

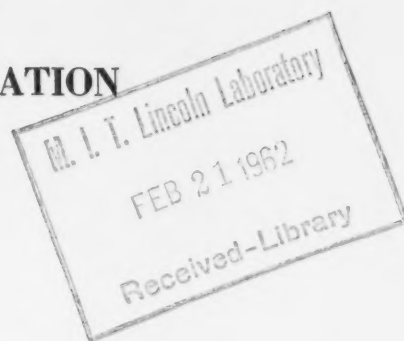
Д О К Л А Д Ы
АКАДЕМИИ НАУК СССР

*Volume 137, Nos. 1-6
March-April, 1961*

PROCEEDINGS OF THE ACADEMY OF SCIENCES OF THE USSR

(DOKLADY AKADEMII NAUK SSSR)
Physical Chemistry Section

IN ENGLISH TRANSLATION



CONSULTANTS BUREAU

2 outstanding new Soviet journals

KINETICS AND CATALYSIS

The first authoritative journal specifically designed for those interested (directly or indirectly) in kinetics and catalysis. This journal will carry original theoretical and experimental papers on the kinetics of chemical transformations in gases, solutions and solid phases; the study of intermediate active particles (radicals, ions); combustion; the mechanism of homogeneous and heterogeneous catalysis; the scientific grounds of catalyst selection; important practical catalytic processes; the effect of substance — and heat-transfer processes on the kinetics of chemical transformations; methods of calculating and modelling contact apparatus.

Reviews summarizing recent achievements in the highly important fields of catalysis and kinetics of chemical transformations will be printed, as well as reports on the proceedings of congresses, conferences and conventions. In addition to papers originating in the Soviet Union, KINETICS AND CATALYSIS will contain research of leading scientists from abroad.

Contents of the first issue include:

- Molecular Structure and Reactivity in Catalysis.** A. A. Balandin
- The Role of the Electron Factor in Catalysis.** S. Z. Roginskii
- The Principles of the Electron Theory of Catalysis on Semiconductors.** F. F. Vo'kenshtein
- The Use of Electron Paramagnetic Resonance in Chemistry.** V. V. Voevodskii
- The Study of Chain and Molecular Reactions of Intermediate Substances in Oxidation of *n*-Decane.** Z. K. Maizus, I. P. Skibida, N. M. Emanué' and V. N. Yakovleva
- The Mechanism of Oxidative Catalysis by Metal Oxides.** V. A. Roiter
- The Mechanism of Hydrogen-Isotope Exchange on Platinum Films.** G. K. Borekov and A. A. Vasilevich
- Nature of the Change of Heat and Activation Energy of Adsorption with Increasing Filling Up of the Surface.** N. P. Keier
- Catalytic Function of Metal Ions in a Homogeneous Medium.** L. A. Nikolaev
- Determination of Adsorption Coefficient by Kinetic Method. I. Adsorption Coefficient of Water, Ether and Ethylene on Alumina.** K. V. Topchieva and B. V. Romanovskii
- The Chemical Activity of Intermediate Products in Form of Hydrocarbon Surface Radicals in Heterogeneous Catalysis with Carbon Monoxide and Olefins.** Ya. T. Éidus
- Contact Catalytic Oxidation of Organic Compounds in the Liquid Phase on Noble Metals. I. Oxidation of the Monophenyl Ether of Ethyleneglycol to Phenoxycetic Acid.** I. I. Ioffe, Yu. T. Nikolaev and M. S. Brodskii

Annual Subscription: \$150.00

Six issues per year — approx. 1050 pages per volume

JOURNAL OF STRUCTURAL CHEMISTRY

This significant journal contains papers on all of the most important aspects of theoretical and practical structural chemistry, with an emphasis given to new physical methods and techniques. Review articles on special subjects in the field will cover published work not readily available in English.

The development of new techniques for investigating the structure of matter and the nature of the chemical bond has been no less rapid and spectacular in the USSR than in the West; the Soviet approach to the many problems of structural chemistry cannot fail to stimulate and enrich Western work in this field. Of special value to all chemists, physicists, geochemists, and biologists whose work is intimately linked with problems of the molecular structure of matter.

Contents of the first issue include:

- Electron-Diffraction Investigation of the Structure of Nitric Acid and Anhydride Molecules in Vapors.** P. A. Akishin, L. V. Vil'kov and V. Ya. Rosolovskii
- Effects of Ions on the Structure of Water.** I. G. Mikhailov and Yu. P. Syrnikov
- Proton Relaxation in Aqueous Solutions of Diamagnetic Salts. I. Solutions of Nitrates of Group II Elements.** V. M. Vdovenko and V. A. Shcherbakov
- Oscillation Frequencies of Water Molecules in the First Coordination Layer of Ion in Aqueous Solutions.** O. Ya. Samilov
- Second Chapter of Silicate Crystallochemistry.** N. V. Belov
- Structure of Epididymite $\text{NaBeSi}_3\text{O}_8\cdot\text{OH}$. A New Form of Infinite Silicon—Oxygen Chain (band) $[\text{Si}_3\text{O}_{11}]$.** E. A. Podedimskaya and N. V. Belov
- Phases Formed in the System Chromium—Boron in the Boron-Rich Region.** V. A. Épel'baum, N. G. Sevast'yanov, M. A. Gurevich and G. S. Zhdanov
- Crystal Structure of the Ternary Phase in the Systems $\text{Mo(W)}-\text{Fe(CO,Ni)}-\text{Si}$.** E. I. Gladyshevskii and Yu. B. Kyz'ma
- Complex Compounds with Multiple Bonds in the Inner Sphere.** G. B. Bokii
- Quantitative Evaluation of the Maxima of Three-Dimensional Patterson Functions.** V. V. Ilyukhin and S. V. Borisov
- Application of Infrared Spectroscopy to Study of Structure of Silicates. I. Reflection Spectra of Crystalline Sodium Silicates in Region of $7.5-15\mu$.** V. A. Florinskaya and R. S. Pechenkina
- Use of Electron Paramagnetic Resonance for Investigating the Molecular Structure of Coals.** N. N. Tikhomirova, I. V. Nikolaeva and V. V. Voevodskii
- New Magnetic Properties of Macromolecular Compounds with Conjugated Double Bonds.** L. A. Blyumenfel'd, A. A. Slinkin and A. E. Kalmanson

Annual Subscription: \$80.00

Six issues per year — approx. 750 pages per volume

Publication in the USSR began with the May-June 1960 issues. Therefore, the 1960 volume will contain four issues. The first of these will be available in translation in April 1961.



CONSULTANTS BUREAU 227 W. 17 ST., NEW YORK 11, N. Y.

Volume 137, Nos. 1-6

March-April, 1961

PROCEEDINGS OF THE ACADEMY OF SCIENCES OF THE USSR

(DOKLADY AKADEMII NAUK SSSR)

Physical Chemistry Section

A publication of the Academy of Sciences of the USSR

IN ENGLISH TRANSLATION

Year and issue of first translation:

Vol. 112, Nos. 1-6 Jan.-Feb. 1957

Annual subscription
Single issue

\$160.00
35.00

Copyright © 1961

CONSULTANTS BUREAU ENTERPRISES, INC.
227 West 17th Street, New York, N. Y.

*A complete copy of any paper in this issue may
be purchased from the publisher for \$5.00*

*Note: The sale of photostatic copies of any
portion of this copyright translation is expressly
prohibited by the copyright owners.*

Printed in the United States of America

PROCEEDINGS OF THE ACADEMY OF SCIENCES OF THE USSR

Physical Chemistry Section

Volume 137, Numbers 1-6

March-April, 1961

CONTENTS

	PAGE	RUSS. ISSUE	RUSS. PAGE
Polymerization Induced by the Electrical Charges formed at Phase Boundaries. G. P. Gladyshev and S. R. Rafikov	227	1	113
The Interaction between Non-Bonded Carbon and Hydrogen Atoms. A. I. Kitaigorodskii	231	2	116
The Rate Constant for the Reaction $\text{HO}_2 + \text{H}_2\text{O} = \text{H}_2\text{O}_2 + \text{OH}$. V. N. Kondrat'ev	235	1	120
The Nature of "The Fluctuating Bands of Boric Acid". A. A. Mal'tsev, V. K. Matveev, and V. M. Tatevskii	239	1	123
The Relation between the Amount of H_2O_2 Evolved and the Number of Oxide Molecules Formed in the Atmospheric Corrosion of Mg and Al. I. L. Roikh and I. P. Bolotich	243	1	126
Theoretical Treatment of the I(t)-Curves for the Reduction of Anions on a Dropping Mercury Electrode in the Presence of Adsorbed Catalysts. A. Ya. Gokhshtein	247	2	345
The Nature of the Induction Period in the Autoxidation of Fats and Fatty Acids. N. S. Drozdov	251	2	349
Polanyi's Rule for Proton Transitions and the Hydrogen Bond. E. A. Pshenichnov and N. D. Sokolov	255	2	352
A Spectrophotometric Study of Zirconium Chloride Solutions in Connection with the Adsorption of Zirconium on Fluoroplast-4. I. E. Starik, I. A. Skul'skii, and V. N. Shchebetkovskii	259	2	356
Mechanism of the Transfer of Iodine under Conditions of Internal Kinetics of Adsorption on to Carbons from Various Solvents. A. N. Kharin and N. A. Kataeva	263	2	359
The Change in the Spectral Distribution of the Intrinsic and Sensitized Photoeffects in Weakly Illuminated Silver Halides. I. A. Akimov	267	3	624
Radioactive Catalysts. The Dehydration of Cyclohexanol on Magnesium Sulfate and Calcium Chloride. A. A. Balandin, Vikt. I. Spitsyn, N. P. Dobrosel'skaya, and I. E. Mikhailenko	271	3	628
Certain Quantitative Relationships in Thermography. L. G. Berg and L. A. Borisova	275	3	631
The Mechanism of Ozone Formation in the Electrolysis of Concentrated Perchloric Acid Solutions. M. A. Gerovich, R. I. Kaganovich, Yu. A. Mazitov, and L. N. Gorokhov	279	3	634
The Nature of the Interaction of Benzene Molecules with Hydroxyl Groups. A. V. Kiselev, Ya. Koutetski, and I. Chizhek	283	3	638
The Effect of Chloride Ions on the Electrochemistry of Zirconium and Its Corrosion. Ya. M. Kolotyarkin and V. A. Gil'man	289	3	642
Electrical Properties of Alkaline Earth, Rare Earth, and Thorium Hexaborides. Yu. B. Paderno and G. V. Samsonov	293	3	646
The Mobility of Atoms on the Surface of a Crystal at Its Melting Point. V. I. Shimulis and V. M. Gryaznov	295	3	648

CONTENTS (continued)

	PAGE	RUSS. ISSUE	RUSS. PAGE
Mechanical and Structural Properties of Protein Fibers. N. V. Grigor'eva, V. A. Pchelín, and P. A. Rebinder	301	4	889
Catalysis on Organic Semiconductors Prepared from Polyacrylonitrile by Thermal Treatment. E. S. Dokukina, S. Z. Roginskii, M. M. Sakharov, A. V. Topchiev, M. A. Geiderikh, B. Z. Davydov, and B. A. Krentsel'	305	4	893
The Adsorption of Hydrogen Ions at a Negatively Charged Mercury-Electrolyte Interface. A. N. Frumkin, O. A. Petrii, and N. V. Nikolaeva-Fedorovich	309	4	896
The Kinetics of Electrode Processes and the Mechanisms of Spontaneous Dissolution of the N- and P-Types with Different Specific Resistances. E. N. Paleolog, A. Z. Fedotova, and N. D. Tomashov	313	4	900
The Effect of Adsorbed Halogens on the Electron Work Function of Iron. G. M. Popova, H. A. Shurmovskaya, and P. Kh. Burshtein ..	317	4	904
The Role of Convection Mixing in the Combustion of Solid Mixtures. N. N. Bakhman	321	5	1141
The Statics of Exchange for a Mixture of Ions. N. K. Galkina, R. N. Rubinshtein, and M. M. Senyavin	325	5	1144
The Use of High Pressure in the Study of Collective Interaction in Polymerization Processes. M. G. Gonikberg	329	5	1147
Investigation of the Kinetics of the Electroreduction of Iron on the Dropping Mercury Electrode. V. F. Ivanov and Z. A. Iofa	331	5	1149
Nuclear Magnetic Resonance Spectra of Irradiated Perfluorooctadiene and Perfluorododecadiene. N. M. Pomerantsev, V. A. Khramchenkov, L. V. Sumin, and A. V. Zimin	335	5	1153
The Effect of Polymorphism on Thermal Conductivity. G. B. Ravich and Yu. N. Burtsev	337	5	1155
The Influence of Surface Active Substances on the Solution Kinetics of Calcium Carbonate in Mineral Acids. Vikt. I. Spitsyn, V. A. Pchelkin, and I. V. Goncharov	341	5	1158
The Kinetics of the Oxidation of Propylene to Acrolein Studied by the Circulating-Flow Method. V. M. Belousov, Ya. B. Gorokhovatskii, M. Ya. Rubanik, and A. V. Gershingorina	345	6	1396
Thermodynamic Properties of Iron-Tellurium Alloys in the Solid State. V. A. Geiderikh, Ya. I. Gerasimov, and A. V. Nikol'skaya ..	349	6	1399
An Investigation of the Mechanism of the Formation of Ozone at the Anode in Sulfuric Acid Solutions. V. A. Lunenok-Burmakina, A. P. Potemskaya, and A. N. Brodskii	353	6	1402
The Effect of a Magnetic Field on Particle Movement in Electrolyte Solutions. V. A. Myamlin, V. A. Kibardin, and Yu. Ya. Gurevich ..	357	6	1405
Interaction of Weak Compression Waves with a Flame Front. S. S. Novikov and Yu. S. Ryazantsev	363	6	1409
Spreading of Mercury Over a Free Zinc Surface, as Connected with the Study of Strength Reduction by Adsorption. B. D. Summ, Yu. V. Goryunov, N. V. Pertsov, and E. D. Shchukin	367	6	1413
The Manifestation of Autonomy by Electron Groupings in the Luminescence Spectra of Complicated Molecules. D. N. Shigorin, N. A. Shcheglova, and N. S. Dokunikhin	371	6	1416
Reaction Kinetics for the Reduction of Diphenyl-m-Tolylcarbinol with Isopropyl Alcohol by Transfer of Negatively Charged Hydrogen in the System $H_2SO_4-H_2O$. S. G. Éntelis, R. P. Tiger, G. V. Épple, and N. M. Chirkov	377	6	1420
Errata, Vol. 135, Nos. 1-6, November-December, 1960	381		

POLYMERIZATION INDUCED BY THE ELECTRICAL CHARGES FORMED AT PHASE BOUNDARIES

G. P. Gladyshev and S. R. Rafikov

(Presented by Academician N. N. Semenov, October 15, 1960)

Translated from Doklady Akad. Nauk SSSR, Vol. 137, No. 1,

pp. 113-115, March, 1961

Original article submitted October 15, 1960

The presence of ordinary phase boundaries (in the simplest case the point of contact between the reaction mixture and the vessel), the formation of new phases, or normal phase transitions play a very important role in a great number of chemical reactions.

Polymerization has been detected during the melting of certain solid monomers (methyl methacrylate, styrene, etc.) [1,2,3]. It is also reported that the polymerization rate increases at low temperatures if a solid phase is present [4]. When a powder is added to help the reaction the rate depends on the particle size but is apparently independent of the nature of the powder [1]. Recently Adler, Ballantine, et al. have reported [5] liquid phase polymerization on the surface of solid lumps of polymer. Abkin has noted [6] that the walls of the reaction vessel are definitely involved in the radiation-induced polymerization of styrene in an ethyl chloride solution at -78° . Of some interest is also the recent work of Kargin, Kabanov, Platé, and others [7], who have used molecular beam methods for the investigation of polymerization induced by freshly ground solid particles. In studying the polymerization of sodium acrylate in the presence of certain salts the above-mentioned workers have discovered that presence of a crystalline solid phase has a great effect on the reaction rate.

We can also cite several examples of chemical reactions induced by phase changes. The chlorination and hydrochlorination at the melting point of the reaction mixtures [1,8], reactions of alkali oxides and alkaline earth oxides with oxides and chlorides of group IV elements at temperatures where one of the reaction components exhibits a polymorphic transition [1,9], and many other reactions have already been described. Medvedev emphasized the importance of surface effects in the induction and chain propagation of emulsion polymerization [10].

In our opinion all the above-discussed phenomena can, to a large extent, be attributed to the electric charges which normally appear on phase boundaries, or are formed during phase transitions, or else arise as a result of mechanical disintegration and similar causes. A number of workers have reported observing such charge accumulations under these circumstances [11]. Alexander and Rideal [12] have proposed that if an activated complex should acquire a charge the reaction rate in a monomolecular layer would be proportional to the factor $e^{-E\varphi/RT}$, where φ is the potential drop. Moreover Danielli and Davies [13] have shown that PH_s (in the surface layer) is related to PH_b (in the bulk of the solid) by the formula

$$PH_s = PH_b + \frac{\Psi_s}{0.058}.$$

Some workers have presumed that the charge acts through the activation energy of the chemical reaction, while others claim that the effect is only confined to a solid surface (heterogeneous catalysis) [14]. One would naturally assume that a potential difference at a phase boundary would promote a certain orientation of the molecules near the interphase which (according to Semenov [1]) is very important in low-temperature polymerization.

In our opinion a potential drop should affect not only the frequency factor in the Arrhenius equation, but in all the cases where the activated complex acquires a charge it should also change the activation energy.

If we write the rate equation (for a reaction away from a surface) in its usual form,

$$V = A_1 e^{-E_1/RT},$$

then the same reaction near a potential drop (on the phase boundary) will be represented by the equation where

$$V = A_2 e^{-E_2/RT},$$

$A_2 \neq A_1$, $E_2 = E_1 - E_\varphi$, $E_\varphi = n 23060 (\varphi - T \frac{d\varphi}{dT})$ (the sign of E_φ depends on the system).

Consequently one would expect that on account of a potential drop under certain experimental conditions the polymerization should be very rapid due to decreased activation energy and increased frequency factor.

In order to find out whether polymerization can indeed be induced by a surface charge we investigated the polymerization of certain unsaturated compounds on phase boundaries at relatively low temperatures and in the absence of any of the known initiators and catalysts for these reactions. We have also investigated the effects of certain impurities (surface active compounds, inhibitors) on the polymerization rate in layers adjacent to the boundary between the monomer and a solid surface. The monomers used in our work were purified to remove stabilizing agents and peroxides and fractionally distilled in vacuo. Other reagents were purified by ordinary methods until their physical constants were in good agreement with those given in the literature. In each case examined by us we carefully checked the reagents to make sure no peroxides were present and also carried out a parallel set of control experiments; in the latter ones the polymerization was studied in a homogeneous system in the presence of benzoyl peroxide and certain other compounds which were earlier found to enhance the polymerization in the presence of two phases.

We have demonstrated experimentally that the polymerization of acrylonitrile (AN) and of methyl methacrylate (MMA) at 20-22° at a phase boundary (liquid-liquid and liquid-solid) can be induced by a surface potential drop even in the absence of ordinary initiators and catalysts.

Thus, for example, after a 1-2 cm layer of AN was maintained for 10-12 hours on the surface of glycerin which contained 1-2% water, at 20-22° we detected large amounts of the polymer in the form of white flakes. The resulting polymer had a molecular weight of 100,000-200,000 (determined from the density of solution). Moreover, the reaction was completely unaffected by air oxygen, which normally inhibits the radical polymerization of AN.

The polymerization of AN at the phase boundary between AN and water (or rather between the two respective saturated solutions) proceeds at a measurable rate only in an atmosphere of CO₂. When the polymerization of MMA is studied in air at the boundary separating the compound from water or mercury a polymeric film can be detected after 30-40 hours, while at the MMA-paraffin and MMA-glycerin phase boundaries film formation is observed in 4-5 hours. Not only is the monomer more rapidly polymerized in carbon dioxide atmosphere, but in several cases appreciable amounts of polymer could be seen to form immediately after oxygen was eliminated from the system.

It is a well known fact that many compounds when introduced into a two-phase system will alter the potential drop at the interface and should therefore affect the reaction rates. In fact when 0.01% of an acid (CH₃COOH, CH₂ClCOOH, HCl) is added to a system consisting of AN and glycerin (containing 1% water) 25-30% of the monomer undergoes polymerization in 15-20 hours at 20°C and the reaction is practically unaffected by oxygen. In an AN + water system (1:1) containing 0.01 moles/liter of acid only about 1.5% of the compound was polymerized after the system had been maintained in an atmosphere of nitrogen for 100 hours, and the polymer had a molecular weight of about 6,000,000 (determined viscosimetrically).

The polymerization rate in the system AN + glycerin + water increases considerably if acid is present, and the reaction takes place in both the upper and lower layers. In the AN layer the polymerization starts at the phase boundary and continues on the surface of polyacrylonitrile particles. In the lower layer (AN + glycerin + water + HCl, AN + water + HCl) the reaction takes place throughout the entire phase; the initiation apparently occurs on microscopic phase boundaries when the components are mixed, since the reaction rate has been found to depend on how thoroughly the components are mixed and on the presence of finely ground solid particles in the system.

As another example to demonstrate the effect of electric charge on polymerization we can cite the polymerization of MMA when the monomer is electrified. Thus when the very thoroughly degassed monomer is vigorously agitated (electrified) in sealed glass tubes at 20° (400-600 vibrations/min) in the absence of any other initiators, its density rapidly increases due to the formation of the polymer. Within 3 hours 5-10% of the monomer will react under these conditions. In this manner our experiments have demonstrated positively that the polymerization of acrylonitrile and methyl methacrylate can be initiated by the electric charge which arises at the interface, even if none of the ordinary initiators are present. It is safe to assume that the polymerization of many other unsaturated compounds can probably be promoted in a similar way. On the basis of the little data available at the present time it is not possible to construct a definite mechanism for the reaction, but the fact that the reaction can be inhibited by certain compounds would suggest a free radical mechanism.

LITERATURE CITED

1. N. N. Semenov, *Khim. i Tekh. Polimerov*, No. 7-8, 196 (1960).
2. J. C. Bevington, R. G. W. Norrish, *Proc. Roy. Soc., A* **196**, 363 (1949).
3. H. A. Rigby, C. J. Danby, C. W. Hinshelwood, *J. Chem. Soc.* 1948, 234.
4. R. Worall, S. H. Pinner, *J. Polym. Sci.*, **34**, 229 (1959).
5. J. Adler, D. Ballantine and Basel, *Intl. Symposium on Macromolec. Chem.*, [in Russian] (Moscow, 1960), Sec. II, p. 396.
6. A. D. Abkin, A. L. Sheinker, et al., *Intl. Symposium on Macromolec. Chem.* [in Russian] (Moscow, 1960), Sec. II, p. 410.
7. V. A. Kargin, V. A. Kabanov, et al., *Vysokomolek. Soed.* **1**, 264 (1959); **1**, 301 (1959); **1**, 330 (1959); **1**, 1853 (1959); **1**, 1859 (1959); **2**, 765 (1960); V. A. Kargin and N. A. Platé, *Intl. Symposium on Macromolec. Chem.* [in Russian], (Moscow, 1960), Sec. II, p. 460.
8. V. A. Lishnevskii and G. B. Sergeev, *Doklady Akad. Nauk SSSR*, **128**, 767 (1959).
9. V. I. Evdokimov, *Zhur. Neorg. Khim.* **3**, 1232 (1957).
10. S. S. Medvedev, *Collection Czechoslovak chem. comm.*, **22**, Suppl. 174 (1957).
11. N. K. Adam, *The Physics and Chemistry of Surfaces* [Russian translation] (Moscow-Leningrad, 1947); A. Nikuradse, *Liquid Dielectrics* [Russian translation] (NKTP SSSR, 1936); H. Saito, K. Tanaka, *Proc. 7th Japan Nat. Congr. Appl. Mech.*, 1957, Tokyo, 1958, p. 35; *Proc. 6th Japan Nat. Congr. Appl. Mech.*, 1956, Tokyo, 1957, p. 205; G. S. Rose, S. G. Ward, *Brit. J. Appl. Phys.*, **8**, 121 (1957); J. Kobatake, J. Inone, *Koll. Zs.*, 159, 168 (1957); L. G. Kuchurin and V. I. Bekryaev, *Doklady Akad. Nauk SSSR*, **130**, 57 (1960).
12. E. Havinga, *Unimolecular Films* [Russian translation] (IL, 1956), p. 222.
13. J. F. Danielli, J. T. Davies, *Adv. in Enzymol.*, **11**, 35 (1951).
14. J. Davies, *Catalysis, A Study of Heterogeneous Reactions* [Russian translation] (IL, 1956) p. 241.

All abbreviations of periodicals in the above bibliography are letter-by-letter transliterations of the abbreviations as given in the original Russian journal. Some or all of this periodical literature may well be available in English translation. A complete list of the cover-to-cover English translations appears at the back of this issue.

2
3
4
5
6
7
8
9
10
11
12
13
14
15
16
17
18
19
20
21
22
23
24
25
26
27
28
29
30
31
32
33
34
35
36
37
38
39
40
41
42
43
44
45
46
47
48
49
50
51
52
53
54
55
56
57
58
59
60
61
62
63
64
65
66
67
68
69
70
71
72
73
74
75
76
77
78
79
80
81
82
83
84
85
86
87
88
89
90
91
92
93
94
95
96
97
98
99
100

THE INTERACTION BETWEEN NON-BONDED CARBON AND HYDROGEN ATOMS

A. I. Kitaigorodskii

Institute of Heteroorganic Compounds, Academy of Sciences, USSR

(Presented by Academician M. I. Kabachnik, September 26, 1960)

Translated from Doklady Akad. Nauk SSSR, Vol. 2, No. 1,

pp. 116-119, March, 1961

Original article submitted September 26, 1960.

1. Introduction. In many problems of physical chemistry it is frequently convenient to treat a molecule as a system of interacting atoms. Quite often the application of this treatment to various problems connected with reactivity, kinetics, adsorption, thermochemistry, etc., requires some knowledge of the interaction energy curves for non-bonded atoms. It is also taken for granted that a curve for the interaction between non-bonded atoms on the same molecule can not be distinguished from a corresponding curve for atoms on two separate molecules.

2. A Generalized Interaction Curve for C and H Atoms. The intermolecular distances in crystals constitute the most accurate experimentally determined parameters in the interaction functions. These distances are, of course, the same for all hydrocarbons [1] (at least to within 5%) and in general for all organic compounds regardless of their chemical nature. Taking into account the fact that the molecules become slightly "compressed" when they form a crystal we will take the following interatomic equilibrium distances (for "isolated" atoms): C...C 3.8 Å, C...H 3.15 Å, and H...H 2.6 Å. These values yield the following intermolecular distances (in the solid phase): C...C 3.6 Å and H...H 2.35 Å, which are identical with the average experimental values.

We will take $z=r/r_0$ to denote the ratio of the actual interatomic distance to the equilibrium distance and transform the 6th power potential $A/r^6 + B \exp[-r/\rho]$ into the form

$$U = U_{2/3} \left[\frac{1}{z^6} - \frac{6}{\alpha} e^{\alpha} e^{-\alpha z} \right] / \left[11.4 - \frac{6}{\alpha} e^{\frac{1}{3}\alpha} \right],$$

where $U_{2/3}$ is the energy at $r=2/3 r_0$ ($2/3 r_0$ represents typical shortening encountered in organic molecules. For example, the distance between two carbon atoms attached to the same atom in an aliphatic chain is about $2/3 r_0$). The parameter $\alpha = r_0/\rho$; the parameter $U_{2/3} = (A/r_0^6)(11.4 - 6e^{\alpha/3}/\alpha)/(1 - 6/\alpha)$; while parameter B can generally be neglected since the equilibrium condition is $B = (6A/\alpha r_0^6)e^{\alpha}$. The above-made transformation makes it considerably easier to determine the unknown parameters and makes the problem more explicit.

It is apparent that $U/U_{2/3}$ is essentially a function of only one variable, α . The second parameter can be readily taken as a dimensionless unit. One can readily show that $U_{2/3}$ is on the order of several kcal/mole. It is very important that α also have a reasonable range of values. In fact if we compute $U/U_{2/3}$ for $z=1$ we can see right away that only if α is in the range between 11 and 18 will the equilibrium interaction energies (which essentially determine the heats of sublimation) have reasonable values. Hence one great advantage of the new form of the 6th power potential resides in the fact that the two parameters (the third, r_0 , is already incorporated in the equation) have a very narrow range of possible values.

As can be seen in Fig. 1 the $U/U_{2/3}$ curves for various α values intersect at $z=2/3$ and attain distinct minima at $z=1$. Since the value of $U/U_{2/3}$ at the minimum is very small the curves are actually bundled in two points. Consequently, since the curve is not very sensitive to α variations of this parameter are not very important; the case is clearly illustrated in the Figure.

The parameters α and $U_{2/3}$ were so chosen as to give the best agreement with experimental data.

It is interesting to note that all three interactions have very similar α and $U_{2/3}$ values. In the early stages of our investigation it is permissible to use the generalized expression (in reduced coordinates):

$$U = 3,5 \left(-0,64/z^6 + 8,6 \cdot 10^3 \cdot e^{-13z} \right). \quad (1)$$

The choice of $\alpha=13$ fixes the values of two other coefficients in the parentheses. $U_{2/3}=3,5$ kcal/mole was chosen independently.

We have therefore made the following advance since our preceding communication [2]. In our previous work the generalized expression $U'(\Delta r/r)$ was used. The present work shows that a generalized curve can be derived to represent the energy itself as well as its derivative. The U/C function used by us before agrees quite well with the corresponding expression used in the present work.

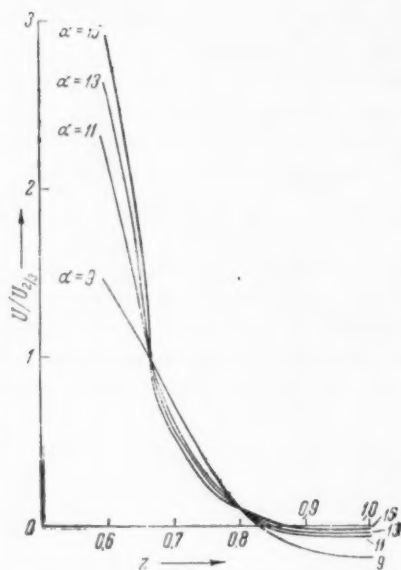


Fig. 1

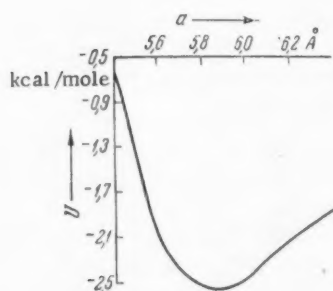


Fig. 2

3. Intermolecular Interactions. In Fig. 2 we have plotted the energy curve for a methane crystal derived with the help of Equation (1). The curve yields a lattice constant which is in good agreement with the experimental value (5.8 Å) and a satisfactory lattice energy (the experimental value computed from the heat of sublimation is 2.6 kcal/mole). The asymmetry of our curve also leads to a reasonable temperature dependence of the lattice parameter.

The energy of methane in the gas-crystalline state (we use the term to denote a state of matter where the molecular centers form the appropriate lattice, but the azimuthal angles of these molecules are randomly oriented relative to the crystallographic axes) turns out to be about the same (within 0.2 kcal/mole). The calculated energies for a quasi-crystalline molecular cluster and for molecules in the closest-packing arrangement are no different from the regular crystal energy. This is hardly surprising, since the energy is practically independent of the lattice parameter in the temperature range from 0°K to the melting point of methane.

One would expect the above-mentioned effect to be of a general nature, since the potential interaction energy between organic molecules at absolute zero is only insignificantly smaller than the corresponding energy at the boiling point of the corresponding liquid. Or in other words, the heat absorbed by the compound is almost entirely converted into the kinetic energy of the molecules.

The equilibrium lattice energies of other compounds have also been calculated [3]. Thus for cyclopentane in the gas-crystalline state the calculations yield 7 kcal/mole as compared to 8 kcal/mole calculated from the heat of sublimation. It is interesting though that in the case of gas-crystalline cyclohexane the calculated and experimental values differ considerably (3 and 9.6 kcal/mole). The discrepancy can be interpreted as follows. The calculations assumed complete randomness in the azimuthal

angles of the molecules. But the cyclohexane molecules are far from being spherically symmetrical. Close packing does not permit orientations in which neighboring molecules have their largest diameters along the same line. And in fact new calculations taking into account the close packing yielded greater repulsion energies and consequently raised the energy level for the system (decreased the absolute value of the total energy).

In the case of benzene the lattice energy calculations are very tedious. We computed the contributions to the total energy coming from the interaction of one molecule with its 12 nearest neighbors, which constitute the first coordination sphere. These interactions contribute 6.5 kcal/mole. From some simpler calculations done for gas-crystalline compounds we know that the first coordination sphere contributed 80-85% of the total energy. Since the experimental lattice energy of benzene is 9-10 kcal/mole, the agreement between the calculated and experimental results is again excellent.

Our energy curve for the atomic interactions practically coincides with the curve derived by Crowell for the interaction between carbon atoms in graphite [4]. Our curve also predicts that the intermolecular distances in crystals of aromatic compounds should decrease with increasing molecular size; such a decline has been observed.

In addition to the energy and equilibrium distance the interaction curve can also be used to compute the compressibility. The calculated compressibility of methane was 0.31 kcal/mole-Å³, the experimental 0.26.

4. Intramolecular Interactions. In order to evaluate the strain energy of a molecule,

$$W_{\text{str}} = \frac{1}{2} \sum C \alpha_i^2 + \sum U_{ih},$$

we have to determine the ideal angle force constant C (see [2]). Using data on the optical force constant γ , one can choose the proper value of C for carbon. $\gamma = [\partial^2 W / \partial \alpha^2]_{\alpha=\alpha_0}$, where α_0 is the equilibrium value of α , and W is the strain energy of an ideal angle plus the interaction energy between non-bonded atoms. To get back values of γ from the chosen C we have to know the form of the interaction curve, since

$$\gamma = \partial^2 W / \partial \alpha^2 = C + U'(r) \partial^2 r / \partial \alpha^2 + U''(r) (\partial r / \partial \alpha)^2.$$



A value of $C = 35$ kcal/mole together with our expression for the potential curve yields $\gamma_{\text{CCC}} = 95$ kcal/mole and $\gamma_{\text{HCH}} = 79$ kcal/mole, both of which are in full agreement with the optical data. Using this value of C we computed the strain energies and the optimal conformations of several hydrocarbon molecules. The experimental and calculated data are presented in Table 1.

The present conformation data agree quite well with those presented in the preceding paper. The new approach enabled us to calculate also the strain energies. One can readily see in the Table that the main contribution to the strain energy comes from the repulsion of non-bonded atoms and not from the deviation of the angle from a tetrahedral value. Thus even in cyclobutane $\frac{1}{2} C \alpha^2 = 2$ kcal/mole whereas the strain energy per CH_2 -group is 21 kcal/mole. It is quite obvious that the situation arises as a result of a new and, in our opinion, more correct determination of the strain energy. In the classical literature strain energy was defined as excess energy over that of alkanes. Two thirds of the strain energy thus defined came from the deformation of the tetrahedral bond angles.

We would like to point out that the calculated excess strain energies are considerably smaller than the calorimetrically determined experimental. This indicates that half the strain must result from changes in the interaction between bonded atoms (bond strain).

The examples given in this paper show that the generalized potential gives reasonable results when used for calculating a number of physical properties. Future work should reveal whether the interaction curves could be improved any more. In our opinion a method of calculating and predicting properties to within less than one order of magnitude already deserves some attention.

TABLE 1

Molecule	Angle	Size of angle in °C			Strain energy per CH ₂ group, kcal /mole	Excess strain energy over that of alkanes	
		theoretical		exptl.		theoretical	exptl.
		current work	(*)				
Ethane	HCH	109,4	—	109,3	—	—	
Alkanes	CCC	112	111,5	112	18	—	
	HCH	110	108	—			
Cyclopropane	HCH	116,5	118	118,2	23	5	10
Cyclobutane	HCH	113	112	114	21	3	7
Cyclopentane	HCH	110,5	109	—	18,5	0,5	1
Cyclohexane	CCC	112,5	112				
	HCH	110	108	—	18	0	0
Nortricyclene	θ	98,5	96	96,5	—	—	
	β ₁	112	121	—			
	β ₂	113	112	—			
							
Norcamphane	α ₁	114	109,5	—	—	—	
	α ₂	103	103*				
	α ₃	91	92				
	β ₁	106	108,5				
	β ₂	112	107,5*				
	β ₃	114	113*				
							

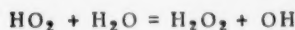
* The α₂, β₂, and β₃ angles given in [2] were in error.

LITERATURE CITED

1. A. I. Kitaigorodskii, Organic Crystal Chemistry [in Russian] (IZd AN SSSR, 1955).
2. A. I. Kitaigorodsky, Tetrahedron, 9, 183 (1960).
3. A. I. Kitaigorodskii and K. V. Mirskaya, Kristallografiya (in press).
4. A. D. Crowell, J. Chem. Phys., 29, 446 (1958).

All abbreviations of periodicals in the above bibliography are letter-by-letter transliterations of the abbreviations as given in the original Russian journal. Some or all of this periodical literature may well be available in English translation. A complete list of the cover-to-cover English translations appears at the back of this issue.

THE RATE CONSTANT FOR THE REACTION



Academician V. N. Kondrat'ev

Translated from Doklady Akad. Nauk SSSR, Vol. 2, No. 1,
pp. 120-122, March, 1961

Original article submitted December 7, 1960

V. A. Poltorak and V. V. Voevodskii have shown [1] that in vessels coated with potassium chloride the third ignition limit of hydrogen-oxygen mixtures is a chain instead of a thermal process. Even before that it has been shown [2] that in addition to reactions involving H, O, and OH radicals the reactions $\text{HO}_2 + \text{H}_2 = \text{H}_2\text{O}_2 + \text{H}$ and $\text{HO}_2 + \text{H}_2\text{O} = \text{H}_2\text{O}_2 + \text{OH}$ play an important part in the region of the third ignition limit.

From the known reaction mechanism the equation

$$\left[\frac{(p + 6.3p_{\text{H}_2\text{O}})k_6}{2k_2} - 1 \right] \frac{k_7^0}{(2/3 k_8 p + k_9 p_{\text{H}_2\text{O}})(p + p_{\text{H}_2\text{O}})} = 1, \quad (1)$$

can be derived, where k_2 , k_6 , $k_7 = k_7^0(p + p_{\text{H}_2\text{O}})$, k_8 , and k_9 are the respective rate constants for the reactions:



p is the sum of the partial pressures of H_2 and O_2 and $p_{\text{H}_2\text{O}}$ is the partial pressure of H_2O . Using the relationship between temperature and pressure in the third limit with the assumption that ignition takes place the instant the $2\text{H}_2 + \text{O}_2$ mixture is practically entirely converted to water (i.e. when $p=0$ and $p_3 = 3/2 p_{\text{H}_2\text{O}}$) and also assuming $k_8 \ll k_9$ Poltorak and Voevodskii evaluated the rate constant for reaction (V) and got $k_9 = 2 \cdot 10^{-16} e^{-8000/RT} \text{ cm}^3 \cdot \text{molecule}^{-1} \cdot \text{sec}^{-1}$.

Since, however, $E_9 = 8000 \text{ cal/mole}$ is considerably smaller than the heat for the endothermic reaction (V) (which is about 30,000 cal/mole) Poltorak and Voevodskii concluded that there must be two forms of the HO_2 radical with different degrees of stability (see also [3]). But we are going to show that more exact calculations based on the same experimental data of Poltorak and Voevodskii yield an activation energy for reaction (V) which is very close to the heat of reaction, and consequently there is no need to postulate two types of HO_2 radical.

Using the relationship $p = p_0 - 3/2 p_{\text{H}_2\text{O}}$ [1] and substituting the initial pressure of the stoichiometric mixture of H_2 and O_2 p_0 for the pressure p in Equation (1) we get the expression

$$p_0^2 - 2 \left(a - \frac{3b-4}{4} p_{\text{H}_2\text{O}} \right) / p_0 + \left(c - 9.6 a p_{\text{H}_2\text{O}} - \frac{3b-3}{4} p_{\text{H}_2\text{O}}^2 \right) = 0,$$

where $a = (3/8)[(k_6 k_7^0 / k_2 k_8)]$, $b = k_9 / k_8$, and $c = (3/2)[(k_7^0 / k_8)]$.

Now, assuming that ignition occurs at a certain minimum p_0 ($p_{0\min} = p_3$) determined from the condition that $dp_0/dp_{H_2O} = 0$ we can derive the following relationship connecting p_3 and p_{H_2O} :

$$p_{H_2O} = \frac{3b-4}{3(b-1)} p_3 - \frac{6.4a}{b-1}.$$

Substituting this value of p_{H_2O} into our quadratic equation and rearranging the resulting expression we get

$$p_3^2 - 2a \frac{12(5.8b-7.4)}{(3b-2)^2} p_3 + 12 \frac{c(b-1) + 4.8 \cdot 6.4a^2}{(3b-2)^2} = 0. \quad (2)$$

The data of Willbourn and Hinshelwood [4] indicate that at 586°C the rate constant k_9 exceeds k_8 by a factor of ten [3]. Since the experiments of Poltorak and Voevodskii were carried out in the vicinity of this temperature we will consider $b = k_9/k_8 \gg 1$. As a result Equation (2) can be rewritten as

$$\alpha^2 - 2 \frac{2.9 \frac{k_2}{k_6} p_3 - \frac{k_2^2}{k_6^2}}{5.76} \alpha + \frac{p_3^2 \frac{k_2^2}{k_6^2}}{5.76} = 0, \quad (3)$$

where $\alpha = k_7^0/k_9$.

Solving the equation for α we get

$$\alpha = \frac{2.9 p_3 - k_2/k_6 \frac{k_2}{k_6}}{5.76} \left(1 \pm \sqrt{1 - \frac{5.76 p_3^2}{(2.9 p_3 - k_2/k_6)^2}} \right). \quad (4)$$

Using Poltorak's and Voevodskii's data we evaluated α at three temperatures spanning the entire temperature range covered by the authors. In Fig. 1 we have plotted $\log \alpha$ as a function of $1/T$. The slope yields an activation energy $E_9 = 30$ kcal/mole for the reaction $HO_2 + H_2O = H_2O_2 + OH$; the value is almost identical with the heat of the reaction (which is about 30 kcal/mole). Considering that the reported experiments covered a very narrow temperature range our E_9 value could be off by several kcal/mole. The heat of reaction (V), which is also known to only within several kcal/mole*, constitutes the lower limit of the activation energy. The upper limit can be determined by adding the activation energy for the reverse reaction $E_9^*(OH + H_2O_2 = H_2O + HO_2)$ to the heat of reaction. The activation energy for the reverse reaction can be determined in the following manner. Frost and Oldenberg found that the OH radicals formed by discharge in H_2O_2 disappear in about 0.01 sec [7]. Assuming that the rate of hydroxyl radical disappearance determines the rate of the reaction $OH + H_2O_2 = H_2O + HO_2$ and that during a time interval $t = 0.01$ sec the OH concentration will decrease to one tenth its value we can use the equation

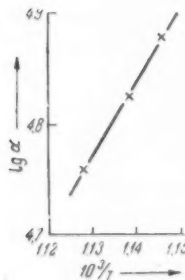


Fig. 1

$$\frac{[OH]}{[OH]_0} = e^{-k_6(H_2O_2)t}$$

to evaluate the rate constant for the reaction: $k_9^* = 10^{-14} \text{ cm}^3 \cdot \text{molecule}^{-1} \cdot \text{sec}^{-1}$ ($p_{H_2O_2} = 1 \text{ mm Hg}$, $T = 400^\circ K$).

* Using the data tabulated in [5] and the following heats of dissociation: $D_{O-H} = 102.4$ kcal/mole and $D_{O_2-H} = 47 \pm 4$ kcal/mole, together with the heat of formation of H_2O_2 , $\Delta H_{298} = 32.5$ kcal/mole [6] we get -29.6 ± 4.5 kcal/mole as the heat of reaction for the reaction $HO_2 + H_2O = H_2O_2 + OH$ under standard conditions.

Writing k_9' in the form $k_9' = k_9^0 e^{-E_9'/RT}$ and assuming that k_9^0 can not exceed $10^{-11} \text{ cm}^3 \cdot \text{molecule}^{-1} \cdot \text{sec}^{-1}$ we get $E_9' = 5 \text{ kcal/mole}$ as the upper limit of E_9' . Hence the upper limit of E_9 could hardly exceed $30 + 5 = 35 \text{ kcal/mole}$.

Using the α values determined by us we find that $k_7^0 : k_9^0 = 2.3 \cdot 10^{13} \text{ cm}^3 \cdot \text{molecule}^{-1}$ ($E_9 = 30,000 \text{ cal/mole}$) and taking $k_7^0 = 700 \text{ sec}^{-1}$ we get $k_9^0 = 3 \cdot 10^{-11} \text{ cm}^3 \cdot \text{molecule}^{-1} \cdot \text{sec}^{-1}$ and consequently $k_9 = 3 \cdot 10^{-11} e^{-30000/RT} \text{ cm}^3 \cdot \text{molecule}^{-1} \cdot \text{sec}^{-1}$.

We will also evaluate $b = k_9 : k_8$. Using the k_9 determined above and k_8 which can be evaluated from the approximate equation $k_8 = 2 \cdot 10^{-13} e^{-24000/RT} \text{ cm}^3 \cdot \text{molecule}^{-1} \cdot \text{sec}^{-1}$ [3] we find that at 586°C $b = 5$, whereas calculations based on the data of Willbourn and Hinshelwood yielded $b = 11$ [3, 4].

Before concluding we would like to consider one more problem. We had assumed above that k_8 represents reaction (IV) the heat of which is -15 kcal/mole . In addition to this reaction, however, we can also have an exothermic reaction,



with a heat of reaction $+ 53 \text{ kcal/mole}$.

It can be demonstrated that the general form of Equation (1) will not change if both reactions are taken into account except that the constant k_8 will have to be replaced by the sum $k_8 + k_8'$.

On the basis of the available experimental data one can not as yet decide whether both or only one of the two constants should enter Equation (1) (within the investigated temperature range). An activation energy of 24 kcal/mole seems quite compatible with the endothermic reaction (IV) which has a $\Delta H = -15 \text{ kcal/mole}$. On the other hand reaction (IV') which involves a rupture of two bonds (H-H and HO-O) should have a large activation energy and a small frequency factor which is also compatible with the value of k_8 (or k_8') $= 2 \cdot 10^{-13} e^{-24000/RT} \text{ cm}^3 \cdot \text{molecule}^{-1} \cdot \text{sec}^{-1}$.

LITERATURE CITED

1. V. A. Poltorak and V. V. Voevodskii, *Zhur. Fiz. Khim.* **24**, 299 (1950).
2. V. V. Voevodskii, *Zhur. Fiz. Khim.* **20**, 1285 (1946); A. B. Nalbandyan and V. V. Voevodskii, *The Mechanism of Oxidation and Ignition of Hydrogen* [in Russian] (Izd AN SSSR, 1949).
3. V. V. Voevodsky, *Seventh Symposium on Combustion*, London, 1959, p. 34.
4. A. H. Willbourn, C. N. Hinshelwood, *Proc. Roy. Soc., A* **185**, 353, 369 (1946); *A* **188**, 1 (1947).
5. *Selected Values of Chemical Thermodynamic Properties*, Washington, 1952.
6. P. Gray, *Trans. Farad. Soc.*, **55**, 408 (1959).
7. A. A. Frost, O. Oldenberg, *J. Chem. Phys.*, **4**, 781 (1936).

All abbreviations of periodicals in the above bibliography are letter-by-letter transliterations of the abbreviations as given in the original Russian journal. Some or all of this periodical literature may well be available in English translation. A complete list of the cover-to-cover English translations appears at the back of this issue.

* This number was obtained from the equation $k_7^0 = 39.9D_1/d^2$, where D_1 is the diffusion coefficient at a pressure of 1 mm Hg and d is the diameter of the spherical reaction vessel ($d = 4 \text{ cm}$). The diffusion coefficient of the HO_2 radicals is comparable to that of O_2 , which under standard temperature and pressure has a diffusion coefficient of $0.2 \text{ cm}^2/\text{sec}$.



THE NATURE OF "THE FLUCTUATING BANDS OF BORIC ACID"

A. A. Mal'tsev, V. K. Matveev, and V. M. Tatevskii

(Presented by Academician V. N. Kondrat'ev, October 5, 1960)

Lomonosov Moscow State University

Translated from Doklady Akad. Nauk SSSR, Vol. 2, No. 1,

pp. 123-125, March, 1961

Original article submitted October 3, 1960

It is well known that when boron or its compounds are introduced into a flame, it becomes green. This green luminescence is caused by a series of so-called "fluctuating bands of boric acid" [1] which are located in the region from 3700 to 6800 Å. It is utilized in the spectrophotometric determination of boron. Although these fluctuating bands were first discovered in the last century [2], their nature has remained unknown up to the present. The bands were attributed to boric acid [2], to the BO [3] and BOH [4] radicals, and to the molecule B_2O_3 [5, 6]. In work carried out in our laboratory [7] it was shown, by means of analysis of the isotopic displacement in the band heads of the fluctuating bands, that attributing these bands to the BO radical [3] is incorrect, and that the molecule which gives the spectrum of "boric acid" does not contain hydrogen but appears to be a multi-atom oxygen boron compound of the composition B_xO_y . If the fluctuating bands were caused by a molecule containing two atoms of boron - the B_2O_3 molecule for example - as Soulen, Sthapitanonda, and Margrave assert [5, 6] then, in a compound containing the isotope B^{10} , about 50% of the spectrum would consist of three systems of band heads, caused by the three isotopic molecules $B_2^{10}O_3$, $B^{10}B^{11}O_3$, and $B_2^{11}O_3$.

By using a discharge tube with a hollow hot cathode [7] on a D F S - 3 spectrograph with a dispersion of 2 Å/mm, we photographed emission spectra of the fluctuating bands in the 5470, 5800, and 6300 Å regions, varying the isotopic concentration of boric oxide (the concentrations of the isotope B^{10} were 18, 55, and 90%). In Figure 1 are shown the isotopic displacements in the 5470 Å band. In the spectrum one can see only two sys-

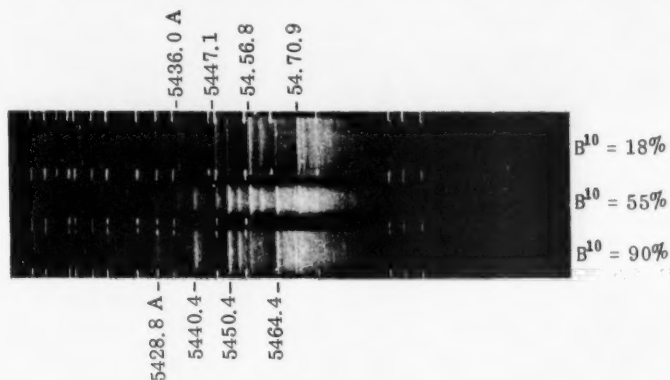


Fig. 1. Isotopic displacements in the band λ 5470 Å.

tems of isotopic band heads that can be caused by a molecule containing one atom of boron. Of course it is not impossible, though highly improbable, that the isotopic displacements between a molecule of $B^{10}B^{11}O_3$ and either of the molecules $B_2^{10}O_3$ or $B_2^{11}O_3$ are so small that they cannot be observed.

Since the isotopic bands do not give an unequivocal solution to the problem of the nature of the fluctuating bands, we studied the emission and absorption spectra of the vapors over boric oxide. This was done in both the visible and infrared bands at temperatures of 1200-1550 deg in inert (He, Ar, N₂), oxidizing (O₂) and reducing (H₂) atmospheres and in the presence of steam.

Boric oxide was placed in a tube of thermally resistant porcelain and heated in a graphite furnace. By means of glass adapters with windows the tube was attached to a vacuum pump which served to pump out and fill the system with various gases. Before beginning the study, the boric oxide was carefully degassed at 1000 deg by continuous pumping (the thermally resistant porcelain tube made it possible to obtain a vacuum of the order of $1 \cdot 10^{-5}$ mm of Hg at 1550 deg). The temperature inside the tube was measured by a platinum-platinumrhodium thermocouple or by an optical pyrometer. The emission and absorption spectra in the visible range were taken on an I S P - 22 spectrophotograph. The absorption spectrum was recorded with the aid of a spectrophotometric adapter made according to Dianov-Klokov [8]. The emission and absorption spectra in the infrared region were taken on an I K S - 6 machine [9]. Since analysis of the spectra in the visible and infrared regions showed that the emission and absorption spectra coincided perfectly in all the atmospheres studied, the research was confined to absorption spectra.

There is mention in the literature of the reaction of boric oxide with the porcelain of the tubes [5]. Therefore the influence of the material of the tube on the spectrum of the vapors over heated boric oxide was examined. This was done by placing a cylinder, folded from platinum foil, inside the porcelain tube. Experiment showed, however, that this precaution was not necessary.

Figure 2 shows the dependence of the intensity of the fluctuating absorption bands on the type of atmosphere. In an inert atmosphere the fluctuating bands appear only at temperatures of 1400-1550 deg and even then their intensity is very slight.

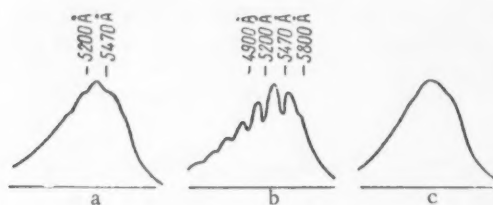


Fig. 2. Influence of various atmospheres on the intensity of the "fluctuating absorption bands" at 1500 deg (gas pressure 250 mm). a - He, b - O₂, c - H₂.

The addition of oxygen even in small quantities (3 mm of Hg) sharply increases the intensity of the fluctuating bands, and with increasing oxygen pressure the intensity of the bands further increases. With oxygen at atmospheric pressure luminescence appears as low as 1200 deg. In the presence of hydrogen the fluctuating bands do not appear at all; moreover, hydrogen extinguishes already existing luminescence. The passage of steam over heated boric oxide brings about a vigorous transfer of the substance as a result of the formation of boric acid and in this case the fluctuating bands are absent.

Mass-spectrometric studies of the vapors over boric oxide [10,11] at temperatures of the order of 1300 deg have shown that, in a vacuum or an inert atmosphere,

they consist essentially of molecules of B₂O₃. Therefore the anomalous influence of oxygen on the intensity of the fluctuating bands, in comparison with an inert atmosphere, indicates that these bands result from another oxygen compound of boron with a higher oxygen content than the B₂O₃ molecule. In our opinion, this is the radical BO₂ [12]. In this case the increase in the intensity of the fluctuating bands may be explained by the reaction $B_2O_3 + \frac{1}{2} O_2 = 2BO_2$, and the appearance of the fluctuating bands in an inert atmosphere at temperatures of 1400-1500 deg would be caused by a slight dissociation of boric oxide, $B_2O_3 = BO + BO_2$. Quantitative measurements of the dependence of the intensity of the fluctuating bands on the oxygen pressure [13] fully confirm the fact that the carrier of the fluctuating bands is the radical BO₂. This conclusion agrees well with the isotopic displacements which were discussed above.

In studying the infrared spectra in the region from 3 to 12 μ only one band of about 2000 cm^{-1} was detected, which was caused by the oscillations of the double bond B = O of the B₂O₃ molecule [14]. The intensity of the 2000 cm^{-1} absorption band is identical in an atmosphere of helium, argon, nitrogen, oxygen or hydrogen, and increases greatly when steam is passed through, apparently as a result of an increase in the concentration of molecules containing the B = O group. In the presence of steam such a molecule, other than B₂O₃, might be HBO₂. The fact that oxygen has practically no influence on the 2000 cm^{-1} band indicates that the concentration of the BO₂ radical at 1550 deg is small in comparison with the concentration of B₂O₃ molecules.

The conclusion to which we came in 1958, namely, that the fluctuating bands are caused by the BO_2 radical [12] has been confirmed by Kaskan and Millikan's work on the intensity of the fluctuating bands in trimethylborate flames, which has only just been published.

LITERATURE CITED

1. R. W. Pearse, A. G. Gaydon, "The Identification of Molecular Spectra," London, 1950.
2. H. Kayser, Handbuch der Spectroskopie, 5, 1910.
3. N. L. Singh, Proc. Indian Acad. Sci., A29, 424 (1949).
4. E. Pungor, I. Kankoly Thege, Acta chim. Acad. Sci. Hung., 13, 39 (1957).
5. J. R. Soulen, P. Sthapitanonda, J. L. Margrave, J. Phys. Chem., 59, 132 (1955).
6. J. R. Soulen, J. L. Margrave, J. Am. Chem. Soc., 78, 2911 (1956).
7. A. A. Mal'tsev, V. G. Vinokurov, V. M. Tatevskii, Fiz. sborn. L'vovsk. univ., No. 3 (8), 480 (1957).
8. V. I. Dianov-Klovov, Zav. Lab. 21, 361 (1955).
9. M. N. Markov, Zh. T. F., 24, 1867 (1954).
10. P. Bradt, National Bureau of Standards Report, 3016, January 1954.
11. M. G. Inghram, R. F. Porter, W. A. Chupka, J. Chem. Phys., 25, 498 (1956).
12. V. M. Tatevskii and others, "Scientific report for the second quarter of 1958 of the laboratory for molecular spectroscopy," No. 210, Khimfak, MGU, 1958 [in Russian].
13. V. K. Matveev, A. A. Mal'tsev, V. M. Tatevskii, Vestn. Moskovsk. Univ., No. 1, (1961).
14. D. White, P. N. Walsh, D. E. Mann, J. Chem. Phys., 28, 508 (1958).
15. W. E. Kaskan, R. C. Millikan, J. Chem. Phys., 32, 1273 (1960).

All abbreviations of periodicals in the above bibliography are letter-by-letter transliterations of the abbreviations as given in the original Russian journal. *Some or all of this periodical literature may well be available in English translation.* A complete list of the cover-to-cover English translations appears at the back of this issue.

1
2
3
4
5
6
7
8
9
10
11
12
13
14
15
16
17
18
19
20
21
22
23
24
25
26
27
28
29
30
31
32
33
34
35
36
37
38
39
40
41
42
43
44
45
46
47
48
49
50
51
52
53
54
55
56
57
58
59
60
61
62
63
64
65
66
67
68
69
70
71
72
73
74
75
76
77
78
79
80
81
82
83
84
85
86
87
88
89
90
91
92
93
94
95
96
97
98
99
100

THE RELATION BETWEEN THE AMOUNT OF H_2O_2 EVOLVED
AND THE NUMBER OF OXIDE MOLECULES FORMED
IN THE ATMOSPHERIC CORROSION OF Mg AND Al

I. L. Roikh and I. P. Bolotich

I. V. Stalin Odessa Technological Institute

(Presented by Academician A. N. Frumkin, September 5, 1960)

Translated from Doklady Akad. Nauk SSSR, Vol. 2, No. 1,

pp. 126-129, March, 1961

Original article submitted September 5, 1960

The photographic method of studying atmospheric corrosion is based on the ability of the hydrogen peroxide formed in oxidation to produce a latent photographic image. The sensitivity of the photographic emulsion to the action of H_2O_2 vapors has been increased to the extent that it is now possible to study the corrosion in its very early stages, some fractions of a second after oxidation has been initiated [1]. In this respect the photographic method is not only simple, but superior to all other known procedures. Validation of the method requires proof that the H_2O_2 formed in the oxidation of metals is one of the principal links in the corrosion process [2]. Such proof can be obtained by showing agreements between the results of a photographic study of the kinetics of atmospheric corrosion and a study by some other method whose validity has been checked both theoretically and experimentally. A basis for such comparison is found in the Drude [3] optical polarization method of studying thin films, which has been refined and widely applied by Tronstad and Winterbottom [4] in their work on metallic corrosion. This method involves a study of the parameters of elliptically polarized light (Δ and ψ) which is reflected from the metallic surface. These parameters are functions of the optical properties of the metal and the thickness of the oxide film carried on its surface and they therefore alter as oxidation progresses. Their relation to the depth and index of refraction of the oxide film is covered by the equations:

$$L = \frac{\Delta - \bar{\Delta}}{A \left(1 - \frac{1}{n_1^2} \right)}; \quad n_1^2 = \frac{1 + \frac{2\psi - 2\bar{\psi}}{\Delta - \bar{\Delta}} \cdot \frac{\cos^2 \varphi - a}{a' \sin 2\psi}}{\cos^2 \varphi}, \quad (1)$$

where

$$A = -\frac{4\pi}{\lambda} \frac{\cos \varphi \sin^2 \varphi (\cos^2 \varphi - a)}{(\cos^2 \varphi - a)^2 + a'^2}; \quad a = \frac{1 - \kappa^2}{n^2 (1 + \kappa^2)^2}, \quad a' = \frac{2\kappa}{n^2 (1 + \kappa^2)^2},$$

and L is the film depth, n_1 is its refractive index, λ is the wave length of the incident monochromatic light, n is the refractive index of the metal, κ is the absorption coefficient of this metal, φ is the angle of incidence of the beam onto the metallic surface, ψ is the angle of inclination of the plane of vibration of the incident plane polarized light to the plane of incidence, the factor which fixes the relative alternation of the amplitudes of the component of the reflected light in, and perpendicular to, the plane of incidence.

The amplitude and phase of these components is altered as a result of reflection. The phases of the components after reflection will be designated by $\delta_{||}$ and δ_{\perp} , so that $\delta_{||} - \delta_{\perp} = \Delta$. The bars over $\bar{\Delta}$ and $\bar{\psi}$ will indicate parameters referring to the clean metallic surface, while similar quantities without the bar designate parameters measured in the presence of an oxide film. The optical constants of the metal are related to Δ and ψ through the following approximation equations:

$$n = \frac{\sin \varphi \operatorname{tg} \varphi \cos 2\bar{\psi}}{1 - \cos \Delta \sin 2\bar{\psi}}, \quad \kappa = \sin \bar{\Delta} \operatorname{tg} 2\bar{\psi}. \quad (2)$$

The experimental technique must be such that the conditions of reflection are uniform over the entire area of impingement of the ray, and the plane and angle of incidence are well defined. This condition was assured by subjecting the Mg and Al to a fine polishing with GOI paste. The height of the non-uniformities in the profile of the metallic surface fell within the limits assigned to Classes 10 and 11 ($N_{sk} = 0.14-0.1 \mu$). The prepared specimen was then set on the table of a polarizing goniometer which had been constructed in this laboratory* and initial values of $\bar{\Delta}$ and $2\bar{\psi}$ determined for the clean metallic surface. Equation (2) was then used to obtain the constants κ and n of the metal from these measured values. Measurements of Δ and 2ψ were then carried out as the oxide film formed on the metallic surface. These values substituted into Equation (1) permitted evaluation of L and n_1 for the oxide film carried by the metal at various stages of oxidation. An accuracy of 2-3 Å in the measured values of L was assured by the use of a SVD-120A lamp with a luminosity of 5000 stilbs, by careful adaptation of the eye (15 minutes), and by taking pains to assure that the specimen remained fixed in its position on the table during the entire study of the kinetics (5 hours). The following values were obtained for n , κ , and n_1 : at $\lambda = 5890 \text{ Å}$ and $\varphi = 60^\circ$; for Al, $n = 2.37$, $\kappa = 1.53$, and $n_1 = 1.51$; for Mg, $n = 0.484$, $\kappa = 6.93$, and $n_1 = 1.7$. These results were used in constructing the kinetic curves for oxide formation on Mg and Al which are shown in Fig. 1.

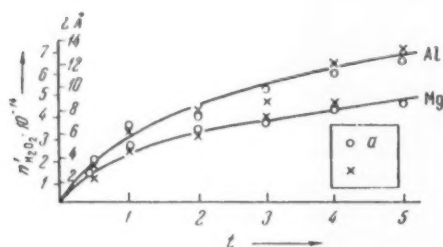


Fig. 1. Kinetic curves for the oxidation of Mg and Al obtained by the photographic and by the optical methods: a) Optical method; b) photographic method.

These studies were carried out at $20 \pm 1^\circ$ and a relative humidity, r , of $63 \pm 5\%$. Each point on the graph represents a mean of ten measurements in the case of Al, and eight, in the case of Mg.

It must be remembered that no one of the metallic surfaces was entirely free of oxide film at the beginning of observation [5]. Moreover, optical studies [6] have shown that an adsorbed gaseous film is formed on all metals which are undergoing oxidation, reaching a depth of 9 Å in the case of Al. On the basis of these data the values of $\bar{\Delta}$ and $2\bar{\psi}$ for Al must be altered by $1-1.5^\circ$ and $10-12'$, respectively, because of the total depth of initial film. Variations of this order in the values originally accepted for the clean metal are of no consequence for calculations of n and κ from Equation (2); they would introduce an error of around 2-3% in the calculated value of L .

Thus the graph showing increase in depth of oxide film on Mg and Al can be considered as entirely acceptable. The depth, L , of oxide film on Al at the end of 24 hours was 17-20 Å. The rate of further growth of the oxide film was considerably lower, L increasing by less than 4 Å in the next 24 hours. On Mg the increase in depth of oxide film after 2-3 days was: $L_{24h} \sim 15 \text{ Å}$; $L_{48h} \sim 22 \text{ Å}$.

The curves of Fig. 1 giving the increase in L over the experimental time interval of five hours are covered by the equations: Al, $L^2 = 31 t$; Mg, $L^{2.66} = 63 t$. The kinetics of oxidation of Mg and Al were also investigated by the photographic method, working at the same temperature and humidity as before and preparing the specimens in the same manner.

* We take the opportunity to express our thanks to V. A. Marchenko who constructed the mechanical portion of this goniometer with great care.

The test metals had the following chemical compositions (contaminants expressed in percentages):

	Fe	Si	Mg	Cu
Mg	0,004	0,009	0,0021	—
Al	0,0016	0,0016	—	0,001

Carefully polished specimens of Mg and Al were placed on a photographic plate and allowed to remain in contact with it for 0.5, 1, 2, 3, 4, and 5 hours. The optical density, D , of the darkening of the emulsion resulting from the action of the H_2O_2 liberated in oxidation was determined photometrically (Fig. 2). The absolute number of evolved H_2O_2 molecules was then calculated from the optical density of darkening, using mean values from six experiments. For these calculations it was necessary to:

1. Establish a relation between the density of darkening, D , and the concentration of the H_2O_2 solution responsible for the darkening.

2. Determine the amount, v , of H_2O_2 solution which evaporated under the experimental conditions. A photoplate was set 2 mm above the surface of the vaporizing solution, emulsion downward, at $20 \pm 1^\circ$ and with $r = 63 \pm 5\%$, and held there for 1 minute. The resulting value of v , namely $0.218 \text{ mg}/(\text{cm}^2 \cdot \text{min})$, was constant for H_2O_2 solutions whose concentrations fell in the working interval which ranged from 0.05 to 2%.

3. Determine the mole fraction, y_h , of H_2O_2 in the vapors above a hydrogen peroxide solution of known concentration. This could be done through the equation of Skatchard, et al. [7]. The number of H_2O_2 molecules responsible for the observed darkening, n' , could be obtained from v and y_h since the number of H_2O_2 molecules evolved and the number falling on the photoemulsion are related linearly [1] by:

$$n'_{H_2O_2} = v y_h N / M_h \quad (3)$$

N being the Avogadro Number, and M_h , the molecular weight of the H_2O_2 solution. But the photographic plate was set 2 mm above the solution surface and $n'_{H_2O_2}$ diminishes exponentially with height [8] so that

$$n'_{H_2O_2} = n^0_{H_2O_2} e^{-0.417 \cdot z} \quad (4)$$

would give the number of H_2O_2 molecules which, if evolved from 1 cm^2 of solution surface, would give rise to the darkening observed on 1 cm^2 of apparent surface of the photographic plate if the latter were in direct contact with the solution. The calibration curve, $D = D(n')$, of Fig. 2 was constructed from $n'_{H_2O_2}$ values obtained in this manner. This curve served as a basis for passing to the kinetics of H_2O_2 evolution in the oxidation of Mg and Al (Fig. 1).

The concordance between the kinetic curves for the oxidation of Mg and Al obtained by the photographic and the optical methods points to the existence of a linear relation between the number of H_2O_2 molecules evolved and the depth of the oxide film. From this it can be concluded that the elementary act of formation of an oxide molecule is accompanied by the production of a strictly defined number of H_2O_2 molecules. As a result, the evolution of H_2O_2 during oxidation can serve as a basis for the study of the corrosion processes of a metal.

The relation between the number of H_2O_2 molecules evolved and the number of molecules of MgO and Al_2O_3 oxides formed was elucidated in further work. A knowledge of the true surface of the oxidizing specimen was necessary for this calculation. Special studies were carried out on a profileograph (a profile meter of the

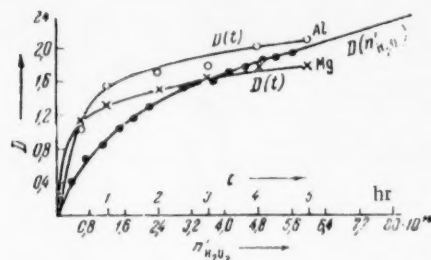
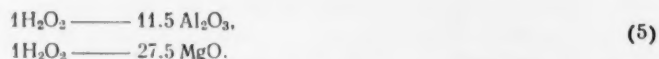


Fig. 2. Curves showing the relation between the optical density, D , the time of exposure of Mg and Al on the photographic plate, and the number of H_2O_2 molecules falling on the photoemulsion.

"Calibr - VE1" type, whose vertical magnification could be varied from 2000 to 120000 in development of the surface profile and whose horizontal magnification could be altered from 117 to 4200) in order to determine the effect of the class of polishing on the true surface of the metal. The length of the profile curve for the metal surface was determined for various treatments, allowance being made for the vertical and horizontal magnification chosen for each type of polishing. The extent by which the true surface exceeded the geometrical surface was estimated by comparing the length of the profile curve with the length of the corresponding straight line. It was thus established that a non-uniformity in the surface profile falling within the limits $0.01-2 \mu$ would increase the geometrical surface by no more than 3%. Erbacher has measured the number of ions adsorbed on metals [9] and concluded on this basis that the true metallic surface is 2.5 times greater than the geometrical surface, regardless of the type of polishing. A comparison of our own data with those of Erbacher shows the difference between the geometrical and true surfaces of a metal to result from the presence of non-uniformities which lie beyond the limits of the highest type of treatment of the metal. A coefficient of roughness of 2.5 led to the following relations between the number of H_2O_2 molecules evolved in oxidation and the corresponding number of molecules of the oxide:



We will give an illustration of the calculations leading to (5). A two-hour exposure of a photoplate to Mg gave a darkening, D, of 1.51. To this value of D there corresponds a $n'H_2O_2$ value of $3.15 \cdot 10^{14}$, the number of molecules evolved from 1 cm^2 apparent metal surface [Equations (3) and (4) and Figure 2]. This 1 cm^2 of surface of the photoplate corresponds to $2.5 \cdot 1 \text{ cm}^2$ of true metallic surface if the coefficient of roughness is assumed to be 2.5. The number of oxide molecules, $n'MgO$, which are contained in volume V of the oxide formed on such a Mg surface in two hours is:

$$n'MgO = \frac{(2.5 \cdot 1) \text{ cm}^2 \cdot L \cdot 10^{-8} \text{ cm} \cdot 1 \cdot \text{g/cm}^3 \cdot N \text{ 1/mole}}{M_{MgO} \text{ g/mole}} = 85.3 \cdot 10^{14}.$$

Thus in the case of Mg, the number of evolved molecules, $n'H_2O_2$, is $3.14 \cdot 10^{14}$ and the corresponding value of $n'MgO$, $85.3 \cdot 10^{14}$, or $1 H_2O_2 - 27.2 MgO$. Relations (5) result from carrying through similar calculations for all of the experimental values of D and L, and then averaging. In [2] it was shown that formation of one oxide molecule is accompanied by the appearance of one molecule of H_2O_2 . This result combined with (5) would lead to the conclusion that a very considerable part of the hydrogen peroxide must decompose on the metallic surface.

LITERATURE CITED

1. I. L. Roikh, *Fiz. Khim.*, **31**, 1959 (1957).
2. T. M. Abramova, I. L. Gankina, and A. S. Fomenko, *Doklady Akad. Nauk SSSR*, **129**, 4 (1959).
3. P. Drude, *Wied. Ann.*, **36**, 532, 865 (1889); **39**, (1890).
4. L. Tronstad, *Trans. Farad. Soc.*, **31**, 1151 (1935); B. Winterbottom, *Det. kgl. Norske Videnskabers selskabs skrifter*, No. 1 (1955).
5. N. A. Shishakova, V. V. Andreeva, and N. K. Andrushchenko, *The Structure and Mechanism of Formation of Oxide Films on Metals* [in Russian] (Acad. Sci. USSR Press, 1959).
6. V. V. Andreeva, *Trans. Institute of Physical Chemistry of the Acad. Sci. USSR*, **6**, 79 (1957); L. Vlasakova, *Werkstoffe und Korrosion* No. 8/9, 536 (1958).
7. G. Skatchard, G. Kavanagh, and L. Ticknor, *J. Am. Chem. Soc.*, **74**, 3715 (1952); Schumb, Satterfield, and Wentworth, *Hydrogen Peroxide* [Russian translation] (Foreign Literature Press, 1958).
8. I. L. Roikh and I. P. Bolotich, *Doklady Akad. Nauk SSSR*, **120**, 116 (1958).
9. O. Erbacher, *Zs. Phys. Chem.*, **A**, **163**, 196 (1933).

THEORETICAL TREATMENT OF THE $I(t)$ CURVES
FOR THE REDUCTION OF ANIONS ON A DROPPING
MERCURY ELECTRODE IN THE PRESENCE OF ADSORBED
CATALYSTS

A. Ya. Gokhshtein

Institute of Electrochemistry, Academy of Sciences USSR
(Presented by Academician A. N. Frumkin, December 1, 1960)
Translated from Doklady Akad. Nauk SSSR, Vol. 137, No. 2,
pp. 345-348, March, 1961
Original article submitted January 29, 1960

Weber, Koutecky, Koryta, and Kuta have arrived at some interesting results in their theoretical study of polarographic currents in the presence of surface-active agents the adsorption of which was diffusion-controlled. The authors have thoroughly examined the cases where the reaction rate is linearly dependent on surface coverage [1], and neglecting the concentration polarization effects they were also able to obtain the initial portion of the $I(t)$ curve for the exponential dependence case [2].

The present work was stimulated by the work of A. N. Frumkin, O. A. Petriya, and N. V. Nikolaeva-Fedorovich [3] who detected definite maxima on the $I(t)$ curves when they reduced polyvalent anions in the presence of adsorbed cations. In the present work an attempt was made to take into account concentration polarization and to derive a relationship between characteristic points on the $I(t)$ -curve (over its entire length) and the parameters which determine the discharge kinetics of ions.

The current I , which we are trying to determine as a function of t , results from an irreversible reaction taking place at a constant potential φ on the surface of an expanding spherical electrode. The spherical volume increases at the rate of m/γ where m is the flow rate of mercury (in g/sec) and γ is the specific gravity of mercury (in g/cm³). The initial anion and catalyst concentrations are C and C_0 while the respective diffusion coefficients are D and D_0 . When a supporting electrolyte is added and the thickness of the diffusion layer is small in comparison with the electrode radius, the equation for the diffusion current assumes the form [4]:

$$\partial C / \partial t - (2x/3t) \partial C / \partial x = D \partial^2 C / \partial x^2; \quad (1)$$

where $C(x, t)$ is the cation concentration at a distance x from the electrode surface. The boundary condition can be derived from Frumkin's equation [5].

$$\frac{I}{nFS} = D \frac{\partial C(0, t)}{\partial x} = C(0, t) k \exp \left(\frac{(n + \alpha) F \psi_1}{RT} \right) \exp \left[- \frac{\alpha F \varphi}{RT} \right], \quad (2)$$

where α is the barrier coefficient, n is the number of electrons, and k is the specific reaction rate. The surface density of the adsorbed compound can be determined from the Ilkovic Equation [1],

$$Q(t) = 2(3/7\pi)^{1/2} D_0^{1/2} C_0 t^{1/2} \quad (\text{moles/cm}^2). \quad (3)$$

We will use ψ_{10} to denote the ψ_1 potential in the absence of the catalyst, and assume that

$$\psi_1(t) = \psi_{10} + \sigma Q(t), \quad (4)$$

where the coefficient σ is determined by the reaction kinetics.

Equations (2), (3), and (4) yield the expression

$$D \frac{\partial C}{\partial x}(0, t) = C(0, t) k \exp \left\{ \frac{F}{RT} [(n + \alpha) \psi_{10} - \alpha \varphi] \right\} \exp \left[2 \left(\frac{3}{7\pi} \right)^{1/2} \frac{F}{RT} \sigma (n + \alpha) D_0^{1/2} C_0 t^{1/2} \right]. \quad (5)$$

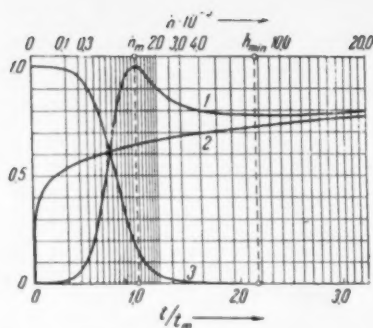


Fig. 1. 1) Theoretical $I(t)$ curve; 2) limiting current with I_{\max} as unity; 3) $C(0, t)/C_p = 10^6$.

If we change the variables as shown below

$$y = t^{1/2}x, \quad h = st^{1/2}, \quad s = \left[2 \left(\frac{3}{7\pi} \right)^{1/2} \frac{F}{RT} \sigma(n+\alpha) D_0^{1/2} C_0 \right]^{2/3} \quad (6)$$

then Equations (1) and (5) assume the form

$$\frac{\partial C}{\partial h} = \frac{3D}{7s} \frac{\partial^2 C}{\partial y^2}, \quad \frac{\partial C}{\partial y} = s^{1/2} \frac{k}{D} \quad (7)$$

$$\exp \left\{ \frac{F}{RT} [(n+\alpha)\psi_{10} - \alpha\varphi] \right\} h^{-1/2} e^{h^{3/2}} C(0, h).$$

The first of the two equations reduces to

$$C(0, h) = C - \left(\frac{3D}{7\pi s} \right)^{1/2} \int_0^h \frac{[\partial C(0, \xi)/\partial y] d\xi}{\sqrt{h-\xi}} \quad (8)$$

when $C(y, 0) = C$.

Eliminating $C(0, h)$ from Equations (7) and (8) we introduce a new function,

$$f(h) = \frac{1}{C} \left(\frac{3D}{7\pi s} \right)^{1/2} \frac{\partial C(0, h)}{\partial y} \quad (9)$$

and replacing the constants by the simpler terms given in Eq. (6) we get for $f(h)$ the integral equation

$$f(h) = \frac{1}{p} h^{-1/2} e^{h^{3/2}} \left[1 - \int_0^h \frac{f(\xi) d\xi}{\sqrt{h-\xi}} \right], \quad (10)$$

which contains the parameter

$$p = \frac{2F}{RT} \frac{\sigma(n+\alpha) D_0^{1/2} D^{1/2} C_0}{k \exp \frac{F}{RT} [(n+\alpha)\psi_{10} - \alpha\varphi]}; \quad (11)$$

f , h , and p are all dimensionless. Equation (11) can be conveniently split up as shown below:

$$p = \frac{vC_0}{\omega}, \quad v = \sigma(n+\alpha) D_0^{1/2}, \quad \omega = \frac{RT}{2F} D^{-1/2} k \exp \frac{F}{RT} [(n+\alpha)\psi_{10} - \alpha\varphi]. \quad (12)$$

A set of experiments is then carried out where p is varied by changing the catalytic concentration C_0 while

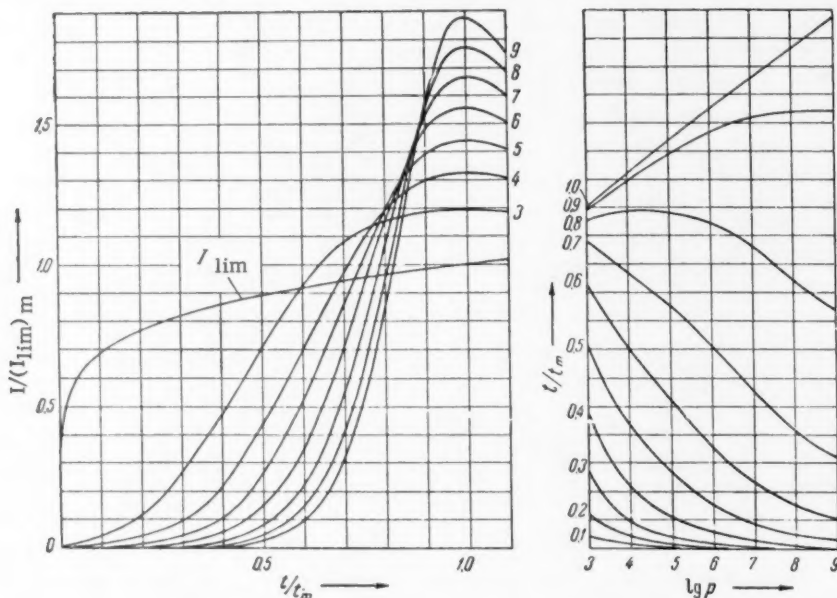


Fig. 2. The $I(t)$ curves at $p = 10^3, 10^4, 10^5, 10^6, 10^7, 10^8$, and 10^9 , and the limiting current. The right hand graph is an interpolation nomogram.

ν and ω are maintained constant. When the integral contained in the brackets of Equation (10) is evaluated we find that for $h > 10^3$ and $p > 10^4$ (these values do not constitute the limits in practical calculations) the singular point of the $f(h)$ function at $h=0$ can be neglected without introducing any errors in the fourth power.

Numerical solutions of Equation (10) at various p were obtained by a method described before [6]. After determining the function $f(h)$ from Eq. (10) and restoring our original variables and coefficients we can get the equation

$$I = nFDS(t) \partial C(0, t) / \partial x = 6.458 F (F/RT)^{1/2} (m/\gamma)^{1/2} nCD^{1/2} (\nu C_0)^{1/2} ft^{1/2} \quad (13)$$

for the current flow from the entire electrode surface $S(t)$ at time t . Using the relationship connecting t and h (see Eq. (6)) we can express the function f in terms of either set of variables, $f(h) = f(st^{2/3})$. The current is proportional to $ft^{4/3}$ and consequently to $fh^{4/3}$. It follows therefore that I and f attain their maxima at different values of h . The value of f and h at which the current attains its maximum (I_{\max}) will be denoted by f_m and h_m . These can be determined by simply multiplying the evaluated $f(h)$ function by $h^{4/3}$. The resulting maximum will yield h_m since $f_m = f(h_m)$. Using the relationships derived earlier for the descending portions of polarograms [7] we can prove that $f(h)$ can be expressed by the equation

$$f(h) = 0.318 (h - h_a)^{-1/2} \quad (14)$$

at a certain distance from the maximum. In this equation only h_a depends on p ; when $p = 10^6$, $h_a = 0.972 \cdot 10^5$. Equation 14 indicates that the curve of $I-t$ should have a minimum (I_{\min}) right after the maximum. The corresponding h_{\min} can be determined from the condition for a minimum of the function $fh^{4/3}$. From Equation (14) we get

$$h_{\min} = 8h_a, \quad f_{\min} = 0.318 (7h_a)^{-1/2} \quad (15)$$

Using Equation (14) we can extend $f(h)$ beyond the point where $h \approx 3h_a$. After determining $f(h)$ and $f(h)h^{4/3}$ we determine $f(st^{2/3})t^{4/3}$ (Fig. 1), which when substituted in Eq. (13) yields the current as a function of time. Figure 1 also shows how the concentration in the vicinity of the electrode changes with time. Multiplying the right side of Eq. (13) by $h^{1/2}st^{1/6} = 1$ [cf. (6)] we get another expression for $I(t)$:

$$I = 13.093 F (m/\gamma)^{1/2} nCD^{1/2} h^{1/2} ft^{1/2} = 2.30 F m^{1/2} nCD^{1/2} h^{1/2} ft^{1/2} \quad (16)$$

It follows from Eq. (14) that as h increases $h(h^{1/2}f) \rightarrow 0.318$. Substituting this limit into Eq. (16) we get the well-known Ilkovic equation as a special case. Thus for large h , $I/I_{\lim} = \sqrt{h/(h-h_a)}$,

while for $h \gg h_a$ the curve of $I-t$ approaches the limiting current curve. In Fig. 2 we have plotted some nomograms which can be used to construct the curve of $I-t$ at any p within the range $10^3 \leq p \leq 10^9$.

We will now derive expressions for the maximum on the $I(t)$ curve. The corresponding values of $f_m, h_m, C(0, t_m)/C$, were calculated from Eq. (10) at various p and are given in Fig. 3. The selected range of values $10^3 \leq p \leq 10^9$ includes most of the p values encountered in practice. It is noteworthy that $h_m^{1/2}f_m$ is almost linearly dependent on $\lg p$.

$$h_m^{1/2}f_m = 0.290 + 0.0341 \lg p, \quad 10^3 < p < 10^9. \quad (17)$$

Substituting expression (17) into the Equation (16) we get the principal equation for the current at the maximum of the $I(t)$ curve.

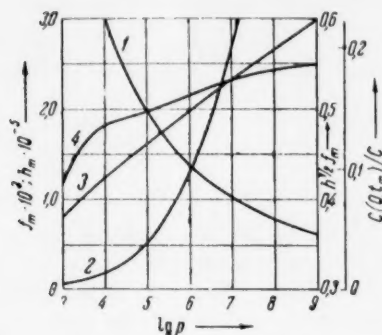


Fig. 3. f_m (1), h_m (2), $h_m^{1/2} f_m$ (3) $C(0, t_m)/C$ (4), all as a function of p

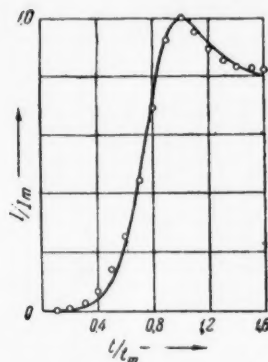


Fig. 4. Experimental points and the calculated curve for $p = 10^6$, in relative units.

$$I_{\max} = (0.666 + 0.0782 \lg p) F m^{1/2} n c D^{1/2} t_m^{1/2}. \quad (18)$$

Dividing Equation (18) by the limiting current at time t_m we get a very convenient equation:
 $I_{\max}/I_{\lim} = 0.91 + 0.107 \lg p$, (19).

Using Eq. (19) we can determine p without having to determine first a large number of experimental parameters. The limiting current can be either determined experimentally or (even more precisely) by extrapolating the $I(t)$ curve well beyond the maximum. When $p = 10^6$, $I_{\max}/I_{\lim} = 1.55$ (Fig. 1). Using Eq. (6) we can determine the time required to attain the maximum:

$$t_m = \frac{7\pi}{12} \left(\frac{RT}{F} \right)^2 \frac{h_m^{1/2}}{v^2 C_0^2}, \quad t_{m, (20^\circ)} = 1.169 \cdot 10^{-3} \frac{h_m^{1/2}}{v^2 C_0^2}, \quad t_{m, (25^\circ)} = 1.209 \cdot 10^{-3} \frac{h_m^{1/2}}{v^2 C_0^2}. \quad (20)$$

The exact values of h_m are given in Fig. 3; for $10^4 < p < 10^9$ the approximate equation $h_m^{3/7} = 4 (\lg p)^{2.04} \approx 4 \lg^2 p$ holds well. For two $I(t)$ curves at different catalyst concentrations (C_{01} and C_{02}) Eq. (20) yields

$$t_{m1}/t_{m2} = (C_{02}/C_{01})^2 (h_{m1}/h_{m2})^{1/2}. \quad (21)$$

When $(C_{02}/C_{01}) < 2$, $(h_{m1}/h_{m2})^{3/7}$ is close to 1 and $(t_{m1}/t_{m2}) \approx (C_{02}/C_{01})^2$, i.e. t_m is very sensitive to any change in C_0 , which fact may be used for analytical purposes. In contrast Equation (19) is not very sensitive to changes in $\lg C_0$. We can determine ν and ω from experimental data by determining p from Eq. (19) and using Equations (20) and (12). Since the experimentally determined limiting current may be off by 10%, the value of p obtained from Eq. (19) should normally be verified and corrected if necessary with the help of the ascending portion of the nomogram in Fig. 2. For the shift in ψ_1 at the maximum we get $\Delta \psi_{1m} = [RT/(n + \alpha)F] h_m^{3/14} \approx 2 \cdot [RT/(n + \alpha)F] \lg p$. Substituting $C(0, t_m)/C$ (Fig. 3) into Eq. (2) we get a simple relationship between the maximum current and the rate constant.

In Fig. 4 we have compared the experimental results obtained [3] in a solution of $5 \cdot 10^{-4}$ M $K_2S_2O_8 + 2.5 \cdot 10^{-3}$ M $Na_2SO_4 + 3 \cdot 10^{-5}$ M $(C_4H_9)_4N$ at 20° with a theoretical curve calculated for $p = 10^6$. Equations (20) and (12) yield for this case ($C_0 = 3 \cdot 10^{-8}$ moles/cm³): $\nu = 0.75 \cdot 10^7$ cm/mole \cdot sec^{1/2}, $\omega = 2.25 \cdot 10^{-7}$ sec^{1/2}, $\sigma = 1.44 \cdot 10^9$ cm² \cdot v/mole, and $\Delta \psi_{1m} = 0.14v$.

The author wishes to express his gratitude to Academician A. N. Frumkin, who directed this work.

LITERATURE CITED

1. J. Weber, J. Koutecky, J. Koryta, Zs. Elektrochem., **63**, 583 (1959).
2. I. Kuta, J. Weber, J. Koutecky, Coll. Czechoslov. Chem. Comm., **25**, 2376 (1960).
3. A. N. Frumkin, O. A. Petrii, and N. V. Nikolaeva-Fedorovich, Doklady Akad. Nauk SSSR, **135**, No. 5 (1960).
4. V. G. Levich, Physicochemical Hydrodynamics [in Russian] (Moscow, 1959), p. 538.
5. A. N. Frumkin, V. S. Bagotskii, Z. A. Iofa, and B. N. Kabanov, The Kinetics of Electrode Processes [in Russian] (Moscow, 1952), p. 209.
6. Ya. P. Gokhshtein and A. Ya. Gokhshtein, Doklady Akad. Nauk SSSR, **128**, 985 (1959).
7. Ya. P. Gokhshtein and A. Ya. Gokhshtein, Zhur. Fiz. Khim, **34**, 1654 (1960).

All abbreviations of periodicals in the above bibliography are letter-by-letter transliterations of the abbreviations as given in the original Russian journal. Some or all of this periodical literature may well be available in English translation. A complete list of the cover-to-cover English translations appears at the back of this issue.

THE NATURE OF THE INDUCTION PERIOD IN THE AUTOXIDATION OF FATS AND FATTY ACIDS

N. S. Drozdov

N. I. Pirogov Moscow State Medical Institute

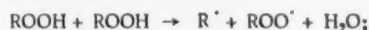
(Presented by Academician B. A. Kazanskii, September 27, 1960)

Translated from Doklady Akad. Nauk SSSR, Vol. 137, No. 2,

pp 349-351, March, 1961

Original article submitted September 26, 1960.

It is known that the initial reaction in the autoxidation of fats and fatty acids is addition of molecular oxygen to the compound being oxidized with formation of peroxides (hydroperoxides), which serve as initiators for the further autocatalytic chain mechanism of the whole autoxidation process:



Indeed in many cases of autoxidation of natural fats and fatty acids, a very small increase of the rate is observed at the beginning of the process. The interval between the initial contact of the substance being oxidized with oxygen and the moment when a satisfactorily high rate of the oxidation process is reached, is designated the induction period, since this term is generally associated with the introduction of the initial reactions of formation of peroxides, which on attaining a certain concentration, autocatalytically accelerate the further oxidation process. Such a view of the nature of the induction period is wide-spread and is accepted by many investigators.

A number of authors, however, failed to detect an induction period during oxidation of chemically pure substances [1]. In an experimental study of the absorption of oxygen by well-purified and freshly distilled oleic acid at 20-60 deg we also did not observe an induction period [2]. This agrees with the results of Hamilton and Olcott [3], who found that an induction period did not occur during oxidation of pure methyl oleate.

Independent investigators consider [1] that, particularly in the case of oxidation of fatty substances, the appearance of an induction period can be explained by the presence of natural inhibitor impurities (HA), readily oxidizable substances which terminate the autoxidation chain process:



or



since A^{\cdot} cannot maintain the autoxidation chain reaction.

In our investigation it was established that autoxidation of unsaturated fatty acids and fats, which did not contain natural inhibitors of the oxidation, took place at 40-60 deg, without an induction period. During this, even in the very first stages of the process, besides formation of peroxides, a rapid accumulation of hydroxyepoxy-compounds were observed. One of our experiments on the autoxidation at 40 deg of pure oleic acid, giving no Kreis [4] reaction, (the results of which are presented in Fig. 1), may serve as an example. In this experiment during the autoxidation process determinations were made of the total oxygen absorption [2], peroxides (according to

Wheeler), epoxide oxygen [5] and oxygen of hydroxy groups [6]. The results of the determinations are given in Fig. 1 as milligrams of oxygen per gram of oleic acid.

As seen from Fig. 1, the absorption of molecular oxygen (curve 1), the accumulation of epoxide oxygen (curve 2) and of the oxygen of OH-groups (curve 3) in the autoxidation products proceeded without any induction period. If judged by the accumulation of peroxide oxygen (curve 4), then the existence of such an induction period might be assumed.

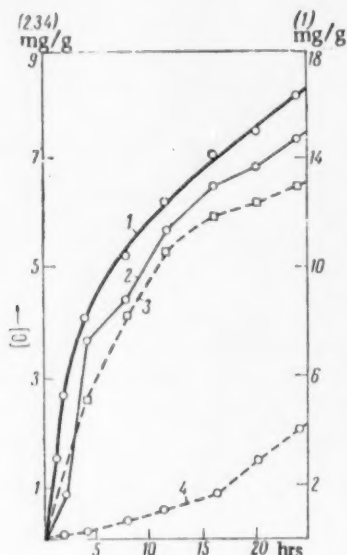


Fig. 1

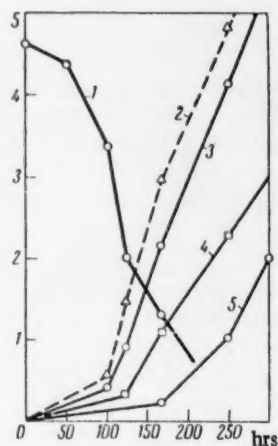
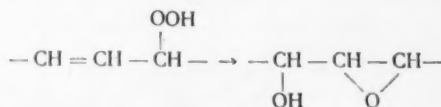


Fig. 2

This is explained by the fact that in the initial stages of the autoxidation process, as seen in Fig. 1, concurrently with the formation of peroxides, their rapid conversion into hydroxyepoxy compounds takes place



which also accumulate in the autoxidation products. Due to such conversion the peroxide content in the autoxidation products during the initial stage of the oxidation remains relatively low, while the oxygen of the peroxides amounts to only an insignificant part of the absorbed oxygen. The main part of the oxygen is present in the autoxidation products, during the primary phase, as a hydroxyepoxy compound. Hence, it is not possible to estimate the extent and the rate of oxidation by the quantity of peroxide which is formed, and such a method can only result in detection of a false induction period.

During the autoxidation of fats, containing substances forming part of the unsaponifiable fraction (and including a number of natural inhibitors), almost the whole oxidation process from the very beginning is concentrated on these additional components of the fat. An experiment on the oxidation of refined milk fat, containing carotinoids may serve as an example of such a type of autoxidation.

In Fig. 2 are given experimental results of the oxidation of such a fat with an iodine value of 35.6. The experiment was conducted at 70° in air with complete exclusion of light. During the autoxidation process determinations were made of: carotinoids (photometrically), iodine value according to Rosenmund and Kuhnenn [7], peroxides (according to Wheeler), epoxide oxygen [5], and oxygen of the hydroxy groups [6]. The results of the determinations are expressed for carotinoids (curve 1) in grams of carotene per gram of fat; oxygen of OH-groups

(curve 3), of epoxy groups (curve 4) and of peroxides (curve 5) in milligrams of oxygen per gram of fat, and the decrease of the iodine values (curve 2) as a difference.

From the results of the experiment it is seen that from the start of the process and in the course of 100 hours the triglycerides of the fat had been oxidized only insignificantly compared to the carotinoids of the fat which had been subjected to energetic oxidation. Only after that as the oxidation of the carotinoids approached the final phase was a sudden increase in the rate of oxidation of the triglycerides observed. Thus, the observed "induction period" depends on the fact that initially an energetic oxidation of carotinoids occurs, which protects the triglycerides from oxidation in the early stages. Because of this, the term "induction" naturally loses its meaning since the initial inhibition of oxidation of the triglycerides in the present case has quite a different nature.

Analogous results were also obtained in experiments on autooxidation of other natural fats, containing carotinoids, for example beef fat, and also on oxidation of mixtures of triglycerides of a natural fat and carotinoids. All these results show that in a number of cases of oxidation of triglycerides of natural fats, the induction period which is observed is dependent on the oxidation of easily oxidizable substances of the unsaponifiable fraction present in the fat. Furthermore, from the data obtained in the autooxidation experiments described, it is obvious that by studies limited to observations of formation of any one autooxidation product, for example peroxides, a false induction period will be detected. Thus not only is the determination of oxygen absorption and determination of the various autooxidation products necessary, but also a study of the oxidation of all the main components of the complex system of the natural fat, including a number of substances in the unsaponifiable fractions.

LITERATURE CITED

1. K. Beili, The Inhibition of Chemical Reactions [in Russian] (Moscow, 1940).
2. N. S. Drozdov and N. P. Materanskaya, Nauchn. Dokl. Vyssh. Shkoly, 1, No. 3, 536, (1958).
3. L. Hamilton, H. Olcott, Oil and Soap, 13, 127 (1936); Ind. and Eng. Chem., 29, 217 (1937).
4. N. Drozdov and N. Materanskaya, Zhur. Anal. Khim., 7, 74 (1952).
5. N. Drozdov and N. Materanskaya, Myasnaya Industriya, No. 3, 50 (1954).
6. C. Ogg, W. Porter, Ind. and Eng. Chem., 17, 395 (1945).
7. K. W. Rosenmund, W. Kuhnenn, Zs. Unters. Nahr. u. Genussmittel, 46, 154 (1923).

All abbreviations of periodicals in the above bibliography are letter-by-letter transliterations of the abbreviations as given in the original Russian journal. *Some or all of this periodical literature may well be available in English translation.* A complete list of the cover-to-cover English translations appears at the back of this issue.

111

POLANYI'S RULE FOR PROTON TRANSITIONS AND THE HYDROGEN BOND

E. A. Pshenichnov and N. D. Sokolov

Institute of Chemical Physics Academy of Science USSR

M. V. Lomonosov Moscow State University

(Presented by Academician V. N. Kondrat'ev, October 22, 1960)

Translated from Doklady Akad. Nauk SSSR Vol. 137, No. 2,
pp. 352-355, March, 1961

The connection between the change of activation energy $\Delta \mathcal{E}$ and the change of heat of reaction Δq for a number of monotypical reacting substances, known as Polanyi's Rule,

$$\Delta \mathcal{E} = k \Delta q, \quad 0 < k < 1, \quad (1)$$

is observed for many reactions, in which the determinative stage is the transfer of a proton from one molecule to another [1]: $A-H + B \rightarrow A-H \cdots B \rightarrow A^- + H^+B$. Since the mass of the proton is considerably less than the masses of the atoms A and B, then to a first approximation it is possible to assume that during the time of transition of a proton from one potential well to another the distance between A and B in a complex with a hydrogen bond $A-H \cdots B$ does not change. Generally the movement of the proton during this transfer is considered as classical. In agreement with this, Polanyi's Rule (1) is treated as a consequence of the fact that during the transfer from one substance to another the points on the potential curve for the proton are displaced in the same direction along the energy axis so that the displacement of the peak of the potential barrier is less than the displacement of the second medium i.e. $\Delta U < \Delta Q$ (Fig. 1, see for example [2]). In a paper by one of us [3] it was shown that the proportionality between ΔU and ΔQ is easily proved, if for a number of substances under consideration the energy of the system $A-H \cdots B$ depends only on a small variable parameter. However the inequality $\Delta U > \Delta Q$ is difficult to prove theoretically in a neat fashion. More than that, as will be seen further on, the facts indicate that for proton transition processes this inequality is not fulfilled during the time that Polanyi's Rule can be shown to apply correctly.

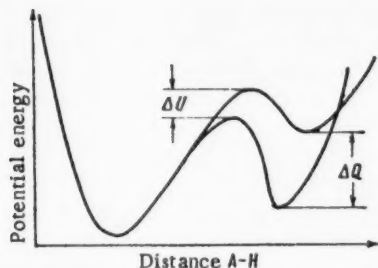


Fig. 1. Potential curves for transfers of a proton in the system $A-H \cdots B$ for two different species of B.

It is, in fact, impossible to consider classically the movement of a proton from one potential well to another. The energy of the proton in the double potential well is quantized and transition of the proton is, apparently, a multi-stage process of its gradual excitation to one of the vibration levels, situated somewhat above the barrier, and then a "drop" into the fundamental state of the right-hand well. For this, the activation energy \mathcal{E} (at absolute temperature $T = 0$) will be equal to the distance between the zero level of the left well and the intermediate level shown. The distance between the zero levels of the two potential wells corresponds to the heat of reaction q (at $T = 0$). In order to substantiate Polanyi's Rule it is necessary to study how \mathcal{E} and q change for a given

series of substances. We will assume that this series is chosen so that q is diminished by the endothermic tendency of the reaction (the basicity of substance B increases).

Calculation of the energy levels in an unsymmetrical double potential well in the general case is a problem attended by great mathematical difficulty. • Applying the Schrodinger equation for one dimension to this problem we arrived at a quasi-classical approximation, on the assumption that the proton moves in a potential field $V(Z)$, having the following form •• (see Fig. 2):

$$\begin{aligned} V(Z) &= \frac{1}{2} \mu \omega_a^2 (Z+a)^2, & -\infty < Z \leq -a; \\ V(Z) &= U^a [1 - (Z/a)^2], & -a \leq Z \leq +b; \\ V(Z) &= \frac{1}{2} \mu \omega_b^2 (Z-b)^2 + Q & +b \leq Z < +\infty \end{aligned} \quad (2)$$

$$(Q \equiv U^a [1 - (b/a)^2]).$$

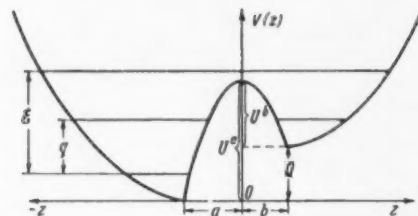


Fig. 2. Shape of the double unsymmetrical potential well (formula 2).

Here μ is the reduced mass of the proton; U^a is the height of the potential barrier, reckoned from the minimum of the deeper potential well (a); the meaning of the parameters a and b is evident from Fig. 2. Instead of the independent parameters a , b and U^a we introduce the following dimensionless values

$$U_0^a = U^a / \hbar \omega_a, \rho_0 = (a/2\hbar) \cdot \sqrt{2\mu U^a}, s = b/a. \quad \text{We also}$$

$$\text{introduce the symbols: } Q_0 = Q/\hbar \omega_a, U_0^b = (U^b/\hbar \omega_a) =$$

$$= U_0^a - Q_0, E_0 = E/\hbar \omega_a \quad (E = \text{energy}). \quad \text{The calculation is}$$

made on the assumption that the frequencies ω_a and ω_b are equal.

In order to follow the change of the relative position of the energy levels depending on the parameters ρ_0 and U_0^a , we will vary the latter simultaneously in such a way that the equality $\rho_0 = U_0^a$ is fulfilled, i.e. so that the moving together of the minima of the potential curve (decrease of a) will be accompanied by a simultaneous

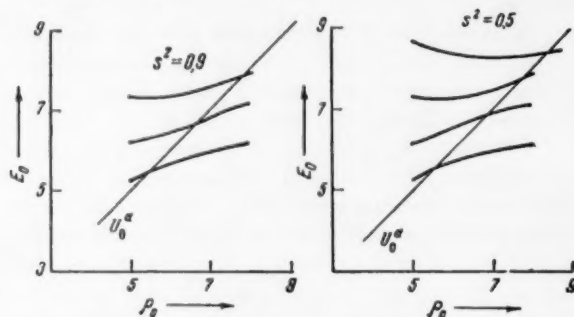


Fig. 3. Dependence of the energy levels E_0 on ρ_0 (U_0^a) for $s = \text{const}$.

lowering of the height of the potential barrier U^a . One may expect that precisely such a situation will be realized in fact, for example, for a transfer from weak bases to stronger ones. In future, for brevity, we will simply speak of the approach of the minima. Values for the energy $E_{0,n}(\rho_0, U_0^a, s)$ resulting from solution of the problem, are presented graphically in Figs. 3 and 4. Values of $E_{0,n}$, plotted along the ordinate axis are reckoned from the lower minimum (a). The values of the parameter $U_0^a = \rho_0$ are also plotted on the vertical axis. In this way the points of the energy curves lying on the graphs below (above) the straight line $U_0^a = \rho_0$ obviously correspond with such values of the parameter ρ_0 at which the calculated $E_{0,n}$ lies below (above) the peak of the barrier. In Fig. 3, for $s^2 = 0.9$ and $s^2 = 0.5$, the behavior is shown of some levels, selected from those for which the "parent" is the deeper potential well (a) [these levels relate to the well (a) with separation of the minima to infinity]. In Fig. 4 the curves $E_{0,n}$ are given for two cases: with the assumption that $U_0^b = \text{const}$ and with the assumption $Q_0 = \text{const}$. For the calculations the three parameters ρ_0 , U_0^a and s were varied simultaneously. Numbers with a prime relate to levels for which the "parent" is the potential well (b).

In conformity with the usual treatment [1-3] for the direct process $A \cdot H \dots B \rightarrow A^- \dots H^+ B$ the relationship between the height of the potential barrier U^a and the value Q is:

• Blinc and Hadzi [4] solved this problem by representing the wave function of the proton as a linear combination of the wave functions of two harmonic oscillators, each of which corresponds to the appropriate potential well.

•• In order to construct a quasi-classical function, which is accurate close to the peak of the potential barrier, we took advantage of the fact that for a barrier of parabolic form an exact solution of the wave equation is known. For a detailed account of the method of solution, see [5].

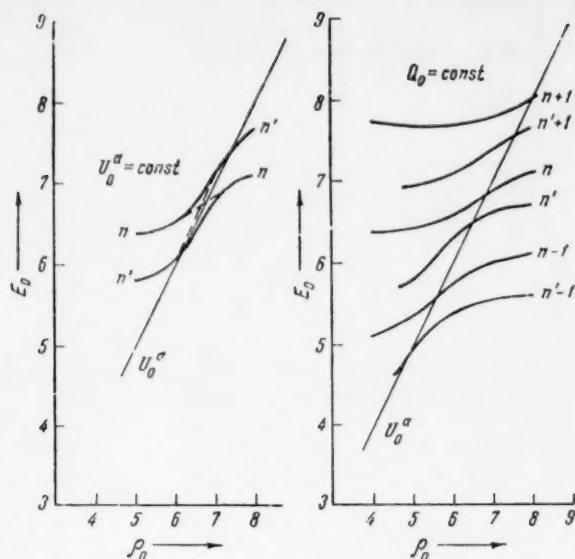


Fig. 4. Dependence of the energy levels E_0 on $\rho_0 (=U_0^a)$

ence $\Delta\nu = \nu' - \nu$ for the transfer to stronger bases is decreased. Within the framework of our model such a regularity is secured only in that case where by a decrease of ρ_0 both quantities U^b and Q are decreased, i.e. U^a decreases more rapidly than Q . Hence, according to Fig. 4 with $U_0^b = \text{const}$ with an increase of ρ_0 the diffuse level is lowered more rapidly than the non-diffuse level whereby for large values of ρ_0 (in the region of interest to us on the right of the straight line $U_0^a = \rho_0$, i.e., below the peak of the potential barrier) $\nu' > \nu$, which conflicts with the experimental data. In another limited case, when $Q_0 = \text{const}$ the sign and shift of $\Delta\nu$ for each overtone over the range of variation of ρ_0 (curves \underline{n} and \underline{n}' ; $\underline{n} - 1$ and $\underline{n}' - 1$) are obtained in qualitative agreement with these data. A more rapid fall of U^a in comparison with Q for a decrease of ρ_0 indicates that a contraction of the hydrogen bond during transfer to a stronger base has a greater effect on the height of the barrier than on the position of the minimum (b) consequently it is found that $k' > 1$ (see (3) and (4)).

Polanyi's Rule (1) can be substantiated in the following way. First of all we note that with the approach of the minima the energy levels are at first lowered, and then gradually begin to increase (Figs. 3 and 4). Low levels are controlled similarly by the higher levels but a considerable change in them starts at the smallest values of ρ_0 . As the calculations showed, a lowering of the level, immediately preceding attainment of its minimal value, takes place in that range of variation of ρ_0 (its own range of ρ_0 for each level), where the quantum effects of the above-barrier repulsion are small. Transition of a proton from one well to another occurs across such a level (we designate it by E_m). It is clear that on the average the gradient of these levels in the indicated range of variations of ρ_0 will be less than for lower diffuse levels, which attain their own minimal values for the smallest ρ_0 (see for example Fig. 4 levels \underline{n} and $\underline{n}' - 1$ in the range $4 < \rho_0 < 6$). Therefore it is possible to write $\partial E_m / \partial \rho_0 < \partial E_{l'} / \partial \rho_0$, $m > l'$, because $\delta = E_m - E_{\text{och}}$, $q = E_{l'} - E_{\text{och}}$, then $\Delta\delta = ((\partial E_m / \partial \rho_0) - (\partial E_{\text{och}} / \partial \rho_0)) \cdot \Delta\rho_0$ and $\Delta q = ((\partial E_{l'} / \partial \rho_0) - (\partial E_{\text{och}} / \partial \rho_0)) \Delta\rho_0$. Here l' is the number of the ground level of the potential well (b). From these equalities we find

$$\frac{\Delta\delta}{\Delta q} = \left(\frac{\partial E_m}{\partial \rho_0} - \frac{\partial E_{\text{och}}}{\partial \rho_0} \right) / \left(\frac{\partial E_{l'}}{\partial \rho_0} - \frac{\partial E_{\text{och}}}{\partial \rho_0} \right) = k < 1, \quad (5)$$

where k is approximately constant. If E_{fund} lies considerably below the fundamental level of the right-hand well (b), then the change in the position of the latter is small, say to the position of E_{fund} , i.e. $(\partial E_{\text{fund}} / \partial \rho_0) \approx 0$, and hence $k > 0$. With this condition, formula (5) expresses Polanyi's Rule.

$$\Delta U^a = k' \Delta Q. \quad (3)$$

In order to demonstrate Polanyi's Rule it must be assumed that $0 < k' < 1$. Since $U^a = U^b + Q$, it follows from (3) that

$$\Delta U^b = -(1 - k') \Delta Q, \quad (4)$$

i.e. with a decrease of Q the height of the barrier for the reverse process is increased. This statement does not agree however with the results from the vibration spectra of the hydrogen bond. In fact, in agreement with Barrow [6] in the spectra of a series of complexes $A \cdots H \cdots B$, with a strong enough base B , there is an additional frequency ν' which arises owing to a splitting of the levels of the two potential wells and the intensity of which is increased by transfer to stronger bases. This frequency in Fig. 4 corresponds to a transition from the fundamental level E_{fund} of the well (a) (not reproduced in the figure) to an excited diffuse level. In agreement with the experimental data ν' is found to be smaller than the "non-diffuse" frequency ν , whereby the differ-

LITERATURE CITED

1. J. Horiuti, M. Polanyi, Acta Physicochim. URSS, 2, 505 (1935); R. P. Bell, Acid-base Catalysis, Oxford, 1941.
2. R. D. Brown, Quart. Rev., 6, 63 (1952).
3. N. D. Sokolov, Doklady Akad. Nauk SSSR, 112, 710 (1957)
4. R. Blinc, D. Hadzi, Molecular Physics, 1, 391 (1958).
5. E. A. Pshenichnov and N. D. Sokolov, Optika i Spektroskopiya, 10, No. 5, (1961)
6. C. L. Bell, G. M. Barrow, J. Chem. Phys., 31, 300 (1959); 31, 1158 (1959).

All abbreviations of periodicals in the above bibliography are letter-by-letter transliterations of the abbreviations as given in the original Russian journal. *Some or all of this periodical literature may well be available in English translation.* A complete list of the cover-to-cover English translations appears at the back of this issue.

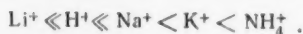
A SPECTROPHOTOMETRIC STUDY OF ZIRCONIUM CHLORIDE SOLUTIONS IN CONNECTION WITH THE ADSORPTION OF ZIRCONIUM ON FLUOROPLAST - 4

Corresponding Member, Acad. Sci. USSR I. E. Starik,
I. A. Skul'skii, and V. N. Shchebetkovskii

V. G. Khlopin Radium Institute, Academy of Science USSR
Translated from Doklady Akad. Nauk SSSR, Vol. 137, No. 2,
pp. 356-358, March, 1961

Original article submitted December 19, 1960

Earlier we showed that the distribution coefficient of zirconium-95 between a solution and the non-ionogenic surface of fluoroplast-4 was decreased by an increase in the HCl concentration and depended on the nature of the cations for first group chlorides. At constant ionic strength the adsorption of zirconium-95 increased through the series (Fig. 1):



Decrease of zirconium-95 adsorption with increase in HCl concentration was explained by the reduction in the degree of hydrolysis of zirconium and the increase in the proportion of chloride-ions in neutral complexes of the type $[\text{Zr}(\text{OH})_x \text{Cl}_{4-x}]$, which were adsorbed on the fluoroplast-4. It was assumed of course that the effect of the nature of the cations on the amount of adsorption also depended on differences in the degree of hydrolysis and complex formation of zirconium with chloride ions in the solutions of the corresponding chlorides. It was known that active HCl concentration increased through the series $\text{KCl} < \text{NaCl} < \text{LiCl}$ and therefore the degree of hydrolysis of zirconium in this direction must be reduced. In order to clarify the effect of the nature of the cations on the complex formation of Zr with Cl^- ions we employed a spectrophotometric method.

Optical Density of Zirconium Chloride Solutions in the presence of cations of the First Group (zirconium concentration $2 \cdot 10^{-2} \text{M}$)

Composition of solution	$D \cdot 10^3$ at $\lambda = 214 \text{ m}\mu$	Composition of solution	$D \cdot 10^3$ at $\lambda = 214 \text{ m}\mu$
$\mu = 2.2$		$\mu = 3.0$	
2.2N HCl	192	3.0N HCl	525
0.2N HCl + 2.0N LiCl	113	1.0N HCl + 2.0N LiCl	180
0.2N HCl + 2.0N NaCl	62	1.0N HCl + 2.0N NaCl	125
0.2N HCl + 2.0N KCl	54	1.0N HCl + 2.0N KCl	114
0.2N HCl + 2.0N NH_4Cl	44	1.0N HCl + 2.0N NH_4Cl	98

Measurements were made on a SF-4 spectrophotometer. All reagents were carefully recrystallized or distilled. Spectrally pure zirconium hydroxyl chloride was used to prepare the solutions. The data cited below relate to equilibrium solutions and are expressed as optical density or molar extinction coefficient.

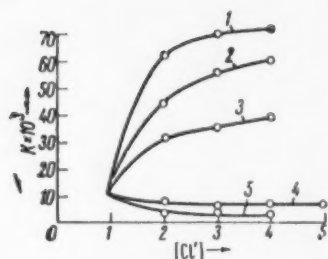


Fig. 1. Dependence of zirconium-95 adsorption of fluoroplast-4 from 1 N HCl on the concentration of first group chlorides. 1) NH_4Cl , 2) KCl , 3) NaCl , 4) HCl , 5) LiCl , $K = G/C$ where G = g-atoms Zr per 1 cm^2 , C = g-atoms Zr per 1 ml.

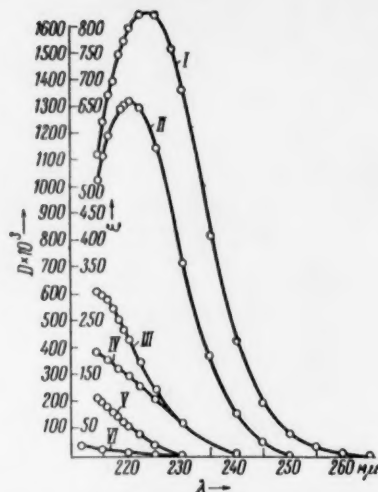


Fig. 2. Absorption spectra of zirconium solutions ($2 \cdot 10^{-3} \text{ M}$) in hydrochloric and perchloric acid. I) 9 N HCl; II) 8 N HCl; III) 6 N HCl; IV) 2 N HCl; V) 2 N HCl; VI) 1 N HClO_4 . D = optical density; ϵ = molar extinction coefficient.

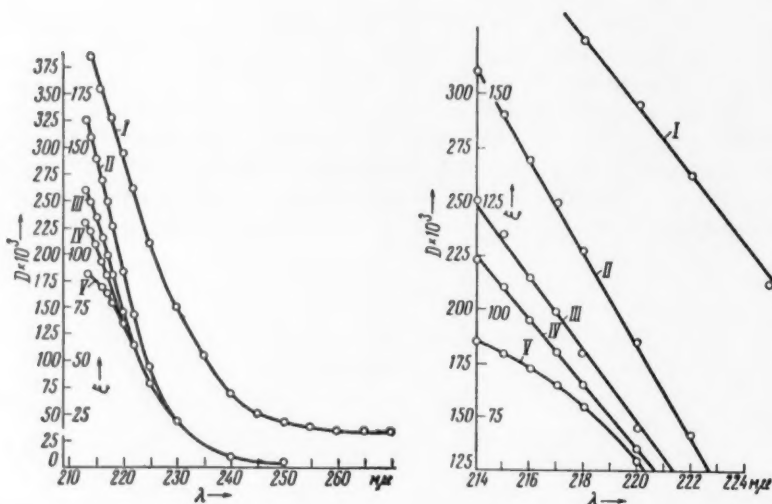


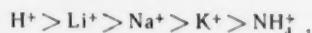
Fig. 3. Absorption spectra of zirconium chloride solutions ($2 \cdot 10^{-3} \text{ M}$, $\mu = 2$). I) 2N HCl; II) 0.2N HCl + 1.8N LiCl ; III) 0.2N HCl + 1.8N NaCl ; IV) 0.2N HCl + 1.8N KCl ; V) 0.2N HCl + 1.8N NH_4Cl . D = optical density, ϵ = molar extinction coefficient (In Fig. 3 on the right, part of the spectra is shown on an enlarged scale.)

As seen from Fig. 2, in 2N perchloric acid, where zirconium is mostly present as ZrO^{2+} or Zr^{4+} ions, the absorption is very small. In hydrochloric acid the optical density of zirconium solutions decreased owing to

formation of $ZrCl(x-y)^+$ complexes. In 8N and 9 N HCl a maximum in the 220-225 $m\mu$ region appeared on the absorption spectrum corresponding, probably, to the formation of $ZrCl_5^-$ and $ZrCl_6^{2-}$ complexes.

Thus the integral value of the optical density of zirconium chloride solutions in the 213-250 $m\mu$ region characterizes the degree of complexation of zirconium with chloride ions.

In Figs. 3 and 3a are shown the absorption spectra of zirconium in solutions of first group chlorides. Differences in the spectra are especially noticeable in the short wave regions and show that the degree of complex formation decreases through the series:



In Table 1 are presented optical density values of more concentrated zirconium solutions. The cation series was maintained. Consequently the degree of complex formation of zirconium with chloride ions depended on the nature of the cation of the neutral salts.

The optical densities of solutions of Zr in NaCl, KCl, NH_4Cl were very close to one another. A clear dependence of the amount of adsorption of zirconium on its state was shown in the present case for two groups of solutions: NaCl, KCl, NH_4Cl on the one hand, and HCl, LiCl on the other. With increase of the NaCl, KCl, or NH_4Cl concentration, the adsorption of zirconium (Fig. 1) increased in comparison with its adsorption from pure acid; with addition of HCl and LiCl the adsorption decreased. Apparently in NaCl, KCl or NH_4Cl solutions formation of zirconium complexes with chloride ions occurs mainly at the expense of the free valencies, without displacement of hydroxyl groups from the inner sphere of the complexes. This leads to an increase in the proportion of neutral forms of zirconium in the solution, with retention of their adsorbability. The adsorption of zirconium increases ("salting-out" effect).

With increase of the HCl and LiCl concentration, the complex formation of zirconium is probably accompanied by a significant increase in its degree of hydrolysis and a decrease of the adsorbability of the neutral complexes which are formed.

With equal concentration of chloride ions in NaCl, KCl and NH_4Cl solutions the amount of zirconium adsorption was considerably higher than in HCl and LiCl solutions. This agreed with the spectrophotometric data, showing that in the presence of Na^+ , K^+ and NH_4^+ the degree of complexation of zirconium with chloride ions was considerably lower than in solutions containing H^+ and Li^+ ions.

All abbreviations of periodicals in the above bibliography are letter-by-letter transliterations of the abbreviations as given in the original Russian journal. Some or all of this periodical literature may well be available in English translation. A complete list of the cover-to-cover English translations appears at the back of this issue.



MECHANISM OF THE TRANSFER OF IODINE UNDER CONDITIONS OF INTERNAL KINETICS OF ADSORPTION ON TO CARBONS FROM VARIOUS SOLVENTS

A. N. Kharin and N. A. Kataeva,

Taganrog Radiotechnical Institute

(Presented by Academician M. M. Dubinin, October 8, 1960)

Translated from Doklady Akademii Nauk SSSR, Vol. 137, No. 2, pp. 359-362, March, 1961

Original article received October 5, 1960.

The mechanism of the transfer of dissolved substances on to powdered adsorbents has not, unlike that of gases [1], been much studied.

We have studied the transfer of molecular iodine under conditions of intramolecular adsorption kinetics, from various solvents on to various carbons. The solvents used were dehydrated and redistilled ethanol, benzene and carbon tetrachloride, in addition to distilled water. Carbons BAU, KAD and AG were used as adsorbents.

TABLE 1.

Carbons	BAU	KAD	AG	Carbons	BAU	KAD	AG
Gravimetric specific gravity, Δ , g/cm ³	0.21	0.35	0.52	Pore vol. = $1/\delta - 1/\rho$, cm ³ /g	2.30	1.01	0.63
Apparent sp. gr., δ , g/cm ³	0.35	0.64	0.88	Porosity = $(\rho - \delta)/\rho$	0.805	0.65	0.55
True sp. gr., ρ , g/cm ³	1.80	1.82	1.98	Micropore vol.,* cm ³ /g	0.180	0.193	0.196
Vol. of 1 g C, $1/\delta$, cm ³ /g	2.85	1.56	1.14	in percent	7.8	19.1	31.8
				Ash, %	0.2	10.3	6.3
				Moisture, %	0.67	1.87	3.80

* This volume is calculated from the ratio: $126.9a_{\max}/4930$, where a_{\max} is calculated from the adsorption isotherm of iodine from water (cf. Table 2) at equilibrium concentration $y = 2.3$ mg-equiv/liter, equal to the solubility of iodine in water at 20° (cf. Table 3).

Carbons BAU, KAD and AG were used as adsorbents. Carbons BAU and AG were washed with hydrochloric acid, and carbon AG was additionally oxidized by iodine. The carbons were subsequently washed with water, and heated in a muffle furnace at 800-850° to 10% weight loss for BAU, and 40% for AG (that is, until hydrochloric acid and iodine were completely absent from the issuing gases). Carbon KAD was not submitted to treatment. All the carbons were screened, and dried at 100°. The work was performed on fractions of mean grain diameter 0.25 cm.

The statics of the adsorption of iodine were investigated by methods described earlier [2,3] at a temperature of 18-23°. The results of equilibrium adsorption (obtained by analysis for iodine on samples BAU and AG) are shown in Fig. 1. If the adsorption isotherms obtained for carbon KAD were shown on the same figure, they

would lie between the isotherms obtained for carbons BAU and AG. Table 2 gives the constants (\underline{z} and y_1) for the Langmuir equation: $a = zy/(y_1 + y)$, found by the method of least squares from the experimental points. \underline{z} is given in mg-equiv/g, and y_1 in mg-equiv/liter.

TABLE 2

Adsorption of iodine	On BAU		On KAD		On AG	
	\underline{z}	y_1	\underline{z}	y_1	\underline{z}	y_1
From H_2O	7.31	1.063	8.05	0.24	10.12	0.75
C_2H_5OH	1.13	1.22	1.00	0.23	0.95	0.52
C_6H_6	1.54	0.42	1.22	0.30	0.95	0.30
CCl_4	2.85	0.23	1.61	0.38	1.60	0.69

the carbon granules, and conditions of internal diffusion saturation could be assumed. Our experiments were conducted at 60 r.p.m. To maintain the initial iodine concentration at certain times the liquid over the carbon was replaced by new portions of the initial iodine solution. At the appropriate time the carbon was transferred to a mortar, in which the adsorbed iodine was determined in the way described earlier [2,3]. Deviation from the mean of the results obtained was around $\pm 5\%$. The mean results for the saturation (a) of carbons BAU and AG are shown against time in Fig. 3. From these curves the time of half-saturation (t) was found, corresponding to $a/a_0 = 0.5$;

TABLE 3

Diffusion of Iodine in Carbon Granules

Carbons	Medium	Heat of wetting, 20°, cal/g	Equilibrium adsorption a_0 , mg-equiv/g	D_{ef} , (cm ² /sec) · 10 ⁷	Half saturation, min	$g = \frac{a_0 \delta}{C_s}$	$\frac{D_L \epsilon / \Gamma}{(\text{cm}^2/\text{sec}) \cdot 10^7}$	$\frac{D_a \Gamma}{D_L \epsilon}$	$\frac{D_a}{\text{cm}^2/\text{sec}} \cdot 10^7$
BAU	H_2O	7.3	6.88	0.265	300	2750	0.038	5.0	0.227
	C_2H_5OH	18.0	0.93	0.245	325	371	0.24	—	—
	C_6H_6	19.8	1.09	0.271	294	436	0.36	—	—
	CCl_4	12.6	2.32	0.083	960	930	0.12	—	—
KAD	H_2O	11.2	6.65	0.230	346	4250	0.020	9.5	0.216
	C_2H_5OH	19.2	0.81	0.072	1100	519	0.14	—	—
	C_6H_6	19.2	0.94	0.083	960	602	0.21	—	—
	CCl_4	16.7	1.17	0.083	960	750	0.12	—	—
AG	H_2O	12.3	5.78	0.210	380	5090	0.014	12.9	0.196
	C_2H_5OH	19.8	0.62	0.040	1980	547	0.11	—	—
	C_6H_6	22.8	0.72	0.066	1200	633	0.17	—	—
	CCl_4	19.7	0.95	0.080	1000	830	0.09	—	—
Diffusion coefficient of iodine at 20° $D_L \cdot 10^5$.						$B \ H_2O, \sim 1.3$	$C_2H_5OH, \sim 1.1$	$C_6H_6, 1.95$	$CCl_4, 1.36$
Solubility of iodine at 20° in mg-equiv/liter.						2.3	1698.2	946.0	190.4

successive approximations were then used to calculate the effective coefficients of internal diffusion (D_{ef}) by means of the equation:

$$a/a_0 = 1 - \frac{6}{\pi^2} \sum_{n=1}^{n=\infty} \frac{1}{n^2} \cdot e^{-\frac{n^2 \pi^2 D_{ef} t}{R^2}}, \quad (1)$$

not less than 4 terms of the series being taken (Table 3). This gives the heats of wetting of the carbons by the solvents, which were determined in small Dewar vessels by means of bead-thermistors of type T8S2. The deviations from the mean amounted to ca. 0.3-0.4 cal/g.

It is seen that the thermal effect of wetting the carbons by each liquid increases from carbon BAU to carbon AG. The heats of wetting by water are smaller than by the nonaqueous liquids. The micropore volume accessible to iodine increases from BAU to AG, while the total porosity drops abruptly (Table 1). The values of a_0 diminish from BAU to AG, in the opposite direction to the change in the heats of wetting. On each carbon the values of a_0 diminish in the solvent order: water, carbon tetrachloride, benzene, ethanol (cf. also Fig. 1) in accordance

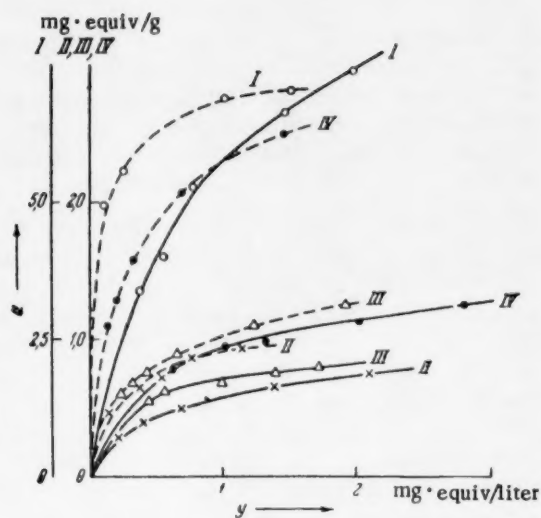


Fig. 1. Static adsorption of iodine on Carbon BAU (broken lines) and on carbon AG (solid lines). I) from water; II) from ethanol; III) from benzene; IV) from carbon tetrachloride. A) mg-equiv/g B) mg-equiv/liter.

as distinct from the usual use of the term to denote the capacity of the adsorbent in 1 ml column of the material. In our experiments $= a_0 \delta / C_0$ (4), where δ is the apparent specific gravity of the carbon. Utilizing (2) and (3) we obtain:

$$D_{ef} = \frac{D_1 \epsilon}{\Gamma} \left(1 + \frac{D_a \Gamma}{D_1 \epsilon} \right). \quad (5)$$

Assuming that for the adsorption of iodine from water the effective porosity of the carbons will differ little from that calculated from the specific gravity, and using the values of ϵ given in Table 1, we have found the

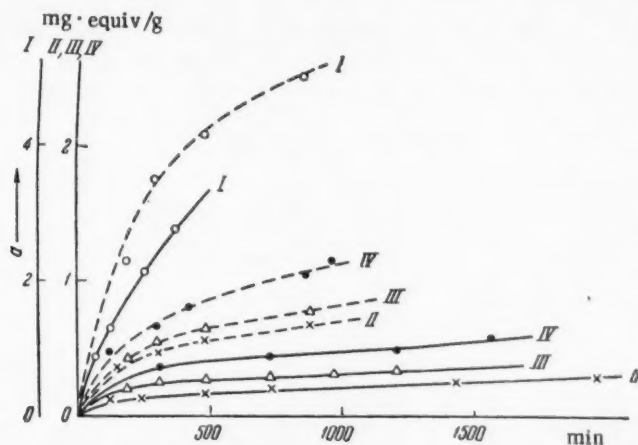


Fig. 2. Kinetics of the adsorption of iodine on the carbons BAU and AG (designation as in Fig. 1)

with the rule that adsorption diminishes with increased solubility of the substance in the solvent (Table 3). The curves $a = f(t)$ for each carbon lie one over the other also in accordance with the static adsorption (Fig. 2), and the relative saturation curves, $a/a_0 = f(t)$ show peculiarities connected with the porosity of the carbons.

If we assume with Damkohler that the transfer of iodine in the granules on the walls of the pores proceeds with a diffusion coefficient D_a , and in the volume of the pores in the liquid occupying them with a diffusion coefficient D_p , we may write:

$$D_{ef} = \frac{D_p}{\Gamma} + D_a = \frac{D}{\Gamma} \left(1 + \frac{D_a \Gamma}{D_p} \right). \quad (2)$$

The ratio $D_a \Gamma / D_p$ is a measure of the part played by transfer along the pore walls relative to that in the volume of the pores [1]. If we assume that diffusion in the bulk of the macropores proceeds at least as easily as in the free liquid, the diffusion coefficient may be written:

$$D_p = D_1 \epsilon, \quad (3)$$

where ϵ is the effective porosity of granules filled with liquid; Γ is the adsorption coefficient, denoting in our experiments the capacity of 1 ml of carbon granules,

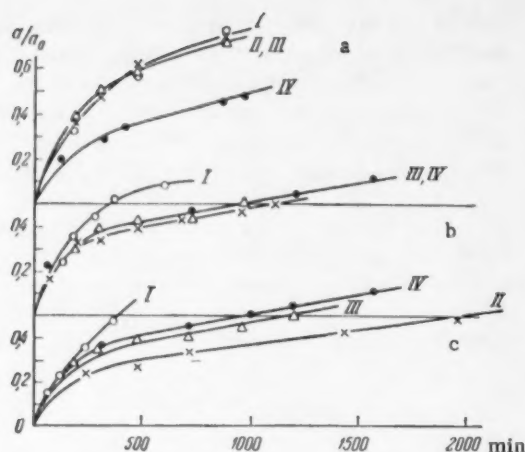


Fig. 3. Kinetics of relative saturation of carbons with iodine; for BAU (a), KAD (b), and AG (c) (designation as in Fig. 1).

Then, writing $D_1 \epsilon' / \Gamma \approx D_{ef}$, we may find effective porosity, ϵ' , of the carbons. For BAU, KAD and AG the value of this is found to be 0.60, 0.26 and 0.20 respectively, and the ratios ϵ / ϵ' are 1.34, 2.50 and 2.75; that is, for the less porous carbons the effect of benzene on "reduction of the open space in the pores" is naturally found to be great.

Owing to the difference in the fundamental mechanism of the iodine transfer in the pores of the carbons during adsorption from water and from nonaqueous liquids, the effect of the porosity of the carbon is also very different. In adsorption from water, D_{ef} is little dependent on the porosity, since the transfer takes place principally on the pore walls; and it is also found that D_a is little dependent on the kind of carbon used. In adsorption from benzene (and from alcohol), D_{ef} depends greatly on the type of carbon, since in these cases the major diffusion takes place in the volume of the pores, determined by the value of $D_1 \epsilon' / \Gamma$, which may vary several fold from carbon to carbon. It seems that, in the adsorption of iodine from carbon tetrachloride, surface transfer is not entirely eliminated, as it is in the cases of benzene and ethanol, and therefore the difference of value of D_{ef} for different carbons in this medium is smoothed out.

In the internal diffusion transfer of iodine when it is adsorbed from water on to carbons, surface transfer on the walls of the pores seems to be the major factor. This mechanism loses significance for the adsorption of iodine from nonaqueous media (carbon tetrachloride, ethanol and benzene), especially from the two last. In these cases the diffusion of iodine in the volume of the pores predominates, and so the effective diffusion coefficient may vary greatly on different carbons, depending on their effective porosity and adsorptive power.

LITERATURE CITED

1. D. P. Timofeev, *Uspekhi. Khim.*, **29**, 3, 404 (1960).
2. A. N. Kharin and L. G. Svintsova, *Zhurn. Fiz. Khim.*, **30**, 8, 1776 (1956).
3. A. N. Kharin and V. I. Vereshchagin, *Zhurn. Fiz. Khim.*, **32**, 8, 1878 (1958).
4. G. Damkohler, *Zs. phys. Chem.*, **A174**, 222 (1935).

All abbreviations of periodicals in the above bibliography are letter-by-letter transliterations of the abbreviations as given in the original Russian journal. Some or all of this periodical literature may well be available in English translation. A complete list of the cover-to-cover English translations appears at the back of this issue.

values of $D_1 \epsilon' / \Gamma$, $D_a \Gamma / D_1 \epsilon$ and D_a (Table 3).

In the adsorption of iodine from water, $D_1 \epsilon' / \Gamma$ is always considerably less than D_{ef} , while D_a is large, and diminishes somewhat in moving from BAU to AG. The criterion of surface transfer, $D_a \Gamma / D_1 \epsilon$ increases greatly from BAU to AG, since with reduction in the porosity of the carbon the value of $D_1 \epsilon' / \Gamma$ diminishes by a factor of about 3.

In adsorption from nonaqueous media, on the other hand, D_{ef} is found to be smaller than $D_1 \epsilon' / \Gamma$. It is clear that the molecules of these liquids, being themselves adsorbed, form adsorbed layers of different thicknesses, as a result of which retardation of transfer occurs, not only on the pore walls (D_a close to zero), but also of that due to diffusion in the pore volume, on account of "reduction of the free open space in the pores". It is possible that this retardation is an expression of the necessity to displace the liquids from the pores when iodine diffusion takes place in them. If it is supposed that D_a is approximately zero in experiments using benzene,

THE CHANGE IN THE SPECTRAL DISTRIBUTION OF THE INTRINSIC AND SENSITIZED PHOTOEFFECTS IN WEAKLY ILLUMINATED SILVER HALIDES

I. A. Akimov

(Presented by Academician A. N. Terenin, October 31, 1960)

Translated from *Doklady Akad. Nauk SSSR*, Vol. 2, No. 3,

pp. 624-627, March, 1961

Original article submitted October 25, 1960

Photochemical reactions introduce complications in the study of the photoelectric properties of the silver halides. It is for this reason that monocrystals with low photochemical sensitivity are usually used in measuring the photoconductivities of these substances [1]. There are, however, many cases (e.g., the study of the optical sensitization of the photoeffect) in which it is necessary to employ dispersed layers. At the same time it is clear that most of the photocurrents which have been measured in layers of powdered silver halides [2-4] are characteristic of the exposed specimens. In determining the spectral distribution of the photoconductivity of silver halide emulsions this difficulty was circumvented by using a new, unexposed section of film for each successive measurement [5,6]. This approach is practicable only with films which are rather extensive and uniform.

An apparatus for measuring the spectral distribution of the photoconductivity of photochemically sensitive semiconductors under weak illumination was developed in the present work. This apparatus was used in studies on layers of powdered silver bromide and chloride.

EXPERIMENTAL

A schematic lay-out of the apparatus is given in Fig. 1. Light from the incandescent lamp was modulated by the disk D to 600 pulses per second and then focused on the entrance slit of the autocollimating monochromator of a high-speed spectrometer (see Fig. 10 of [7]). This light was passed through a quartz prism onto the mirror A which was rocking to and fro at a frequency of 1 vib/sec* under the action of the cam-mechanism K. With each oscillation of the mirror the entire region of the spectrum from 1000 m μ to 350 m μ was made to pass before the exit slit of the monochromator, once in the forward and once in the reverse direction. A shutter operated by a relay which was synchronized to close at the beginning of the sweep through the spectrum from 1000 m μ to 350 m μ opened once every 0.5 second to pass the light coming from the monochromator onto a photoresistor.

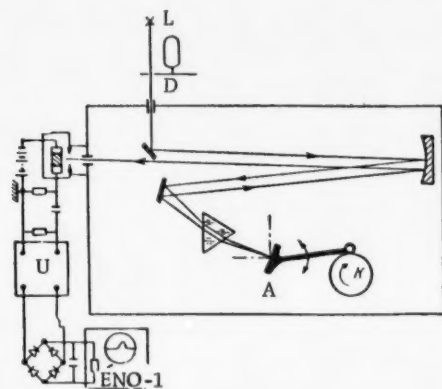


Fig. 1. Schematic lay-out of the apparatus for measuring the spectral distribution of the photoconductivity.

* Photocurrent relaxation times of the silver halides layers were measured with a taumeter and proved to be of the order of 10^{-4} second. Thus the rate of scanning which was adopted for this work was such that the inertia of the receiver introduced no distortion into the measurements.

A photoresistor consisting of a layer of powdered silver halide deposited on a glass plate with platinum electrodes was used as a radiation detector in the studies on photoconductivity while a condenser consisting of a layer of powdered silver halide between mica spacers served the same purpose in the studies on photo-emf. All of the preliminary operations on the silver halides were performed in inactive light. The measurements were carried out with a monochromator slit opening of 0.5 mm (the dispersion was 80 Å/mm at 400 mμ and 240 Å/mm at 700 mμ) so that the energy transferred to the layer in a single scanning of the spectrum was of the order of 10^{-5} watt/cm². The photocurrent signal was fed into a narrow band amplifier*, U, with a band-pass width of 600 ± 15 kc and an amplification factor of 70,000. The output from this amplifier was rectified and fed into an ÉNO-1 oscillograph the ray of which was triggered by a slave sweep synchronized with the scanning of the spectrum.

Thus the screen of the oscillograph showed a curve representing the spectral distribution of the photocurrent, or photo-emf, of the layer which was under study, no reduction being made to unit incident energy. The apparatus was combined with a synchronous detector [8,9] so as to permit the sign of the charge of the photocurrent carriers to be determined in various portions of the spectrum while the photo-emf was being measured by the condenser method.

DISCUSSION OF RESULTS

These measurements were carried out on colorless silver halides and also on silver halides which had adsorbed certain organic dyes to act as sensitizers. A number of spectral measurements were made on each specimen. The difference between one spectrum and its predecessor was due to photochemical changes which had occurred in the layer during the earlier exposure (0.5 second) to radiation.

Figure 2 shows how exposure progressively changed the spectra of photo-emf (2a) and photoconductivity (2b) of silver bromide. Similar changes were observed in silver chloride. The photo-emf of unexposed silver bromide showed a red limit at 480 mμ and a maximum at 390 mμ while the corresponding values for silver chloride were 395 and 365 mμ, respectively. Progressive exposure caused the appearance of a break in the spectral curve for photo-emf in AgBr at 415 mμ, a similar break appearing in the AgCl curve at 380 mμ. New maxima appeared on the long-wavelength side of the spectra (at approximately 450 mμ for the silver bromide and 385 mμ for the silver chloride) while the photo-emf diminished over the entire region of short wavelengths.

Measurements with the synchronous detector showed the sign of the photo-emf in the unexposed powders of AgBr and AgCl to be that corresponding to the diffusion of electrons from the illuminated surface into the body of the layer. The electron diffusion current diminished with successive exposures and a new maximum appeared at the long-wavelength limit as a result of the diffusion of positive holes into the layer.

The changes observed in the photoconductivity spectra were of a different type. The photoconductivity of unexposed silver bromide powders showed a red limit at 490 mμ and a maximum at 450 mμ, corresponding values for silver chloride being 400 mμ and 380 mμ, respectively. Figure 2 shows that the second exposure of the layer brought about a uniform 20-30% increase in the photoconductivity over the entire spectrum. The photoconductivity diminished in subsequent exposures. The most marked alteration in the photoconductivity occurred in the short-wave portion of the spectrum.

These irreversible alterations in the photo-emf and photoconductivity of AgBr and AgCl were obviously due to photochemical changes.

The formation of colloidal silver particles gave rise to bands in the photoeffect in the 580-620 mμ region after only 10-15 exposures of AgBr and after 20-30 exposures of AgCl.

These observations can be explained only if the photoconductivity is assumed to be bipolar. It has been shown earlier that such is the case in molten films of silver bromide and chloride [10]. The electronic component predominates in the unexposed layer (it has been shown in [11] that hole mobility is much less than electron mobility in monocrystals of AgBr and AgCl). It is possible that exposure causes the appearance of acceptor levels

* A narrow-band amplifier could be used in place of the wide-band amplifiers which are commonly employed with high-speed spectrometers [7] because the bands in the photoconductivity spectra are rather wide. This made it possible to study photocurrents of the order of 10^{-13} amp.

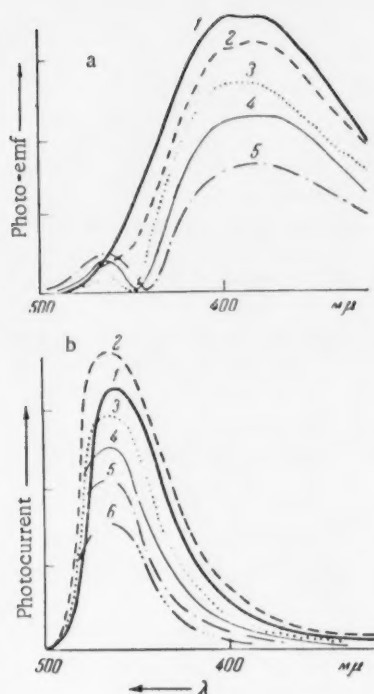


Fig. 2. Spectral distribution of photo-emf (a) and photoconductivity (b) in layers of powdered silver bromide: 1) First measurement of spectrum; 2) second measurement, etc.

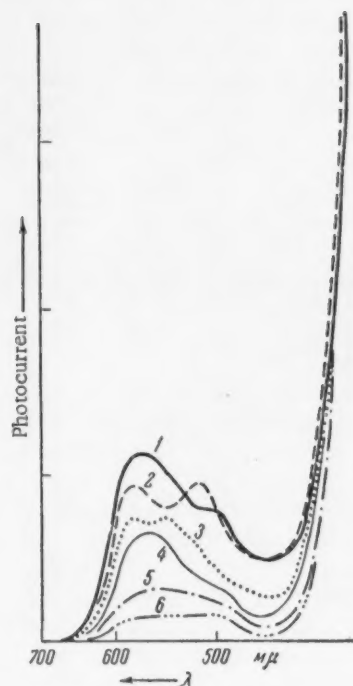


Fig. 3. Spectral distribution of photoconductivity of a layer of silver bromide which had been colored with the dye 1,1'-diethyl-3,3,3',3'-tetramethylthiacarbocyanine iodide at a concentration of 10^{-4} mole/liter: 1) First measurement of spectrum; 2) second measurement, etc.

in the forbidden zone of the crystal and that these capture electrons, thereby increasing the contribution of the hole component [9]. At the same time, the centers which are formed produce an additional band at the absorption limit of the crystal [10]. Moreover, the alteration of the diffusion of the photocurrent carriers could be due in part to a reduction in the upward bend of the zone of the unexposed crystals as a result of screening from the surface electron levels which arise during exposure [12].

It has been observed earlier that dyes will markedly sensitize the internal photoeffect in silver and thallium iodides although their effect on the bromides is quite small [13-16,4]. A study of the effect of exposure on the photoconductivity spectra of layers of powdered bromides and iodides which had been treated with cyanine dyes to act as sensitizers led to the following results.

The sensitized photoeffect in AgI was entirely unaltered by exposure. Exposure of a layer of AgBr led to a rapid diminution of the photoelectric sensitivity in the neighborhood of the absorption of the dye to the point where it was insignificant in comparison with the photoeffect in the region of absorption of the semiconductor itself. Figure 3 shows how successive exposures altered the spectral photoconductivity curve for silver bromide colored with the thiacyanine dye.

The observed disappearance of the sensitized photoeffect in silver bromide is naturally explained by the breakdown of the dye under action of the bromide liberated in photochemical decomposition of the AgBr. It should be noted, however, that the effectiveness of sensitization of the photoeffect was one order lower in silver bromide than in silver iodide, even in unexposed layers. This is obviously due to energy transfer from the dye-sensitizer to the local electron levels on the surface of the semiconductor [4,9,13-16].

In conclusion we would like to express our thanks to Academician A. N. Terenin for his continued interest in this work and for his valuable advice.

LITERATURE CITED

1. O. Stasiw and J. Teltow, *Ann. Phys.*, **40**, 181 (1941).
2. E. A. Kirillov, *Zs. Wiss. Photogr.* **26**, 235 (1929).
3. M. Tamura, M. Kaga, and N. Tatsuuma, *Sci. Ind. Photogr.*, **25**, 70 (1954); *Photogr. Sens.*, **1**, 47 (1956).
4. I. A. Akimov, *Doklady Akad. Nauk SSSR*, **121**, 311 (1958).
5. W. West and B. H. Carroll, *J. Chem. Phys.*, **15**, 529 (1947); **19**, 417 (1951).
6. L. G. Gross, *Zhur. Nauchn. i. Priklad. Fotogr. i Kinematogr.*, **5**, 54, 219 (1960).
7. O. D. Dmitrievskii, B. S. Neporent, and V. A. Nikitin, *UFN*, **64**, 447 (1958).
8. U. Kh. Nymm and L. Ya. Uibo, *Trans. Institute of Physics and Astronomy, Acad. Sci. Estonian SSR*, **4**, 124 (1956).
9. I. A. Akimov and E. K. Putseiko, *Collection, Photoelectrical and Optical Effects in Semiconductors* [in Russian] (Kiev, 1959), p. 301.
10. P. V. Meiklyar and E. K. Putseiko, *Doklady Akad. Nauk SSSR*, **73**, 63 (1950); *Zhur. Éksp. i Teor. Fiz.*, **21**, 341 (1951).
11. J. W. Mitchell, *J. Photogr. Sci.*, **6**, 57 (1958); *UFN*, **67**, 293 (1959).
12. V. E. Kozhevnikov and V. E. Loshkarev, *Radiotekhnika i Elektronika*, **2**, 260 (1957).
13. E. K. Putseiko and A. N. Terenin, *Zhur. Fiz. Khim.*, **23**, 676 (1949); *Doklady Akad. Nauk SSSR*, **70**, 401 (1950).
14. A. G. Gol'dman and I. A. Akimov, *Zhur. Fiz. Khim.*, **27**, 355 (1953).
15. I. A. Akimov, *Zhur. Fiz. Khim.*, **30**, 1007 (1956).
16. A. Terenin, E. Putseiko, and I. Akimov, *J. Chim. Phys.*, **54**, 716 (1957); *Wissenschaft. Photogr. Intern. Konfer. Köln, 1956, Darmstadt-Wien, 1958*, S. 117.
17. A. Terenin and I. Akimov, *Zs. Phys. Chem. (DDR)*, (in litt).

All abbreviations of periodicals in the above bibliography are letter-by-letter transliterations of the abbreviations as given in the original Russian journal. Some or all of this periodical literature may well be available in English translation. A complete list of the cover-to-cover English translations appears at the back of this issue.

RADIOACTIVE CATALYSTS

THE DEHYDRATION OF CYCLOHEXANOL ON MAGNESIUM SULFATE AND CALCIUM CHLORIDE

Academician A. A. Balandin, Academician Vikt. I. Spitsyn, N. P. Dobrosel'skaya, and I. E. Mikhailenko

Institute of Physical Chemistry, Academy of Sciences, USSR

Translated from *Doklady Akad. Nauk SSSR*, Vol. 2, No. 3, pp. 628-630, March, 1961

Original article submitted December 24, 1960

In a previous communication [1] it has been shown that the catalytic dehydration of cyclohexanol on $MgSO_4$ is vitally affected by the presence of radioactive sulfur-35 in the catalyst.

The present work is a study of the relation between the reaction yield and the radiation energy of the applied isotope at fixed value of the absolute activity of the radioactive catalyst. The effect of the S^{35} ($E_{max} = 0.167$ Mev) was compared with that of the β -emitter Ca^{45} ($E_{max} = 0.254$ Mev). A high specific activity of Ca^{45} was obtained by irradiating calcium carbonate enriched with the stable isotope Ca^{44} with slow neutrons at a flux density of $0.8 \cdot 10^{13}$ ev/cm²·sec. Identification of the resulting radioactive isotopes was carried out on a scintillation spectrometer with a 100-channel amplitude analyzer. The β -spectrum showed the presence of Ca^{45} . The product also showed a weak γ -activity which is not characteristic of calcium-45. Measurements by a relative method using a radium standard showed this activity to be equivalent to 0.010 mg/eq Ra per 1 g $CaCO_3$ and to be due to the presence of an infinitesimal amount of Fe^{59} .

TABLE 1

Dehydration of Cyclohexanol on $MgSO_4 + CaCl_2$

Catalyst No.	Characteristics of catalyst		Apparent activ. energy for dehydration of cyclohexanol, kcal/mole
	$CaCl_2$ content, wt. %	absolute ac. mCu/g	
1	0	0	15,1
2	100	0	—
2*	100	93,7	—
3	13,82	0	17,8
3*	13,93	12,0	14,2
4	27,05	0	18,2
4*	26,99	24,6	18,3
5	49,87	0	16,4
5*	49,82	45,1	15,5

Radioactive calcium chloride was obtained by dissolving the $CaCO_3$ in 18% HCl, evaporating the solution to dryness, and then heating the resulting salt to 400°. The absolute activity of the $CaCl_2$ was measured with an end-window counter and a π -counter.

Study was made of the dehydration of cyclohexanol on mixtures of $MgSO_4$ and $CaCl_2$. The radioactive catalysts were prepared in the following manner. Non-radioactive magnesium sulfate was moistened with a definite amount of the $CaCl_2$ solution. The mixture of salts was then brought to 400° and held at this temperature for two hours. The non-radioactive catalysts were prepared in the same manner and contained the same amount of $CaCl_2$.

The characteristics of these catalysts are given in Table 1.

Dehydration of the cyclohexanol was studied over the temperature interval from 350 to 420°. The apparatus which was used here has been described in [1]. The cyclohexanol was fed at a rate of 0.2 ml/min. The charge of catalyst, which was in the form of grains 1-2 mm

in diameter and weighed approximately 0.25 g. was placed in a removable reactor. The reaction products were collected in a water-cooled receiver. The unsaturated hydrocarbons in the catalyzate were determined by bromometric titration.

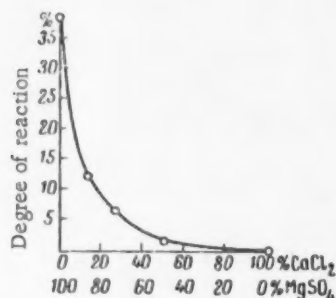


Fig. 1. Relation between catalytic activity of MgSO_4 and amount of added CaCl_2 (380°).

Pure magnesium sulfate proved to have the highest catalytic activity, comparison being based on the degree of reaction of the alcohol at fixed temperature. A marked diminution in catalytic activity resulted from the addition of calcium chloride to the magnesium sulfate (Fig. 1). Calcium chloride without magnesium sulfate was inert in this reaction.

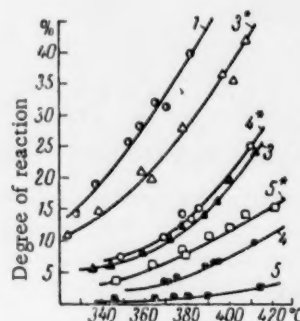


Fig. 2. The effect of the radioactive radiation of the catalyst on the catalytic activity.

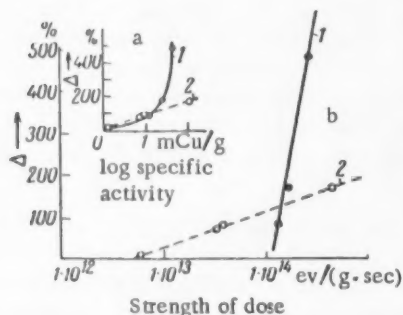


Fig. 3. Increase in the degree of reaction of cyclohexanol as a function of the specific radioactivity of the catalyst (a), and the strength of dose absorbed by the catalyst (b) (410°). 1) $\text{MgSO}_4 + \text{CaCl}_2$. 2) $\text{MgSO}_4 + \text{Na}_2\text{SO}_4$.

Introduction of radioactive Ca^{45} into a $\text{MgSO}_4 - \text{CaCl}_2$ mixture resulted in a decrease in the catalytic activity in every case. Pure CaCl_2 containing as much as 93.7 mCu/g of Ca^{45} resembled the non-radioactive compound in being inert in this reaction. Thus it can be affirmed that it is not the β -radiation of the radioactive isotope that affects the dehydration of the cyclohexanol but rather the excitation resulting from the β -particles and the secondary electrons which they dislodge from the atoms of the MgSO_4 catalyst.

The data on the relation between the temperature and the degree of reaction of cyclohexanol are presented in Fig. 2. Catalysts of the same composition carry the same number, but the radioactive specimens are starred. Thus it can be seen that the degree of conversion of cyclohexanol at 410° is 87% greater on catalyst 3* than on catalyst 3, 170% greater on catalyst 4* than on catalyst 4, and 486% greater on catalyst 5* than on catalyst 5. The relation between the degree of reaction and the specific activity of the catalyst is shown in Fig. 3a. The dotted line in this figure covers our earlier relation [1] between the increase in the degree of reaction of cyclohexanol and the logarithm of the specific activity of magnesium and sodium sulfates containing radioactive sul-

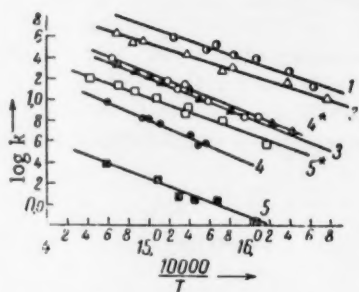


Fig. 4. Relation between reaction rate constant and reciprocal temperature.

fur-35. The difference in these two curves is clearly due to the difference in the radiation energy and the accompanying secondary effects from the action of the high-energy β -particles on the catalyst. Figure 3b shows the relation between the increase in the degree of reaction and the dose strength of the irradiation received by catalysts containing sulfur-35 and calcium-45. These dose strengths were calculated by assuming all of the emitted β -particles to be absorbed by the catalyst. It can be concluded that the degree of reaction is linearly dependent on the logarithm of the dose of radiation absorbed by the catalyst in both cases, the line corresponding to the β -particles of higher energy having the greater slope.

Apparent activation energies were calculated from the data on the temperature dependence of reaction yield (see Fig. 4 and Table 1). These energies rise rapidly with increase in the amount of added CaCl_2 . The values of E_{app} for the radioactive catalysts are somewhat lower.

LITERATURE CITED

1. A. A. Balandin, Vikt. I. Spitsyn, N. P. Dobrosel'skaya, and I. E. Mikhailenko, *Doklady Akad. Nauk SSSR*, 121, 495 (1958).

All abbreviations of periodicals in the above bibliography are letter-by-letter transliterations of the abbreviations as given in the original Russian journal. *Some or all of this periodical literature may well be available in English translation.* A complete list of the cover-to-cover English translations appears at the back of this issue.



CERTAIN QUANTITATIVE RELATIONSHIPS IN THERMOGRAPHY

L. G. Berg and L. A. Borisova

Kazan Section of the Academy of Sciences USSR
(Presented by Academician B. A. Arbuzov, October 29, 1960)
Translated from *Doklady Akad. Nauk SSSR*, Vol. 2, No. 3,
pp. 631-633, March, 1961
Original article submitted October 15, 1960

Thermographic analysis constitutes one of the principal methods for the determination of the phase composition of a number of synthetic and natural products. However, quantitative thermographic relationships have still not been worked out thoroughly enough. We still don't know whether the areas determined from the differential curves of compounds with different thermal conductivity coefficients can be validly compared, since the heat of phase transition is proportional to the product of the thermal conductivity coefficient K and the area S formed by the shift of the differential curve during the reaction. By the thermal conductivity coefficient we mean the sum of all the factors affecting the rate of heat loss, i.e., the coefficients of: heat transfer, heat conduction, specific heat, distance from the thermocouple junction to the sample surface and to the calibrating instrument, the surface area, etc. [1].

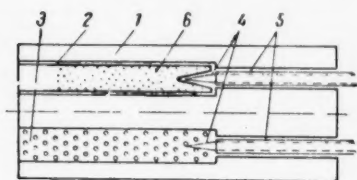


Fig. 1. Schematic diagram of the block and the thermocouple attachment: 1) block made of heatproof steel; 2) a pyrex reaction vessel; 3) powdered Al-metal; 4) multiple junction thermocouple; 5) porcelain tubing; 6) a weighed sample of the investigated compound.

L. G. Berg [1] has demonstrated mathematically that areas obtained from various thermograms for compounds with different values of K can be compared if they are reduced to areas with a common value of K ; this can be done by means of the equation:

$$S'' = S' \cdot \frac{\Delta t''}{\Delta t'} \quad (I)$$

In this case $\Delta t'$ and $\Delta t''$ are the respective temperature differences between the furnace and the sample. These can be determined independently from the thermograms.

Should the thermal conductivity coefficient change during the phase transition we will use the average coefficient and Equation (I) assumes the form

$$S'' = S' \cdot \frac{\frac{\Delta t_1'' + \Delta t_2''}{2}}{\frac{\Delta t_1' + \Delta t_2'}{2}} = S' \cdot \frac{\Delta t_1'' + \Delta t_2''}{\Delta t_1' + \Delta t_2'} \quad (II)$$

We have verified Equation (II) experimentally by measuring the areas representing the polymorphic transition in KNO_3 . Changes were introduced into the thermal conductivity coefficient by adding to the KNO_3 compounds with known greatly different conductivities in amounts such as to maintain the same specific heat in all the experimental mixtures.

Heating curves were recorded on a self-recording automatic potentiometer (model ÉPP-09) which was rendered extremely sensitive by decreasing the resistance of the shunt in the rheostat (from 235 to 4.5 ohms) and increasing the resistance R_{int} , so as to shift the initial section of the plot to the extreme left [2]. In this way a potential drop of 0.5 mv could be obtained across the rheostat. The junction of the differential thermocouple was located inside the block. Since the position of the junction of a simple thermocouple has a strong effect on the area of the peak representing phase transition, it is very difficult to get reproducible results when the thermocouple is placed above the sample. We attached our thermocouples rigidly from below so that the junction remained in a fixed position. At the bottom of the reaction vessel we had a pocket for the thermocouple junction (Fig. 1). Since the area of a phase transition peak increases with increasing sample size to a limiting value and then remains constant, we always determined the maximum weight n_{max} and subsequently used samples weighing considerably less than n_{max} ; in this way we were able to get the true areas corresponding to the respective weights.

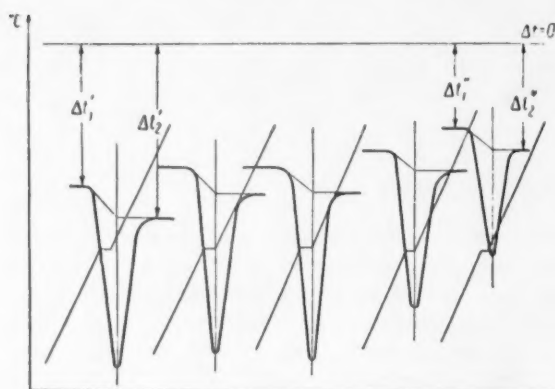


Fig. 2. Heating curves 1, 3, 4, 5, and 8.

Thus most of the factors influencing the rate of heat transfer remained the same in all of our experiments with the exception, of course, of thermal conductivity, which was varied from experiment to experiment.

We reduced the areas corresponding to the polymorphic transitions in KNO_3 samples with various values of K (refractory clay, CuO , Ag, and Al were introduced into weighed samples of KNO_3) to the corresponding areas with a common K, and the results are presented in Table 1. The area of curve 1 was used as reference for the reduction of all other curves. When the thermal conductivity was constant we obtained reproducible peak areas and reproducible shifts Δt_1 and Δt_2 of the differential curves from the zero line (Nos. 7, 8, and 9).

TABLE 1

Expt. Nos.	Compound	Δt_1 , in mm	Δt_2 , in mm	Δt_{av} , in mm	S, in rel. units	$S_{\text{red.}}$, in rel. units	Relative % error
1	3g KNO_3 + 1.5g of refractory clay	46,0	59,0	52,50	6,80	—	—
2	The same	48,0	58,0	53,0	7,08	6,98	+2,65
3	3g KNO_3 + 1.5 g NaNO_3	46,0	56,0	51,0	6,50	6,66	-2,06
4	3g KNO_3 + 3g CuO	46,0	56,0	51,0	6,56	6,77	-0,44
5	3g KNO_3 + 1.5g Al (met.)	39,0	47,0	43,0	5,46	6,66	-2,06
6	The same	44,0	52,0	48,0	6,20	6,72	-1,15
7	3g KNO_3 + 6g Ag (met.)	31,5	40,0	35,75	4,70	6,87	+1,03
8	The same	31,5	39,5	35,50	4,6	6,77	-0,44
9	" "	31,5	39,0	35,25	4,66	6,93	+1,91

Table 1 shows that unless the areas are reduced in the above-described manner the same amount of material, depending on the thermal conductivity may yield very different values, as for example $S_1 = 4.6$ and $S_2 = 6.8$ (Nos. 1 and 8). After we reduce the former to compare it with the area S_2 we get $S_1 = 6.77$, with the absolute error reduced to only 0.03 relative units and the relative error to 0.45%. Mixtures having the same specific heat were selected before our measurements. However, since the specific heat is insignificantly small in comparison with thermal conductivity, the former can be neglected without significantly increasing the errors in reduced areas.

Thus, in practice such a reduction decreases the errors obtained in quantitative phase analysis and makes it possible to utilize the heating curves of various compounds obtained from different thermograms for quantitative calculations; at the same time heats of transition obtained from the same thermogram can be compared, since the errors do not exceed 3%.

LITERATURE CITED

1. L. G. Berg, Trans. 1st Confer. on Thermography [in Russian] (Izd AN SSSR, 1955), p. 59; L. A. Pashkevich, Zavodskaya Lab. No. 4, 482 (1959).

All abbreviations of periodicals in the above bibliography are letter-by-letter transliterations of the abbreviations as given in the original Russian journal. *Some or all of this periodical literature may well be available in English translation.* A complete list of the cover-to-cover English translations appears at the back of this issue.



THE MECHANISM OF OZONE FORMATION IN THE ELECTROLYSIS OF CONCENTRATED PERCHLORIC ACID SOLUTIONS

M. A. Gerovich*, R. I. Kaganovich, Yu. A. Mazitov, and L. N. Gorokhov

The M. V. Lomonosov Moscow State University

(Presented by Academician A. N. Frumkin, November 26, 1960)

Translated from *Doklady Akad. Nauk SSSR*, Vol. 2, No. 3,

pp. 634-637, March, 1961

Original article submitted November 18, 1960

There has been relatively little work done to elucidate the mechanism of anodic formation of ozone [1-4]. This is because the process is complicated by oxidation of the electrodes, anodic oxygen evolution, per-acid formation, and other processes which occur at the potentials for ozone evolution.

In this paper we present the results of an investigation of the mechanism of anodic ozone formation from concentrated perchloric acid solutions at low temperature, using the labelled atom method in association with the recording of polarization curves.

As in the previous investigation at room temperature [5], we electrolyzed solutions of perchloric acid labeled with heavy oxygen isotope, or solutions of normal perchloric acid in water enriched with O^{18} ; samples were taken of the oxygen and ozone formed at various potentials, and their isotopic compositions were determined by mass spectrometry.

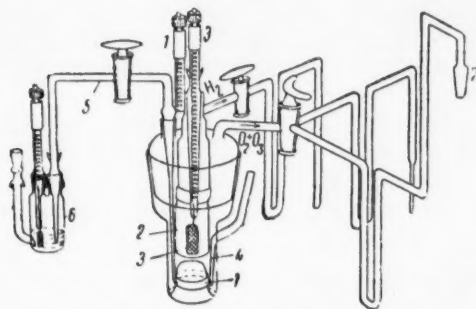


Fig. 1. Cell for electrolysis of perchloric acid at low temperature: 1) Anode; 2) diaphragm; 3) cathode; 4) capillary for thermocouple; 5) tap for measuring anode potential relative to hydrogen electrode 6; 7) ground joint for connection to receiver trap.

The use of perchloric acid as electrolyte, instead of sulfuric acid, was found to be more convenient, since it avoided the complications associated with per-acid formation and oxygen exchange between water and acid. The absence of these complications in the electrolysis of $HClO_4$ solutions was demonstrated in our previous paper [5].

Electrolysis was carried out in the cell shown in Fig. 1. The anode consisted of a platinum plate, 0.5 to 20 cm^2 in area according to the current density required. The cathode was a platinum grid. The anodic and cathodic compartments were separated by a porous glass diaphragm; this was in the form of a cylinder enclosing the cathode. A low temperature at the anode was maintained by surrounding the cell with a cooling mixture of methanol and solid carbon dioxide. The temperature was measured by means of an iron-constantan thermocouple, placed in a fine sleeve in contact with the anode. The cell was so constructed that polarization curves could be recorded, and samples of gas evolved from the anode

could be collected at different potentials. Before starting electrolysis, the anode was treated with sulfuric and hot nitric acids, washed with twice-redistilled water, and then polarized anodically at a current of 10^{-6} to 10^{-4} amp for 30 min

* Deceased.

After electrolysis for 1.5 to 2 hours at a given temperature, the electrolyte was practically saturated with the gases evolved at the anode, and these gases then began to condense in the receiver trap (Fig. 2) made of molybdenum glass. The condensation temperature was achieved by surrounding the receiver trap with a copper block, 6, cooled by liquid nitrogen. Special ampoules, for collecting samples for mass spectrometric analysis, were sealed beforehand to the receiver connections. In order to adjust the pressure in the receiver while gas was being condensed, the outlet 9 remained unsealed and was only closed by water drops. At the end of the electrolysis the receiver taps 1 and 2 were closed, the current was switched off, the outlet 9 was dried and rapidly sealed, the copper block 6 was totally immersed in liquid nitrogen, and the receiver was connected by the joint 7 to a vacuum line to pump off oxygen.

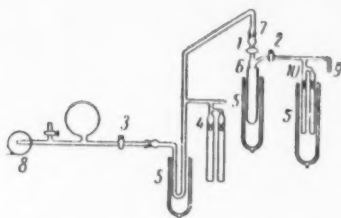


Fig. 2. Diagram of system for collecting samples of ozone and oxygen.

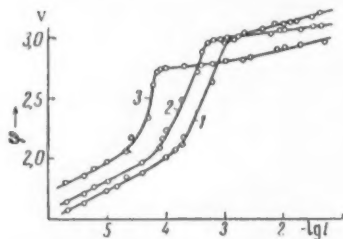


Fig. 3. Anodic polarization curves for a platinum electrode in perchloric acid at -40° : 1) 6.3 N; 2) 7.1 N; 3) 10 N.

was reduced. In fact, as can be seen from Table 1, the oxygen evolved at low temperature when using HClO_4^{18} was enriched with heavy oxygen, thus showing that the acid anion played a part in the process of oxygen formation [5].

It might have been expected that parallel samples of oxygen and ozone would have nearly the same isotopic compositions, which would have shown that they were formed by similar mechanisms. However, although the acid anion played a part in the processes of formation of oxygen and ozone, the results in Table 1 show that there was a difference.

From the isotopic compositions of the oxygen and ozone we calculated the fractional shares of the water in the formation of ozone (n_{Oz}) and of oxygen (n_{Ox}) from the oxygen in the water and the acid anion. For solutions of normal perchloric acid in labelled water, n_{Oz} and n_{Ox} were calculated as the ratios of the O^{18} contents of the ozone and oxygen to that of the original H_2O^{18} . For solutions of labeled acid the fractional shares of the acid in the formation were calculated as above, and these values were subtracted from 1 to give n_{Oz} and n_{Ox} . It can be seen from Table 1 that n_{Oz} was always greater than n_{Ox} .

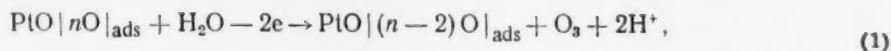
It is reasonable to suppose, on the basis of these results, that oxygen chemisorbed on the anode was diluted with oxygen from water in the process of ozone formation. Table 1 shows values of $Q = (n_{\text{Oz}} - n_{\text{Ox}}) / (1 - n_{\text{Ox}})$; it is easy to show that this represents the fractional share of water in formation of ozone from oxygen and water, in

Before collecting the oxygen sample, the space up to tap 1 (Fig. 2) was first evacuated and then filled by evaporation from the oxygen receiver. Then the ampoules 4 were sealed off for determination of the oxygen isotopic composition by mass spectrometry. The other ampoules were next filled with ozone; this was done by evacuating the system for 1.5 hours, raising the temperature of the copper block, and cooling the ampoules 10 with liquid nitrogen so that the ozone condensed in them. These ampoules were then sealed off and heated, first to room temperature and then in an oven at $150-200^\circ$, so as to decompose the ozone to oxygen before determining its isotopic composition.

Some of the results obtained are shown in Fig. 3 as polarization curves recorded at -40° , and some results are also shown in Table 1. The notation $\text{HClO}_4^{18}/\text{H}_2\text{O}$ in Table 1 means that the solution investigated was of labeled perchloric acid in normal water, and $\text{HClO}_4/\text{H}_2\text{O}^{18}$ means a solution of normal perchloric acid in labeled water. Data is given on the isotopic composition of the starting materials (HClO_4^{18} and H_2O^{18}) and of the reaction products liberated at the anode (O_2 and O_3).

It is clear from Fig. 3 that the polarization curves recorded at low temperature were similar in form to those obtained previously [5-9] at room temperature. For the low temperatures, the sections of the curves showing an abrupt increase in overvoltage shifted in the direction of lower current density and more positive potential; the relation between overvoltage and acid concentration, observed at room temperature, was retained. We can therefore conclude that the mechanism of oxygen evolution did not alter when the temperature

accordance with the reaction $(1-Q) O + QH_2O \rightarrow \frac{1}{3} O_3$. Q should be $\frac{1}{3}$ if the ozone were produced by an electrochemical desorption mechanism in accordance with the equation:



and the oxygen were produced by direct decomposition of surface oxides of platinum.

TABLE 1

Composition and concentration of electrolyte	Anode temp., °C	Current density, $\frac{2}{cm}$	Oxygen source	Enrichment, %	Fractional share of water in formation process		Q
					oxygen, n_{ox}	ozone, n_{oz}	
5,8N $HClO_4^{18}/H_2O$	-40	$2,2 \cdot 10^{-2}$	$HClO_4^{18}$	0,399	—	—	0,35
			O_2	0,059	0,85	—	
			O_3	0,038	—	0,90	
$HClO_4/H_2O^{18}$	-40	$1,2 \cdot 10^{-1}$	H_2O^{18}	0,742	—	—	0,50
			O_2	0,680	0,91	—	
			O_3	0,710	—	0,95	
6,3N $HClO_4^{18}/H_2O$	-40	$2 \cdot 10^{-2}$	$HClO_4^{18}$	1,780	—	—	0,39
			O_2	0,482	0,73	—	
			O_3	0,296	—	0,83	
$HClO_4/H_2O^{18}$	-50	$2 \cdot 10^{-2}$	H_2O^{18}	0,738	—	—	0,48
			O_2	0,519	0,70	—	
			O_3	0,624	—	0,84	
7,1N $HClO_4^{18}/H_2O$	-40	$2 \cdot 10^{-2}$	$HClO_4^{18}$	1,780	—	—	0,30
			O_2	0,46	0,74	—	
			O_3	0,32	—	0,82	
$HClO_4/H_2O^{18}$	-50	$2 \cdot 10^{-2}$	H_2O^{18}	2,481	—	—	0,41
			O_2	1,193	0,48	—	
			O_3	1,723	—	0,69	
8,6N $HClO_4^{18}/H_2O$	-50	10^{-2}	$HClO_4^{18}$	1,78	—	—	0,37
			O_2	1,005	0,44	—	
			O_3	0,633	—	0,64	
$HClO_4/H_2O^{18}$	-50	$5 \cdot 10^{-2}$	H_2O^{18}	0,455	—	—	0,51
			O_2	0,148	0,32	—	
			O_3	0,305	—	0,67	
10N $HClO_4^{18}/H_2O$	-40	$2 \cdot 10^{-3}$	$HClO_4^{18}$	0,569	—	—	0,35
			O_2	0,413	0,27	—	
			O_3	0,270	—	0,53	
$HClO_4/H_2O^{18}$	-50	$2 \cdot 10^{-2}$	H_2O^{18}	4,36	—	—	0,38
			O_2	1,235	0,28	—	
			O_3	2,411	—	0,55	

The experimental values of Q were slightly greater than $\frac{1}{3}$. Experiments with H_2O^{18} gave a mean Q of 0.45 ± 0.05 ; experiments with $HClO_4^{18}$ gave a mean Q of 0.36 ± 0.05 ; the combined average was $Q = 0.4 \pm 0.05$ (15 other experiments, besides those shown in Table 1, were used in calculating the mean value).

Considering the scatter in the experimental results, equation (1) may be taken as correct to a first approximation.

In conclusion, we would like to thank Academician A. N. Frumkin for valuable discussions on the experiments and their interpretation, and Academician of the Academy of Sciences of the Ukrainian SSR A. I. Brodskii for fruitful discussions on the results.

LITERATURE CITED

1. F. Forster, *Elektrochemie wässriger Lösungen*, 1922.
2. F. Fischer and K. Massener, *Zs. anorg. Chem.*, 52, 202 (1907).
3. T. R. Beck and R. W. Moulton, *J. Electrochem. Soc.*, 103, 247 (1957).
4. V. I. Veselovskii, *Proceedings of the Fourth Conference on Electrochemistry [in Russian] (Academy of Sciences of the USSR, 1959)*, p. 241.
5. M. A. Gerovich, R. I. Kaganovich, V. M. Vergelesov, and L. N. Gorokhov, *Doklady Akad. Nauk SSSR*, 114, 1049 (1957).
6. N. A. Izgaryshev and E. A. Efimov, *Zhur. Fiz. Khim.*, 27, 130, 310 (1953).
7. V. L. Khelfets and I. Ya. Rivlin, *Zhur. Priklad. Khim.*, 28, 12, 129 (1955).
8. R. I. Kaganovich, M. A. Gerovich, and É. Kh. Enikeev, *Doklady Akad. Nauk SSSR*, 108, 107 (1956).
9. A. A. Rakov, V. I. Veselovskii, et al., *Zhur. Fiz. Khim.*, 32, 12, 2702 (1958).

All abbreviations of periodicals in the above bibliography are letter-by-letter transliterations of the abbreviations as given in the original Russian journal. *Some or all of this periodical literature may well be available in English translation.* A complete list of the cover-to-cover English translations appears at the back of this issue.

THE NATURE OF THE INTERACTION OF BENZENE MOLECULES WITH HYDROXYL GROUPS

A. V. Kiselev, Ya. Kouterski, and I. Chizhek

The Institute of Physical Chemistry of the Academy of Sciences of the USSR
The Institute of Physical Chemistry of the Czechoslovak Academy of Sciences
(Presented by Academician A. A. Balandin, October 19, 1960)
Translated from *Doklady Akad. Nauk SSSR*, Vol. 2, No. 3,
pp. 638-641, March, 1961
Original article submitted October 10, 1960

The adsorption of aromatic and unsaturated hydrocarbons and of nitrogen is very sensitive to the degree of hydration of the adsorbent. The adsorption heat of benzene on graphite [1] and MgO [2], in conformity with the results [2] of calculation of the energy of electrokinetic interaction, is less than that of n-hexane. The adsorption heats of olefins on graphite are less than those of paraffins [3]. However, on magnesium hydroxide [4] or silica [5,6], the adsorption heats of benzene [4,5] and propene [6] are greater than those of n-hexane and propane. In accordance with this, when benzene is adsorbed on hydrated silica, the infrared absorption bands of the surface hydroxyl groups are shifted to a greater extent than when n-hexane is adsorbed [7,8]. This shift is also greater for adsorbed nitrogen than for adsorbed argon [9], whereas on graphite the adsorption heats of these gases are similar [10]. Dehydration of the silica surface reduces the adsorption heat of benzene to a value less than that for n-hexane [5].

The first attempt to investigate the nature of this increased interaction of benzene with surface hydroxyl was made by D. P. Poshkus and one of us [11]; this was based on an approximate appraisal of the distribution of π -electron charge in the benzene molecule and the Coulomb interaction of this charge and the residual charges of the carbon skeleton with the point charges of the hydroxyl group. It was of interest to make a more complete calculation of the electron density distribution both in the adsorbate molecule and in the adsorbent surface. In the present paper we have carried out a second step: We have considered the interaction of a benzene molecule with a dipole using a crude model, in which the dipole is considered, as before, as a pair of point charges, but account is taken of both the π - and σ -bonds in the benzene molecule, using the method of molecular orbitals*.

Geometry of the System. The C-C spacing in the benzene molecule was taken as 1.39 Å, and the C-H spacing as 1.04 and 1.12 Å (the range of values in the literature is 1.08 ± 0.04 Å). The OH dipole was assumed to be in a straight line perpendicular to the plane of the benzene ring and passing through its center; two sets of values were taken for the distances of the H and O atoms from its center: 1) H atom 2.15 Å, O atom 3.12 Å, and 2) H atom 3.12 Å, O atom 4.09 Å. The first pair of values corresponded to the closest possible packing of the dipole with the molecule [11], the second was chosen to facilitate calculation, since the H atom center in the second variant coincided with the O atom center in the first variant. This pair of values was close to the sum of the Van der Waals semithickness of the benzene molecule and the Van der Waals radius of an H atom. The effective terminal charge of the dipole was taken as $q_O = q_H = 1.6 \cdot 10^{10}$ absolute units [11].

Model of the Benzene Molecule. Slater's form was used for the wave function of the electrons in the intermolecular bonds of the molecule. It was assumed that the σ -bonds were localized and the π -bonds delocalized. The various component molecular orbitals to be considered were:

* A detailed description of the calculation is given in [12].

1) The molecular orbitals localized at the bonds between the carbon atoms C_i and C_{i+1} , in the form:

$$^1\psi_{i,i+1} = \frac{1}{\sqrt{2(1+S_{C-C})}} (\chi_{i,i+1} + \chi_{i+1,i}), \quad (1)$$

where $\chi_{i,i+1}$ is the sp^2 orbital of the atom i in the direction of the atom $i+1$, and S_{C-C} is the overlap integral.

2) The molecular orbitals forming bonds between C_i atoms and adjacent H atoms, in the form:

$$^2\psi_i = \frac{1}{\sqrt{1+2aS_{C-H}+a^2}} (\chi_{iH} + a\eta_i), \quad (2)$$

where χ_{iH} is the sp^2 orbital of the atom C_i in the direction of the adjacent H atom, η_i is the $1s$ orbital of this H atom, and S is the overlap integral. Since no precise value is known for the coefficient a , associated with the polarity of the C-H bond, we used values of 1.2, 1.0, 0.8, and 0.6; the H atom is the more positive, so that the most probable value is between 0.8 and 1.0. The dipole of the C-H bond does not determine a .

3) The molecular orbitals of the delocalized π -bonds, in the form:

$$^3\psi_1 = \frac{1}{\sqrt{6(1+2S)}} \sum_{j=1}^6 (p_z)_j; \quad ^3\psi_{2,3} = \frac{1}{\sqrt{6(1+S)}} \sum_{j=1}^6 e^{\pm 2\pi i j/6} (p_z)_j, \quad (3)$$

where S is the overlap integral of the p_z orbitals with adjacent C atoms.

If the x axis is taken in the direction of the C_i-C_{i+1} bond, then the orbitals are:

$$\chi_{i,i+1} = \frac{1}{\sqrt{3}} (2s)_{C_i} + \sqrt{\frac{2}{3}} (2p_x)_{C_i}. \quad (4)$$

The hybridized atomic orbitals χ_{iH} are determined similarly, if the x axis is taken in the direction of the C-H bond.

The atomic orbitals are expressed by the wave functions:

$$\begin{aligned} (1s)_H &= \sqrt{1/\pi} e^{-r}; & (2s)_C &= \kappa \sqrt{\gamma^3/3\pi} r e^{-\gamma r} - \omega \sqrt{\beta^3/\pi} e^{-\beta r}; \\ (2p_x)_C &= \sqrt{e^0/\pi} r e^{-\epsilon r} \sin \vartheta \cos \varphi; & (2p_y)_C &= \sqrt{e^0/\pi} r e^{-\epsilon r} \sin \vartheta \sin \varphi; \\ & & (2p_z)_C &= \sqrt{e^0/\pi} r e^{-\epsilon r} \cos \vartheta \end{aligned} \quad (5)$$

The following values were used for the parameters: $\kappa = 1.054$, $\omega = 0.249$, $\gamma = 1.68$, $\beta = 4.52$, $\epsilon = 1.51$ [13] (r, ϑ, φ are spherical coordinates).

Calculation of the Interaction Energy. Deformation of the electronic cloud of the molecule could be neglected in view of the large distance between molecule and dipole, so that the interaction energy could be calculated by the perturbation method, only considering first order terms. We found the difference in interaction energy of the molecule with both poles of the dipole. The change in energy of the molecule under the influence of the point charge q , whose position is given by the vector R , is determined by the equation:

$$\frac{\Delta E}{eq} = -2 \sum_{i=1}^N \int \frac{|\psi_i(r)|^2}{|R-r|} d^3r + \sum_{k=1}^M \frac{z_k}{|R-\rho_k|}, \quad (6)$$

where N is the number of occupied orbitals in the molecule, M is the number of atoms, and z_k and ρ_k are the

nuclear charge and radius-vector of the k -th atom. Expressing the molecular orbitals ψ_i in terms of the atomic orbitals φ_j , in accordance with the equation $\psi_i = \sum c_{ij} \varphi_j$, we obtain:

$$\int \frac{|\psi_i(\mathbf{r})|^2}{|\mathbf{R} - \mathbf{r}|} d^3\mathbf{r} = \sum_j |c_{ij}|^2 \alpha_j + \sum_{j \neq k} \bar{c}_{ij} c_{ik} \beta_{jk}, \quad (7)$$

where

$$\alpha_j = \int \frac{|\varphi_j(\mathbf{r})|^2}{|\mathbf{R} - \mathbf{r}|} d^3\mathbf{r}; \quad \beta_{jk} = \int \frac{\varphi_j(\mathbf{r}) \varphi_k(\mathbf{r})}{|\mathbf{R} - \mathbf{r}|} d^3\mathbf{r}. \quad (8)$$

Equations (6), (7), and (8) are general in character. For interaction of a benzene molecule with an OH dipole, the change in energy must have the form:

$$\Delta E = \Delta E_{C-C} + \Delta E_{C-H} + \Delta E_{\pi}. \quad (9)$$

The separate contributions to the interaction energy can be expressed as the sums of the Coulomb terms $\Delta E^{(Q)}$ and the exchange terms $\Delta E^{(V)}$.

The latter have no classical analogy and depend on the bond conditions, i.e., on the distribution of atomic orbitals with regard to molecular orbitals.

Calculation of Integrals. In calculating the Coulomb integrals, the hybridized wave functions are expressed as in (5). The corresponding bicentric integrals were calculated as in [14], and it was found sufficient to retain only the terms expressing the dipole and quadrupole interactions. The tricentric integrals in β_{jk} were accordingly calculated using the quadrupole approximation. For the same reason, the integrals of all types were calculated using this approximation.

RESULTS AND DISCUSSION

The Coulomb $F^{(Q)}$, exchange $F^{(V)}$, and total $F^{(T)}$ interaction energies of benzene with the dipole, whose poles are at distances Z_1 and Z_2 from the center of the benzene ring, were calculated from the equation:

$$F^{(L)} = \Delta E^{(L)}(Z_1) - \Delta E^{(L)}(Z_2); \quad L = Q, V, T \quad (10)$$

where $\Delta E^{(L)}(Z_1)$ and $\Delta E^{(L)}(Z_2)$ are the interaction energies of poles 1 and 2 with the different bonds of the molecule. The highest absolute values of the contributions to the total energy $F^{(T)}$ arise from interaction of the dipole σ -bonds. Thus, for a mean value of a between 1.0 and 0.8, and with $Z_1 = 2.15$ A, $F_{C-C}^{(T)} = -13.3$, $F_{C-H}^{(T)} = +15.7$, $F_{\pi}^{(T)} = -5.8$, so that $F^{(T)} = -3.4$ kcal/mole (with $Z_1 = 3.12$ A, $F_{C-C}^{(T)} = -4.7$, $F_{C-H}^{(T)} = +6.1$, and $F_{\pi}^{(T)} = -2.9$, so that $F^{(T)} = -1.5$ kcal/mole). The contributions of the σ -bonds C-C and C-H have opposite signs and partially compensate for each other, so that in this calculation, as in [11], the π -bond contributions is more important, but is comparable in magnitude to the total σ -bond contribution. The interaction energies $F^{(Q)}$ and $F^{(T)}$ for the whole benzene molecule are shown in Table 1. They vary only slightly with the possible variations in length of the C-H bond, but are strongly dependent on a . For the most probable value of $a = 0.8$ to 1.0, they are in agreement with the measured difference in the heats of adsorption of benzene on a silica surface with and without hydroxyl groups (up to 3 kcal/mole [5]). However, this agreement should not be overrated, since the energy is obtained as the difference between large terms, and the physical nature of the effect is complicated. Thus the Coulomb integral type terms in the total energy largely cancel each other, and it is the exchange terms

* The exchange terms $\Delta E^{(V)}$ are formed from the terms β_{ik} in (7).

which actually determine the energy, but these are very sensitive to the choice of model, particularly to the value of a . It is very difficult to estimate to what extent the calculated value of the energy depends on the atomic orbital parameters.

Calculations were made for only one position of the molecule with respect to the dipole. The values and signs of the contributions of the different groups are very sensitive to the geometry of the system for a complex molecule. The contributions of the single bonds, in particular, strongly depend on the orientation of the molecule with respect to the dipole. Great interest therefore attaches to similar calculations for different relative positions and orientations of benzene molecule and hydroxyl.

TABLE 1

Calculated Interaction Energies of a Benzene Molecule with an OH Dipole. $F^{(Q)}$ in kcal/mole for Different Distances to the Dipole Centers Z_1 and Z_2 , and for Different Lengths of the C-H Bond

a		C-H 1.04 Å		C-H 1.12 Å	
		$Z_1 = 2.15$ Å	$Z_1 = 3.12$ Å	$Z_1 = 2.15$ Å	$Z_1 = 3.12$ Å
		$Z_2 = 3.12$ Å	$Z_2 = 4.09$ Å	$Z_2 = 3.12$ Å	$Z_2 = 4.09$ Å
0.6	$F^{(Q)}$	3.94	1.48	4.19	1.59
	$F^{(T)}$	-6.63	-2.92	-7.47	-3.33
0.8	$F^{(Q)}$	1.38	0.45	1.60	0.54
	$F^{(T)}$	-4.31	-1.82	-4.84	-2.08
1.0	$F^{(Q)}$	-0.49	-0.31	-0.31	-0.24
	$F^{(T)}$	-2.47	-0.98	-2.78	-1.09
1.2	$F^{(Q)}$	-1.90	-0.88	-1.75	-0.82
	$F^{(T)}$	-1.06	-0.27	-1.14	-0.29

It should also be appreciated that the experimental values for the differences in heat of adsorption on hydrated and dehydrated silica surfaces may be affected by differences in geometry as well as by the different contributions of the dispersive forces in both cases. We therefore consider that the greatest interest attaches, not so much to the agreement of the calculated value for the interaction energy of a benzene molecule and an OH dipole with the measured change in the adsorption heat of benzene on dehydrated silica, but rather to the establishment of a method for calculating the connection between this effect and the quantum-mechanical nature of the model used. It has already been noted that the main contribution to the interaction energy comes from the exchange integral. For this reason the observed difference in behavior of benzene and hexane on a hydrated surface is more quantitative than qualitative in character, in conformity with the changes in the infrared spectra [8,9].

Theoretical and experimental work in this direction should undoubtedly help to elucidate the nature of these effects in concrete cases. It would be of interest to investigate the adsorption of molecules of different structure and to make the most detailed possible calculations of the electron structure of adsorbate and adsorbent. The possible role of the pure exchange effect should be studied.

LITERATURE CITED

1. N. N. Avgul', G. I. Berezin, and A. V. Kiselev, *Izvest. Akad. Nauk SSSR, Otdel. Khim. Nauk*, 1304 (1956); A. A. Isirikyan and A. V. Kiselev, *Zhur. Fiz. Khim.*, **35** (1961).
2. N. N. Avgul', A. A. Isirikyan, et al., *Izvest. Akad. Nauk SSSR, Otdel. Khim. Nauk*, 1314 (1957); 1196 (1959); A. V. Kiselev and D. P. Poshkus, *Zhur. Fiz. Khim.*, **32**, 2824 (1958).
3. B. A. Bezus, V. P. Dreving, and A. V. Kiselev, *Kolloid. Zhur.*, **23** (1961).
4. A. V. Kiselev and D. P. Poshkus, *Kolloid. Zhur.*, **29**, 25 (1960).
5. L. D. Belyakova and A. V. Kiselev, *Collection: The Production, Structures, and Properties of Adsorbents* [in Russian] (1959), p. 180.

6. A. B. Bezus, V. P. Dreving, and A. L. Klyachko-Gurvich, *Kolloid. Zhur.*, 23 (1961).
7. A. N. Terenin, *Collection: Surface Chemical Compounds and their Role in Adsorption Phenomena* [in Russian] (Moscow State University, 1957), p. 206.
8. A. V. Kiselev and V. I. Lygin, *Kolloid. Zhur.*, 23 (1961).
9. R. S. McDonald, *J. Am. Chem. Soc.*, 79, 850 (1957); G. J. C. Frohnsdorff and G. L. Kington, *Trans. Farad. Soc.*, 55, 1173 (1959).
10. S. Ross and W. Winkler, *J. Colloid. Sci.*, 10, 319 (1955).
11. A. V. Kiselev and D. P. Poshkus, *Doklady Akad. Nauk SSSR*, 120, 834 (1958).
12. Ya. Koutetski and I. Chizhek, *Zhur. Fiz. Khim.*, 35 (1961).
13. P. M. Morse, L. A. Young, and E. S. Haurwitz, *Phys. Rev.*, 48, 948 (1935).
14. C. C. J. Roothan, *J. Chem. Phys.*, 19, 1445 (1951).

All abbreviations of periodicals in the above bibliography are letter-by-letter transliterations of the abbreviations as given in the original Russian journal. *Some or all of this periodical literature may well be available in English translation.* A complete list of the cover-to-cover English translations appears at the back of this issue.



THE EFFECT OF CHLORIDE IONS ON THE ELECTROCHEMISTRY OF ZIRCONIUM AND ITS CORROSION

Ya. M. Kolotyркиn and V. A. Gil'man

L. Ya. Karpov Institute of Physical Chemistry

(Presented by Academician A. N. Frumkin, October 20, 1960)

Translated from *Doklady Akad. Nauk SSSR*, Vol. 2, No. 3,

pp. 642-645, March, 1961

Original article submitted October 13, 1960

The available data indicate [1-4] that zirconium and many of its alloys are highly stable to corrosion by alkaline and mineral acid solutions, including solutions of HNO_3 and H_2SO_4 at moderate concentrations. On the other hand, the stability of Zr toward chloride ion solutions varies markedly from case to case depending on the nature of the other substances which may be present. Thus Zr is highly stable to corrosion by solutions of HCl or various metallic chlorides [1-3] although the metal is quite soluble in mixed HCl, HNO_3 solutions and in solutions of FeCl_3 and CuCl_2 [2,3].

The results of [1-4] do not give an adequate basis for understanding these variations in the corrosional resistance of zirconium towards various solutions. The authors of these papers limited themselves, unfortunately, to a mere determination of corrosional losses without taking any account of the electrode potential of the corroding metal. It is obvious, however, that the behavior of Zr varies because the potential established on the metal in various solutions is not constant. This fact has been definitely confirmed in [5,6] where it has been shown that the above-noted high corrosional stability of the metal toward solutions of pure HCl and alkali metal chlorides can be broken down by subjecting the metal to anodic polarization and displacing its electrode potential to a certain critical value.

A more detailed study of the relation between the rate of dissolution of Zr and its potential has been carried out in the present work with a view to elucidating the observed effects of solution composition and other factors on the corrosional behavior of the metal.

This problem was attacked through the potentiostatic method which has been described in [7,8], measurements on HCl solutions of 1.0, 0.1, and 0.01 N concentration being compared with measurements on 1.0 N solutions of H_2SO_4 , KBr, and KI. Sheets of zirconium foil with apparent surface areas of 1 and 3 cm^2 were used as electrodes. This Zr was 99.8% pure and contained 0.065% hafnium. These sheets were degreased prior to experiment by treatment with ethyl ether, after which they were briefly etched in 5% HF, and then washed in tap water and in doubly distilled water. The solutions were prepared from doubly distilled water and triply distilled, chemically pure, HCl and H_2SO_4 . Purified nitrogen was used to saturate each solution for an extended period prior to experiment and was also passed through the solution during the experiment.

The measurements showed the stationary potential and rate of spontaneous dissolution of zirconium in 1.0 N H_2SO_4 to be -0.16 to -0.18 v* and $5 \cdot 10^{-7}$ amp/ cm^2 ** , respectively. The potentiostatic curve (Fig. 1, Curve 1) shows that Zr is passive in 1 N H_2SO_4 even before anodic polarization and that this passivity is maintained over the entire range of potentials.

* The potentials quoted here and in the sequence are measured relative to the normal hydrogen electrode.

** These results are rather close to the values obtained by Balashova and Kabanov [15].

Passage to HCl solutions brings about no appreciable alteration in either the stationary potential or the rate of spontaneous dissolution. The relation between potential and rate of dissolution is at first the same here as in the H_2SO_4 solution. This relation is maintained, however, only up to a certain critical potential, φ_c , where the dissolution of the Zr becomes unlimited in the sense that the potential remains essentially constant as the current density is increased under stationary conditions. For potentiostatic measurements, this amounts to saying that an increase in the anodic current is accompanied by only a brief displacement of the potential in the direction of positive values, after which there is a rapid return to the original value φ_c (Fig. 2). Figure 2 also shows that reduction of the current density at φ_c leads to no more than brief displacement of the potential in the negative direction with a subsequent rapid return to the original value.

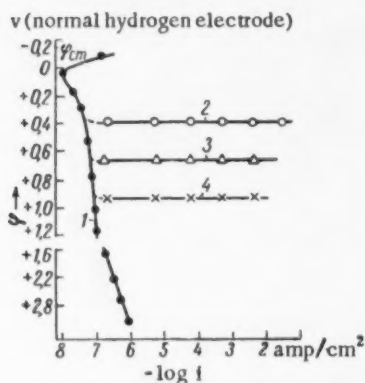


Fig. 1. Potentiostatic curves for Zr in the following solutions: 1) 1 N H_2SO_4 ; 2) 1 N HCl; 3) 1N KBr; 4) 1 N KI.

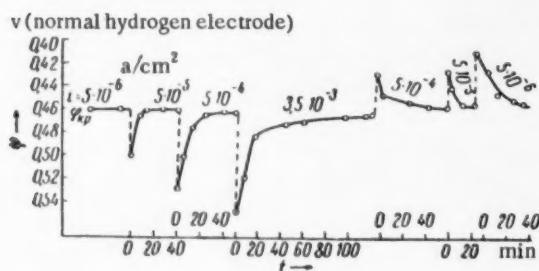


Fig. 2. Alteration of the potential while successively increasing and diminishing the current density in 0.1N HCl.

reversible in the sense that elimination of the sources of activation will return the metallic surface into its passive condition. This reversibility can be accounted for by supposing that two mutually competing reactions are in progress on the metallic surface under the conditions which are in question here, namely: passivating adsorption of the oxygen of the water and the displacement of this oxygen by the halide ions.*

The fact that the halide ions can begin to displace oxygen only after a definite potential has been established justifies the conclusion that pitting corrosion can result only when the corroding metal has a higher affinity for oxygen than for the corresponding halide under normal conditions. Anodic polarization and the resulting in-

These results are confirmed by the charging curves of Fig. 3 which show that the Zr is initially polarized to potentials which are much more positive than φ_c . It was found here that the maximum departure of the potential from φ_c increases with an increase in the current density at fixed Cl^- ion concentration and rises with a diminution of the Cl^- ion concentration at fixed current density. The magnitude of φ_c is markedly dependent on the Cl^- concentration and completely independent of the pH of the solution. A ten-fold increase in the chloride ion concentration was accompanied by an approximate 65 mv displacement of φ_c in the direction of negative values. This observation is in good agreement with the results obtained earlier in [5,6].

The behavior of Zr in bromide and iodide solutions is essentially the same as in chloride solutions. Figure 1 shows that passage from Cl^- to Br^- to I^- serves only to displace the value of φ_c in the positive direction. By special experiments it was proven that the addition of trivalent iron to a HCl solution has the same effect on the behavior of Zr as anodic polarization, the potential being displaced in the positive direction until a certain critical value, φ_c , is reached and then remaining constant as the Fe^{3+} ion content of the solution is increased further.

Pitting results once this critical value, φ_c , is reached (either by anodic polarization or by the introduction of Fe^{3+} ions into the solution) and dissolution of the zirconium surface is seen to be a definitely localized process. The extent of pitting is increased by increasing the density of the polarizing current, reduction of this current leading, in turn, to the passivation of the pits which had been formed earlier.

On the basis of these data it can be concluded that the aggressive action of the chloride ions is related to the depassivation of a part of the metallic surface, the observed effect being essentially dependent on the polarizing current density and completely

* A similar mechanism for the anodic action of Fe in alkaline chloride solutions was proposed earlier by Vanyukova and Kabanov [14].

crease in the positive charge of the metallic surface are accompanied by polarization and increased chemical activity of the halide ions. Thus the establishment of this certain potential on the surface produces those conditions under which the affinity of the metal for the halide begins to exceed its affinity for oxygen.

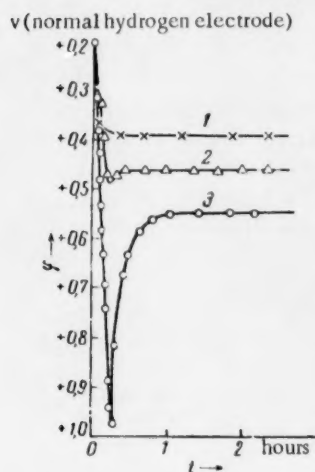


Fig. 3. Charging curves at $i = 5.0 \cdot 10^{-6}$ amp/cm² in HCl solutions of the concentrations: 1) 1.0 N; 2) 0.1 N; 3) 0.01 N.

It is clear that the possibility of adsorptional displacement of the passivating oxygen by halide ions is determined not only by the magnitude of the electrode potential but also by the concentration of halide ions at the metallic surface. This concentration must reach a certain critical value. Engell and Stolica [9] have recently shown that chloride ions will stimulate the corrosion of passive iron only after their concentration has reached a certain critical value.

The question naturally arises as to why it is not the entire surface that is depassivated but only individual, comparatively small, sections whose number increases as the current density rises. We believe that this is due to the fact that current transfer is the principal means of furnishing halide ions to the metallic surface. This supposition is supported by the observed relation between the effectiveness of the chloride ions and the nature and concentration of the basic electrolyte. For example, our measurements show that the above-mentioned effect of Cl⁻ ions on the anodic dissolution of zirconium in sulfate solutions disappears completely when the concentration ratio of sulfate to chloride approaches five. However, the critical concentration ratio is practically doubled if a perchlorate (with a univalent anion) is used as the basic electrolyte and approaches 9-11.

The anodic current is not uniformly distributed over the surface since the dissolution of a solid metal is always non-uniform to a certain degree and it is natural to expect that the concentration of halide ions would first reach the critical value over those few sectors where the dissolution is most rapid. The initiation of activation on these sectors will clearly give rise to a still more pronounced non-uniformity in the current distribution and a still more preferentially directed supply of ions to them. The value of ϕ_c for zirconium in chloride solutions of ordinary concentrations is considerably more positive than the passivation potential of the metal so that dissolution can be expected to be limited by diffusion and an increase in the polarizing current must then invariably lead to an increase in the number and dimensions of the pits. The true current density will, for this reason, remain constant, and it is obviously this fact which accounts for the observation that the potential remains constant over a wide interval of current densities calculated from apparent surface areas.

After displacing the passivating oxygen, the halide ions might be reasonably supposed to participate directly in the elementary act of ionization of the zirconium atoms [10,11], forming complexes of the type $ZrCl_n^{(4-n)+}$ as initial dissolution products. A retardation of reaction would be expected under these conditions, however, since the halide ions are fed into the reaction zone quite slowly. Our measurements have failed to confirm this conclusion, since they show no marked deviation of the potential from the critical value, with increase of the current density up to 100 ma/cm², even at comparatively low Cl⁻ ion concentrations (Fig. 1). This result can be explained by taking account of the above-mentioned fact that the metal has a higher affinity for oxygen than for the chlorine. Under these conditions, complex ions of the type in question must invariably hydrolyze as they diffuse from the metallic surface into solution thereby forming oxygen-metal complexes and free halide ions which can again participate in the reaction. Thus the halide ions function as special catalysts for the corrosion of zirconium although they themselves do not enter into the chemical products of the reaction.

The available data make it appear likely that the mechanism proposed for the formation and development of pits in Zr would also be applicable to such metals as Mg [12], Al [13], and Fe [14].

LITERATURE CITED

1. E. A. Gee, L. B. Golden, and W. E. Lusby, *Ind. and Eng. Chem.*, **41**, 1668 (1949).
2. D. F. Taylor, *Ind. and Eng. Chem.*, **42**, 639 (1950).
3. L. B. Golden, I. R. Lane, and W. L. Acherman, *Ind. and Eng. Chem.*, **44**, 1930 (1952); **45**, 782 (1952).
4. I. R. Lane, L. B. Golden, and W. L. Acherman, *Ind. and Eng. Chem.*, **45**, 1067 (1953).

5. N. Hackerman and O. B. Cecil, *J. Electrochem. Soc.*, 101, 419 (1954).
6. M. Maraghini, G. B. Adams, and P. Van Rysselberghe, *J. Electrochem. Soc.*, 101, 400 (1954).
7. Ya. M. Kolotyrkin and V. M. Knyazheva, *Zh. Fiz. Khim.*, 30, 1990 (1956).
8. V. M. Knyazheva and Ya. M. Kolotyrkin, *Doklady Akad. Nauk SSSR*, 114, 1265 (1957).
9. H. J. Engell and N. D. Stolica, *Zs. Phys. Chem., N. F.*, 20, 113 (1959).
10. Ya. M. Kolotyrkin and L. A. Medvedeva, *Zhur. Fiz. Khim.*, 29, 1477 (1955).
11. V. V. Losev and A. I. Molodov, *Doklady Akad. Nauk SSSR*, 130, 111 (1960).
12. D. V. Kokoulina and B. N. Kabanov, *Doklady Akad. Nauk SSSR*, 112, 682 (1957); 120, 558 (1958).
13. N. D. Tomashov and V. N. Modestova, *Studies on the Corrosion of Metals [in Russian] (Acad. Sci. USSR Press, 1951)*, p. 75.
14. L. V. Vanyukova and B. N. Kabanov, *Doklady Akad. Nauk SSSR*, 59, 917 (1948).
15. N. Balashova and B. N. Kabanov, *Doklady Akad. Nauk SSSR*, 121, 126 (1958).

All abbreviations of periodicals in the above bibliography are letter-by-letter transliterations of the abbreviations as given in the original Russian journal. *Some or all of this periodical literature may well be available in English translation.* A complete list of the cover-to-cover English translations appears at the back of this issue.

ELECTRICAL PROPERTIES OF ALKALINE EARTH,
RARE EARTH, AND THORIUM HEXABORIDES

Yu. B. Paderno and G. V. Samsonov

Institute of Metal Ceramics and Special Alloys, Academy of Sciences Ukr. SSR

(Presented by Academician A. N. Frumkin, November 18, 1960)

Translated from Doklady Akad. Nauk SSSR, Vol. 2, No. 3,

pp. 646-647, March, 1961

Original article submitted November 17, 1960

An investigation of the electrical properties of the hexaborides of alkaline earth and rare earth metals and of the actinides is of considerable interest not only because it would lead to a better understanding of the nature of their physical properties, but also in connection with the many uses which these compounds have found as cathodes in the electronic components of high-power generators [1]. A number of papers have been devoted to the study of the electrical resistance [2-4] and the thermal e.m.f.'s [4,5] of some of these borides and the Hall coefficients of lanthanum and samarium borides [3,6]. The data, however, were not systematic, the experiments were carried out under diverse conditions, and in some cases the effects of porosity (which was sometimes as high as 50%) were not taken into account.

In the present work the specific electrical resistance, the Hall effect, the thermal e.m.f., and the temperature coefficient of electrical resistance of each compound were all determined on the same sample. The samples were cut out of hot-rolled boride bars by the electrical erosion method in the shape of parallelepipeds $12 \times 2.5 \times 0.5$ mm. The samples had porosities ranging from 1.5 to 22%. Good electrical contacts were ensured by depositing some copper electrolytically on the ends of each sample.

The Hall effect was measured in a 12500 oersted field. The thermal e.m.f. of copper, which served as one component of the experimental couples, was taken into account in calculating the absolute thermal e.m.f.'s of our samples [7].

We used from 3 to 8 samples of each compound in our measurements, which enabled us to extrapolate satisfactorily the obtained resistances and Hall effects to zero porosity (using the method of least squares).

The results are compiled in Table 1. In order to see if a single-band model could be used to represent these compounds (as was done in [8]) we determined the values of $\delta \approx R/ep^2 \approx n_+ u_+^2 - n_- u_-^2$ [since if charge carriers of both signs are assumed the Hall coefficient will be $R = (1/e) (n_+ u_+^2 - n_- u_-^2) / (n_+ u_+ + n_- u_-)^2$ and the resistance $p = (1/e) 1 / (n_+ u_+ + n_- u_-)$], which are also listed in Table 1.

One can readily see that with the exception of SmB_6 all the compounds have fairly large absolute values of δ , which indicates that electronic conduction is quite important in the hexaborides. Keeping this in mind and assuming a single-band model we calculated the concentrations n^* (per metal atom) and the mobilities u^* of the effective charge carriers.

In all the cases, with the exception of SmB_6 , the number of effective charge carriers in the hexaborides of trivalent rare earth metals come out very close to integral numbers which provides additional evidence that a single-band model can be used for these compounds.

The concentration of free electrons in the hexaborides of divalent metals (calcium, strontium, barium, europium, and ytterbium) is very low since all of the valence electrons participate in bond formation, i.e., the valence levels are filled. The relatively low resistance of these compounds can be attributed to the high mobility

of charge carriers which in turn is connected with the fact that these carriers are not spread throughout the filled levels. The mobility is particularly high in ytterbium hexaboride, in which a high-lying 4f-level is filled.

TAP

Electrical Properties of Hexaborides

Boride	Sp. el. res. ρ , in ohm · cm	Hall coeff. $R \cdot 10^4$, $\text{cm}^3/\text{coulomb}$	Thermal e.m.f., $\mu\text{V}/\text{deg}$	Temp. coeff. of el. res., $\alpha \cdot 10^3 \text{ deg}^{-1}$ (0-100°)	Charge carrier conc., n^* , el./Met. atom.	Carrier mobility u^* , $\text{cm}^2/\text{v} \cdot \text{sec}$	$\delta \cdot 10^{23}$, $\text{cm}^3/\text{v}^2 \cdot \text{sec}^2$
Ca B ₆	222	-91,0	-32,8	+1,16	0,05	41,0	-11,5
Sr B ₆	111	-76,3	-30,3	+0,83	0,06	68,7	-38,7
Ba B ₆	77	-57,5	-26,2	+1,08	0,08	74,7	-60,5
Y B ₆	40	-4,56	-0,5	+1,24	0,96	11,4	-17,8
La B ₆	15,0	-4,96	+0,1	+2,68	0,90	33,1	-137,8
Ce B ₆	29,4	-4,18	+2,8	+1,00	1,06	14,2	-30,2
Pr B ₆	19,5	-4,33	-0,6	+1,92	1,02	22,2	-71,1
Nd B ₆	20,0	-4,39	+0,4	+1,93	1,00	22,0	-68,5
Sm B ₆	207,0	+1,54	+7,6	-0,42	2,86	0,74	+0,2
Eu B ₆	84,7	-50,2	-17,7	+0,90	0,09	59,3	-43,7
Gd B ₆	44,7	-4,39	+0,1	+1,40	0,94	9,8	-13,7
Tb B ₆	37,4	-4,57	-1,1	+1,31	0,94	12,2	-20,4
Yb B ₆	46,6	-83,6	-25,5	+2,34	0,05	179,4	-240,3
Th B ₆	14,8	-2,18	-0,6	+2,31	1,99	14,7	-62,1

The hexaborides of trivalent rare earth metals are characterized by the presence of a single free electron per metal atom, while tetravalent thorium derivatives have two free electrons. This is fully consistent with the observed similarity of the bonds in all isomorphous hexaborides.

The hexaborides of trivalent metals and of thorium have very small thermal e.m.f.'s due to the high concentration of free electrons. The borides of divalent metals have considerably higher thermal e.m.f.'s, which also slightly decline in the order: CaB₆, SrB₆, BaB₆.

The temperature thermal coefficients of electrical resistance remain positive in the 0-100° temperature range, with the exception, again, of samarium hexaboride, in which it is negative (up to 300°, above the temperature the resistance begins to increase). It is also worth noting that in samarium metal the Hall effect also exhibits anomalous temperature dependence.

LITERATURE CITED

1. G. V. Samsonov, Uspekhi Khim. 27, 189 (1959).
2. G. V. Samsonov and A. E. Grodshstein, Zhur. Fiz. Khim. 30, 379 (1956).
3. J. Lafferty, J. Appl. Phys., 22, 299 (1951).
4. U. B. Paderno and G. V. Samsonov, Doklady Akad. Nauk Ukr. SSR, No. 11, 1215 (1959).
5. G. V. Samsonov and N. S. Strel'nikova, Ukr. Fiz. Zhur. 3, 135 (1958).
6. B. Post, D. Moskovich, and F. Glezer, Coll. Refractory and Corrosion-Resistant Metal Ceramics [in Russian] (Moscow, 1959), p. 183.
7. A. A. Rudnitskii, The Thermoelectric Properties of Noble Metals and Their Alloys [in Russian] (Izd AN SSSR, 1956), p. 25.
8. S. N. L'vov, V. F. Nemchenko, and G. V. Samsonov, Doklady Akad. Nauk SSSR, 135, No. 3 (1960).

THE MOBILITY OF ATOMS ON THE SURFACE OF A CRYSTAL AT ITS MELTING POINT

V. I. Shimulis and V. M. Gryaznov

M. V. Lomonosov Moscow State University

(Presented by Academician M. M. Dubinin, November 14, 1960)

Translated from *Doklady Akad. Nauk SSSR*, Vol. 2, No. 3,
pp. 648-651, March, 1961

Original article submitted November 11, 1960

The thermodynamics of certain adsorption processes shows that the entropy of two-dimensional translatory movement of the adsorbate molecules must be taken into account, even at relatively low temperatures [1]. Mobility of the surface atoms of a crystal is observed at temperatures in excess of $0.3 T_{mp}$ (see [2], for example) and is designated as mobile autoadsorption in what follows. Mobile autoadsorption of surface atoms has been drawn on to explain the details of the catalytic activity of platinum and palladium at high temperatures [3-5]. The experimentally determined values of frequency factors for catalytic reactions are in satisfactory agreement with the values obtained from calculations in which allowance is made for the entropy of two-dimensional movement of the metal atoms [4]. These facts lend interest to an evaluation of the degree of mobility of atoms on the surface of a crystal at its melting point.

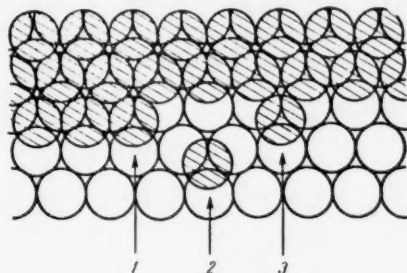


Fig. 1. Schematic representation of a section of a densely packed face: 1) Atom in a step kink; 2) atom which has undergone immobile adsorption on face; 3) atom which has undergone immobile adsorption at the step.

Experimental and theoretical studies of the transfer of matter between crystal and vapor, or crystal and melt, have shown [6] the crystal face to carry incompleting layers, one particle in depth, whose edges function as steps. A schematic representation of a section of a densely packed face is given in Fig. 1. The shaded atoms are ones which are located in the uppermost layer. Surface atoms in positions 1, 2, and 3 differ with respect to the number of bonds which are shared with other atoms. Let φ represent the energy of bonding of a surface atom to its nearest neighbor and φ' , the energy of bonding of this same atom to its next nearest neighbor. The difference in the number of bonds for two positions of a given atom can be considered as a measure of the change in enthalpy per atom in passage of the system from the one state to the other. Mere reduction of the strength of one or two of these bonds can carry the individual atom from a state of immobile adsorption on a face into a state of mobile adsorption, even though the bonds are not ruptured. This fact is reflected in Table 1 by the coefficient α , a quantity less than unity. The value of α is fixed by the nature of the crystal and by the face which is under consideration and is constant for a given substance throughout any one line of Table 1. Evaluation of the energy of bonding on the basis of the usual assumptions that ΔH_4^0 is equal to the heat of sublimation and that $\varphi \gg \varphi'$ has led to the φ values for 28 metals at their melting points which are given in Table 2.

The transfer of an atom from the body of the lattice into positions 1, 2, or 3 (Fig. 1) involves only a slight change in entropy [6,7]. On the other hand, passage into a state of mobile autoadsorption in which each atom

has one vibrational and two translational degrees of freedom relative to the lattice, will be accompanied by a considerable change in the entropy. In the isotropic crystal the frequency of vibration of an atom which has undergone mobile adsorption can be assumed to be lower, and the anharmonicity higher, than that of an atom in the body of the lattice since bonding with the lattice is weaker than bonding at a crystal lattice point. Thus the vibrational entropy of a mobile adsorbed atom must be higher than the entropy which an atom located at a crystal lattice point possesses because of its vibration along a normal coordinate. Since the magnitude of the entropy is a measure of the degree of disorder of the system, it follows that the entropy associated with a single degree of vibration of any type will be less than that associated with a single degree of translatory movement.

TABLE 1

Enthalpy Changes Accompanying Certain Types of Transfer of Atoms

Lattice type	Face	ΔH_1^0	ΔH_2^0	ΔH_3^0	ΔH_4^0
Hexagonal close packed, A3	(0001)	3 ϕ	$\alpha\phi$	3 $\phi + \alpha\phi$	6 $\phi + 3\phi'$
Face-centered cubic, A1	(111)	3 ϕ	$\alpha\phi$	3 $\phi + \alpha\phi$	6 $\phi + 3\phi'$
Body-centered cubic, A2	(100)	2 $\phi + 2\phi'$	2 $\alpha\phi$	2 $\phi(1 + \alpha) + 2\phi'$	6 $\phi + 3\phi'$
	(110)	2 $\phi + \phi'$	$\alpha(\phi + \phi')$	$\phi(2 + \alpha) + \phi'(1 + \alpha)$	4 $\phi + 3\phi'$
	(100)	2 ϕ	2 $\alpha\phi$	2 $(\phi + \alpha\phi)$	4 $\phi + 3\phi'$

Note. ΔH_1^0 - step kink - adsorption on face; ΔH_2^0 - adsorption on face - mobile autoadsorption; ΔH_3^0 - step kink - mobile autoadsorption; ΔH_4^0 - step kink - vapor.

TABLE 2

Calculated Values of the Heat of Transfer of Certain Metal Atoms from a Step Kink into a State of Mobile Autoadsorption

Lattice type	Element	Melting point, °K	$\Delta S^* T_{mp}$, entropy units		$\Delta H^* T_{mp}$, kcal/g-at		Bond energy, ϕ , kcal/g-at	No. of ruptured bonds	
			min	max	min	max		min	max
A2	U	1406	19.4	22.4	27.3	31.5	28.0	1.0	1.1
	Li	453.7	19.4	23.9	8.8	10.8	9.57	0.9	1.1
	Th	1968	19.0	21.6	37.3	42.4	32.5	1.1	1.3
	Rb	312	17.6	21.2	5.5	6.6	4.90	1.1	1.3
	Cs	301.8	17.0	20.5	5.1	6.5	4.65	1.1	1.4
	Tl	577	20.6	25.3	11.9	14.6	10.6	1.1	1.4
	Na	370.97	19.6	24.2	7.3	9.0	6.5	1.1	1.4
	K	336.4	18.1	22.1	6.1	7.4	5.35	1.1	1.4
	Hf	2250	22.5	26.8	50.6	60.5	41.4	1.2	1.5
	Zr	2125	21.5	25.2	45.6	53.5	36.0	1.3	1.5
	Nb	2770	22.8	27.0	63.0	74.8	44.0	1.4	1.7
	Ti	1950	21.0	24.6	41.0	48.0	27.0	1.5	1.8
	V	2190	22.0	25.9	48.2	56.6	29.6	1.6	1.9
	Fe	1812	21.2	25.0	38.4	45.3	23.5	1.6	1.9
A1	Pt	2043	23.2	27.3	47.4	55.9	22.0	2.2	2.5
	Au	1336	23.1	28.1	30.8	37.5	13.8	2.2	2.7
	Ni	1728	22.0	26.4	38.0	45.6	16.4	2.3	2.8
	Rh	2239	22.9	27.2	51.2	61.0	21.5	2.4	2.8
	Co	1768	21.9	25.4	38.7	44.9	16.3	2.4	2.8
	Cu	1356	23.1	28.1	31.3	38.2	13.2	2.4	2.9
	Ag	1234	22.6	27.4	27.9	33.8	11.1	2.5	3.0
	Ir	2727	23.7	28.2	64.6	77.1	24.4	2.7	3.1
	Pd	1823	22.8	27.2	41.5	49.6	15.2	2.7	3.2
A3	Ru	2700	24.2	29.0	65.3	78.2	23.7	2.8	3.3
	Os	3000	24.8	30.0	74.5	90.0	26.3	2.8	3.4
	Cd	594	21.4	26.6	12.7	15.5	4.37	2.9	3.5
	Zn	692.7	22.0	27.2	15.2	18.8	5.1	3.0	3.7
	Mg	923	21.3	25.7	20.0	23.7	5.75	3.4	4.1

Thus an atom which passes into a state of mobile autoadsorption will exchange two degrees of vibrational freedom for two degrees of translational freedom and its vibrational entropy relative to the lattice will fall some-

where between one-third of the entropy of an atom in the body of the lattice and the entropy corresponding to one-dimensional translation. The minimum value of the standard entropy change for passage into a state of mobile autoadsorption will be given by:

$$\min \Delta S_T^0 = {}_2S_T^0 - 0,67cS_T^0. \quad (1)$$

Here ${}_2S_T^0$ is the standard entropy for two-dimensional translatory movement of a mole of substance in the form of an ideal gas at temperature T , and cS_T^0 is the standard entropy per mole of this same substance in the crystalline state at temperature T under a pressure of one atmosphere. The expression for the maximum value of the change in entropy has the form:

$$\max \Delta S_T^0 = {}_3S_T^0 - cS_T^0, \quad (2)$$

where ${}_3S_T^0$ is the entropy for three-dimensional translatory movement in a mole of ideal gas of molecular weight M under a pressure of one atmosphere, a quantity which can be calculated from the expression:

$${}_3S_T^0 = R \ln M^{3/2} T^{5/2} - 2,30. \quad (3)$$

The expression for the translatory entropy of a two-dimensional gas has the form:

$${}_2S_T^0 = R \ln MTA + 65,80, \quad (4)$$

A being the area per adsorbed molecule. The standard state for the two-dimensional gas was chosen by Kimball and Rideal [8] to be that in which the volume per mobile adsorbed molecule would be the same as the volume of the individual molecule in a three-dimensional gas at a pressure of one atmosphere. These authors set the depth of the adsorbed layer at 6 \AA , and then obtained the expression $22.53T \text{ \AA}^2$ for the value of A in the standard state.

Values of the standard entropy change for the passage of $6 \cdot 10^{23}$ atoms from step kinks into the state of mobile autoadsorption have been calculated from Equations (1-4) and are presented in Table 2. It is easily seen that these values are close to the Trouton constant, although the mean values for metals with high-temperature lattices of the A2 type ($\min \Delta S_{T_{mp}}^0 = 20 \pm 3$ and $\max \Delta S_{T_{mp}}^0 = 24 \pm 3$) are somewhat lower than for metals of lattice types A1 and A3 ($\min \Delta S_{T_{mp}}^0 = 23 \pm 1$; $\max \Delta S_{T_{mp}}^0 = 28 \pm 1$).

It can be readily proven that the pressure in a mobile autoadsorbed layer is independent of the concentration of the step kinks. This pressure can therefore be determined from the condition that equilibrium exist between the mobile adsorbed atoms and the atoms in the step kinks, namely:

$$\ln p = \Delta S_T^0/R - \Delta H_T^0/RT. \quad (5)$$

The choice of standard state for the calculation of ΔS_T^0 from Equations (1-4) requires that the pressure p in this equation be expressed in atmospheres; ΔH_T^0 is the change in enthalpy accompanying the transfer of $6 \cdot 10^{23}$ atoms from step kinks into a state of mobile autoadsorption under standard conditions.

It is seen from Table 1 that the number of Me-Me bonds which must be broken in the passage of atoms from step kinks into a state of mobile adsorption will vary for faces of low indices whose structure may be identical with that of an incompleated layer on any given surface of the crystal. This points to differences in equilib-

rium pressures of mobile adsorbed atoms on crystal layers of different structure. This equilibrium pressure will increase as the density of packing of the surface layer of the crystal diminishes. For lattices of types A1 and A2, layers less dense than those whose edges function as steps will have the same structures as a (100) face, while such layers will have the structure of a (0001) face in the case of lattices of A3 type. Thus the change in enthalpy for the transfer of $6 \cdot 10^{23}$ atoms from kinks in less densely packed steps into the state of mobile adsorption must lie within the limits:

$$\text{for the A2 type lattice: } \varphi \leq 2(\alpha\varphi + \varphi') \leq 2\varphi; \quad (6)$$

$$\text{for the A1 type lattice: } 2\varphi < 2\varphi(1 + \alpha) + 2\varphi' \leq 3\varphi; \quad (7)$$

$$\text{for the A3 type lattice: } 3\varphi < 3\varphi + \alpha\varphi < 4\varphi. \quad (8)$$

The maximum pressure in the mobile autoadsorbed layer on any metal can be obtained by substituting the value of φ at the melting point from Table 2 into the inequalities (6)–(8) and making use of the value $\Delta S_{T_{mp}}^0$ from this same table. This pressure proves to be of the order of one atmosphere, regardless of the nature of the metal and the type of lattice. On this basis, it can be postulated that there should be a relation of the form:

$$T_{mp} \cdot \Delta S_{T_{mp}}^0 = \Delta H_{T_{mp}}^0 \quad (9)$$

in which T_{mp} is the melting point under a pressure of one atmosphere, and $\Delta S_{T_{mp}}^0$ and $\Delta H_{T_{mp}}^0$ are determined from (1)–(4) and (6)–(8), respectively, in order to be in line with the choice of standard state adopted from [8].

Equation (9) has been used for the calculation of values of $\Delta H_{T_{mp}}^0$ for 28 metals (see Table 2). The requisite thermodynamic data were taken from [9] and the high-temperature structures of the metals obtained from the monograph [10]. Table 2 shows that the values of $\Delta H_{T_{mp}}^0$ actually fall within the limits marked out by the inequalities (6)–(8).

It should be noted that the information concerning the crystal structures of metals in the neighborhood of T_{mp} is contradictory, in many cases. Thus, one set of data shows chromium to have an A1 structure directly below the freezing point [11] while other data point to an A2 type structure [12]. The text of G. B. Bokii [13] gives A1 as the high-temperature structure type for thallium, titanium, and thorium, and A3 as the type for hafnium. Calculated values of the mean number of bonds which are ruptured in the passage of atoms from step kinks into a state of mobile autoadsorption based on these data agree with inequalities (7) and (8) only in the case of titanium. Similar calculations carried out for the structure A2 (which, according to monograph [10] is the type shown by all four of these elements at high temperatures) yield results which are consistent with (6), while the results of titanium will satisfy inequalities (6) and (7) if this element is assigned the structural types A2 and A1, respectively. On the other hand, assumption of an A3 structure for calcium gives better results [13] than can be obtained from assumption of an A2 structure [10]. Concordance can be obtained in the case of beryllium with both A3 [10,13] and A2 [12] structures, and the same is true in the case of barium.

Thus the indication is that the pressure in a mobile layer autoadsorbed on less densely packed surface layers whose edges function as steps will reach a value of the order of one atmosphere at the melting point. On this basis it should be possible to predict certain crystal structures in the neighborhood of the melting point from the known values of the melting temperature and heat of sublimation and a relation between heat capacity and temperature which is valid up to the melting point.

LITERATURE CITED

1. Catalysis, Problems of Theory and Method of Investigation [in Russian] (Moscow, 1955).
2. V. Zait, Diffusion in Metals [in Russian] (Moscow, 1958).
3. V. I. Shimulis, V. M. Gryaznov, and A. E. Cherkashin, *Kinetika i Kataliz*, **1**, 3 (1960).
4. V. I. Shimulis, V. M. Gryaznov, and A. E. Cherkashin, *Kinetika i Kataliz*, **2**, 1 (1961).
5. V. M. Gryaznov, V. I. Shimulis, and V. D. Yagodovskii, *Doklady Akad. Nauk SSSR*, **136**, 5 (1961).
6. Elementary Processes in the Growth of Crystals [in Russian] (Moscow, 1959).
7. O. M. Poltorak *Zhur. Fiz. Khim.*, **29**, 1650 (1955).

8. C. Kemball and E. K. Rideal, *Proc. Roy. Soc. A* **187**, 53 (1946).
9. *Thermodynamic Properties of the Elements*, American Chemical Society, 1956.
10. W. B. Pearson, *A Handbook of Lattice Spacings and Structures of Metals and Alloys*, London-New York-Paris-Los Angeles, 1958.
11. E. Abrahamson and N. Grant, *J. Metals*, **8**, 975 (1956).
12. A. T. Grigor'ev, L. N. Guseva, et al., *Zhur. Neorg. Khim.*, **4**, 2168 (1959).
13. G. B. Bokil, *Crystal Chemistry* [in Russian] (Moscow, 1960).

All abbreviations of periodicals in the above bibliography are letter-by-letter transliterations of the abbreviations as given in the original Russian journal. *Some or all of this periodical literature may well be available in English translation.* A complete list of the cover-to-cover English translations appears at the back of this issue.



MECHANICAL AND STRUCTURAL PROPERTIES OF PROTEIN FIBERS

N. V. Grigor'eva, V. A. Pchelin, and Academician P. A. Rebinder

Fur Industry Scientific Research Institute, M. V. Lomonosov Moscow State University

Translated from Doklady Akad. Nauk SSSR, Vol. 137, No. 4,

pp. 889-892, April, 1961

Original article submitted January 2, 1961

As was shown [1, 2] physicochemical mechanics connected the mechanical properties of the system which were studied with the fine chemical features of the structure. The present work is concerned with an investigation of the mechanical and structural properties of individual protein (gelatine) fibers and with the change of these properties in the tanning process. Such fibers represent a model of the structural elements of the complex protein microheterodisperse system — the tanned skin. A study of the effect of tanning agents on the mechanical properties of such "model" protein fibers may give a basis for further clarification of the mechanism of the tanning process, and will have great practical value.

Gelatine fibers are more convenient materials for investigation than natural collagen fibers since they have constant cross-section over the whole length of the fiber and can be prepared of any length. We used fibers prepared according to the method of A. V. Yudin and M. P. Kotov [3], by salting out from a 40% aqueous gelatine solution by means of extrusion through a die and spinning in a saturated ammonium sulfate solution (drawn out 700%). The spun "untreated" fibers in the form of small skeins consisting of 175 elementary fibers (diameter of each 20 μ) were kept in the same $(\text{NH}_4)_2\text{SO}_4$ solution at room temperature.

Tanning of the fibers was carried out according to A. V. Yudin by treatment, while stretched, at 20° for 7 hours with a solution of sulfate — glucose — chromate extract, basicity 35%, with addition of 1.34 mole of sodium formate per 1 g-atom Cr at pH \approx 4.9, Cr_2O_3 content 40 g/liter, liq. coef. = 5.

We studied the kinetics of the deformation (elongation) of the fiber, while it was subjected to uniaxial tension under a fixed constant load (from 50 g to 5 kg) and the kinetics of the diminution of the deformation after removal of the load.

The elongation was measured with an accuracy of 0.01 mm. The fibers were tested both in the air-dried (after drying at room temperature) and also in the fully wet conditions (in a saturated ammonium sulfate solution). Both prolonged as well as short-duration experiments were carried out. We give here the results of an investigation with a 60 min period under load and without load.

The character of the deformation curves (Fig. 1) shows that both untreated and tanned fibers have nearly the same yield point $P_k \sim 10 \text{ kg/mm}^2$, which corresponds to a load of 0.5-1.0 kg per sample. Also, the conventional instantaneous deformations ϵ_0 and therefore also the corresponding moduli $E = P/\epsilon_0$ ($\approx 600 \text{ kg/mm}^2$) were practically the same for the dry condition.

However, differences, significant enough even in the air-dried state, are revealed, after unloading, in the reversible part of the deformation $\beta = [(\epsilon_0 - \epsilon_p)/\epsilon_0] 100$ (due to the true elasticity and high elasticity) or still more visually in the part of the practical measure of conventional residual deformation $(\epsilon_p/\epsilon_0) 100 = 100 - \beta$ after a sufficiently long time from unloading.

As we showed, the values of these characteristic practical measures do not depend on the duration of loading, but are determined, apparently, in the main by the very rapid relaxation processes, operating on unloading. Therefore, later on we confined ourselves to a study of the diminution of the deformation on removal of the conventional instantaneous stress during a time adequate for visual reading of the developed elongation (~ 1 sec).

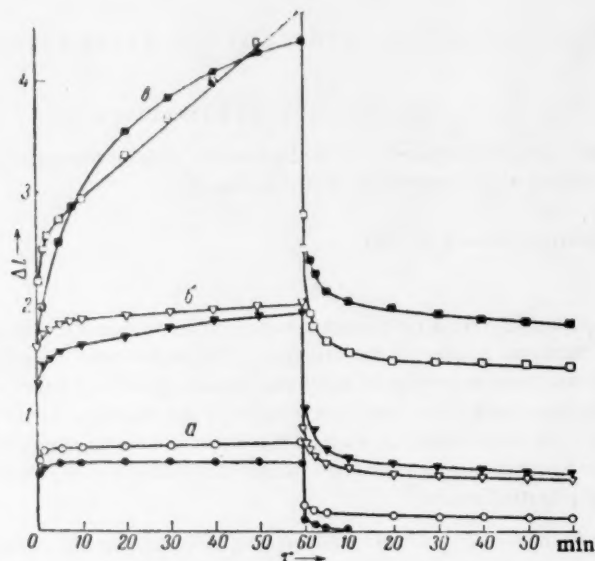


Fig. 1. Curves of the development and diminution of deformation of dry gelatine fibers under load and without load. Black points - untreated fibers, Open points - tanned fibers. a) Load 0.5, b) 1.0, c) 1.25 kg.

The relevant curves (Fig. 2) show that for a 1.25 kg load, after 2 hours, the value of the reversible part of the deformation in the dry fiber was $\beta = 94\%$, and the residual part of the deformation 6% ; in the same fiber tanned, they were 98 and 2% , respectively.

The whole rapidly diminishing high-elastic deformation

$$\beta = \frac{\epsilon_0 - \epsilon_p}{\epsilon_0} \cdot 100,$$

where ϵ_p = deformation remaining after 30 min, for the untreated fibers was 90% and $100 - \beta = 10\%$; for the tanned fibers $\beta = 95\%$, $100 - \beta = 5\%$.

The kinetics of the diminution of deformation, as our experiments showed, in fact gives a convenient graphical method of evaluating the structural and mechanical properties of protein fibers and tanned skins together with measurements of the tensile strength and of the maximum elongation through stretching, by calculation of the rate of loading.

By measurements in an aqueous medium, the method of the without-load plots of the type II elastic after-effect (after unloading), particularly characterizes, in a graphical way, the tanning process and the effectiveness of the tanning agents.

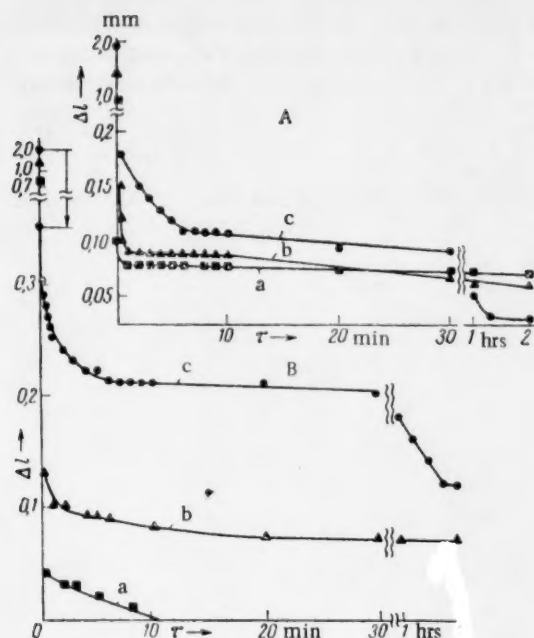


Fig. 2. Kinetic curves of the diminution of deformation of dry gelatine fibers after conventional instantaneous loading. A) Tanned fiber; B) untreated fiber. a) Load 0.5, b) 1.0, c) 1.25 kg.

high-elastic deformation, the "rapid" part of which has completely developed by the time of the first visual reading (1 sec). Later on the "slow" high-elastic deformation increases only a little in value for comparatively small tensions. Only for considerable tensions exceeding the yield point (i.e., the lowest tensile strength) was there observed an appreciable increase and a residual deformation as a result of the gradually developing breaks in the structure which lead to uninterrupted growth of the true tension with the passage of time under load.

After removal of the load the remaining intact elementary fibers which strive to contact, bring about a gradual diminution of the deformation. This diminution will be retarded at the greatest possible tensions near to the breaking point, due to the fact that the entropic lateral stresses remaining in a small number of untorn fibers will be inadequate to bring about restoration of the original length of the sample.

For small tensions this diminution will also be slow, since the internal frictional resistance in a system of practically intact fibers is relatively very great.

Diminution of the deformation is most rapid after application of tensions of sufficiently high average value with regard to the breaking point: in Fig. 2 it can be well seen that the tanned fiber reveals a 2-fold reduction of the conventional residual deformation in comparison with the untreated fiber, both at 30 min, and at 2 hours at the greatest loading, but with loadings much smaller than the lowest tensile strength, i.e., the yield point shows the reverse effect in comparison with the untreated fiber, viz:—

Load in kg	0.5	1.0	1.25
100 - β for tanned fibers	0	5	6
100 - β for untreated fibers	9	10	2

Tanning, which results, as is known, in the blocking of polar groups in the protein molecule on the accessible inner surface of the primary fibers, can cause some decrease of the tensile strength in the dry (seasoned) fiber and consequently of the tanned skin [5].

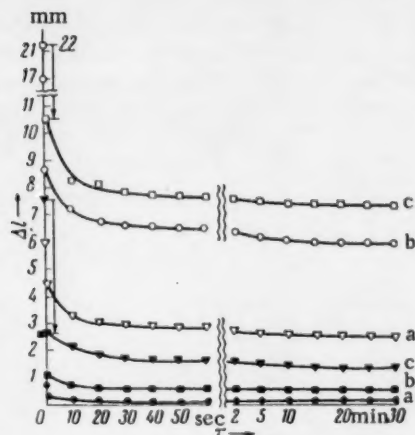


Fig. 3. Kinetic curves of the diminution of the deformation of gelatine fibers in a saturated ammonium sulfate solution after a conventional instantaneous loading. Black points — tanned fiber, open points — untreated fiber. a) Load 0.25, b) 0.5, c) 0.75 kg.

For this it is necessary to take into account the following: all the deformation in the protein stereochemical structure beyond the small true-elastic part (developing with the speed of sound in the sample, i.e., for not more than a millisecond), is the

But, with maximum humidification of the structure, the effect of tanning appears especially clearly by a 2-fold decrease after removal of the load (with $P = 0.75$ kg) of the practical measure of the residual deformation which was, for tanned fibers under maximum humidification, $100 - \beta = 16\%$, and for untreated fibers 33% (Fig. 3).

The conventional equilibrium high-elastic modulus, after removal of the load for 30 min, for the tanned fibers under maximum humidification was $E_e = 100$ kg/mm², and for untreated fibers $E_e = 42$ kg/mm².

The tensile strength (at rapid loading of 600 g/min) for untreated fibers fell at maximum humidification from 25 to 10 kg/mm² (at 60%) and for tanned fibers from 21 only to 15 kg/mm² (at 28%).

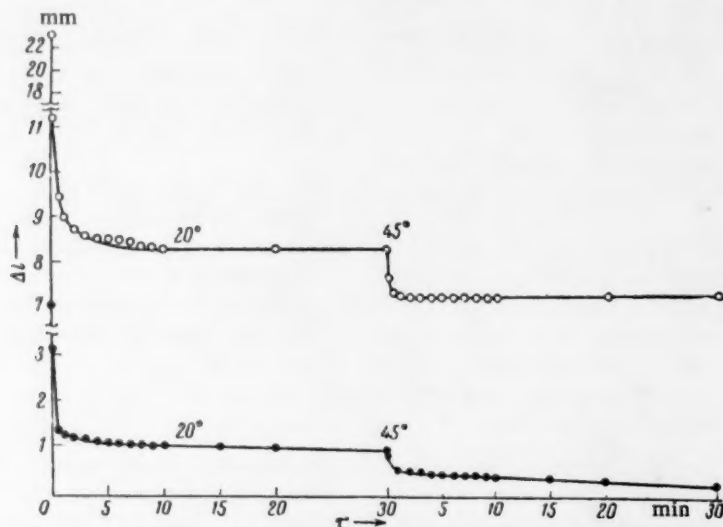


Fig. 4. The effect of increased temperature on the kinetics of the diminution of deformation of gelatine fibers in a saturated ammonium sulfate solution. Open points — untreated fibers; Black points — tanned fiber.

The maximum permissible increase of temperature to 45° somewhat increased, after unloading, the reversible part of the deformation in consequence of the more speedy diminution of the high-elastic deformation (Fig. 4). With such heating up the residual part of the practical measure of the deformation drops still more, being for the tanned fibers $100 - \beta = 4\%$ and for the untreated fibers 30%. This shows still more clearly the effect of tanning on the increased high elasticity.

LITERATURE CITED

1. P. A. Rebinder, Vestn. Akad. Nauk SSSR, No. 10 (1957).
2. P. A. Rebinder, Physicochemical Mechanics [in Russian] (Moscow, 1958); L. V. Ivanova-Chumakova, Advances in the Chemistry and Technology of Polymers [in Russian] (Moscow, 1957) part 2.
3. A. V. Yudin and M. P. Kotov, Tr. Kievskogo Tekhnologich. Inst. Legkoi Promyshlennosti, Kiev, 7 (1955); 10, (1958).
4. G. I. Kutyatin, Investigation of the Physicochemical Properties of Leather [in Russian] (Moscow, 1956).

All abbreviations of periodicals in the above bibliography are letter-by-letter transliterations of the abbreviations as given in the original Russian journal. Some or all of this periodical literature may well be available in English translation. A complete list of the cover-to-cover English translations appears at the back of this issue.

CATALYSIS ON ORGANIC SEMICONDUCTORS PREPARED FROM POLYACRYLONITRILE BY THERMAL TREATMENT

E. S. Dokukina, Corresponding Member, Acad. Sci. USSR
S. Z. Roginskii, M. M. Sakharov, Academician
A. V. Topchiev, M. A. Geiderikh, B. É. Davydov and
B. A. Krentsel'.

Institute of Physical Chemistry, Academy of Science USSR, Institute of
Petrochemical Synthesis, Academy of Science USSR.

Translated from *Doklady Akad. Nauk SSSR* Vol. 137, No. 4

pp. 893-895, April, 1961

Original article submitted December 24, 1960.

Until recently only inorganic substances have been used as solid catalysts in industry and in laboratory practice. By contrast fermentative catalysis, with its very rapid rates and selectivity of the processes, is based on organic microheterogeneous catalysts. In recent years the outstanding catalytic properties of organic ion-exchange resins with respect to a number of acid-base type reactions have been discovered.

The search for organic solid catalysts for acid-base type reactions began comparatively long ago. As is known, metals and inorganic semiconductors [1] are good catalysts for reactions of this type. Therefore, a display of significant catalytic activity, with respect to oxidation-reduction type reactions by organic semiconductors might also be expected. However, in the few known studies [2-4] of catalysis of acid-base reactions in the liquid phase in the presence of such solid organic substances with semiconducting properties, such as phthalocyanine and its complexes with certain metals, only comparatively weak catalytic effects were observed. Concerning the catalytic activity of organic semiconductors with respect to vapor- and gas-phase acid-base reactions, the only work known is that of Tamaru and Shimada [5], who established the absence of catalytic activity of violanthrone in respect to the reaction of H_2-I_2 exchange with HI formation, and of H_2-D_2 exchange.

The reason for the absence of the strong effects in the cases investigated may possibly be sought in the very low electroconductivity and large width of the forbidden band of the organic substances which were used [6]. Recently new polymeric organic materials with semiconducting properties have been prepared which, due to the presence in their structure of multi-atom chains with delocalized electrons, possess a small forbidden band width and a significant electroconductivity at room temperature [7-9, 12]. As already stated in the literature [10, 11] and according to contemporary views on the mechanism of catalysis, it is reasonable to expect that such semiconducting organic materials will have a high catalytic activity with respect to oxidation-reduction type reactions. In support of this point of view only the results relating to the catalytic activity of thermally treated polyacrylonitrile and polyaminoquinone in respect of the decomposition reaction of hydrogen peroxide, obtained by A. V. Topchiev, M. A. Geiderikh and others [7] and by A. A. Berlin, L. A. Blyumenfeld and N. N. Semenov [11], can be advanced as yet. The qualitative character of these results, and also the high susceptibility of hydrogen peroxide to the catalytic influence of very diverse solids, do not permit a simple connection of the found catalytic activity with the prominent electronic properties of the polymeric organic substances mentioned. In this connection, it seemed essential to investigate the catalytic activity of polymeric semiconductors with systems of conjugated bonds in respect to a number of vapor- and gas-phase reactions of the acid-base type. Semiconducting materials prepared from polyacrylonitrile were used in the present investigation. Details of the methods of preparation of semiconductors of this type and their electrical properties are given in references [7, 12].

We have carried out an examination of the catalytic activity of two different samples of thermally treated polyacrylonitrile. The first sample (PAN-1) consisted of polyacrylonitrile into which 0.01% CuCl_2 had been introduced before thermal treatment. The specific surface area of this sample, measured by a volumetric method with krypton, was $0.6 \text{ m}^2/\text{g}$. A second sample (PAN-2) did not contain copper, and its specific surface area was equal to $0.4 \text{ m}^2/\text{g}$.

TABLE 1

Results of Experiments on the Decomposition of Formic Acid over PAN-1 and PAN-2

No. of experiment	Temperature, °C	Rate of formation of gaseous products ml/hr	H ₂ : CO ratio	Rate of introduction of the acid vapors, mol per hr for 1g cat.
PAN-1				
3-1	242	153	2,8	0,02
3-2	255	265		
3-3	272	494		
PAN-2				
6-1	260	66	3,2	0,3
6-2	287	232		
6-3	299	402		
6-4	261	86	3,6	0,3
7-1	264	114		
7-2	288	302		
7-3	304	554	—	0,3
8-1	290	336		

TABLE 2

Rate of Decomposition of Formic Acid over PAN-1 and PAN-2 per Unit Surface Area of Catalyst

PAN-1		PAN-2	
Temp. °C	Decomposition of acid mM/sec · $\text{m}^2 \cdot 10^2$	Temp. °C	Decomposition of acid mM/sec · $\text{m}^2 \cdot 10^2$
242	0,58	261	0,44
255	1,0	287	1,2
272	1,9	299	2,1

10%), then the activation energy of the reaction under study could be determined from the dependence of the logarithm of the rate of decomposition of acid on the reciprocal absolute temperature. In Fig. 1 are presented the relevant graphs plotted from data of experiments 3, 6, and 7. The activation energies for PAN-1 and PAN-2, calculated from these graphs, were 21 and 25 kcal respectively. It may be noted that the observed increase of the activity of PAN-1 and PAN-2 from experiment to experiment has little effect on the activation energy. Thus in experiments 6 and 7 with PAN-2, the activation energy of the process remained practically unchanged.

From the results obtained it follows that, in the temperature range studied, PAN-1 and PAN-2 display a catalytic activity not inferior in magnitude to the catalytic activity of a number of metallic and inorganic semiconducting catalysts of this reaction [14].

* An 85% aqueous solution of formic acid (analytically pure) was used in the work.

Examination of the catalytic activity of these samples with respect to the decomposition of alcohols, formic acid and hydrazine hydrate was carried out in an apparatus essentially similar in pattern to that of Schwab and Theophilides [13]. Experiments on the hydrogenation of ethylene were carried out in a circulation apparatus at pressures somewhat below atmospheric. Before examination of the catalytic activity PAN-1 and PAN-2 were subjected to 1-3 hours treatment at temperatures up to 450 deg. Significant catalytic activity by PAN-1 and PAN-2 was detected only in respect to the decomposition reaction of formic acid.* The relevant results are presented in Table 1.

An appreciable rate of decomposition of formic acid on PAN-1 was already observed at 240°. PAN-2 showed less catalytic activity. With comparable values of the total surface area of PAN-1 and PAN-2 in parallel experiments (0.186 and 0.135 m^2 , respectively), the catalytic activity of PAN-2 attained the same values that PAN-1 had at 20-25° higher. The values of the decomposition rates of formic acid per unit surface area of the catalyst, presented in Table 2, convey very well the indicated relationship of the activities of PAN-1 and PAN-2 in the temperature range 242-299°.

Essentially dehydrogenation of formic acid appeared to be the main course of the decomposition both on PAN-1 and on PAN-2, in the same way as on many inorganic semiconductors. The sample of PAN studied increased in catalytic activity during the initial period of their operation from experiment to experiment. For PAN-2 a steady state of the surface area was attained only after four experiments had been carried out.

Since variation of the decomposition rate of formic acid with increase of temperature was determined by us in one continuous experiment with stepwise increase of temperature, constant rate of introduction of the acid into the reactor and a comparatively low conversion yield (from 1 to

The significant catalytic effect which is observed in the case of PAN-2 leads to the conclusion that even in the case of PAN-1 the presence of copper in it has no decisive value in the development of catalytic activity for this sample of PAN*. PAN-1 and PAN-2 also showed a catalytic effect on the decomposition reaction of hydrazine hydrate in the direction of formation of ammonia and nitrogen. However, a marked catalytic decomposition of hydrazine hydrate takes place at relatively high temperatures (250°), during which the reaction on the glass surface of the reactor, with homogeneous decomposition, plays a substantial role.

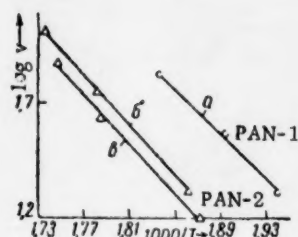


Fig. 1. Dependence of the decomposition rate of formic acid over PAN-1 and PAN-2 on temperature: a) Experiment 3; b) experiment 7; c) experiment 6, v) in mmole/hour · m².

The significant catalytic activity of the samples of PAN studied in respect to the decomposition reaction of formic acid is apparently connected with the chemical structure of the polymer. There are grounds for assuming that the nitrogen atoms in the chains of conjugated double bonds of the polymer might be the centers of adsorption of the acid molecule. It may also be assumed that by controlled modification of the chemical and electrophysical properties of the polymers with a system of conjugated double bonds, highly selective organic catalysts for acid-base reactions might be prepared.

LITERATURE CITED

1. S. Z. Roginskii, *Problemy Kinetiki i Kataliza*, **6**, 9 (1949).
2. M. Calvin, E. G. Cockbain, and M. Polanyi, *Trans. Farad. Soc.*, **32**, 1436, 1443 (1936).
3. A. H. Cook, *J. Chem. Soc.*, 1938, 1761, 1768, 1774.
4. H. Hock, and H. Kropf, *J. Prakt. Chem.*, **9**, 173 (1959).
5. K. Tamaru and T. Shimada, *Bull. Chem. Soc. Japan*, **31**, 141 (1958).
6. A. T. Vartanyan and I. A. Karpovich, *Zhur. Fiz. Khim.*, **32**, 178, 274, 543 (1958); D. D. Eley, *Res. Appl. Ind.*, **12**, 293 (1959).
7. A. V. Topchiev, M. A. Geiderikh et al, *Doklady Akad. Nauk SSSR*, **128**, 312 (1959).
8. A. A. Berlin, *Khim. i Tekhnol. Polimerov*, No. 7-8, 139 (1960).
9. N. N. Semenov, *Khim. i Tekhnol. Polimerov*, No. 7-8, 196 (1960).
10. S. Z. Roginskii, *Khim. Nauka i Prom.*, No. 2, 138 (1957).
11. A. A. Berlin, L. A. Blyumenfel'd and N. N. Semenov, *Izvest. Akad. Nauk SSSR, Otd. Khim. Nauk*, No. 9, 1689 (1959).
12. M. A. Geiderikh, B. É. Davydov et al, *International Symposium on Macromolecular Chemistry*, June 14-18, 1960, Collected Reports and Papers, Section 3, 1960, p. 85.
13. G. M. Schwab, N. Theophilides, *J. Phys. Chem.*, **50**, 427 (1946).
14. G. Rienacker, N. Hansen, *Zs. anorg. u. allgem. Chem.*, **285**, 283 (1956); G. M. Schwab, G. Greger et al., *Zs. phys. Chem.*, **15**, 363 (1959).

All abbreviations of periodicals in the above bibliography are letter-by-letter transliterations of the abbreviations as given in the original Russian journal. Some or all of this periodical literature may well be available in English translation. A complete list of the cover-to-cover English translations appears at the back of this issue.

* The results of the present work were reported by Corresponding Member Acad. Sci. USSR S. Z. Roginskii on March 27, 1960, to the Scientific Soviet of the Institute of Chemical Physics, Academy of Sciences USSR.



THE ADSORPTION OF HYDROGEN IONS AT A NEGATIVELY CHARGED MERCURY-ELECTROLYTE INTERFACE

Academician A. N. Frumkin, O. A. Petrii
and N. V. Nikolaeva-Fedorovich

M. V. Lomonosov Moscow State University

Translated from *Doklady Akad. Nauk SSSR*, 1961. Vol. 137, No. 4,
pp. 896-899, April, 1961

Original article submitted January 7, 1960

It is a known fact that in a number of cases, a definite progression is observed in the change in properties of water solutions containing singly charged cations belonging to the series $H^+ - Li^+ - Na^+ - K^+ - Rb^+ - Cs^+$, the behavior of the lithium and hydrogen cations being very similar. This conclusion follows directly, for example, from a comparison of the variation of the activity coefficients with concentration in aqueous solutions of acids and salts of alkali metals [1]. It was interesting, in this sense, to compare the effects of hydrogen and alkali metal ions on the differential capacitance C of a double layer, as well as on the kinetics of electrode reactions.

As follows from Grahame's measurements [2] in the case of the mercury drop electrode, the values of C are practically identical in 0.1 N solutions of HCl and LiCl at potentials more positive than -0.7 v (normal calomel electrode) while at more negative potentials, C in HCl is 1-2% lower than in 0.1 N LiCl. However, Grahame's measurements were only made up to hydrogen over-voltage $\eta \sim 0.66$ v. We measured the values of C at a mercury drop electrode in 0.1 N solutions of HCl and LiCl at a frequency of 1000 cycles/sec and 25° , with an impedance bridge. The measurements in HCl solution were carried up to $\eta \sim 1.15$ v. The potentials, ϕ , are given in volts against a normal calomel electrode (Fig. 1a). The bridge balancing time was determined with an accuracy of 0.01-0.02 seconds. As distinct from the work of Grahame, in which the second electrode in the cell was a platinum sphere, symmetrically surrounding the test electrode, in our work we used a mercury anode in the form of a cup, over the center of which was placed the mercury drop electrode. The use of a mercury anode was due to the need of avoiding the possibility of contaminating the solution with traces of platinum, which sharply reduces the overvoltage required for the deposition of hydrogen. Since in our experiments the measuring arm of the bridge consisted of series-connected units of capacitance and resistance, and the irreversible electrode reaction represents an impedance equivalent to a leaky capacitor, to make a proper separation of the ohmic and capacitive components of the total impedance at potentials more negative than -1.3 in the HCl solutions, we had to convert the experimental results to the electrical circuit shown in Fig. 1b.

The results obtained are compared with Grahame's data in Fig. 1a. As is clear from the figure, the values of C in 0.1 N HCl, with negative surface charges, is somewhat lower than the values of C in 0.1 N LiCl*. Hence, and from [2] and [3], it follows that the capacitance of the double layer with negative surface charges increases in the order $H^+ < Li^+ < Na^+ < K^+ < Rb^+ < Cs^+$. The reduction in the capacitance of the double layer on replacing Li^+ by H^+ is in agreement with the results of measurements on the potential jump at the free surface of soap solutions [4]. According to Horiuti's hydrogen overvoltage theory [5], the rate of the hydrogen deposition reaction

* The difference between C in acid and in salt decreases with increasing negative value of ϕ . This phenomenon may be explained if we assume that the cation H_3O^+ is more hydrated than Li^+ , and is more strongly deformed with negative values of ϕ . One must, however, take into account that the accuracy of measurement in HCl solutions is somewhat lowered at hydrogen deposition potentials. The explanation of this effect requires further investigation.

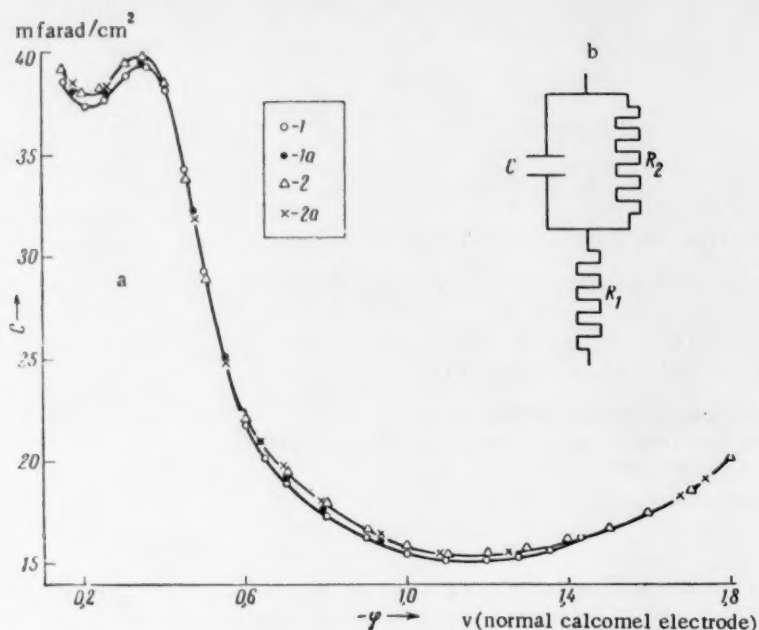


Fig. 1. a) Curves of differential capacitance in 0.1 N HCl (1) and LiCl (2); 1a and 2a) Grahame's data for 0.1 N HCl and LiCl respectively; b) equivalent electrical circuit of the cell and electrode, at which the irreversible reaction occurs; C) capacitance of double layer; R_1) resistance of solution; R_2) polarization resistance.

on mercury is determined by the irreversible discharge of the ions of the molecular hydrogen H_2^+ , adsorbed on the surface of the electrode, and remaining in equilibrium with the H^+ ions in solution. A. N. Frumkin [6] has shown that the differential capacitance of a Helmholtz layer, with an ionic covering made up of H_2^+ ions, should have twice the value of C occurring in neutral solutions. Matsuda [7], considering the effect of the gradual transition to H_2^+ ions of H^+ ions attracted to the surface, with increasing η , which should occur according to Horiuti's theory, came to the conclusion that the $C-\varphi$ curve in acid solutions, at potentials more negative than the electrocapillary zero, ought to show a maximum greater than $2C$, after which, with further increase in φ , the capacitance again reaches its normal value. The experimental results obtained by Grahame in the paper quoted show a complete absence of any such effects, and, consequently, the falsity of the idea of the existence of H_2^+ ions, adsorbed on the mercury surface. It should be noted that normal values of capacitance at the mercury electrode in 1 N acid solutions were found by Watanabe, Tsuji, and Ueda, using the resonance method [8].

It is well known that the reduction rate of the anions $S_2O_8^{2-}$ [9], $S_4O_6^{2-}$ [10], $Fe(CN)_6^{3-}$ [11], and $PtCl_4^{2-}$ [12] rises rapidly in the series $Li^+ < Na^+ < K^+ < Rb^+ < Cs^+$. A. N. Frumkin, N. V. Nikolaeva-Fedorovich, and B. B. Damaskin [9] have explained this phenomenon, starting with the idea of non-uniform distribution of potential in the double layer, at the same time that Gierst [13] proposed that the ions that undergo reduction are of the type $MeS_2O_8^{2-}$, formed in the volume of the solution, or (at more negative potentials) are activated complexes of the same composition. The effect of the nature of the cathode, in the framework of this hypothesis, is to be explained by the way in which the formation of complexes is facilitated as the radius of the cathode is increased. Comparing the pK values for the dissociation $NaSO_4^+$ and KSO_4^+ [14] leads to the conclusion that there is some increase in the stability of the ion pairs formed by a cathode of large dimensions, which could serve as an argument in favor of Gierst's explanation. Since pK for HSO_4^+ at 25° is equal to 1.99 [14], thus considerably exceeding the value of pK for $NaHSO_4$, which is equal to 0.72, we should expect, if we accept Gierst's scheme, that the cation H_3O^+ would show a considerably stronger accelerating action on the electro-reduction of anions than, for example, the cation Na^+ .

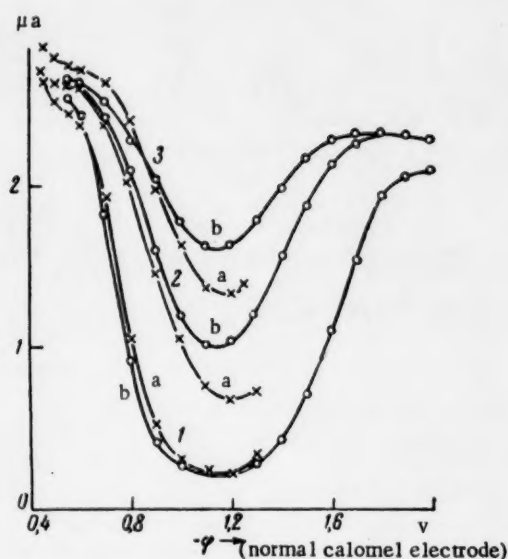


Fig. 2. Polarization curves for the reduction of 10^{-3} N $K_2S_2O_8$ in the presence of HCl (a), and LiCl (b) at the concentrations: 1) 10^{-2} N; 2) $5 \cdot 10^{-2}$ N; 3) 10^{-1} N.

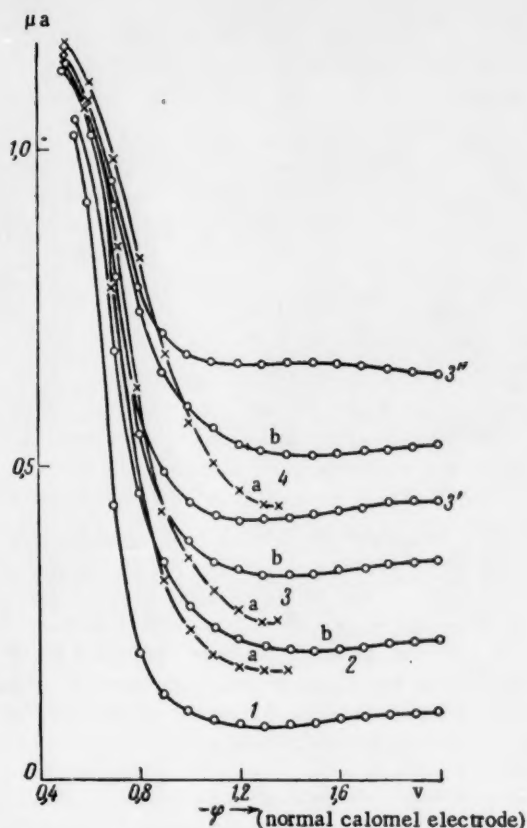


Fig. 3. Polarization curves for the reduction of 10^{-3} N $K_3Fe(CN)_6$ in the presence of HCl (a), and LiCl (b) at the concentrations: 1) 0, 2) $5 \cdot 10^{-4}$ N, 3) 10^{-3} N, 4) $2 \cdot 10^{-3}$ N, and in the presence of 10^{-3} N KCl (3') and 10^{-3} N CsCl (3'').

We studied the effect of H^+ ions on the rate of reduction of the anions $S_2O_8^{2-}$, $Fe(CN)_6^{3-}$, and $PtCl_4^{2-}$ with negative surface charges. The previously de-oxygenated solutions of the salts $K_2S_2O_8$, $K_3Fe(CN)_6$ or K_2PtCl_4 , and the HCl solutions, were mixed to form a solution of the required composition immediately before measurement, to avoid falsifying the results from changes which might have occurred over the course of time, in acid solutions of the anions in question. The polarization curves were corrected for background currents. In studying the reduction of $K_3Fe(CN)_6$ it was found that in acid solution reproducible results are obtained only after preliminary treatment of the glass cell and the capillary with several portions of the solution under investigation. This, apparently, is a matter of the acid solution washing traces of multiply charged cations out of the glass, as these greatly increase the reduction rate of $Fe(CN)_6^{3-}$ [11].

The results of measurements on solutions of 10^{-3} N $K_2S_2O_8$ and 10^{-3} N $K_3Fe(CN)_6$, with additions of acid and of salts of alkali metals, are given in Figs. 2 and 3. As may be seen from the data, the cation H_3O^+ exerts an influence on the reduction of anions, comparable with the influence of Li^+ , or even weaker, which is in agreement with its small adsorbability on the negatively charged mercury surface. The polarization curves, measured in 10^{-3} N $K_2S_2O_8$ with additions of KCl and KOH, are practically coincident, as well as the curves taken for the solutions 10^{-3} N $K_3Fe(CN)_6$ + 10^{-3} N $K_3Fe(CN)_6$ + 10^{-3} N KOH.

In the reduction of $PtCl_4^{2-}$, additions of HCl in concentrations $< 10^{-2}$ N, as well as additions of inorganic salts in the same concentrations [12] show little effect. With large additions of HCl, the wave of deposition of

hydrogen, strongly displaced to the positive potential side in the presence of traces of platinum, which are formed at the cathode, is added onto the PtCl_4^{2-} reduction current, which complicates the interpretation of the results for this case.

It should, however, be emphasized that any conclusion as to the relatively small adsorptivity of the hydrogen ion or the weakness of its interaction with the anions in the surface layer refers only to the surfaces of the region, carrying a negative charge, which attract hydrogen ions and repel anions. It cannot be distributed over the uncharged surfaces in the presence of specific anion adsorption, as follows from the increased adsorbability of acids, as compared with the neutral layers on mercury at the maximum of the electrocapillary curve [15] and on the free surface of water [16]. It is possible that in these cases undissociated acid molecules are formed in the adsorbed layer.

It should, however be emphasized that any conclusion as to the relatively small adsorptivity of the hydrogen ion or the weakness of its interaction with the anions in the surface layer refers only to the surfaces of the region, carrying a negative charge, which attracts hydrogen ions and repels anions. It cannot be distributed over the uncharged surfaces in the presence of specific anion adsorption, as follows from the increased adsorbability of acids, as compared with the neutral layers, on mercury, at the maximum of the electrocapillary curve [15] and on the free surface of water [16]. It is possible that in these cases undissociated acid molecules are formed in the adsorbed layer.

LITERATURE CITED

1. R. Robinson, R. Stokes, *Electrolyte Solutions*, London, 1955.
2. D. Grahame, *J. Electrochem. Soc.*, **98**, 343 (1951).
3. A. N. Frumkin, B. B. Damaskin, and N. V. Nikolaeva-Fedorovich, *Doklady Akad. Nauk SSSR*, **115**, 751 (1957); B. B. Damaskin, N. V. Nikolaeva-Fedorovich, and A. N. Frumkin, *Doklady Akad. Nauk SSSR*, **121**, 129 (1958).
4. B. Pethica, A. Few, *Disc. Farad. Soc.*, **18**, 258 (1954).
5. J. Horiuti, T. Keii, K. Hirota, *J. Res. Inst. Catalysis Hokkaido Univ.*, **2**, 1 (1951); J. Horiuti, *ibid.*, **3**, 52 (1954); A. Matsuda, J. Horiuti, *ibid.*, **6**, 231 (1958).
6. A. Frumkin, 115-th Meeting, Theor. Div. Am. Electrochem. Soc., Philadelphia, May, 1959.
7. A. Matsuda, *J. Res. Inst. Catalysis, Hokkaido Univ.*, **8**, 29 (1960).
8. A. Watanabe, F. Tsuji, S. Ueda, *J. Electrochem. Soc. Japan*, **22**, 521 (1954); *Bull. Inst. Chem. Res., Kyoto Univ.*, **34**, 1 (1956).
9. A. N. Frumkin, *Transactions of the 4th Conference on Electrochemistry* (1956) *Akad. Nauk SSSR Press* (1959), page 21; N. V. Nikolaeva-Fedorovich, *Transactions of the 4th Conference on Electrochemistry* (1956) *Akad. Nauk SSSR Press* (1959), page 150; A. Frumkin, *Zs. Elektrochem.*, **59**, 807 (1955).
10. I. Zetzula, *Chem. Listy*, **47**, 492 (1953).
11. A. N. Frumkin, O. A. Petrii, N. V. Nikolaeva-Fedorovich, *Doklady Akad. Nauk SSSR*, **128**, 1006 (1959).
12. N. V. Nikolaeva-Fedorovich, O. A. Fokina, O. A. Petrii, *Doklady Akad. Nauk SSSR*, **122**, 639 (1958).
13. L. Gierst, *Cinetique d'approche et reactions d'electrodes irreversibles*, Bruxelles, 1958.
14. R. Parsons, *Handbook of Electrochemical Constants*, London, 1959.
15. G. Gouy, *Ann. chim. phys.*, (7) **29**, 145 (1903).
16. A. Frumkin, *Zs. phys. Chem.*, **109**, 34 (1924).

All abbreviations of periodicals in the above bibliography are letter-by-letter transliterations of the abbreviations as given in the original Russian journal. *Some or all of this periodical literature may well be available in English translation.* A complete list of the cover-to-cover English translations appears at the back of this issue.

THE KINETICS OF ELECTRODE PROCESSES
AND THE MECHANISM OF SPONTANEOUS DISSOLUTION
OF GERMANIUM OF THE n- AND p- TYPES WITH DIFFERENT
SPECIFIC RESISTANCES

E. N. Paleolog, A. Z. Fedotova, and N. D. Tomashov

Physical Chemistry Institute, Academy of Sciences, USSR

(Presented by Academician A. N. Frumkin, November 18, 1960)

Translated from Doklady Akademii Nauk SSSR, Vol. 137, No. 4

pp. 900-903, April, 1961

Original article submitted November 10, 1960

In our earlier works [1,2] it was shown that the evolution of hydrogen and reduction of hydrogen peroxide on hole-type germanium is greatly retarded, i. e. takes place at a much lower velocity than on n-type germanium. Since the chemical composition and surface state of n-type germanium are practically identical to those of p-type germanium, these results can only be explained by taking account of differences in their semiconducting properties.

In a number of works [3,4] it has been suggested that the difference in the rates of evolution of hydrogen on n- and p- germanium is related to the participation in this reaction of electrons from the free zone only. For n-type germanium, the free electrons are the major charge carriers and their concentration is fairly high, so that reduction reactions on n-type germanium involving free electrons should take place without hindrance.

For hole-type germanium the rate of a cathodic process for this reaction mechanism is limited by the low concentration of free electrons. By analogy with the limiting current due to holes for electronic germanium with anodic polarization, the cathodic polarization curves for p-germanium should show a region corresponding to a "limiting" current due to free electrons. The values of the "limiting" cathodic current should depend on the specific resistance of the specimen, increasing with increase in the resistance ρ for a given value of the diffusion length L of the minor carrier or with increase in the ratio ρ/L [5].

From general theories of semiconductor physics, however, cathodic reduction reactions on semiconductors can in principle involve not only free electrons but also electrons from the valence zone, as has been confirmed experimentally in a number of cases [6,7]. Energetically, this is possible with the condition that the energy level into which the electron moves during the reduction process lies below the Fermi level of the germanium. The extent to which electrons from different zones in this system take part in the reaction will be determined by the type of conductivity of the germanium, by the energetic position of the level to which the electrons move during the reduction, and by the magnitude of the potential of the given cathodic reaction, i. e. it depends both on the nature of the semiconductor and on the nature of the ion being reduced.

On the basis of these theories, we put forward the suggestion that the cathodic reduction of hydrogen peroxide on p-germanium involves predominantly the electrons from the valence zone [1]. In this case increase in the specific resistance of the hole-type germanium (i. e. decrease in the number of holes in it) should lead to a decrease in the rate of the cathodic process as a result of the marked impoverishment, with respect to holes, in the electrode layer next to the surface. The change in the rate of a cathodic process on p-germanium with change in its specific resistance can thus be used as an indirect criterion for judging the correctness of one of the above mechanisms for the cathodic reaction.

In the present work we carried out polarization measurements and determined the rate of spontaneous dissolution for n- and p- type germanium specimens with different specific resistances.

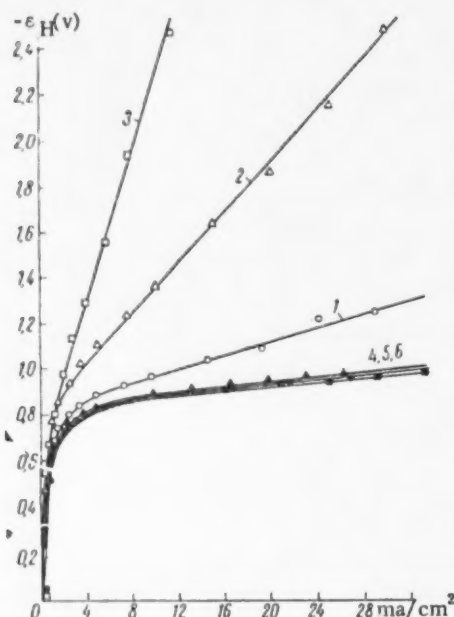


Fig. 1. Cathodic polarization of germanium in H_2SO_4 solution ($pH=1.0$). p-Type germanium: 1) $\rho = 1.3$ ohm-cm; 2) $\rho = 12$ ohm-cm; 3) $\rho = 20$ ohm-cm. n-Type germanium: 4) $\rho = 1.0$ ohm-cm; 5) $\rho = 10$ ohm-cm; 6) $\rho = 20$ ohm-cm.

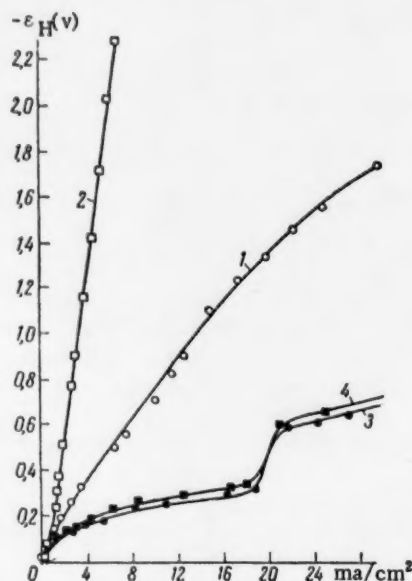


Fig. 2. Cathodic polarization of germanium in H_2SO_4 ($pH=1.0$) + 0.2 N H_2O_2 solution. p-Type germanium: 1) $\rho = 1.3$ ohm-cm; 2) $\rho = 20$ ohm-cm. n-Type germanium: 3) $\rho = 1$ ohm-cm; 4) $\rho = 20$ ohm-cm.

The characteristics of the germanium used in the work are given below.*

	n-type germanium	p-type germanium
Specific resistance ρ , ohm-cm	1.0; 10.0; 20.0	1.3; 12.0; 20.0
Diffusion length L , mm	0.5; 1.3; 1.5	0.4; 1.0; 1.5
ρ/L	2.0; 7.7; 13.3	3.2; 12.0; 13.3

All the experiments were carried out in the following solutions: H_2SO_4 ($pH=1.0$); H_2SO_4 ($pH=1.0$) + 0.2 N H_2O_2 ; 0.5 N Na_2SO_4 + 0.05 N $K_3Fe(CN)_6$; the procedure corresponded to the conditions of our earlier measurements [1].

The results obtained are given in Figs. 1, 2, and 3. For p-type germanium the rate of the cathodic process is practically independent of the specific resistance.** For hole-type germanium (Figs. 1 and 2), the retardation of the cathodic reactions of hydrogen evolution and H_2O_2 reduction are greater, the higher the specific resistance of the p-germanium, i. e., the lower the concentration of major carriers in it. The cathodic polarization curves for p-germanium in H_2SO_4 ($pH=1.0$) and H_2SO_4 ($pH=1.0$) + 0.2 N H_2O_2 solutions have a constant slope and show no region corresponding to a limiting current due to free electrons. The rate of the cathodic reduction of $[Fe(CN)_6]^{3-}$ on p-germanium over a wide range of current density is found to be even higher than on n-type germanium and for hole-type germanium it is independent of the specific resistance (Fig. 3). The sharp change in the slope of the polarization curves for n- and p-germanium is related to the attainment of a limiting current for the $[Fe(CN)_6]^{3-}$ ions.

*It should be pointed out that for these germanium specimens the change in the specific resistance was much greater than the change in the diffusion length.

**All figures give polarization curves with allowance for the ohmic potential drop within the volume of the specimen.

The decrease in the rates of discharge of hydrogen ions and reduction of H_2O_2 which we observed on hole-type germanium with increase in its specific resistance (or correspondingly in the ratio ρ/L) and the fact that the curves show no limiting current due to the minor carriers indicate that the suggestion that only free electrons take part in these reactions is incorrect. The experimental results which have been obtained confirm our theory that in these cathodic processes the major current carriers, i. e. free electrons for n-germanium and electrons from the valence zone for p-type germanium, play a predominant part.

The greater polarizability of p-germanium compared with n-type germanium in the reactions $2\text{H}^+ + 2\text{e}^- \rightarrow \text{H}_2$ and $\text{H}_2\text{O}_2 + 2\text{e}^- + 2\text{H}^+ \rightarrow 2\text{H}_2\text{O}$ may be due in this case to the additional ohmic potential drop in the electrode layer next to the surface, which is impoverished with respect to holes. The layer impoverished with respect to holes in p-germanium is formed during its polarization, i. e. when the p-germanium surface is negatively charged with respect to the solution. The presence of this layer, directed into the depth of the semiconductor, is equivalent to an increase in the effective resistance at the germanium-solution boundary, so that it leads to a certain additional ohmic potential drop which at constant polarizing current density is greater, the greater the specific resistance of the original p-germanium.

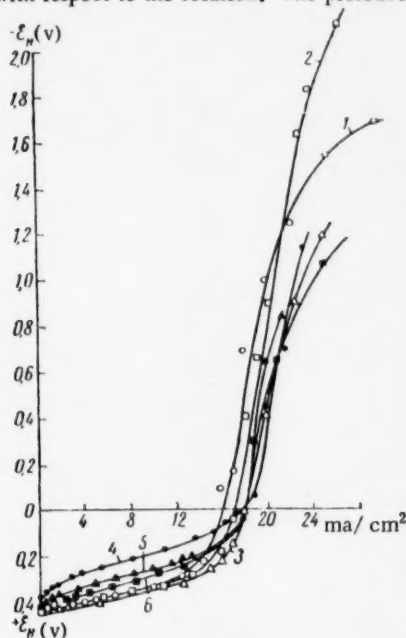


Fig. 3. Cathodic polarization of germanium in $0.5 \text{ N Na}_2\text{SO}_4 + 0.05 \text{ N K}_3[\text{Fe}(\text{CN})_6]$. p-Type germanium: 1) $\rho = 1.3 \text{ ohm} \cdot \text{cm}$; 2) $\rho = 12 \text{ ohm} \cdot \text{cm}$; 3) $\rho = 20 \text{ ohm} \cdot \text{cm}$. n-Type germanium: 4) $\rho = 1 \text{ ohm} \cdot \text{cm}$; 5) $\rho = 10 \text{ ohm} \cdot \text{cm}$; 6) $\rho = 20 \text{ ohm} \cdot \text{cm}$.

The magnitude of the potential at which the impoverishment of the surface layer of p-germanium with respect to holes begins is determined by the position of the zero point of the germanium under these conditions may differ for different solutions. A layer impoverished with respect to holes is not formed on a positively charged p-germanium surface. The fact that no retardation of the reduction of $[\text{Fe}(\text{CN})_6]^{3-}$ takes place on p-germanium (Fig. 3) is apparently due to the fact that, as a result of the high positive value of the reduction potential of this ion on the germanium electrode, the impoverishment with respect to holes of the surface of the p-germanium in this case is extremely small or zero.

The rate of anodic dissolution of p-germanium in all the above solutions is independent of the specific resistance. For electronic germanium in the same solutions, as expected, the anodic saturation current is greater, the higher the specific resistance (or the ratio ρ/L) of the original material.

It is shown below that the rate of spontaneous dissolution of germanium in H_2SO_4 ($\text{pH} = 1.0$) + $0.2 \text{ N H}_2\text{O}_2$ solution is practically independent of the conductivity type and specific resistance.

For n-type germanium with a specific resistance to $1.0 \text{ ohm} \cdot \text{cm}$, the rate of spontaneous dissolution exceeds the anodic saturation current by a factor of 3.

The results obtained show that in the spontaneous dissolution process, the semiconducting properties of the germanium have no specific effect and the electrode reactions for both electronic and hole-type conductivity take place in this case without retardation.

	Ge n-type	Ge p-type
Rate of spontaneous dissolution, $\text{mg}/\text{cm}^2 \cdot \text{hr}$		
for $\rho = 1.0 \text{ ohm} \cdot \text{cm}$	0.91	0.98
for $\rho = 20.0 \text{ ohm} \cdot \text{cm}$	0.87	0.92

For n-type Ge with $\rho = 1.0 \text{ ohm} \cdot \text{cm}$, $I_{\text{sat}} \approx 0.4 \text{ ma}/\text{cm}^2$, and with $\rho = 20.0 \text{ ohm} \cdot \text{cm}$, $I_{\text{sat}} \approx 1.2 \text{ ma}/\text{cm}^2$.

We have associated this last feature with the existence of a positive charge on the surface of n- and p-type germanium at a stationary potential in H_2SO_4 ($\text{pH} = 1.0$) + $0.2 \text{ N H}_2\text{O}_2$ solution, i. e. with an increased surface concentration of holes under these conditions.

The rate of spontaneous dissolution of germanium in the presence of hydrogen peroxide for n- and p-type germanium should in this case be determined by the kinetics of the cathodic process on n-germanium and by the kinetics of the anodic process on p-germanium. The values of the stationary potential and the rate of spontaneous dissolution of n- and p-type germanium in H_2SO_4 ($\text{pH} = 1.0$) + 0.2 N H_2O_2 solution, obtained from the polarization diagrams constructed on this principle, show good agreement with data obtained by direct measurement.

LITERATURE CITED

1. N. D. Tomashov, E. N. Paleolog, and A. Z. Fedotova, *Zhur. Fiz. Khim.*, **34**, No. 4 (1960).
2. E. N. Paleolog, A. Z. Fedotova, and N. D. Tomashov, *Doklady Akad. Nauk SSSR*, **129**, No. 3 (1959).
3. W. Brattain, G. Garrett, *Bell System Techn. J.*, **34**, No. 1 (1955).
4. J. B. Flynn, *J. Electrochem. Soc.*, **105**, 715 (1958).
5. Yu. A. Vdovin, V. G. Levich, and V. A. Myamlin, *Doklady Akad. Nauk SSSR*, **126**, No. 6 (1959).
6. H. Gerischer, F. Beck, *Zs. phys. Chem.*, **13**, 389 (1957).
7. Yu. V. Pleskov, *Doklady Akad. Nauk SSSR*, **126**, No. 1 (1959).

All abbreviations of periodicals in the above bibliography are letter-by-letter transliterations of the abbreviations as given in the original Russian journal. Some or all of this periodical literature may well be available in English translation. A complete list of the cover-to-cover English translations appears at the back of this issue.

THE EFFECT OF ADSORBED HALOGENS ON THE ELECTRON WORK FUNCTION OF IRON

G. M. Popova, N. A. Shurmovskaya, and R. Kh. Burshtein

Electrochemical Institute, Academy of Sciences, USSR

(Presented by Academician A. N. Frumkin, November 9, 1960)

Translated from *Doklady Akad. Nauk USSR*, Vol. 137, No. 4

pp. 904-907, April, 1961

Original article submitted October 30, 1960

Work in our laboratory [1-3] on the effect of adsorbed oxygen on the electron work function in iron, nickel, and platinum has shown that not only the magnitude, but even the sign of the contact potential difference is determined by the way in which the gas interacts with the metal. Thus, for the same amount of oxygen adsorbed on iron or nickel, the electron work function is increased or decreased, depending upon the temperature at which the gas interacts with the metal. Change in sign of the surface charge, in the case of iron, likewise occurs if the quantity of adsorbed oxygen is changed. An analogous effect of chemisorbed oxygen on the surface charge has recently been observed by other authors [4].

In connection with the data mentioned above, it was of interest to study the effect on the electron work function of other electronegative gases, such as halogens, adsorbed on metals. Literature data concerning the effect of halogen adsorption on the electron work function is extremely limited. The work of Oullet and Rideal [5] has shown that iodine and bromine, adsorbed on a gold surface, and iodine on silver, produce an increase in the electron work function. Iodine also increases the electron work function in zirconium and titanium [6]. The change in work function in the case of Ag, Au, and Zr amounted to 0.2-0.4 v, and for Ti, $\Delta\phi$ reached 0.9 v. A different behavior was observed when the halogens were adsorbed on metals of the alkali group, where the adsorption leads to a reduction in the electron work function [7].

The present paper gives results of a study of the effect on the electron work function of chlorine and iodine adsorbed on iron under various conditions. The measurement of the contact potential difference was carried out by the vibrator-capacitor method [8], in an apparatus in which the molybdenum comparison electrode was soldered with glass, as described in the paper by R. Kh. Burshtein and L. A. Larin [9]. The test electrode was a $20 \times 20 \times 0.2$ mm plate of "Hilger" spectroscopically pure iron.

The chlorine was prepared by the thermal decomposition of gold chloride [10]. After treatment in vacuum, the gold chloride or the iodine was heated, and the chlorine or iodine vapor formed was condensed in a side tube, immersed in liquid nitrogen. To introduce the chlorine or iodine into the apparatus, a definite halogen vapor pressure was maintained, which was accomplished by immersing the side tube with the condensate in various cooling mixtures. Thus, ampules were prepared with different pressures of chlorine or iodine. The following cooling mixtures were used with chlorine: solid isopentane ($t_{mp} = -142^\circ$), solid ethyl alcohol ($t_{mp} = -106^\circ$), and a mixture of solid CO_2 and acetone ($t = -78^\circ$), which corresponded with chlorine vapor pressures in the ampule of $4 \cdot 10^{-2}$, 5, and 63 mm of mercury [11]. After breaking the ampule, the vapor pressure of chlorine in the system was $4 \cdot 10^{-4}$, $5 \cdot 10^{-2}$, and $6.3 \cdot 10^{-1}$ mm of mercury. The vapor pressure of iodine in the system, in our experiments, was 0.01 and 0.07 mm of mercury. To check the accuracy of the halogen concentration, analytic determinations of the chlorine and iodine contained in the ampules were made by the iodometric method. The analytical data agreed satisfactorily with the quantity of halogen given by the equilibrium value of vapor pressure.

The preliminary treatment of the iron electrode consisted of repeated reduction in hydrogen at 400°, followed by prolonged degassing down to $2 \cdot 10^{-6}$ mm of mercury, with high frequency heating up to 700°. Then the cell was placed on a copper mesh screen, and to take off any polish, it was heated to 200° with direct current. After cooling the apparatus to room temperature, the contact potential difference was measured between the iron and the comparison electrode. Breaking the ampule inside the system introduced chlorine or iodine vapor. The iron electrode was maintained in the halogen vapor at room temperature (20°) for 15-17 hours, and the contact potential difference was again measured.

To find out how the electron work function varies with the way in which chlorine interacts with iron, we measured the contact potential differences between pure iron, and iron which had adsorbed chlorine, first, with different halogen pressures in the system, and then at the same pressure, but at different temperatures (20-300°). Regardless of the conditions under which the interaction took place, all the contact potential differences were measured at 20°. The results obtained are given in Figs. 1 and 2. The values of contact potential difference given are mean values from a number of experiments. The greatest deviation from the mean was 25%.

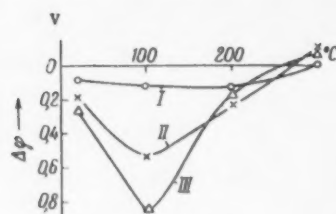


Fig. 1. Contact potential differences. Iron with chemisorbed chlorine heated in vacuum at various temperatures. 1) Chemisorption at 20°, $p = 5 \cdot 10^{-4}$ mm of mercury; 2) the same, $p = 5 \cdot 10^{-2}$ mm of mercury; 3) the same, $p = 6 \cdot 10^{-1}$ mm of mercury.

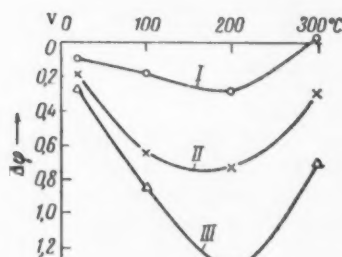


Fig. 2. Change in contact potential difference as a function of the temperature of interaction between chlorine and iron at different chlorine pressures in the gas phase. 1) $p = 5 \cdot 10^{-4}$ mm of mercury; 2) $p = 5 \cdot 10^{-2}$ mm of mercury; 3) $p = 6 \cdot 10^{-1}$ mm of mercury.

The change in the electron work function when chlorine is adsorbed on iron is brought about by an irreversible chemisorption. This is clear from the fact that, if the apparatus is degassed after a chlorine absorption, the work function does not change. This also argues in favor of the idea that the chlorine does not affect the comparison electrode. If the chlorine is adsorbed at 20°, an investigation of the electron work function shows that a pressure change from $4 \cdot 10^{-4}$ to $6.3 \cdot 10^{-1}$ mm of mercury causes a change in contact potential difference from 0.1 to 0.27 v. Heating iron with chemisorbed chlorine at 100° in the absence of chlorine in the gaseous phase (the chlorine was frozen out with liquid nitrogen) causes an additional increase in the work function, which, as can be seen from curve III, reaches 0.85 v. If the electrode temperature is raised to 200-300°, a decrease in the electron work function is observed, relative to the preceding values. If the electrode is heated to 300°, the electron work function becomes less than for reduced iron. Curves II and III show that it is as much as 0.1 v less.

If chlorine is present in the gaseous phase (Fig. 2), a similar temperature variation is observed. The only difference is that, in this case, the maximum contact potential difference of 1.3 v occurs at 200°. Heating at 300° produces some reduction in the electron work function, but it is always greater than for the reduced metal. The variation of the contact potential difference with the vapor pressure of chlorine in the gaseous phase at different absorption temperatures is given in Fig. 3. Fig. 3 shows that over the whole temperature interval from 20 to 300° raising the chlorine pressure in the system raises the electron work function.

The increase in the electron work function of iron, when chlorine is adsorbed on it at room temperature, can be explained by the formation of surface dipoles, with the negative sign turned outward. The further increase in the electron work function, observed when iron interacts with the chlorine at a high temperature, cannot be explained merely by a change in the amount of halogen adsorbed. This is based on the fact that a similar increase occurs after vacuum heating of iron with chemisorbed chlorine, i. e. under conditions where any additional adsorption is impossible. To explain the phenomenon described here, one must assume that increasing the temperature causes a change in the nature of the bond between the chlorine and the surface atoms of the iron. The reduction, relative to the maximum value, in the contact potential difference at temperatures above 100° in vacuum, and above 200° in the presence of chlorine in the gaseous phase, is the result of two concurrent processes. First, there is removal of chlorous iron

salts from the surface of the electrode, which can be concluded from the occasional appearance of small dark brown deposits on the walls of the cell. From data in the literature [12], the vapor pressure not only of ferric, but of ferrous chloride as well, is beginning to get appreciable at temperatures of 200° and higher. Second, it is possible for the halogen atoms to penetrate beneath the top layer of iron atoms, or for the iron atoms to come

out on the surface of the chloride. This follows from the fact that the electron work function for iron, which has absorbed a certain quantity of chlorine, becomes less after heating to 300° than for the reduced and degassed electrode. If the chlorine is present in the gaseous phase over the temperature range 100-200°, additional absorption of halogen takes place, which causes a change in the electron work function, amounting to 1.3 v.

To show the effect of adsorbed iodine on the electron work function for iron, a series of experiments was carried out at pressures of 0.01 and 0.07 mm of mercury. The results obtained are given in Fig. 4.

In contrast with the results obtained with chlorine, the maximum increase in the electron work function is observed with iodine when it has been chemisorbed on iron at 20°. The contact potential difference at 0.07 mm of mercury reaches 0.5 v. Removing the iodine from the gaseous phase after chemisorption on the iron surface produces no change in the contact potential difference, which shows the irreversibility of the process. Raising the temperature at which the iodine reacts with the iron produces a gradual reduction in the electron work function, relative to the 20° value. After heating to 300°, the electron work function becomes less than for pure iron by 0.1-0.15 v. It follows from the results obtained that the value of the contact potential difference increases with increasing iodine pressure, which may be related to an increase in the chemisorption with increasing iodine pressure.

On the basis of the data, it may be assumed that the absorption of iodine atoms at room temperature is accompanied by an electron transition from metal to halogen, which causes a negative charge to appear on the surface. The subsequent reduction in the electron work function, as the interaction temperature is raised, is due, apparently, to evaporation of the ferrous iodide [13] formed, as shown by the yellow-brown deposit on the walls of the cell, in which the iron ions were formed.

The reduction relative to the value for the pure metal, in the electron work function for iron with chemisorbed iodine, found after heating to 300°, can be explained in the same way as the analogous phenomenon with chlorine, described above.

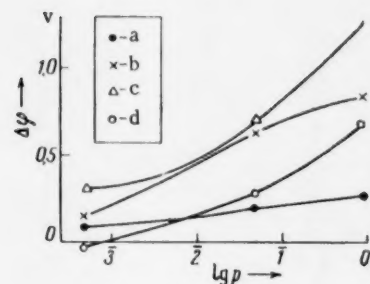


Fig. 3 Effect of chlorine pressure on the contact potential difference. a) 20°; b) 100°; c) 200°; d) 300°.

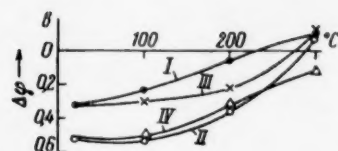


Fig. 4. Iron with chemisorbed iodine. Change in contact potential difference as a function of temperature. 1) Heating in vacuum after chemisorption of iodine at $p=1 \cdot 10^{-2}$ mm Hg and 20°; 2) the same, at $p=7 \cdot 10^{-2}$ mm and 20°; 3) heating with iodine pressure in the gaseous phase, $p=1 \cdot 10^{-2}$ mm Hg; 4) the same, at $p=7 \cdot 10^{-2}$ mm.

It follows from the data obtained, that when halogens are chemisorbed on iron, just as in the case of chemisorption of oxygen, whether the electron work function is increased or reduced depends upon how the interaction took place.

LITERATURE CITED

1. R. Kh. Burshtein, M. D. Surova, I. A. Zaidenman, *ZhFKh*, **24**, 214, (1950).
2. N. A. Shurmovskaya, R. Kh. Burshtein, *ZhFKh*, **31**, 1150 (1957).
3. T. V. Kalish, R. Kh. Burshtein, *Doklady Akad. Nauk SSSR*, **81**, 1093 (1950).
4. J. S. Anderson, D. F. Klemperer, *Nature*, **184**, 899 (1959); R. Suhrmann, *Advances in Catalysis*, **9**, 497 (1957).
5. C. Oullet, E. K. Rideal, *J. Chem. Phys.*, **3**, 150 (1935).

6. H. Malamud, A. D. Krumbein, J. Appl. Phys., 25, 591 (1954).
7. W. Geiger, Zs. Phys., 140, 608 (1955).
8. B. M. Tsarev, Contact Potential Differences (1949) [in Russian].
9. R. Kh. Burshtein, L. A. Larin, ZhFKh, 32, 194 (1958).
10. Gmelin, Handb. anorg. Chem., 62, 695 (1954).
11. J. D'Ans, Taschenbuch für Chemiker und Physiker, Berlin, 1943, S. 864.
12. Gmelin, Handb. anorg. Chem., 59 (B), 189, 232 (1932); 59 (B), 338 (1932).
13. Gmelin, Handb. anorg. Chem., 59 (B), 338 (1932).

All abbreviations of periodicals in the above bibliography are letter-by-letter transliterations of the abbreviations as given in the original Russian journal. *Some or all of this periodical literature may well be available in English translation.* A complete list of the cover-to-cover English translations appears at the back of this issue.

THE ROLE OF CONVECTION MIXING IN THE COMBUSTION OF SOLID MIXTURES

N. N. Bakhman

Institute of Chemical Physics, Academy of Sciences USSR

(Presented by Academician V. N. Kondrat'ev, December 2, 1960)

Translated from Doklady Akad. Nauk SSSR, Vol. 137, No. 5,

pp. 1141-1143, April, 1961

Original article submitted November 3, 1960

When solid mixtures undergo combustion it has frequently been observed that if the particles exceed a certain size (several microns) the normal combustion rate u_n becomes practically independent of the particle size d *; this is particularly true in the important special case where vaporization precedes the mixing of components [1]. This can be readily explained provided one assumes that if d is large enough then despite molecular diffusion convection mixing becomes very important and consequently the coefficients of mass and heat transfer increase with d .

A special feature of this particular problem is that one can expect in this case two different types of turbulence. The first type has to do with the fact that the initial solid mixture, in which particles of various sizes are randomly distributed, constitutes a sort of "frozen" turbulence which "comes to life" when the components are vaporized. We are therefore dealing with an artificially created turbulence which resembles that generated by mechanical stirring. Turbulence of this type is not directly connected with the parameters (in particular the Re number) regulating a steady flow of vaporization and combustion products. The artificial turbulence is most intense in the vicinity of the solid (s-phase) surface, i.e., in the zone which most strongly affects the combustion rate. Further in the flow the artificial turbulence subsides. The dimensions of such turbulence should be given in units proportional to d .

In addition to this at fairly large Re numbers the flow of vaporization and combustion products will give rise to the ordinary turbulence on a scale proportional to G , where G is the diameter of the combustion channel (or of the cylindrical charge when combustion takes place at one end). If we were to limit ourselves to the case where combustion takes place at one end of a charge such turbulence will obviously have little effect on the combustion rate since it can only become pronounced at a great distance from the surface of the s-phase.

Let us now stop and consider the physical aspects of the mixing taking place in the artificially created turbulence. Let us examine the factors responsible for the interpenetration of the volumes filled with the vaporized products of the original components. Among such factors we should include the fact that the various vaporized materials do not flow in parallel streams and that their absolute flow velocities are not equal.

Experiments have shown that provided d is not too small the solid phase surface facing the flame is not flat but shows wedge-shaped cavities along the line of contact between the components of the mixture (Fig. 1) which increase with increasing d . In the immediate vicinity of the s-phase surface the vaporized products move in a

* We will examine the frequently encountered case where one component is plastic (or is composed of particles much smaller than those of the second) and forms a medium throughout which the solid particles of the other component are distributed. If the latter ones are all of about the same size d then the interlayers of the first one are also proportional to d .

direction normal to the surface, since there are no tangential forces. Hence the gaseous flow velocity varies from point to point on the surface, and collisions between the gaseous streams near the surface produce the observed mixing.



Fig. 1

The absolute velocities of the vaporized products can be derived from the law of conservation of flow, and for each component we get:

$$v_1 = \frac{\rho_1 u_1}{(\rho_1)_v}; \quad v_2 = \frac{\rho_2 u_2}{(\rho_2)_v}, \quad (1)$$

where ρ and ρ_v are the densities of the solid component and its vaporization product respectively, while u is the vaporization rate (rate at which the s-phase disappears).

The mean values of \bar{u}_1 and \bar{u}_2 (time averages) are both proportional to u_n and to each other, but the instantaneous values of u_1 and u_2 (at any given time) may be interrelated in any odd fashion. Since ρ_1 and ρ_2 as well as $(\rho_1)_v$ and $(\rho_2)_v$ may also be related in about any random fashion then in general $v_1 \neq v_2$.

Due to the fact that the vaporized materials do not have the same velocities intermixing is enhanced in the tangential direction (perpendicular to u_n) and convective mixing in the axial direction (parallel to u_n) becomes possible. Let us actually analyze the situation at the instant when component 1 replaces component 2 at a fixed point. Since generally $v_{1a} \neq v_{2a}$, we should get along the line of flow either an elementary shock wave (when $v_{1a} > v_{2a}$), or an elementary rarefaction wave (when $v_{1a} < v_{2a}$), as these waves become reflected from pockets of uneven density in the gas stream and from the s-phase surface they generate progressively weaker secondary, tertiary, etc., waves. Consequently, in the case of $v_{1a} > v_{2a}$, for example, the stream of gas 1 will penetrate gas 2 while the boundary between the two will become diffused by the periodic variations of velocity and pressure which arise during the passage of elementary waves through the gas.

However, we would like to point out that gaseous mixing in the axial direction is relatively unimportant in comparison with the tangential mixing, since when a cubical piece of solid undergoes vaporization we get a rectangular gas volume with the base area unchanged and the height (and also the displacement in the axial direction) increased by a factor of ρ/ρ_v (by 1-3 orders of magnitude under ordinary conditions).

For the artificial turbulence examined by us we have one parameter with the dimensions of length (d) and another with the dimensions of velocity ($v_1 - v_2$); these can be combined to yield a function with the dimensions of the coefficient of turbulent exchange (cm^2/sec):

$$D_{\text{turb.}} \sim d(v_1 - v_2); \quad (2)$$

when considering mixing in the tangential direction we have to take $(v_{1t} - v_{2t})$, while for axial mixing we take $(v_{1a} - v_{2a})$.

Substituting the terms given in Equation (1) into (2) and assuming that $\bar{u}_1 \sim \bar{u}_2 \sim u_n$, we get

$$D_{\text{turb.}} \sim du_n \frac{\rho}{\rho_v} \sim \frac{au_n}{\rho}. \quad (3)$$

Let us now assume that the molecular diffusion coefficient

$$D_{\text{molec.}} \sim \frac{1}{\rho} \quad (4)$$

and is independent of \underline{d} , and also that usually $u_n \sim \rho^{0.5-0.7}$. It follows therefore that with increasing \underline{d} and p convection mixing assumes a more important role. It should also become more important when the curvature of the s-phase surface is increased, since the angle at which the streams collide increases and tangential displacement becomes considerably smaller than the axial.

Of course, Formula (3) is inadequate for determining the value of \underline{d} at which convection mixing in a given system becomes comparable in magnitude with molecular mixing, since we have no idea as to the magnitude of the proportionality constant on the right-hand side of expression (3). In order to verify at least qualitatively the proposed ideas regarding the role of convection mixing we designed certain experiments (in cooperation with Yu. V. Frolov) in which by using a movie camera and a set of light filters we determined the height h of the cores of flames obtained from cylindrical charges ($G = 1$ cm) consisting of $KClO_4$ mixed with bitumen of approximately the same particle size as the $KClO_4$; the sizes studied were: $d \approx 10, 180$, and 1700μ . The flame was maintained inside a large vessel filled with nitrogen at 1 atm and $20^\circ C$. We found out that the height of the flame core instead of increasing actually declined slightly when we changed from $d \approx 10 \mu$ to $d \approx 1700 \mu$, which would indicate that the coefficient of mass transfer increases with increasing \underline{d} .

We also determined the function $h(d)$ for the combustion of a single "particle". This was done by compressing powdered $KClO_4$ inside a thick plexiglass film into pellets of various internal diameters (from 0.4 to 1.4 cm). Let us note that in this case we have to assume that $G = d$.

Dimensional reasoning yields the expression

$$h \sim \frac{vd^2}{D} \sim \frac{ud^2}{\rho_v D}, \quad (5)$$

where \underline{u} is practically independent of \underline{d} [2]. Hence in the case of molecular mixing we should have $h \sim d^2$. If on the other hand the mixing is turbulent ($D_{turb.} \sim d$) then $h \sim d$. In our experiments we found that $h \sim d$ which provides additional evidence for the importance of convection mixing.

We wish to thank A. S. Sokolnik, O. I. Leipunskii, and B. V. Novozhilov for a discussion of this work and valuable comments.

LITERATURE CITED

1. N. N. Bakhman and A. F. Belyaev, *Doklady Akad. Nauk SSSR*, **133**, No. 4, 866 (1960).
2. N. N. Bakhman, *Doklady Akad. Nauk SSSR*, **129**, No. 5, 1079 (1959).

All abbreviations of periodicals in the above bibliography are letter-by-letter transliterations of the abbreviations as given in the original Russian journal. Some or all of this periodical literature may well be available in English translation. A complete list of the cover-to-cover English translations appears at the back of this issue.

2-1-12

THE STATICS OF EXCHANGE FOR A MIXTURE OF IONS

N. K. Galkina, R. N. Rubinshtein, and M. M. Senyavin

V. I. Vernadskii Geochemistry and Analytical Chemistry Institute,
Academy of Sciences, USSR

(Presented by Academician A. P. Vinogradov, November 28, 1960)

Translated from Doklady Akademii Nauk SSSR, Vol. 137, No. 5,
pp. 1144-1146, April, 1961

Original article submitted November 19, 1960

The chief aim in the application of ordinary ion-exchange processes and ion-exchange chromatography is the absorption and separation of mixtures; in spite of this the statics of exchange for ions has up to the present been studied separately. At the same time the independence of exchange of each pair of ions has been assumed [1-7]. The degree of this approximation for solutions of different concentrations has been insufficiently studied, chiefly because of the necessity for laborious calculations.

The aim of the present work was to find a simple method for calculating the equilibrium ratios in a multi-component system with known initial concentrations, from the given values of the exchange constants, and to compare the calculated data with the experimental results.

The calculation involved the solution of a system of equations including the material balance equation and the exchange isotherms for each ion, with the assumption that the activity coefficients of the ions in the solution and resin are equal to unity:

$$\frac{A_i^{1/z_i}}{A_j^{1/z_j}} = K_{ij} \frac{C_i^{1/z_i}}{C_j^{1/z_j}}, \quad i, j = 1, 2, \dots, n; \quad (1)$$

$$m(A_i - A_{0i}) = V(C_{0i} - C_i); \quad (2)$$

$$A_0 = \sum_{i=1}^n A_i = \sum_{i=1}^n A_{0i}; \quad (3)$$

$$C_0 = \sum_{i=1}^n C_i = \sum_{i=1}^n C_{0i}; \quad (4)$$

where A_i and A_j are the quantities of i -th and j -th ions sorbed per unit mass of ion exchanger; C_i and C_j are the equilibrium concentrations of the i -th and j -th ions in the solution; A_{0i} and A_{0j} are the initial quantities of the i -th and j -th ions on unit mass of the ion exchanger; C_{0i} and C_{0j} are the initial concentrations of the i -th and j -th ions in the solution; A_0 is the static exchange capacity of the ion exchanger; V is the volume of solution; m is the mass of ion exchanger; and z_i and z_j are the charges on the ions.

Since in the absorption and separation of mixtures of the elements the ion exchanger is usually used in the form of a singly charged ion, the ion in the form of which the ion exchanger exists initially is denoted by the subscript 1, $A_{01} = A_0$; $A_{02} = A_{03} = \dots = A_{0n} = 0$ and z is put equal to 1.

The solution of the system of equations (1), (2), (3), and (4) is found as follows. By means of the equation

$$\left(\frac{C_{0i}}{C_i} - 1\right)^{1/z_i} = K_{i1} \left(\frac{V}{m}\right)^{1-1/z_i} \frac{1}{\frac{A_0}{A_1}(1+b) - 1} \quad (5)$$

[where $b = (V/m)(C_{01}/A_0)$], which follows from Equations (1) - (4), a series of all values of C_i for an arbitrary given value of A_1 is calculated. These values of C_i are then used to calculate the value of

$$A_1^1 = A_0 - \frac{V}{m} \left(\sum_{i=2}^n C_{0i} - \sum_{i=2}^n C_i \right). \quad (6)$$

Next, by constructing the graph showing the relationship between A_1^1 and A_1 , we find the solution to the system of equations at the point for which $A_1 = A_1^1$. The calculation from Equation (6) is simplified by using nomograms (Fig. 1).

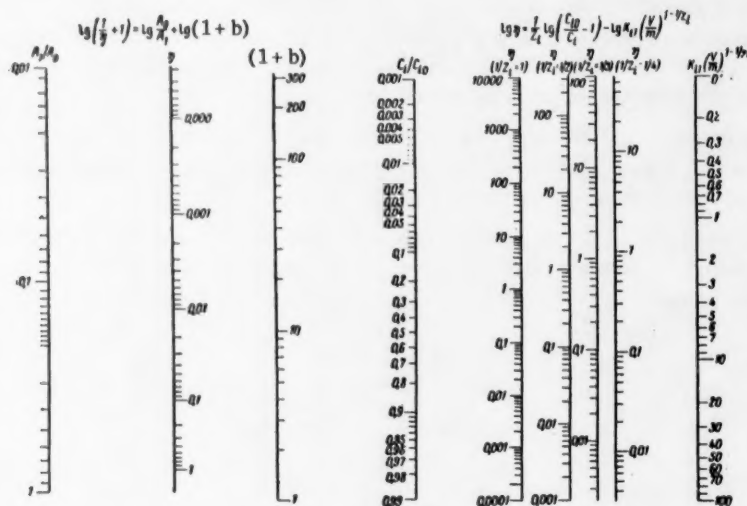


Fig. 1. Nomograms for calculating the equilibrium concentrations of ions for exchange in multicomponent systems.

We have studied the exchange in a three-component system on a cation exchanger in the hydrogen form. The values of the individual exchange constants of the ions, necessary for the calculation of the equilibrium ratios in the mixture, were determined experimentally under static conditions and calculated according to Equation (1).

The experimental equilibrium ratios were studied for the $\text{NaCl}-\text{CsCl}-\text{RH}$ and $\text{NaCl}-\text{CaCl}_2-\text{HCl}-\text{RH}$ systems on KU-2 cation exchanger under static conditions at salt concentrations of up to 1 N and equivalent metal ratio equal to 1:1. The equilibrium concentrations of sodium and cesium were determined radiometrically and the equilibrium concentrations of Ca were determined by complexometric titration with Trilon B (in the resin—after desorption with NaCl solution). For exchange in concentrated solutions (> 0.2 N), where the concentration of hydrogen in the cation exchanger is the smallest quantity, this concentration was determined directly by eluting the hydrogen from the cation exchanger with 2 N NaCl solution and titrating with alkali.

The experimental data obtained for the exchange in the three-component systems and a comparison of these data obtained by calculations assuming independence of exchange of the ions are given in Figs. 2 and 3. It is

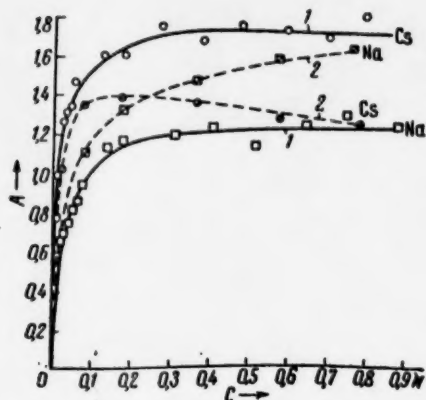


Fig. 2. Isotherms for exchange of sodium and cesium by hydrogen for exchange in a three-component system. 1) Experimental data; 2) data calculated from the nomograms.

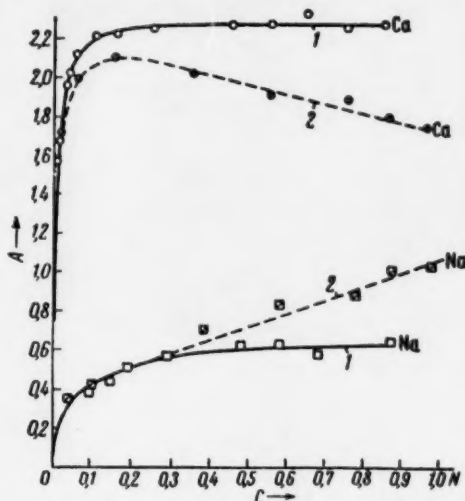


Fig. 3. Isotherms for exchange of sodium and cesium by hydrogen for exchange in three-component system in the presence of 0.1 N hydrochloric acid. 1) Experimental data; 2) data calculated from the nomograms.

clearly seen that there is complete correspondence between the experimental and calculated data up to concentrations of equilibrium solution of, on the average, 0.05 N, together with a regular divergence at higher concentrations of the solution: this divergence cannot apparently be attributed entirely to the change in the activity coefficients of the substances.

LITERATURE CITED

1. B. P. Nikol'skii and V. I. Paramonova, *Uspekhi Khim.*, **8**, No. 10, 1535 (1939).
2. A. M. Trofimov, Collection. *Chromatography* [in Russian] (Leningrad University Press, 1956), p. 15.
3. T. F. Antipova-Karataeva and I. N. Antipov-Karataev, *Kolloid. Zhur.*, **5**, 419 (1939).
4. J. Dranoff and L. Lapidus, *Industr. and Eng. Chem.*, **49**, No. 8, 1297 (1957).
5. G. Jangg, *Osterr. Chem. Ztg.*, **59** No. 23-24, 331 (1958).
6. K. M. Saldadze, A. B. Pashkov, and V. S. Titov, *Macromolecular Ion-Exchange Compounds* [in Russian] (Moscow, 1960), p. 38.
7. A. T. Davydov and I. Ya. Levitskii, *Trudy Nauch.-Issled. Inst. Khim. Khar'kovsk. Gos. Univ.*, **10**, 221 (1953); **12**, 309 (1954); **12**, 316 (1954).

All abbreviations of periodicals in the above bibliography are letter-by-letter transliterations of the abbreviations as given in the original Russian journal. Some or all of this periodical literature may well be available in English translation. A complete list of the cover-to-cover English translations appears at the back of this issue.



FIGURE 1. The relationship between the percentage of patients with a certain condition and the percentage of patients who have been treated. The curves show that the percentage of patients with a certain condition increases rapidly at first and then levels off as the percentage of patients who have been treated increases.

The following table shows the percentage of patients with a certain condition who have been treated by various methods. The methods are listed in the first column, and the percentage of patients treated is listed in the second column.

Method	Percentage of Patients Treated
1. Medical treatment	100
2. Surgical treatment	85
3. Radiation treatment	70
4. Chemotherapy	55
5. Hormone therapy	40
6. Physical therapy	25
7. Psychotherapy	10

The results of the treatment of patients with a certain condition are shown in the following table. The methods are listed in the first column, and the percentage of patients who have been treated is listed in the second column. The percentage of patients who have been treated is shown in parentheses.

THE USE OF HIGH PRESSURE IN THE STUDY OF COLLECTIVE INTERACTION IN POLYMERIZATION PROCESSES

M. G. Gonikberg

N. D. Zelinskii Institute of Organic Chemistry, Academy of Sciences, USSR

(Presented by Academician B. A. Kazanskii, December 6, 1960)

Translated from Doklady Akad. Nauk SSSR, Vol. 137, No. 5,

pp. 1147-1148, April, 1961

Original article submitted December 1, 1960

It is generally recognized at the present time that the application of high pressure is a very useful tool in the investigation of the transition state of chemical reactions. In particular, data relative to the influence of pressure on reaction rate in the liquid phase make it possible to arrive at definite conclusions as to the structure of the transitional state (see, for example, [1] and [2]), as well as to the participation of the solvent in the process [3-6]. The essence of the method consists in a calculation, based on the above-mentioned kinetic data, of the magnitude of the volume change when the transitional state is formed, and then comparing this magnitude with the value to be expected on the basis of some model or other of the transitional state. Thus it is even possible to find the actual volume of the transitional state. It is easily seen that this property is very important to the study of collective interactions. It is possible to talk in this way about any kind of reactions which involve the necessity of overcoming a known energy barrier, and, in particular, it applies to collective chemical interactions.

Let us write the equation expressing the reaction rate constant k as a function of pressure [7]:

$$\left(\frac{\partial \ln k}{\partial P}\right)_T = -\frac{\Delta v^\ddagger}{RT} \quad (1)$$

Here, Δv^\ddagger is the change in volume when the transitional state is formed from the initial materials. If n particles participate in the transitional state, then the value of Δv^\ddagger will, roughly speaking, be $(n - 1)$ times greater than in the interaction of two particles.

As an illustration of the application of this method, let us consider the interesting data of Wentworth on the polymorphic transformation of diamond into graphite, presented at the XVII International Congress of Pure and Applied Chemistry in August 1959 (see also Ref. [8]). Wentworth found that graphitization of diamond at temperatures of 1700-2200° is very strongly retarded by increasing pressure. The value of Δv^\ddagger which they found from the kinetic data is about 168 cm³ per gm-atom, that is, 50 times greater than the volume existing per gm-atom in the crystal. Hence, the author naturally concluded that the polymorphic transition that he was studying took place as a collective act, with the participation of a considerable number of atoms.

The polymorphic transformation of diamond into graphite, considered above, is characterized by an increase in volume when the transitional state is formed. An effect of opposite sign is observed in polymerization reactions (see [9]). A particularly large compression should occur when the transitional state is formed in polymerization reactions of the sort (at low temperatures or high pressures), in which the presence of collective interaction of the reacting particles can be assumed [10, 11]. Therefore, reactions of this sort ought to experience considerable acceleration with increasing pressure. This can be illustrated by the following arbitrarily selected example. Let the reduction in volume on formation of the transitional state from two molecules of monomer

(or a radical and a molecule) be 10 cm^3 per mole, and let the number \underline{n} of particles participating in the transitional state be ten. Then increasing the pressure to 1000 atm will, in accordance with Eq. 1, bring about a 43-fold increase in the reaction rate constant.

It follows from what has just been said that a study of the effect of pressure on the polymerization rate in liquid and solid phases can show up cases of collective interaction of the reacting particles, and permit an estimate to be made of the number of "participants" in the interaction.

Considerable interest is also attached to the study of the influence of temperature on the variation of the rate constant with pressure. Combining the Arrhenius equation with the equations for the theory of the transitional state gives the following.*

$$\left(\frac{\partial E}{\partial P}\right)_T = \left(\frac{\partial \Delta H^\ddagger}{\partial P}\right)_T; \quad (2)$$

$$\left(\frac{\partial \ln A}{\partial P}\right)_T = \frac{1}{R} \left(\frac{\partial \Delta S^\ddagger}{\partial P}\right)_T. \quad (3)$$

Using now the well-known thermodynamic equations for the heat content and the entropy as a function of pressure, and substituting them in Eqs. (2) and (3), we get:

$$\left(\frac{\partial E}{\partial P}\right)_T = \Delta v^\ddagger - T \left(\frac{\partial \Delta v^\ddagger}{\partial T}\right)_P, \quad (4)$$

$$\left(\frac{\partial \ln A}{\partial P}\right)_T = -\frac{1}{R} \left(\frac{\partial \Delta v^\ddagger}{\partial T}\right)_P. \quad (5)$$

From Wentworth's data, already cited, the activation energy of the diamond graphitization reaction rises with increasing pressure from zero (vacuum) to 20,000 atm, from 175 to 255 kcal/gm-atom respectively. Substituting these figures in Eq. (4), we find that the right side of the equation is approximately equal to $165 \text{ cm}^3/\text{gm-atom}$. Comparing this figure with the value of Δv^\ddagger equal to about $168 \text{ cm}^3/\text{gm-atom}$ (see above), we can conclude that the change in Δv^\ddagger with temperature is near zero. This means that in the reaction under consideration, a change in temperature within the experimental limits (1700–2200°) does not, in any noticeable fashion, influence the number of atoms taking part in the collective act of polymorphic transformation. The elucidation of this question for collective chemical interactions will stimulate the effort to penetrate into the physical nature and the mechanism of the reactions themselves.

LITERATURE CITED

1. C. Walling, J. Peisach, J. Am. Chem. Soc., **80**, 5819 (1958).
2. M. G. Gonikberg, ZhFKh, **34**, 225 (1960).
3. J. Buchanan, S. D. Hamann, Trans. Farad. Soc., **49**, 1425 (1953).
4. M. G. Gonikberg, V. M. Zhulin, Austr. J. Chem., **11**, 285 (1958).
5. M. G. Gonikberg, B. S. El'yanov, Doklady Akad. Nauk SSSR, **130**, 545 (1960).
6. E. Whalley, Canad. J. Chem., **36**, 228 (1958).
7. M. G. Evans, M. Polanyi, Trans. Farad. Soc., **31**, 875 (1935).
8. H. P. Bovenkerk, F. P. Bundy et al., Nature, **184**, 1094 (1959).
9. M. G. Gonikberg, Chemical Equilibrium and Reaction Rate at High Temperatures [in Russian] Academy of Sciences Press, USSR (1960).
10. N. N. Semenov, Collection: Chemistry and Technology of Polymers [in Russian] (1960) No. 7–8, page 196.
11. M. G. Gonikberg, V. M. Zhulin, B. S. El'yanov, Doklady Akad. Nauk SSSR, **132**, 353 (1960).

* Assuming the transmission coefficient independent of pressure.

INVESTIGATION OF THE KINETICS OF THE ELECTROREDUCTION OF IRON ON THE DROPPING MERCURY ELECTRODE

V. F. Ivanov and Z. A. Iofa

The M. V. Lomonosov Moscow State University

(Presented by Academician A. N. Frumkin, November 30, 1960)

Translated from *Doklady Akademii Nauk SSSR*, Vol. 2, No. 5,

pp. 1149-1152, April, 1961

Original article submitted November 28, 1960

The study of the reduction of bivalent iron ions on the dropping mercury electrode by a polarographic method has been the subject of many publications [1]. Almost all of these, however, have been performed with analysis as their object. It was J. Heyrovsky [2] who first called attention to the large overpotential in the reduction of iron ions at the dropping mercury electrode. Heyrovskii supposed that ions were reduced reversibly, since the reduction potential was in accord with the equation: $\varphi = \text{const} + 0.029 \log (\text{Fe}^{2+})$. He explained the large negative value of the potential by the formation of a metastable amalgam containing highly active iron atoms. This has also been used to explain the absence of retardation on the anodic branch of the polarization curve due to the dissolution of the iron from the amalgam. Indications of the reversibility of the process are also given in [4]. Kolthoff and Lingane [5], however, believe that iron does not form amalgams on the dropping mercury electrode and that the reduction occurs irreversibly.

The present work is devoted to a study of the degree of irreversibility of this reaction, the effect of the concentration of the iron ions, and the effect of the concentration and nature of the base solution on the kinetics of the process.

A visual polarograph was used for the investigation. The potential of the dropping mercury electrode was determined by a compensation method. The comparison electrode was a normal calomel half-cell. The cell used was distinguished by having built in ground joints containing glass and hydrogen electrodes, so that the pH of the solution could be checked at any moment during the experiment. pH was determined with an accuracy of ± 0.05 , and the temperature used was $25^\circ \pm 0.15^\circ$. To facilitate the separation of closely similar half-wave potentials, a number of the experiments were performed on an oscillographic polarograph of type TsLA-01 on the Zvassman system. By means of this oscillograph the peak potentials φ_p were determined from differential polarograms.

The relationship between the limiting current I_d and the concentration of ferrous ions within the range 10^{-4} to 10^{-2} N showed that, in neutral and weakly acidic solutions (pH greater than 4.5), I_d conformed with sufficient accuracy to the Il'kovich equation, taking $n=2$ and the diffusion coefficient as 0.76×10^{-5} cm²/sec (calculated from conductivity data). The experimental data are given in Fig. 1, 1. In the pH range from 4.5 to 2.8 the limiting currents for iron and hydrogen are practically the same. Figure 1, 2 and 3 shows that the limiting diffusion current within the pH range 7 to 2.8 is the sum of the iron and hydrogen currents.

The study has confirmed the conclusions drawn in [3,5] that the half-wave potential of iron is shifted in a positive direction with increase in the concentration of iron ions (cf. Fig. 1, 4). According to published data [6], no corresponding change of half-wave potential with concentration has been found for cobalt and nickel. The magnitude of the shift is not constant, and seems to be a complex function of the concentrations of iron and hydrogen ions in the solution.

Fig. 2, 1-3 shows the results of determining the effect of concentration and nature of base solution on the half-wave potential of iron for $\text{pH} > 4.5$, for which the presence of hydrogen ions exerts little effect on the iron wave. Curve 4 of the same figure shows the relationship between the coefficient $\alpha = 0.029/b^*$ on the concentration of the base (KCl). This curve shows that the value of α diminishes with increase in base concentration, pointing to the irreversibility of the process.

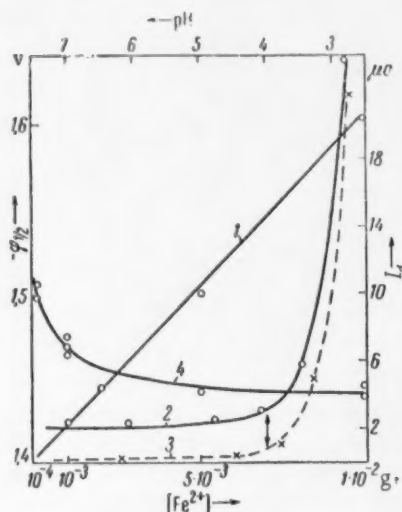


Fig. 1. Curves showing the relationship between: 1) I_d and (Fe^{2+}) , in base of 2N KCl, pH 5.5; 2) I_d and pH, in base of 1N KCl, $(\text{Fe}^{2+}) = 10^{-3}\text{N}$; 3) I_d and pH in base of 1N KCl, $(\text{Fe}^{2+}) = 0$; 4) $\varphi_{1/2}$ and (Fe^{2+}) , in base of 2N KCl, pH = 5.5.

ferrous ions in acid solutions are more negative than those obtained in neutral media (see curves 8 and 9, Fig. 3B).

The correctness of curves so constructed, and the conclusions indicated have been confirmed from data obtained by differential polarography:

Base	1N KCl				10N CaCl_2				10N $\text{Ca}(\text{ClO}_4)_2$		10N LiCl
pH	6.5;	4.5;	3.5;	3.0;	5.0*;	3.5*;	5.0;	3.5	~ 4.5	5.8	
$-\varphi_{1/2}$, v	1.42;	1.45;	1.49;	1.55	—	—	1.13;	1.14	1.42**	1.27**	
$-\varphi_p$, v	1.45;	1.50;	1.55;	—	1.33 *	1.24 *	1.27;	1.27	1.4	—	

* Data from reference [8].

** From the polarographic wave.

These data have shown that the peak potential φ_p on the differential curves for the discharge of hydrogen ions is unchanged when iron ions are present in the solution, and is practically independent of pH. But the value of φ_p for the discharge of iron ions on the same differential curves is shifted in the direction of negative potential by reduction in pH: with pH change from 6.5 to 3.5, $\Delta \varphi_p = \text{ca. } 100 \text{ mv}$. In very acid solutions ($\text{pH} = 2.2$) the peak of the iron ion discharge wave merges with that for hydrogen ion discharge. In the general case the magnitude of the shifts in $\varphi_{1/2}$ and φ_p depends on the ratios of the concentrations of iron and hydrogen ions. Increase in the concentration of iron ions causes a reduction in $\Delta \varphi_{1/2}$.

* b is the coefficient in the equation: $\varphi = \varphi_{1/2} + b \log[(\alpha - i)/i]$.

This reduction in the value of α , and the shift in half-wave potential to the right, are evidently due to a reduction in the negative value of the ψ_1 -potential with increase in base solution concentration. This effect is specially noticeable when sulfates are used as base salts.

The concentration of calcium chloride solutions exerts an opposite effect. In a base of 5M calcium chloride the half-wave potential shows a positive displacement of 300 mv (see Fig. 4). If concentrated calcium perchlorate (sp. gr. ca. 1.4) is used instead, the value of the half-wave potential is about the same as in potassium chloride solutions.

Our experiments on the effect of pH on the half-wave potential for the electrical reduction of ferrous ions gave results shown in Fig. 3A. Curves 4 and 6 show that the half-wave potentials for the simultaneous discharge of iron and hydrogen ions in the pH range 4.5 to 2.8 lie considerably to the positive side of those for hydrogen discharge (see curves 1, 3, and 5), but to the negative side of those for the discharge of iron at $\text{pH} > 5$ (see curve 2). When the pH is reduced, the half-wave potential for the simultaneous wave (as shown in curves 2, 4, 6, and 7), approximates to that of the hydrogen wave ($\varphi_{1/2} = -1.620\text{v}$).

If the hydrogen wave current is subtracted from the overall wave current for various potential values, the difference constitutes the wave for the discharge of iron at the given pH value. The half-wave potentials obtained in this way for discharge of

Published evidence shows that increase in polarization with reduction in pH is found in the electrodeposition of zinc, nickel, cobalt, lanthanum, indium and some other metals [7]. Such data are absent for the deposition of iron.

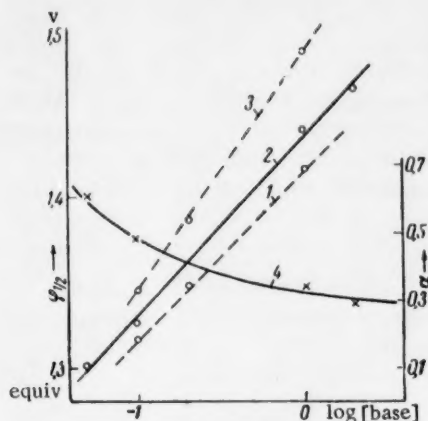


Fig. 2. Curves showing the relationship between $\phi_{1/2}$ and base concentration: 1) KCl; 2) K_2SO_4 ; 3) K_2SO_4 . (Fe^{2+}) = $10^{-3}N$, pH = 5.5; 4) Curve showing the relationship between $\alpha = 0.029/b$ and (KCl). (Fe^{2+}) = $10^{-3}N$, pH = 5.5.

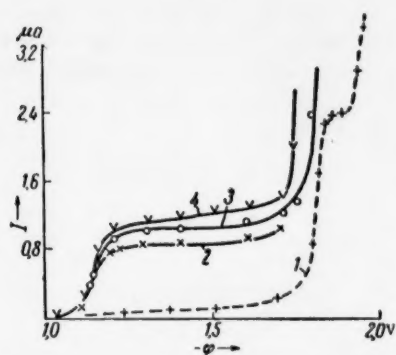


Fig. 4. Curves showing the relationship between I and ϕ in a base of 5M $CaCl_2$: 1) (Fe^{2+}) = 0, pH = 3.65; 2) (Fe^{2+}) = $10^{-3}N$, pH = 3.6; 4) (Fe^{2+}) = $10^{-3}N$, pH = 2.9.

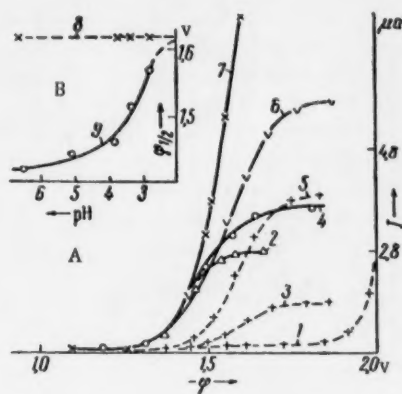
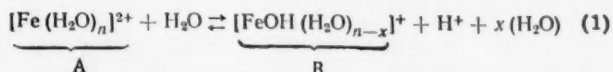


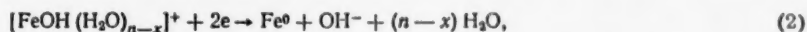
Fig. 3. A. Curves showing the relationship between I and ϕ , when (Fe^{2+}) = 0, in a base of 1N KCl: 1) pH = 6.6; 3) pH = 3.8; 5) pH = 3.3. Curves showing the relationship between I and ϕ , when (Fe^{2+}) = $10^{-3}N$, in a base of 1N KCl: 2) pH = 6.6; 4) pH = 3.8; 6) pH = 3.3; 7) pH = 2.8. B. Relationship between $\phi_{1/2}$ and pH in a base of 1N KCl: 8) (Fe^{2+}) = 0; 9) (Fe^{2+}) = $10^{-3}N$.

tion of iron dropping mercury electrode, with the exception of [8], in which reference is made to the reversible nature of the dependence in a base of 5M calcium chloride. The latter is not, however, in agreement with our own experiments, carried out under similar conditions (see Fig. 4).

All our experimental data may be explained by a single theory if we postulate the following mechanism for the electrodeposition of iron on the dropping mercury electrode. In aqueous solution, through the reaction:



the less hydrated hydroxy-complex B is formed. Ions A are also found in the double layer in a definite concentration ratio, together with B. If it is supposed that the discharge of the more hydrated aqua-complex ions A is more difficult, the rate of the process should be determined by the slowness of the discharge stage of the less hydrated complex B:



Reaction (2) thus represents the stage which determines the rate of the process. Discharge of the B ions may be supplemented by the diffusion of the A ions and their rapid change into B ions on account of the shift in the equilibrium $A \rightleftharpoons B$ in the peri-electrode layer. The size of the limiting current is determined not by the ions B, but by the over-all concentration of the iron ions in the bulk.

In accordance with the suggested mechanism for the electrode reaction, reduction in pH of the solution ought to cause a shift of equilibrium of the bulk reaction (1) in the direction of reducing the concentration of the B ions, and should at the same time increase the polarization. On the other hand, it could be thought that every change tending to reduce the degree of hydration of the iron ions would facilitate their discharge and increase its reversibility. In very concentrated calcium chloride solutions we have actually observed a reduction in the polarization of this process. Replacement of the calcium chloride base solution by one of concentrated calcium perchlorate has shown, however, that it is not the calcium ions which play the decisive role. The cause of the large shift of the half-wave potential in a positive direction in this case is, presumably, not any additional dehydration of the aqua-complexes, but the substitution of hydroxy-complexes by chloro-complexes.

We wish to express our gratitude to Academician A. N. Frumkin for his interest and advice in the course of this work.

LITERATURE CITED

1. S. G. Mikhlin, *Zav. Lab.*, 5, 1167 (1936); Ya. P. Gokhshtein, *Zav. Lab.*, 5, 28 (1936); A. M. Dymov, G. D. Kubyshkina, and N. S. Poliektova, *Zav. Lab.*, 6, 147 (1937); E. S. Burkser and S. G. Mikhlin, *Uspekhi Khim.*, 2, 369 (1937); J. Lingane, *J. Am. Chem. Soc.*, 68, 2448 (1946).
2. J. Heyrovsky, *C. R.*, 179, 1267 (1924).
3. J. Heyrovsky and B. Souček, *C. R.*, 183, 125 (1926); J. Heyrovsky, *Polarographic Methods* [in Russian] (Moscow, 1937); J. Heyrovsky and R. Kalvoda, *Oszillographische Polarographie mit Wechselstrom*, Berlin, 1960.
4. A. A. Gabovich, *Transactions of the M. V. Frunz Agricultural Institute of Kishinev*, 9, 143 (1956).
5. I. Kolthoff and L. Lingane, *Polarography* [in Russian] (1948).
6. Ya. I. Tur'yan, *Doklady Akad. Nauk SSSR*, 113, 631 (1957).
7. S. I. Zhdanov and A. N. Frumkin, *Zhurn. Fiz. Khim.*, 29, 1959 (1955); Z. A. Solov'eva and S. A. Abrarov, *Zhurn. Fiz. Khim.*, 30, 1572 (1956); R. Brdica, *Chem. News*, 142, 336 (1931); A. S. Wensen and G. Glockler, *J. Am. Chem. Soc.*, 71, 1641 (1949).
8. G. Reynolds, H. Shalgosky, and F. Weber, *Anal. Chim. Acta*, 9, 91 (1953).

All abbreviations of periodicals in the above bibliography are letter-by-letter transliterations of the abbreviations as given in the original Russian journal. Some or all of this periodical literature may well be available in English translation. A complete list of the cover-to-cover English translations appears at the back of this issue.

NUCLEAR MAGNETIC RESONANCE SPECTRA OF IRRADIATED PERFLUOROCTADIENE AND PERFLUORDODECADADIENE

N. M. Pomerantsev, V. A. Khranchenkov, L. V. Sumin
and A. V. Zimin

L. Ya. Karpov Physical Chemical Institute

Presented by Academician V. A. Kargin, November 17, 1960

Translated from Doklady Acad. Nauk SSSR, Vol. 137, No. 5,
pp. 1153-1154

Original article submitted November 10, 1960

In the study of the phenomena of radiation chemistry which are produced by irradiating organic systems, very valuable results are obtained from the use of the two methods of infrared spectroscopy and nuclear magnetic resonance (n. m. r.) [1]. However the interpretation of infrared spectra is hampered (particularly with complex molecules) by overlapping of the absorption bands produced by the various functional groups in the molecule. In the n. m. r. spectra, the lines corresponding with these groups are well differentiated, which provides a more reliable answer to the question of whether or not individual functional groups exist.

We have obtained spectra of the magnetic resonance of F^{19} nuclei, un-irradiated and irradiated with Co^{60} (integral dose $\sim 10^{22}$ ev/gm), in perfluorooctadiene and perfluordodecadiene. The spectograms were taken at room temperature with an apparatus which will be described in a separate paper. The chemical shift was measured relative to the F^{19} line of the CF_3 group in trifluoroacetic acid. The values of the chemical shift δ , spread out to the scale of Figs. 1 and 2, are given by the expression $\delta = (H_s - H_f)/H_s \cdot 10^5$, where H_s is the resonance field value for the standard, and H_f is the resonance value for the fluorine in the given functional group.

The published theoretical and experimental data on the chemical shifts for fluoro-carbon compounds make an unambiguous interpretation of the above spectra possible. It can be considered as an established fact that, for compounds containing fluorine, the chemical shift of the F^{19} nuclei is determined, basically, by the form of the chemical bond. For spherically symmetric F^- ions, the paramagnetic term in the expression for the chemical shift is absent. The presence of a co-valent bond causes this term to appear, along with a displacement of the absorption lines toward the weak field end [2, 3]. For fluoro-carbon compounds, containing no other atoms but carbon and fluorine, it has been shown that the absorption lines of the F^{19} nuclei in the CF groups are to be found in rather weak fields. In weaker fields are found the lines from the CF_2 groups, while the lines coming from the F^{19} in the CF_3 groups are located in even weaker fields [4].

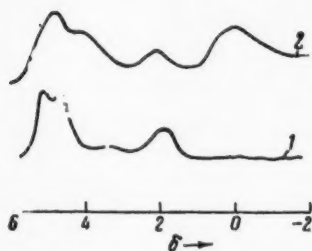


Fig. 1. Magnetic resonance spectrum of F^{19} nuclei in perfluorooctadiene.

Starting with these concepts, the spectra of un-irradiated perfluorooctadiene and perfluordodecadiene may be interpreted as follows. The strong band in the region $\delta = 5.5$ is presumed to consist of a series of unresolved lines belonging to the F^{19} nuclei in the $-CF_2-$ groups, and the molecules $CF_2=CF-(CF_2)_4-CF=CF_2$ and $CF_2=CF-(CF_2)_8-CF=CF_2$. The relatively weak line ($\delta = 1.8$) is assumed to arise from the F^{19} nuclei in the end $=CF_2$ groups. The line coming from CF , which one would expect to find in a weaker field than the line from F^{19} nuclei in the $-CF_2-$ group is not observed, apparently because of its small intensity. The above interpretation of the spectrum lines is supported by considerations based on the line intensities.

The spectra of irradiated perfluorooctadiene and perfluordodecadiene differ from the spectra of the un-irradiated compounds by the presence of a line located in relatively weaker fields, than the lines from the un-irradiated samples. From its position, as we have said above, this line ought to come from

the CF_3 group, which has also been observed in infrared spectroscopy.

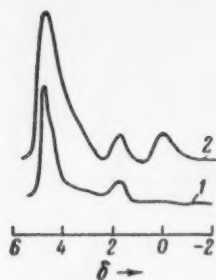


Fig. 2. Magnetic resonance spectra of F^{19} nuclei in perfluorododecadiene.

Some of the changes in form of the band belonging to the F^{19} nuclei in the $-CF_2-$ groups are probably to be explained by the appearance of branching structure, and can be interpreted, if there is better resolution of the lines making up the band. It should be noted that the line widths are greater for the irradiated samples than for the un-irradiated ones. This is to be explained by the viscosity of the irradiated samples and sets a limit to the resolution possible. It is to be expected that measurements at higher temperatures will give spectra with better resolution.

LITERATURE CITED

1. J. A. Pople, W. G. Schneider, and H. J. Bernstein, *High-resolution Nuclear Magnetic Resonance* (New York, 1959).
2. H. S. Gutowsky and C. J. Hoffman, *J. Chem. Phys.* **19**, 1259 (1951).
3. A. Saika and W. P. Slichter, *J. Chem. Phys.* **22**, 26 (1954).
4. N. Muller, P. C. Lauterbur, and G. F. Svatos, *J. Am. Chem. Soc.* **79**, 1807 (1957).

All abbreviations of periodicals in the above bibliography are letter-by-letter transliterations of the abbreviations as given in the original Russian journal. *Some or all of this periodical literature may well be available in English translation.* A complete list of the cover-to-cover English translations appears at the back of this issue.

THE EFFECT OF POLYMORPHISM ON THERMAL CONDUCTIVITY

G. B. Ravich and Yu. N. Burtsev

N. S. Kurnakov Institute of General and Inorganic Chemistry,
Academy of Sciences of the USSR

(Presented by Academician I. V. Tananaev, November 25, 1960)

Translated from *Doklady Akad. Nauk SSSR*, Vol. 137, No. 5,
pp. 1155-1157, April, 1961

Original article submitted November 23, 1960

The change in the thermal conductivity resulting from phase conversions in the solid state, associated with different forms of polymorphism (reversible and non-reversible transitions of modifications) presents considerable scientific and practical interest from the point of view of molecular physics. The first observations in this field, made on inorganic substances, in particular on sulfur [1], revealed a substantial difference in the numerical value of the thermal conductivity for different polymorphic phases.

A dissimilar temperature behavior of the thermal conductivity for different modifications was also established. Papers concerned with the study of thermal conductivity for phase transitions in solid organic substances, and also for the change of state of aggregation of these substances (melting, crystallization) are almost unknown to us. This is associated, apparently, with the substantial methodic difficulties which arise in staging reproducible experiments.

In order to clarify the effect of polymorphism on thermal conductivity we used an apparatus developed by us which allowed us to carry out measurements with satisfactory accuracy (experimental error did not exceed 2%). *p*-Dichlorobenzene was chosen as the material to be studied. As is known from the literature, this substance possesses a clearly defined polymorphism and in particular a reversible transition at $\sim 32^\circ$. The number of phases given by different authors varies between two and three [2-5].

Measurements of the thermal conductivity of *p*-dichlorobenzene were carried out, under static conditions, by a comparison method in an apparatus in the form of two coaxial cylinders, which was constructed so that the thermal conductivity of the substance could be measured in the solid and liquid state.

The apparatus (Fig. 1) was made of glass and consisted of a working cylinder (1) (internal diameter 3-4 mm) passing upwards into a funnel 2 for introducing the substance. Centered along the axis of the working cylinder 1, by means of a teflon stopper 3, was a four-bore glass capillary 4 (external diameter 1.5-2.0 mm) inside which was placed a copper-constantin thermocouple 5 (diameter 0.10 mm) and a nichrome heater 6 (diameter 0.10 mm). The length of the capillary tube 4 was 8-10 cm less than the length of the working cylinder 1, and thus the pit resulting from crystallization of the substance in the cylinder did not reach to the top end of the capillary tube by 2-5 cm. The working cylinder was enclosed within two jackets 7 and 8, through which was passed a thermostating liquid from a Vobzer thermostat. The temperature of the liquid in the apparatus was measured by means of the thermocouple 9 enclosed in the capillary 10. The top of the apparatus was hermetically sealed with a spherical cover 11, having an outlet 12, which was connected through the stopcock 13 to a vacuum pump.

Thermocouples 5 and 9 were connected so that it was possible to measure both the temperature at the walls of the capillary 4 and of the working cylinder 1, and also the difference between these temperatures. The e.m.f. of the thermocouples was measured on a PPTN-1 potentiometer.

In the solid state of $p\text{-C}_6\text{H}_4\text{Cl}_2$ we have detected two stable modifications: a low temperature α (Fig. 2, IV) possessing a low thermal conductivity ($29\text{--}35 \cdot 10^{-5}$ cal/cm \cdot sec \cdot deg), and a high temperature β (Fig. 2, III) possessing a higher thermal conductivity ($37\text{--}40 \cdot 10^{-5}$ cal/cm \cdot sec \cdot deg). The enantiotropic transition between these two modifications $\alpha \rightleftharpoons \beta$, according to our measurements, corresponded to $\sim 32^\circ$. Sometimes through rapid heating, the α -modification became superheated to 40° without undergoing a transition: the β -modification could be supercooled to 30° .

Accurate determination of the temperature of the $\alpha \rightleftharpoons \beta$ transition is possible only by prolonged thermostating.

In addition to the stable modifications of $p\text{-C}_6\text{H}_4\text{Cl}_2$ we detected the presence of metastable forms. By rapid cooling of the melt a metastable β' -modification (Fig. 2, II) was first formed, existing in the temperature range $+32$ to $+53^\circ$, which possessed a thermal conductivity $63\text{--}70 \cdot 10^{-5}$ cal/cm \cdot sec \cdot deg. The thermal conductivity of this modification was detected down to $+20^\circ$.

In the temperature range $+32$ to $+53^\circ$ the β' -modification after 4-5 days changed into the stable β -form. This transition apparently occurred via a series of metastable forms of short existence, since occasionally it is absent from the thermal conductivity curves, lying according to its value between the curves of the β' and β -modifications.

The transition from β to α passes through a metastable form possessing a thermal conductivity $35\text{--}39 \cdot 10^{-5}$ cal/cm \cdot sec \cdot deg.

Thus, we have clearly succeeded in recording in the temperature range -40 to $+53^\circ$ two stable and two metastable modifications. During this, the different polymorphic forms not only alter the value of the coefficient of thermal conductivity but also the value of the temperature coefficient of the thermal conductivity.

This may be of interest both for more detailed treatment of the nature of the conversions and also in connection with various thermophysical problems associated with the passage of heat through solid organic substances.

LITERATURE CITED

1. G. W. C. Kaye and W. F. Higgins, Proc. Roy. Soc., A, 122, 633 (1929).
2. K. Beck and K. Ebbinghaus, Ber. 39, 3870 (1906).
3. M. F. Vuks, Zhur. Éksp. Teor. Fiz. 7, 270 (1937).
4. V. I. Danilov and D. E. Ovsienko, Doklady Akad. Nauk SSSR, 73, No. 6, 1169 (1950).
5. G. A. Jeffrey and W. J. McVeagh, J. Chem. Phys. 23, No. 6, 1165 (1955).
6. G. M. Kondrat'ev, Heat Measurements [in Russian] (Moscow-Leningrad, 1957).

All abbreviations of periodicals in the above bibliography are letter-by-letter transliterations of the abbreviations as given in the original Russian journal. Some or all of this periodical literature may well be available in English translation. A complete list of the cover-to-cover English translations appears at the back of this issue.

1
2
3
4
5
6
7
8
9
10
11
12
13
14
15
16
17
18
19
20
21
22
23
24
25
26
27
28
29
30
31
32
33
34
35
36
37
38
39
40
41
42
43
44
45
46
47
48
49
50
51
52
53
54
55
56
57
58
59
60
61
62
63
64
65
66
67
68
69
70
71
72
73
74
75
76
77
78
79
80
81
82
83
84
85
86
87
88
89
90
91
92
93
94
95
96
97
98
99
100

THE INFLUENCE OF SURFACE ACTIVE SUBSTANCES
ON THE SOLUTION KINETICS OF CALCIUM CARBONATE
IN MINERAL ACIDS

Academician Vikt. I. Spitsyn, V. A. Pchelkin,
and I. V. Goncharov

Translated from Doklady Akad. Nauk SSSR, Vol. 137, No. 5,
pp. 1158-1161, April, 1961

Original article submitted January 7, 1961

Knowledge of the effects of surface active substances on the solution of carbonates in acids is very limited. At the same time, the study of the influence of inhibitors on the rate of solution of carbonates in acids is not only of scientific but also of practical interest, especially in processes of acid leaching of individual elements from carbonate ores. We know of only one paper by P. A. Rebinder [1] directly relating to the present problem, in which the effect of aliphatic and aromatic acids and phenols on the rate of solution of separate crystals of calcite in aqueous solutions of sulfuric and hydrochloric acids was studied. It was discovered that n-heptoic acid decreases the rate of solution of monocrystals of calcite in hydrochloric acid to a considerable extent.

In carrying out the present work the main attention was paid to investigation of new surface active substances which most effectively suppress the solution of calcium carbonate in acids. With this object the effect of more than twenty substances from the following different classes of compounds was studied.

1. Hydrophilic high molecular weight substances: joiners' glue, agar-agar, starch, gelatine, gum arabic and sulphite-alcohol still liquor.
2. Anionic substances: n-heptoic and oleic acids.
3. Cationic substances: (a) salts of aliphatic amines — octadecylamine, triethylamine, triisooamylamine, trioctylamine, amines of the composition $R - CH_2 - CH(NH_2) - CH_3$ where R is a hydrocarbon radical with 13-16 atoms of carbon, mixtures of naphthenic amines; (b) salts of quaternary ammonium bases — trimethylethyl and tetraethyl ammonium.
4. Individual representatives of other classes of compounds, for example, dimethylsiloxane and others.

The selection of depressing agents of the solution of calcium carbonate in acids was based mainly on the differences in their chemical structure, i.e., on the differences of the hydrophilic and hydrophobic radicals and also the differences in the character of the intervening linking groups between them [2]. It was kept in view that establishing the dependence of the properties of surface active substances on their structure was linked with the problem of the choice of the one or the other property for investigation. This problem did not present special difficulties if attention was paid to those physicochemical properties such as surface tension or solubilizing power. On the other hand it proved to be considerably more difficult if the investigation was subject to such technologically important properties as passivating effect, flotation and emulsifying capacity and others.

In the present stage of the work we did not aim at making a profound physicochemical study of the nature of the processes taking place and we restricted ourselves to a study of the qualitative effect of an addition on the rate of solution of calcium carbonate in acids.

In Fig. 1 as examples, curves are presented showing the dependence of the rate of solution of calcite crystals (1500 mm^2) on the time in 0.77 M hydrochloric acid solution for n-heptoic, oleic and isooctylphosphoric acids. These kinetic curves are plotted on the basis of neutralization data for each point from 4-6 experiments. Against the ordinate is plotted the rate of solution in milligrams of CaCO_3 per minute calculated from the volume of the liberated carbon dioxide gas. In all cases, parallel experiments were carried out with and without introduction of surface active substances, which permitted establishing the effect of the latter on the rate of solution. Since the aim of the investigation was to establish the relative change in the rate of the process on introduction of the surface active substances into the solution, then determination of the surface area of the crystals, changing in the course of solution in the present case, was not of interest. As seen from Fig. 1 of these surface active substances isooctylphosphoric acid had the most depressing effect on the solution of calcite.

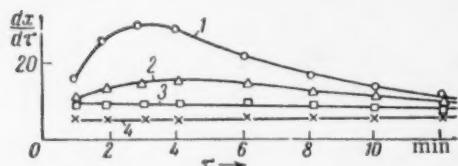


Fig. 1. Influence of surface-active substances on the rate of solution of calcite with time in hydrochloric acid solution. 1) Without addition; 2) 0.00024 mole/liter of n-heptoic acid; 3) 0.00024 mole/liter of oleic acid; 4) approx. 0.0003 mole/liter of isooctylphosphoric acid.

Investigation of the effect of other substances listed above was carried out with calcite ground to -0.5 to $+0.17 \text{ mm}$ in size in sulfuric acid solution. In round flat-bottomed flasks with a narrow neck, of 250 ml capacity, was placed 50 ml of a 0.5 M solution of sulfuric acid and a solution of the surface-active substance. After simultaneously introducing equal weighed portions (2-3 g) of calcite into the solution the contents of the flasks, as in experiments with hydrochloric acid, were mixed by shaking the apparatus for a definite period of time (1.5-2.5 hr). Then the solution was centrifuged and by KOH titration with methyl red the final acidity of the solution was determined. By comparison of the average values of solution of CaCO_3 in blank experiments and experiments with a surface active agent the relative percentage of depression of solution was calculated.

For substances showing a definite passivating effect the curves relating the relative percentage depression of solution of calcite (ϵ) with their concentration (C) were plotted. As seen from Fig. 2 (curve 3) the concentration of cetyl sulfate in solution materially effects the depression of the solution of calcite. From this curve the maximum depression (around 14%) is observed with a relatively low concentration of cetyl sulfate (0.08-0.15 g/liter); a further increase in concentration up to 0.55 g/liter reduced the depression to 6.5%. Addition of glue or agar-agar (curves 2 and 1) proved to be considerably less effective. The sulfates of a mixture of naphthenic amines, p-toluidine, and octadecylamine proved to be fairly effective (curves 4, 5, and 6).

Other amine salts proved to be more effective inhibitors. The maximum passivating effect of the substances we examined was shown by the sulfates of triisoamylamine, trioctylamine, and α -naphthylamine (Fig. 3). As a rule the steepest rise of the curves relating the passivating effect of amine salts with their concentration in solution was observed at low concentrations. In the present case, the study of the effect of addition of α -naphthylamine sulfate was carried out on a -0.175 mm calcite fraction, triisoamylamine and trioctylamine on a -0.40 to $+0.315 \text{ mm}$ fraction.

Investigation of the effect of addition of the sulfate of the amine $\text{R}-\text{CH}_2-\text{CH}(\text{NH}_2)-\text{CH}_3$, and of a representative of the organosilicon class of compounds (dimethylsiloxane), was carried out volumetrically, i.e., from the volume of carbon dioxide liberated, on the -0.40 to $+0.315 \text{ mm}$ calcite fraction. From this experiment, the concentration of amine was 0.63 g/liter, of dimethylsiloxane 1.30 g/liter. The experimental results are given in Table 1.

In the table the sign (+) denotes the accelerating effect, expressed in relative percentages. As seen from the table, the effect of the amine on the solution of calcium carbonate was very unusual. The considerable depression occurring initially quickly diminished and after 8-10 min from the start of the reaction, on the contrary an acceleration of solution of calcite was observed. This behavior occurred under conditions of decreasing concentration of sulfuric acid, and is explained, apparently, by a reduction in stability of the CaSO_4 layer on the surface of the calcium carbonate due to the effect of the inhibitor present [3]. In a similar way to the amine, the passivating effect of addition of dimethylsiloxane diminished with time.

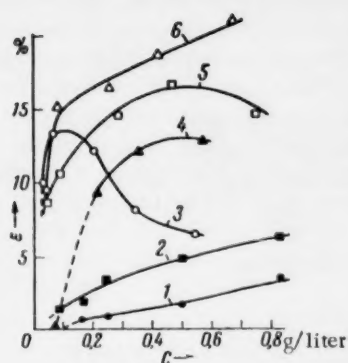


Fig. 2. Effect of the concentration of (1) agar-agar, (2) glue, (3) cetyl sulfate, (4) sulfates of a mixture of naphthenic amines, (5) p-toluidine, (6) octadecylamine on the solution of calcite in 0.5 M H_2SO_4 .

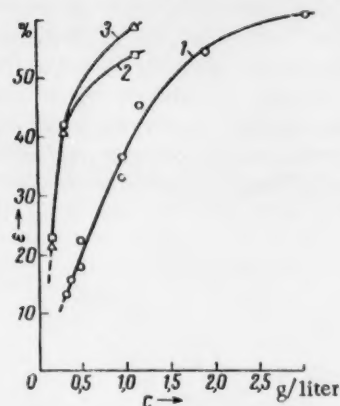


Fig. 3. Effect of the concentration of (1) α -naphthylamine, (2) trioctylamine, and (3) triisoamylamine sulfates on the solution of calcite in 0.5 M H_2SO_4 .

Of the substances we examined, gelatine, starch, gum arabic, cresylic and xylenolic aeroflots, sulfates of triethylamine, aniline, trimethylethyl and tetraethyl ammonium, showed little substantial effect on the solution of calcite independently of concentration (to 3 g/liter) and also of the order of their introduction into the solution.

Effect of the Sulfate of the Amine $R - CH_2 - CH(NH_2) - CH_3$, and of Dimethylsiloxane on the Solution of Calcite in 0.5 M Sulfuric Acid

Time from start of reaction, min	Relative depression of solution of calcite, %	
	sulfate of $R - CH_2 - CH(NH_2) - CH_3$	Dimethylsiloxane
2	+ 45.0	+ 18.0
5	+ 12.9	+ 18.0
10	- 3.3	+ 17.5
20	- 11.0	+ 15.3
30	- 10.0	+ 14.0

Thus, as the result of the investigation of a large variety of substances belonging to different classes of compounds, definite manifestations of the inhibiting effect of surface active substances on the solution of calcium carbonate in sulfuric acid were obtained. Very effective depressions of the solution of calcium carbonate were shown by certain amines. It was characteristic that both for aliphatic and for aromatic amines a definite regularity of the development of the passivating effect with increase of the hydrophobic part of the molecule was observed. For example, in the series aniline, p-toluidine, and α -naphthylamine an increase of the depressant effect corresponding with the complexity of the hydrophobic radical was observed. With equal numbers of carbon atoms in the amines, isomeric amines could apparently possess a greater effect due to their greater hydrophobic properties. As a rule, with decrease of solubility of the amine in water its depressing effect increases. In contrast to the lower representatives of quaternary ammonium salts, which proved to be ineffective, salts of quaternary ammonium bases, containing alkyl groups with a larger number of carbon atoms, for example C_8 and above, could not previously be considered ineffective as depressants of the solution of calcium carbonate in acids.

In conclusion we wish to express sincere acknowledgement to Academician P. A. Rebinder for helpful advice during the conduct of the present work.

LITERATURE CITED

1. P. A. Rebinder and K. P. Rebinder, *Zhur. Fiz. Khim.* 1, No. 2, 175 (1930).
2. A. Schwarz and D. Perry, *Surface-active Substances* [Russian translation] (IL, 1953).
3. K. Beili, *Inhibition of Chemical Reactions* [in Russian] (Leningrad-Moscow, 1940).

All abbreviations of periodicals in the above bibliography are letter-by-letter transliterations of the abbreviations as given in the original Russian journal. *Some or all of this periodical literature may well be available in English translation.* A complete list of the cover-to-cover English translations appears at the back of this issue.

THE KINETICS OF THE OXIDATION OF PROPYLENE TO ACROLEIN STUDIED BY THE CIRCULATING FLOW METHOD

V. M. Belousov, Ya. B. Gorokhovatskii, M. Ya. Rubanik
and A. V. Gershingorina

L. V. Pisarzhevskii Institute of Physical Chemistry, Academy of Sciences, USSR

(Presented by Academician A. A. Balandin, December 10, 1960)

Translated from Doklady Akad. Nauk SSSR, Vol. 137, No. 6

pp. 1396-1398, April, 1961

Original article submitted December 9, 1960

A limited number of papers [1-5] has been devoted to the oxidation of propylene to acrolein over a cuprous oxide catalyst. The aim of the present study was to obtain data on the kinetics of this reaction by using the circulating flow method [6], which is the most suitable one for this purpose.

In order to study the influence of external diffusion we used the method described previously [7]. The data obtained are given in Table 1 and they show that varying the linear velocity by more than four times has no effect upon the rates of acrolein (W_1) and carbon dioxide (W_2) formation, the degree of oxygen conversion (X_{O_2}) and the selectivity ($S_{C_3H_6}$). Therefore, under our conditions the kinetic data were not distorted by external mass transfer.

TABLE 1

Oxidation of Propylene at Various Linear Velocities L of the Flowing Gas (flow rate 253 cm^3/min ; catalyst volume 4 cm^3 ; $[C_3H_6] = 22-24\%$; $t = 379^\circ$; Cu content = 10 g per liter catalyst).

L , m/sec	Stationary conc. in the flow, %			$W_1 \cdot 10^7$, mole. sec ⁻¹ per 1 cc cat.	$W_2 \cdot 10^7$, mole. sec ⁻¹ per 1 cc cat.	X_{O_2} , %	$S_{C_3H_6}$, %
	CO_2	C_3H_6O	O_2				
1,8	2,10	0,73	5,85	3,38	9,78	40	51
0,4	2,10	0,73	5,85	3,38	9,78	40	51

The reaction kinetics were studied on a catalyst containing 2.4 g Cu per liter. The carborundum, granule size 2-3 mm, which was used as a carrier had wide pores (mean diameter $6 \cdot 10^{-2}$ cm), so that it did not give rise to retardation by external diffusion, as was checked experimentally by crushing the granules.

Some of the kinetic data which we have obtained are given in Table 2. From these data it is evident that the rates of acrolein and carbon dioxide formation are proportional to the oxygen concentration and slightly depend upon the propylene concentration. When the concentrations of the original substances in the gas flow are kept constant, the rate falls at rising concentrations of the oxidation products and this indicates that the latter retard the reaction.

The rates of acrolein and carbon dioxide formation at a constant propylene concentration are described by the following kinetic equations:

$$W_1 = \frac{k_1 [O_2]}{1 + b \Delta [O_2]}, \quad W_2 = \frac{k_2 [O_2]}{[C_3H_6O]^{0.7}},$$

where $[O_2]$ represents the oxygen concentration in the flow, $\Delta[O_2]$ the decrease in oxygen concentration, as calculated from the difference between the oxygen concentration in the mixture fed and that in the gas at the outlet; k_1 , k_2 and b are parameters which depend upon temperature. The term $b \Delta[O_2]$ results from the retardation by the products.

TABLE 2

The Rates of Acrolein (W_1) and Carbon Dioxide Formation (W_2) as a Function of the Oxygen and Propylene Content in the Gas Flow and the Flow Rate (catalyst volume 8 cc).

Flow rate, cm ³ /min	Stationary conc. in the flow, %				S _{C₃H₆} , %	W ₁ · 10 ⁷ , mole · sec ⁻¹ per cc cat.	W ₂ · 10 ⁷ , mole · sec ⁻¹ per cc. cat.	k ₁ · 10 ⁷	k ₂ · 10 ⁷
	O ₂	C ₃ H ₆	C ₃ H ₄ O	CO ₂					
t = 335°; b = 2,6									
Catalyst 1									
258	3,05	97	0,19	0,17	76	0,455	0,408	0,07	0,09
303	6,15	94	0,30	0,20	81	0,845	0,565	0,08	0,09
279	13,85	95	0,51	0,35	81	1,325	0,908	0,08	0,09
229	5,70	51,8	0,33	0,27	79	0,702	0,575	0,08	0,10
278	5,90	24,4	0,28	0,27	76	0,723	0,697	0,08	0,11
285	5,80	11,45	0,24	0,35	67	0,640	0,927	0,07	0,13
Catalyst 2									
561	6,05	22,8	0,24	0,26	73	1,252	1,355	0,12	0,19
291	5,95	23,5	0,34	0,36	74	0,920	0,974	0,11	0,17
142	5,95	23,9	0,49	0,60	71	0,647	0,795	0,11	0,17
141	5,90	23,5	0,44	0,62	68	0,576	0,814	0,10	0,18
84	5,80	22,9	0,60	1,00	65	0,470	0,777	0,12	0,20
t = 365°; b = 3,85									
531	6,00	23,6	0,43	0,55	71	2,13	2,73	0,48	0,59
308	5,90	22,7	0,50	0,90	63	1,43	2,58	0,46	0,63
148	5,90	22,5	0,68	1,50	58	0,94	2,06	0,46	0,63
69	5,80	22,0	0,91	2,40	53	0,586	1,54	0,43	0,57

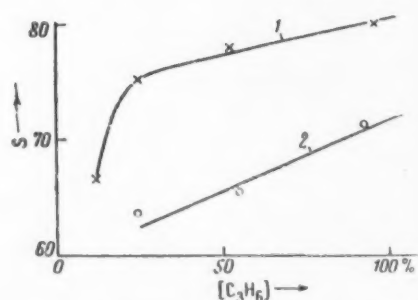


Fig. 1. The way in which the selectivity with respect to propylene ($S_{C_3H_6}$) depends upon the propylene concentration at 335° (1) and 365° (2) and a constant oxygen concentration in the flow, viz., 6%.

The values of the rate constants k_1 and k_2 found by using these equations are given in Table 2. The fact that these values are constant, when the flow rate is varied by seven times and the oxygen concentration by five times, proves that the said equations are valid. The equations proposed do not contain the propylene concentration, though, strictly speaking, the rate and the selectivity of propylene oxidation depend upon the content of this hydrocarbon in the mixture.

When the propylene concentration is raised, the selectivity is somewhat enhanced (Fig. 1). At small variations in the propylene content in the mixture or, when the hydrocarbon is present in a great excess, the rate and the selectivity remain constant and the equations which we have proposed are valid.

When calculated from the rate constants given by these equations the activation energy of C_3H_4O formation E_1 and that of carbon dioxide formation E_2 were found to be equal $E_1=E_2=36 \pm 2.5$ kcal/mole; $b=4.25 \cdot \exp(-10000/RT)$.

In order to find out which of the reaction products retards the reaction we used the method of removing certain products from the gas flow [8] while keeping constant the concentration of the original substances. From the data given in Table 3 it can be seen that the reaction rate increased by 2.5-3 times when acrolein and water were

removed. With all products removed, the degree of oxygen conversion remained the same as when only C_3H_4O and H_2O were removed. Therefore, carbon dioxide has no observable influence upon the reaction rate. If only water was removed and the acrolein concentration remained unchanged, the rate of carbon dioxide formation increased by about 1.5 times.

TABLE 3

Influence of the Reaction Products Upon the Rate (catalyst volume 8 cm^3 , $[C_3H_6]=19-21\%$).

[O ₂] in the outlet, %	Stationary conc. in the flow			Products removed	S _{C₃H₄} , %	W ₁ · 10 ⁷ , mole · sec ⁻¹ per cc cat.	W ₂ · 10 ⁷ , mole · sec ⁻¹ per cc cat.
	O ₂	C ₃ H ₄	CO ₂				
t = 335°, flow rate 280 cm ³ /min							
6,85	5,90	0,29	0,30	—	74 ± 2	0,755	0,778
7,65	5,95	0,05	0,85	C ₃ H ₄ O, H ₂ O	72 ± 2	1,94	2,22
7,65	5,80	0,07	net	CO ₂ , H ₂ O, C ₃ H ₄ O	—	—	—
t = 365°, flow rate 283 cm ³ /min							
7,30	5,70	0,41	0,80	—	60 ± 1	1,07	2,01
9,70	5,85	0,06	1,90	C ₃ H ₄ O, H ₂ O	67 ± 1	3,39	5,00
9,70	5,95	0,05	net	CO ₂ , H ₂ O, C ₃ H ₄ O	—	—	—
7,50*	5,70	0,45	0,90	—	60 ± 1	1,28	2,56
8,25*	5,80	0,43	1,25	H ₂ O	—	—	3,57

* Flow rate 307 cm³/min.

Our data confirm the conclusion of O. V. Isaev and L. Ya. Margolis [5] that the rate of propylene depends upon the oxygen concentration to the first power. At the same time they are not in agreement with the conclusion of those same authors that the reaction products do not retard the oxidation of propylene and that propylene has no influence whatever.

It should be remarked that the mentioned authors [5] worked with a flow method which is less suitable for studying the kinetics of exothermal reactions than is the circulating-flow method. At 335° removal of acrolein from the flow did not result in an enhanced selectivity, as should be the case, if acrolein was further oxidized. At 365° the selectivity is somewhat enhanced by freezing out C_3H_4O ; therefore, at this temperature under the usual conditions a further oxidation of acrolein may take place. These data confirm the conclusion which we have drawn previously [4], namely, that at low temperatures acrolein and carbon dioxide are mainly formed in parallel reactions. Whereas at high temperatures the formation of carbon dioxide constitutes a parallel-consecutive reaction.

The authors express their gratitude to E. N. Popova, D. Ya. Nechiporuk and M. V. Rybakova, who assisted in this investigation.

LITERATURE CITED

1. N. I. Popova, V. I. Belyaev and R. N. Stukova, *Izvest. Vost. Fil. Akad. Nauk SSSR*, No. 7, 40 (1957).
2. O. V. Isaev, L. Ya. Margolis and S. Z. Roginskii, *Zhur. Obshchei Khim.* **29**, 1522 (1959).
3. O. V. Isaev, L. Ya. Margolis and S. Z. Roginskii, *Doklady Akad. Nauk SSSR*, **129**, 141 (1959).
4. V. M. Belousov, Ya. B. Gorokhovatskii, M. Ya. Rubanik and A. V. Gershingorina, *Doklady Akad. Nauk SSSR*, **132**, 1125 (1960).
5. O. V. Isaev and L. Ya. Margolis, *Kinetika i Kataliz*, **1**, 237 (1960).
6. M. I. Temkin, S. L. Kiperman and L. I. Luk'yanova, *Doklady Akad. Nauk SSSR*, **74**, 763 (1950).
7. M. Ya. Rubanik, K. M. Kholyavenko, Ya. B. Gorokhovatskii, A. A. Belaya, E. N. Popova and G. D. Shcherbakova, *Ukrain. Khim. Zhur.* **22**, 190 (1956).
8. Ya. B. Gorokhovatskii, M. Ya. Rubanik and K. M. Kholyavenko, *Doklady Akad. Nauk SSSR*, **125**, 83 (1959).



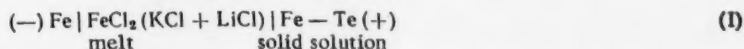
THERMODYNAMIC PROPERTIES OF IRON-TELLURIUM ALLOYS IN THE SOLID STATE

V. A. Geiderikh, Corresponding Member Acad. Sci. USSR
Ya. I. Gerasimov and A. V. Nikol'skaya

Translated from Doklady Akad. Nauk SSSR Vol. 137, No. 6
pp. 1399-1401, April, 1961
Original article submitted January 10, 1961

By means of the method of electromotive forces (e. m. f.) we have investigated solid alloys of iron with tellurium (composition 0-50 at.% iron).

As a function of temperature we have measured the e. m. f. of concentration cells with the following electrodes:



The preparation of the alloys and the procedure of the experiment have been described in the paper [1].

Results obtained by studying the state diagrams of the system Fe-Te are found in the literature [2,3]. State diagrams constructed from the data of Gronvold, Haraldsen and Vihovde [2] are given in the book of Hansen and Andreko [4]. In Fig. 1 the state diagram according to the paper of Chiba [3] is given by the drawn lines, whereas the boundaries of the phase regions, as we propose, are shown by dashed ones.*

At temperatures between 360 and 650° we have investigated iron-tellurium alloys of various compositions belonging to the phase regions $\beta + \text{Te}$, β , $\beta + \gamma$, γ , $\gamma + \alpha$ and $\beta + \alpha$ (altogether 21 alloys). The data obtained for alloys belonging to one and the same two-phase region were treated in the following way. From the entire set of e. m. f. values for all alloys at all temperatures the parameters in the linear relation between the e. m. f. (E)

TABLE 1

Atomic fraction of iron, at. %	Phase comp.	Temperature, °K	E. m. f., mv
0—0,323	$\beta + \text{Te}$	630—700	$344,2 - 97,8 \cdot 10^{-3} T$
0,332	β	650—750	$343,9 - 110 \cdot 10^{-3} T$
0,338	β	740—880	$531,4 - 384 \cdot 10^{-3} T$
0,35—0,51	$\beta + \alpha$	690—786	$-109,5 + 220,6 \cdot 10^{-3} T$
0,35—0,40	$\beta + \gamma$	790—900	$-598,6 + 841 \cdot 10^{-3} T$
0,40—0,425	$\beta + \gamma$	переменная — 900	$-598,6 + 841 \cdot 10^{-3} T$
0,43—0,51	$\gamma + \alpha$	786—900	$80,3 - 21,9 \cdot 10^{-3} T$

*In this paper we have always taken the same denotation of the phase as has been used in the paper by Chiba [3].

Atomic fraction of iron, at. %	Temperature, °K				Temperature, °K			
	phase comp.	ΔG , kcal/g-at	ΔH , kcal/g-at	ΔS , eu/g-at	phase comp.	ΔG , kcal/g-at	ΔH , kcal/g-at	ΔS , eu/g-at
0.338	β	-4.32 ± 0.12	-5.42 ± 0.41	-1.57 ± 0.6	β	-4.13 ± 0.12	-5.40 ± 0.41	-1.57 ± 0.6
0.43	$\alpha + \beta$	-4.08 ± 0.16	-4.20 ± 0.54	-0.45 ± 0.8	γ	-4.07 ± 0.19	-4.33 ± 0.62	$+3.4 \pm 0.8$
0.5	$\alpha + \beta$	-3.84 ± 0.16	-3.06 ± 0.54	$+1.1 \pm 0.8$	$\alpha + \gamma$	-3.92 ± 0.24	-1.63 ± 0.75	$+2.9 \pm 1.0$
0.53	α	-3.71 ± 0.16	-2.65 ± 0.54	$+1.7 \pm 0.8$	α	-3.86 ± 0.21	-1.75 ± 0.75	$+2.7 \pm 1.0$

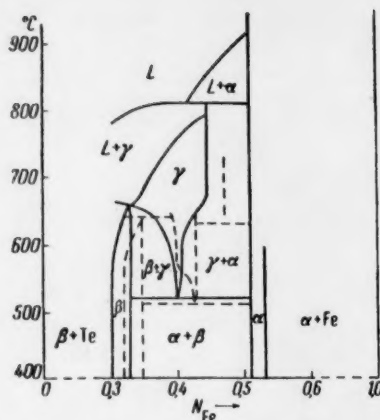


Fig. 1. State diagram of the Fe-Te system; drawn lines according to the paper [3], the dashed lines represent our data.

and absolute temperature were found by means of the least square method. For homogeneous alloys of fixed composition a straight line $E = A + BT$ was drawn through a plot of the experimental points and from this line the coefficients A and B were found.

The equations $E = A + BT$ for electrodes consisting of alloys of various compositions are given in Table 2.

The magnitude of the change in chemical potential when 1 g-at iron is transferred from the pure metal to an alloy of a given composition is obtained from the well-known relation:

$$\Delta\mu_{Fe} = -zFE,$$

where z represents the charge of the carrier ion ($z_{Fe^{2+}} = 2$), and F is Faraday's number ($F = 23064 \text{ cal/v}$).

The partial entropy and enthalpy changes are found from the equations:

$$\Delta\bar{S}_{Fe} = -d\Delta\mu_{Fe}/dT = zFdE/dT,$$

$$\Delta\bar{H}_{Fe} = \Delta\mu_{Fe} + T\Delta\bar{S}_{Fe}.$$

The integral values for the formation of a g-at alloy from pure iron and tellurium are found by means of Gibbs-Duhem's equation:

$$B = N_{Te} \int_0^{N_{Fe}} \bar{B}_{Fe} d\left(\frac{N_{Fe}}{N_{Te}}\right),$$

where B is the integral value (ΔG° , ΔH , ΔS), \bar{B}_{Fe} the corresponding partial value for iron, N_i the atomic fraction of the i-th component. The integration was carried out graphically over the range $N_{Fe} = 0-0.51$ for the temperature 700 and 800° K.

* In conformity with usage in the international literature we have denoted the free energy by G.

The results calculated for 1 g-at alloy are given in Fig. 2 and Table 2. In Fig. 2 the values of the integral thermodynamic functions at 800° K are plotted versus the composition of the alloys. These values for the β -, γ -, α -phase and the heterogeneous alloy of the composition $N_{Fe}=0.5$ are given in Table 2. The data for $N_{Fe}=0.53$ were obtained by extrapolating the function $R(N_{Fe})$ from $N_{Fe}=0.51$ to the region of the homogeneous α -phase.

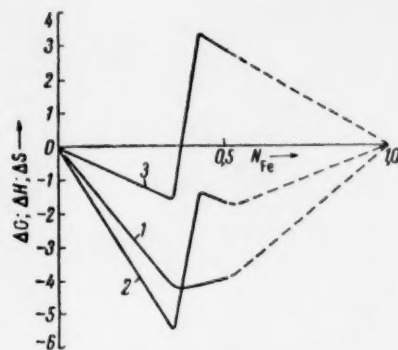


Fig. 2. The thermodynamic functions of the Fe-Te system at 800° K plotted versus the composition of the alloys (dashed lines denote extrapolation). 1) ΔG ($\frac{kcal}{g-at}$); 2) ΔH ($\frac{kcal}{g-at}$); 3) ΔS ($\frac{eu}{g-at}$).

negative in the whole range of concentrations (Fig. 2, Table 2). In the system Fe-Sb [6] we have found a similar relation between alloy composition and formation entropy and enthalpy. When the nature of the analogous phases in both systems is considered, the coincidence appears to be not accidental.

The β -phase of the Fe-Te system has the marcasite structure and the stoichiometric composition $FeTe_2$ lies within the existence region of this phase; $FeSb_2$ is a stoichiometric compound with the marcasite structure. The γ -phase of Fe-Te and the γ -phase of Fe-Sb are Berthollidic phases with a defect structure of the nickel arsenide. Their existence regions do not comprise the composition 1:1, which is the theoretical one for a NiAs type of lattice. The existence region of the Fe-Te γ -phase lies farther away from the 1:1 composition and at the same time has a more positive formation entropy than does the Fe-Sb γ -phase. This is in agreement with our proposition [6] that the defects of a NiAs type lattice have influence upon the formation entropy of intermetallic phases.

By measuring the e. m. f. of a type I cell not only the thermodynamic functions may be determined, but also interferences may be drawn on the boundaries of the phase regions in the state diagram. On the boundary of the phase regions the $E(T)$ relation shows a break. For all the iron-tellurium alloys with compositions $N_{Fe}=0.35-0.51$ a break is found at one and the same temperature (approximately 513° C) and confirms the data [2,3] on the eutectic decomposition of the γ -phase into the α - and β -phases (Fig. 1). The probable boundaries of the phase regions in the Fe-Te system are shown by the dashed lines in Fig. 1. These dashed lines were drawn by combining our e. m. f. data with data from the literature [2,3,7].

LITERATURE CITED

1. A. V. Nikol'skaya, V. A. Geiderikh and Ya. I. Gerasimov, Doklady Akad. Nauk SSSR, **130**, 1074 (1960).
2. F. Grønqvold, H. Haraldsen, J. Vihovde, Acta chem. Scand., **8**, 1927 (1954).
3. S. Chiba, J. Phys. Soc., Japan, **10**, 837 (1955).
4. M. Hansen, K. Anderko, Constitution of Binary Alloys, 1958.
5. O. Kubaschewski and E. L. Evans, Metallurgical Thermochemistry [Russian translation] (1954).
6. V. A. Geiderikh, A. A. Vecher and Ya. I. Gerasimov, Zhur. Fiz. Khim., **34**, No. 6 (1960).
7. L. D. Dudkin and V. I. Vaidanich, Fiz. Tverdogo Tela, **2**, 1527 (1960).

In order to obtain the integral values at 800° K the relations $E(T)$ found experimentally at lower temperatures for alloys with compositions $N_{Fe}=0-0.332$ and given in Table 1 were extrapolated to the said temperature.

The values given in Table 2 are referred to the standard state of "solid iron and tellurium". For reference to the standard state of "solid iron and liquid tellurium" the following data should be used: $\Delta H_{Te}^{melt} = 4.18 \text{ kcal/g-at}$, $\Delta S_{Te}^{melt} = \Delta H_{Te}^{melt} / T_{melt} = 5.78 \text{ eu/g-at}$ and $\Delta G_{Te}^{melt} = (4.18 - 5.78 \cdot 10^{-3} T) \text{ kcal/g-at}$ (neglecting the dependence of ΔH_{Te}^{melt} upon temperature). The values of the melting point and the heat of melting of tellurium have been taken from [5].

RESULTS

From the data in Table 2 it is evident that the entropies of the formation of the α - and γ -phase from the elements is positive, whereas that of the β -phase is negative. The formation enthalpy changes symbolically with the entropy, but it stays

1
2
3
4
5
6
7
8
9
10
11
12
13
14
15
16
17
18
19
20
21
22
23
24
25
26
27
28
29
30
31
32
33
34
35
36
37
38
39
40
41
42
43
44
45
46
47
48
49
50
51
52
53
54
55
56
57
58
59
60
61
62
63
64
65
66
67
68
69
70
71
72
73
74
75
76
77
78
79
80
81
82
83
84
85
86
87
88
89
90
91
92
93
94
95
96
97
98
99
100

AN INVESTIGATION OF THE MECHANISM OF THE FORMATION OF OZONE AT THE ANODE IN SULFURIC ACID SOLUTIONS

V. A. Lunenok-Burmakina, A. P. Potemskaya and Correspondent-Member of the Academy of Sciences of USSR A. I. Brodskii

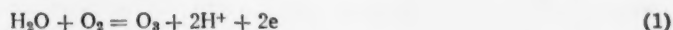
The L. V. Pisarzhevskii Institute of Physical Chemistry, Academy of Sciences USSR

Translated from *Doklady Akademii Nauk SSSR*, Vol. 137, No. 6

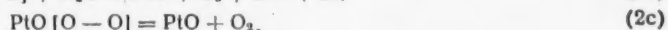
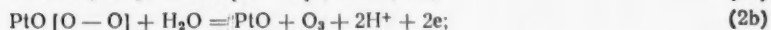
pp. 1402-1405, April, 1961

Original article submitted January 23, 1961

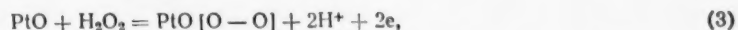
Very little is known about the mechanism of the anodic formation of ozone. By analogy with its formation in the silent electrical discharge, we may propose the over-all scheme: $O_2 + O = O_3$ [1]. It is more probable that water plays some part:



with the possible intermediate formation of oxygen ions or of radicals. A number of authors have carried out the study of the anodic potential curves and of the state of the electrodes [2-4], coming to the conclusion that the anodic formation of ozone is also accompanied by anodic oxidation of oxygen in the form of surface oxides. V. I. Veselovskii and his collaborators [5], in particular, suggest that on platinum electrodes at high overpotentials corresponding to the formation of ozone, higher oxides of peroxide type are formed, which react with water to give ozone or oxygen:



According to scheme (1), the oxygen evolved at the anode does not take part directly in the formation of ozone. On the other hand, we discovered earlier [6] that, in the electrolysis of potassium bisulfate solutions, the yield of persulfate is greatly diminished on addition of hydrogen peroxide, which is a major source of the anodic oxygen. The yield of persulfate increases in step with the reduction in the hydrogen peroxide concentration, and simultaneously the proportion of oxygen from the water increases in the anodic oxygen. This suggested that the higher surface oxides of platinum are formed not only from the water according to (2a), but from peroxidic compounds also, for example:



and that these peroxidic compounds, or their precursors in the anode reaction, also take part in the formation of ozone.

In our study of the formation of ozone we have used heavy oxygen, which has already been used successfully [2, 6-10] for the study of anodic processes.

Electrolysis was carried out in vessels connected to a vacuum system, used for evacuating the ozone and analysis of the anodic gas. The latter, after the water has been frozen out, was passed through a trap containing 5% potassium iodide, in which the ozone was collected and titrated; and the oxygen was determined by volume. For the isotopic analysis the gas was passed into another section of the apparatus where, after further drying, the ozone was frozen out, residual gas was pumped away, and the ozone was purified by redistillation into another vessel, where it was frozen out and decomposed by heating to 150°. The anodic oxygen and oxygen from the ozone were analyzed with respect to their O^{18} content in a mass spectrometer. The completeness of the ozone decomposition was checked in control experiments in which the pressure increased to $1\frac{1}{2}$ times its initial value (within an accuracy of 5%) after the heating of the vessel in which the ozone collected had been evaporated. The completeness of decomposition was also confirmed by the fact that the ozone frozen out from the mixture containing O_2^{18} did not contain excess O^{18} . The O^{18} in sulfuric acid and potassium bisulfate was determined by converting them to lead sulfate, which was heated with degassed carbon at 700°. The carbon dioxide was introduced into a mass spectrometer. The O^{18} content in water was also obtained in the form of carbon dioxide after exchange with the vapor [11]. Heavy sulfuric acid, $H_2SO_4^{18}$ was prepared by addition of the anhydrous acid to H_2O^{18} , and heavy potassium bisulfate, $KHSO_4^{18}$ was obtained from this by neutralization with potassium hydroxide. The electrolyte containing 4-10 g monopersulfuric acid (Caro's acid) in 60-70 ml of 5-6.5 M sulfuric acid in H_2O^{18} was prepared by dissolving 40 g of powdered potassium dipersulfate in 26 ml concentrated sulfuric acid with strong cooling, then adding 50 ml of chilled H_2O^{18} . The liquid was allowed to stand for 1 hour at 20° and then filtered. Electrolysis was conducted at 20° with a current of 4-7 amperes at a potential of 11 volts, the anodic current density being 1-1.5 a/cm² and the volume density 0.1-0.2 a/ml. The hollow platinum anode was cooled additionally with running water. Before the experiment it was washed in nitric acid and again depolarized in a current of 0.1 a/cm². The determination of perdisulfate and permonosulfate in the electrolyte was performed iodometrically [12, 13]. No appreciable quantities of hydrogen peroxide were formed under the conditions of the experiment, while, depending on the experimental conditions, ozone was condensed out at the rate of 2-6 mg/hr, while oxygen was liberated at the rate of ca. 1 liter/hr. In experiments using 4.5-6.8 M sulfuric acid, about 0.004-0.008 moles of permonosulfuric acid were formed in 40-60 ml as a result of the hydrolysis of the persulfate.

TABLE I

Isotopic Composition of Electrolyte, Oxygen and Ozone.

Expt. No.	Composition of electrolyte, mole/liter	Duration of expt., hr	Atomic % of O^{18} in excess of natural					Oxygen calc. from (1)
			in initial sulfate	in final sulfate	in H_2O	in O_2	in O_3	
1	Saturated $KHSO_4$	4	0,85	0,85	0	0,01	0,02	0
2	The same	4	0	0	0,73	0,68	0,72	0,70
3	2,5M H_2SO_4	1	0	—	1,24	1,20	—	—
		2	0	0	1,24	1,18	1,18	1,21
4	4,5M H_2SO_4	1	0	—	0,76	0,62	—	—
		2	0	0,06	0,76	0,63	0,69	0,67
5	6,8M H_2SO_4	2	0	—	1,15	0,44	0,65	0,68
		3	0	0,28	1,15	0,54	0,75	0,73
6	5,5M H_2SO_4 + + 9,9 g H_2SO_5	1,5	0	—	1,18	0,25	—	—
		3,0	0	—	1,18	0,42	0,59	0,60
7	6,0M H_2SO_4 + + 8,7 g H_2SO_5	2	0	0,09	1,18	0,50	—	—
		3	0	0,12	1,18	0,41	0,66	0,67
		4	0	0,17	1,18	0,37	0,66	0,64
8	2,5M H_2SO_4 + + 5,8 g H_2O_2	1	0	0,03	1,00	0,28	0,52	0,52
9	2,6M H_2SO_4 + 3 g + H_2O_2	0,5	0	0,01	0,80	0,36	0,52	0,51

In the electrolysis of saturated solutions of potassium bisulfate in H_2O^{18} , or of KHSO_4^{18} in water, and also 2.5 M sulfuric acid in H_2O^{18} , the ozone had the isotopic composition of the oxygen in the water, and the composition of the oxygen in the sulfate did not change (Table I, experiments 1-3). It was found earlier [6,8] that the oxygen of the water did not participate in the persulfate formed at the same time. These data exclude the possibility that the persulfate (or its possible precursors) participate in the formation of ozone. In agreement with this it is found that the addition of persulfate does not increase the ozone yield [1].

In the electrolysis of more concentrated sulfuric acid solutions in H_2O^{18} , the anodic oxygen is diluted with sulfate oxygen to an extent which increases with the acid concentration, and the ozone has an isotopic composition intermediate between those of the oxygen and the water. The same intermediate composition was found by A. N. Frumkin [2] in the electrolysis of perchloric acid solutions. Increase in the acid concentration was accompanied by an increase in the proportion of O^{18} transferred from the water. This is not due to exchange, which proceeds very slowly under these conditions [14], but to hydrolysis of the persulfate in the course of which, as we discovered earlier [10], oxygen from the water enters into the composition of the sulfate formed. The result of this is the formation of light permonosulfuric acid, whose anodic decomposition dilutes the O_2^{18} with light oxygen. In experiments 4 and 5, using 4.5 and 6.8 M sulfuric acid, the O^{18} content in the ozone was the same as that calculated from (1). To provide a more thorough test of this equation we have increased the difference between the isotopic compositions of anodic oxygen and water, conducting electrolysis after the addition of Caro's acid (experiments 6 and 7) or hydrogen peroxide (experiments 8 and 9). In the experiments using hydrogen peroxide, the concentration of this was maintained constant within ca. 2% by the dropwise addition to the electrolyte of 80% hydrogen peroxide. It is seen from Table I that, in all the experiments, the ratio of 1:2 for oxygen from the water and anodic oxygen is maintained with great accuracy in the ozone formed.

From these experiments it follows that the formation of ozone and of persulfate are two independent parallel processes, the ozone being formed according to the schematic stoichiometric equation (1). Taking into account the electrochemical and other data mentioned above, it must be supposed that the oxygen actually takes part in this process in the form of higher surface oxides, according to scheme (2b), these oxides being formed not only from water in accordance with (2a), but also, in the presence of peroxidic compounds to a predominant degree through the participation of these compounds, as by the process (3) in the presence of hydrogen peroxide. From these oxides anodic oxygen is formed according to (2c) with the same isotopic composition.

As we have indicated above, steps (3) and (2c) also explain the predominance of oxygen from the hydrogen peroxide in anodic oxygen formed during the electrolysis of sulfate or sulfuric acid solutions in the presence of hydrogen peroxide. It would seem that this mechanism is the only one which is able to explain our results.

LITERATURE CITED

1. E. Briner, R. Halfeli, H. Paillard, *Helv. chim. acta*, **20**, 1510 (1957); E. Briner, A. Yalda, *Helv. chim. acta*, **24**, 1829 (1943).
2. A. N. Frumkin, Intern. Committee Elektrochem., Thermodyn. and Kinetics (Proc. 9th Meeting, Paris, 1957), London, 1959, p. 396.
3. R. I. Kaganovich, M. A. Gerovich and E. Kh. Enikeev, *Doklady Akad. Nauk SSSR*, **108**, 107 (1956).
4. V. I. Ginzburg and V. I. Veselovskii, *Zhurn. Fiz. Khim.*, **24**, 366 (1950); K. I. Rozental' and V. I. Veselovskii, *Zhurn. Fiz. Khim.*, **27**, 1163 (1953); G. I. Borisov and V. I. Veselovskii, *Zhurn. Fiz. Khim.*, **27**, 1195 (1953); L. M. Volchikov, L. G. Antonova, and A. I. Krasil'shchikov, *Zhurn. Fiz. Khim.*, **23**, 441, 714 (1949); **27**, 512 (1953).
5. A. A. Rakov, V. I. Veselovskii et alii, *Zhurn. Fiz. Khim.*, **32**, 2703, (1958).
6. A. I. Brodskii, I. F. Franchuk and V. A. Lunenok-Burmakina, *Doklady Akad. Nauk SSSR*, **115**, 934 (1957).
7. K. I. Rozental' and V. I. Veselovskii, *Doklady Akad. Nauk SSSR*, **111**, 637 (1957).
8. A. I. Frumkin, R. I. Kaganovich et alii, *Doklady Akad. Nauk SSSR*, **102**, 981 (1955).
9. M. A. Gerovich, R. I. Kaganovich et alii, *Doklady Akad. Nauk SSSR*, **114**, 1049 (1957).
10. I. F. Franchuk and A. I. Brodskii, *Doklady Akad. Nauk SSSR*, **118**, 128 (1958).
11. A. I. Brodskii, S. G. Demichenko et alii, *Zhurn. Analit. Khim.*, **10**, 256 (1955).
12. A. I. Brodskii, A. S. Afanas'ev and M. G. Dikova, *Zhurn. Priklad. Khim.*, **5**, 929 (1932).
13. I. A. Bodin, *Zav. Lab.*, **7**, 1248 (1938).
14. T. C. Hoering, I. W. Kennedy, *J. Am. Chem. Soc.*, **79**, 56 (1957).



THE EFFECT OF A MAGNETIC FIELD ON PARTICLE MOVEMENT IN ELECTROLYTE SOLUTIONS

V. A. Myamlin, V. A. Kibardin, and Yu. Ya. Gurevich

Institute of Electrochemistry, Academy of Sciences, USSR

(Presented by the Academician A. N. Frumkin, December 6, 1960)

Translated from Doklady Akademii Nauk SSSR., Vol. 137, No. 6

pp. 1405-1408, April, 1961

Original article submitted November 2, 1960

The effect of a magnetic field on the movement of liquid or solid particles in electrolytes has been little studied up to the present time. Consequently, it is interesting to examine several aspects of this movement. As will be shown below, the particle velocity in an electrolyte due to the magnetic field effect is perpendicular to the electrophoresis velocity, and is proportional to the square of the particle radius. It is known that the electrophoresis velocity is proportional to the particle radius; therefore the result obtained from the present work may be used for more accurate determinations of particle dimensions and for separation of particles according to size. Furthermore, the results may prove to be useful for particle structure studies - the determination of particle viscosity, amount of surface charge, and hardness of surface layer. Such problems may arise, for example, in biology.

Consider a particle, which we may assume to be a sphere with radius a , located in an electrolyte solution through which flows a current generating an electric field E . A magnetic field H is applied at right angles to E . The fields E and H are homogeneous and constant at a great distance from the particle.

We introduce a spherical coordinate system with its origin at the particle center and the z polar axis along E . The azimuthal angle φ is measured from the zx plane, and the y axis is aligned with H . In our system the particle is considered to be at rest and the liquid continuously moves with velocity U_0 .

We will first examine the case when no surface charge is formed on the particle. Assuming that the current does not flow through the particle, the potential distribution outside the particle is given by the equation

$$\varphi = (r + a^3/2r^2) E \cos \theta. \quad (1)$$

A spatial force $F = \frac{1}{c} [jH]$ operates on each unit volume of electrolyte, in which flows a current of density

$$= -\kappa \text{ grad } \varphi, \quad (2)$$

Using (1) and (2), we get for the force components:

$$\begin{aligned} F_r &= \frac{\kappa EH}{c} \left(1 + \frac{a^3}{2r^3}\right) \sin \theta \cos \varphi; & F_\theta &= \frac{\kappa EH}{c} \left(1 - \frac{a^3}{r^3}\right) \cos \theta \cos \varphi; \\ F_\varphi &= -\frac{\kappa EH}{c} \left(1 - \frac{a^3}{r^3} + \frac{3a^3}{2r^3} \sin^2 \theta\right) \sin \varphi. \end{aligned} \quad (3)$$

Since the rate of movement is low in the presence of practicable fields, the movement has an essentially viscous nature. In this case, the system of hydrodynamic equation has the form

$$\nabla p = \mu \Delta \mathbf{v} + \mathbf{F}, \quad \operatorname{div} \mathbf{v} = 0; \quad (4)$$

outside the particle, and

$$\nabla p_1 = \mu_1 \Delta \mathbf{v}_1, \quad \operatorname{div} \mathbf{v}_1 = 0. \quad (5)$$

inside the particle.

The boundary conditions, when $r = a$, are:

$$v_r = v_{1r} = 0; \quad v_\theta = v_{1\theta}; \quad v_\varphi = v_{1\varphi}; \quad p_{rr} = p_{1rr}; \quad p_{r\theta} = p_{1r\theta}; \quad p_{r\varphi} = p_{1r\varphi}. \quad (6)$$

In addition, the velocity of the liquids inside and outside the particle must be at their limits when $r = 0$ and $r \rightarrow \infty$ respectively.

As is obvious from (3), it is natural to look for the solution of (4) and (5) in the form

$$v_r = f(r) \sin \theta \cos \varphi; \quad v_\theta = g(r) \cos \theta \cos \varphi; \quad v_\varphi = \sin \varphi [h(r) + t(r) \sin^2 \theta]; \quad (7) \\ p = \mu s(r) \sin \theta \cos \varphi.$$

For determination as a function of the radius, we get, from (4) and (7), the system of equations

$$\begin{aligned} f'' + 4f'/r - s' &= 4\lambda (1/a^3 + 1/2r^3); \\ g'' + 2g'/r - 2g/r^3 - 2t/r^2 + 2f/r^2 - s/r &= 4\lambda (1/a^3 - 1/r^3); \\ f' - 2g/r + 2f/r + t/r &= 0; \quad h = -g; \\ t'' + 2t'/r - 6t/r^2 + 6\lambda/r^3 &= 0; \end{aligned} \quad (8)$$

here $\lambda = \frac{\kappa a^3}{4\mu c} EH$.

The liquid movement inside the particle is described by similar equations if λ is put equal to zero in (8).

Solving system (8) by the usual methods, we obtain the following equations for velocities and pressures:

outside the particle

$$\begin{aligned} f &= \frac{k}{r^3} + \frac{L}{r} + U_0; \quad g = \frac{B-K}{2r^3} + \frac{L+\lambda}{2r} + U_0; \\ t &= \frac{B}{r^3} + \frac{\lambda}{r}; \quad s = \frac{L+\lambda}{r^2} - \frac{4\lambda r}{a^3}; \quad h = -g; \end{aligned} \quad (9)$$

inside the particle

$$f_1 = M + Nr^2; \quad g_1 = M + r^2 (2N + A/2); \quad t_1 = Ar^2; \quad s_1 = 10Nr; \quad h_1 = -g_1, \quad (10)$$

where A, B, etc., are integration constants. The requirements of the limiting velocities, when $r=0$ and $r \rightarrow \infty$, are taken into account in these equations.

The determination of the integration constants from the boundary conditions (6) leads to the system of equations

$$\begin{aligned} M + Na^2 &= 0; & K/a^3 + L/a + U_0 &= 0; & B/a^3 + \lambda/a &= Aa^2; \\ \mu (K/a^5 + 2\lambda/a^2) &= \mu_1 N; \\ \mu \left(\frac{3k-2B}{a^4} - \frac{\lambda}{a^2} \right) &= \mu_1 \left(3Na + \frac{aA}{2} \right); \\ \frac{B-K}{2a^3} + \frac{L+\lambda}{2a} + U_0 &= M + \left(2N + \frac{A}{2} \right) a^2; \\ Aa\mu_1 &= -\mu \left[\frac{4B}{a^4} - \frac{2\lambda}{a^2} \right]. \end{aligned} \quad (11)$$

The solution of this elementary but cumbersome system leads to the determination of the particle velocity relative to the electrolyte velocity, equal to the absolute value in the chosen coordinate system when the electrolyte velocity is infinite.

It appears that the particle moves in a direction perpendicular to the electric and magnetic fields, with velocity

$$U_0 = \frac{\kappa a^2 EH}{2\mu c} \frac{\mu + \mu_1}{2\mu + 3\mu_1}. \quad (12)$$

This movement (magnetophoresis) has a velocity of the order of 0.1 cm/sec when $H = 10^4$ gauss and $j = 10^3$ amp, i. e., the effect has a fully observable magnitude.

In [1], other methods were used to derive an expression for the force acting on a solid particle under similar conditions. In the case of an ideally polarized particle this expression changes into the equation

$$F = \frac{3V}{4c} \kappa EH, \quad (13)$$

where V is the particle volume. From this and Stoke's formula $F = 6\pi\mu aU$ we derive the particle velocity

$$U_0' = \kappa a^2 EH / 6\mu c, \quad (14)$$

which agrees exactly with our results if μ_1 tends to infinity.

Let, now, the particle have a surface charge ϵ . In this case, in an electric field, it will undergo an electrophoretic movement along E , the velocity of which in a wide range of values of ϵ is at least of a higher order than the magnetophoresis velocity.

Assuming that the thickness of the generated electrical double layer is much smaller than the particle radius, we have for the potential outside the particle the equation

$$\varphi = \left[r + \left(\frac{1}{2} - \frac{\epsilon V_0}{\kappa Ea} \right) \frac{a^3}{r^2} \right] E \cos \theta. \quad (15)$$

Here, as is clear from what has been said above, V_0 may be assumed to be equal to the electrophoresis velocity [2]:

$$V_0 = \frac{\epsilon Ea}{2\mu + 3\mu_1 + \epsilon^2 / \kappa}. \quad (16)$$

In addition to the spatial current outside the particle, there is also a spatial current inside the particle generated by movement of the charges on the inner face of the double layer. The force acting because of this on a unit volume of the particle equals [3]

$$F_1 = \frac{1}{c} [\mathbf{j}_1 \cdot \mathbf{H}] = \frac{2V_0 e H}{ac} \mathbf{e}_x, \quad (17)$$

where \mathbf{e}_x is the unit vector along the x axis.

Zero force acts on the magnetic field side of the double layer, because the charges on this face have opposite signs and move in one direction.

Thus, Eq. (4) remains unchanged and force (17) should be allowed for in Eqs. (5).

The small boundary effects, connected with the presence of a surface charge, may be ignored, and conditions (6) are preserved.

In this case, the solutions are:
outside the particle

$$\begin{aligned} v_r &= (K/r^3 + L/r + U) \sin \theta \cos \varphi; \\ v_\theta &= \left(\frac{B-K}{2r^3} + \frac{L+q}{2r} + U \right) \cos \theta \cos \varphi; \\ v_\varphi &= \left[-\left(\frac{B-K}{2r^3} + \frac{L+q}{2r} + U \right) + \left(\frac{B}{r^3} + \frac{q}{r} \right) \sin^2 \theta \right] \sin \varphi; \\ p &= \mu \left(\frac{L+q}{r^2} - \frac{4q}{R^3} r \right) \sin \theta \cos \varphi; \end{aligned} \quad (18)$$

inside the particle [3]

$$\begin{aligned} v_{1r} &= (M + Nr^2) \sin \theta \cos \varphi; \quad v_{1\theta} = (M + Ar^2/a + 2Nr^2) \cos \theta \cos \varphi; \\ v_{1\varphi} &= [-(M + Ar^2/2 + 2Nr) + Ar^2 \sin^2 \theta] \sin \varphi; \\ p_1 &= \mu_1 \cdot 10Nr \sin \theta \cos \varphi + n\mu_1 r \sin \theta \cos \varphi; \\ q &= 2\lambda \left(\frac{1}{2} - \frac{\varepsilon V_0}{\kappa E a} \right); \quad R = a \left[2 \left(\frac{1}{2} - \frac{\varepsilon V_0}{\kappa E a} \right) \right]^{1/6}; \quad n = \frac{2V_0 e H}{ac\mu_1}. \end{aligned} \quad (19)$$

For determination of the constants we get from the boundary conditions a system of equations similar to (11), from which we obtain finally the magnetophoresis velocity equation

$$U = U_0 \left[1 + \frac{8\mu + 15\mu_1}{3(\mu + \mu_1)} \frac{\varepsilon V_0}{\kappa E a} \right], \quad (20)$$

where U_0 is defined by (12) and V_0 by (16).

From (20), it is evident that the surface charge increases from magnetophoresis velocity. Evaluation shows that U must be 3-4 times larger than U_0 ; nevertheless, as before, it is feasible to neglect U in comparison to V_0 in (15).

If the particle is solid, there is no current inside it; consequently, the volume force (17) is absent. In this case, calculation of the magnetophoresis velocity, for a solid particle gives the value

$$U = U_0 (1 + \varepsilon V_0 / \kappa E a), \quad (21)$$

where V_0 is the electrophoresis velocity of a solid particle [2]:

$$V_{\tau} = \frac{\epsilon E d}{\mu + \epsilon^2 d / a \kappa}, \quad (22)$$

and d is the thickness of the double layer. Here, again, the force acting on the magnetic field side of the double layer, no longer equal to zero, is not taken into account because one of the double layer faces is immobile. It is easy to show that the velocity adjustment brought about by this surface effect is of a smaller order than the already obtained value.

If the solution viscosity μ in (22) may be neglected in comparison with $\epsilon^2 d / a \kappa$, then we get from (21)

$$U_{\tau} = 2U_0. \quad (23)$$

From (23) it is obvious that it is possible to separate an uncharged solid particle from uncharged liquids in a magnetic field.

In conclusion, the authors express their appreciation to Corresponding Member, Acad. Sci. USSR, V. G. Levich for valuable discussions.

LITERATURE CITED

1. D. Leenov, A. Kolin, J. Chem. Phys., **22**, 4, 683 (1954).
2. V. G. Levich, Physicochemical Hydrodynamics [in Russian] (Moscow, 1959).
3. V. G. Levich and V. A. Myamlin, Zhur. Fiz. Khim., **31**, 2453 (1957).

All abbreviations of periodicals in the above bibliography are letter-by-letter transliterations of the abbreviations as given in the original Russian journal. Some or all of this periodical literature may well be available in English translation. A complete list of the cover-to-cover English translations appears at the back of this issue.



INTERACTION OF WEAK COMPRESSION WAVES WITH A FLAME FRONT

S. S. Novikov and Yu. S. Ryazantsev

Institute of Chemical Physics, Academy of Sciences USSR

(Presented by Academician V. N. Kondrat'ev, December 7, 1960)

Translated from *Doklady Akad. Nauk SSSR*, Vo. 137, No. 6

pp. 1409-1412, April, 1961

Original article submitted December 3, 1960

The interaction of compression waves with a flame front has received in the past a considerable amount of experimental [1,2] and theoretical [3-7, 10] treatment. Experiments show that a shock wave is sometimes reinforced by such an interaction. The amplification factor for a relaxation interaction between shock waves and a wave front has been determined [6,7]. A possible mechanism has been proposed [10] for the reinforcement of a weak shock wave in the zone of turbulent combustion. We are going to present a gas-dynamical analysis of a non-relaxation interaction between weak compression waves and a flame front; we will take into account changes in the flame propagation velocity produced by the changes which the thermodynamic constants of the burning mixture undergo in a weak wave.

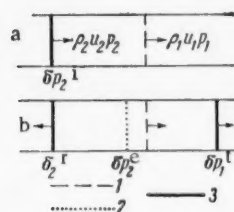


Fig. 1. 1) Flame front; 2) entropy wave; 3) compression wave.

Let us examine the case where a weak compression wave overtakes a flame front (see Fig. 1a). After a compression wave has interacted and passed through the flame it will continue through the burning oxygen while a reflected wave and an entropy wave will be propagated through the combustion products (Fig. 1b). The perturbation on both sides of the flame front can be represented by a set of equations in which the conditions satisfying the laws of conservation of matter, momentum, and energy on the flame front are varied. The conservation of matter, momentum, and energy at the flame front can be represented by the equations:

$$\begin{aligned} \rho_1 U &= \rho_2 (u_1 - u_2 + U); & p_1 + \rho_1 U^2 &= p_2 + \rho_2 (u_1 - u_2 + U)^2; \\ w_1 + U^2/2 &= w_2 + (u_1 - u_2 + U)^2/2. \end{aligned} \quad (1)$$

Variational treatment of (1) with infinitesimals of only the zero and first order in U/c_1 retained (where U is the flame propagation velocity and c_1 the velocity of sound) yields the set of equations shown below:

$$\begin{aligned} \rho_1 \delta U + U \delta \rho_1^t &= \rho_2 (\delta u_1^t - \delta u_2^i - \delta u_2^r + \delta U) + U \frac{c_2^2}{c_1^2} (\delta \rho_2^t + \delta \rho_2^r + \delta \rho_2^e); \\ \delta \rho_1^t + 2\rho_1 U \delta U &= \delta p_2^i + \delta p_2^r + 2\rho_2 U \frac{c_2^2}{c_1^2} (\delta u_1^t - \delta u_2^i - \delta u_2^r + \delta U); \\ \delta \omega_1^t + U \delta U &= \delta \omega_2^i + \delta \omega_2^r + \delta \omega_2^e + U \frac{c_2^2}{c_1^2} (\delta u_1^t - \delta u_2^i - \delta u_2^r + \delta U). \end{aligned} \quad (2)$$

In addition to this the following relationships are maintained on the different waves:
incident compression wave,

$$\delta S_2^i = 0; \quad \delta u_2^i = \frac{\delta p_2^i}{\rho_2 c_2}; \quad \delta w_2^i = \frac{\delta p_2^i}{\rho_2}; \quad \delta p_2^i = \frac{\delta p_2^i}{c_2^2}; \quad (3)$$

reflected compression wave,

$$\delta S_2^r = 0; \quad \delta u_2^r = -\frac{\delta p_2^r}{\rho_2 c_2}; \quad \delta w_2^r = \frac{\delta p_2^r}{\rho_2}; \quad \delta p_2^r = \frac{\delta p_2^r}{c_2^2}; \quad (4)$$

transmitted compression wave,

$$\delta S_1^t = 0; \quad \delta u_1^t = \frac{\delta p_1^t}{\rho_1 c_1}; \quad \delta w_1^t = \frac{\delta p_1^t}{\rho_1}; \quad \delta p_1^t = \frac{\delta p_1^t}{c_1^2}; \quad (5)$$

entropy wave,

$$\delta p_2^e = 0; \quad \delta u_2^e = 0; \quad \delta w_2^e = T_2 \delta S_2^e = -\frac{c_2^2}{\rho_2 (\gamma - 1)} \delta p_2^e \quad (6)$$

The variation in the flame propagation velocity δU can be determined from the relationship $U = f(p_1, T_1)$,

$$\delta U = \left(\frac{\partial f}{\partial p_1} \right)_{T_1} \delta p_1 + \left(\frac{\partial f}{\partial T_1} \right)_{p_1} \delta T_1 = A \delta p_1; \quad A = \left(\frac{\partial f}{\partial p_1} \right)_{T_1} + \frac{\gamma - 1}{\gamma} \frac{T_1}{p_1} \left(\frac{\partial f}{\partial T_1} \right)_{p_1}. \quad (7)$$

Substituting the terms expressed by Equations (3)-(7) into the system of equations (2) and dropping the δp_2^e term we get

$$\begin{aligned} & \left[(\rho_1 - \rho_2) A + \frac{U}{c_1^2} + (\gamma - 1) \frac{U}{c_2^2} - \frac{\rho_2}{\rho_1 c_1} \right] \delta p_1^t = \\ & \gamma \frac{U}{c_1^2} (\delta p_2^i + \delta p_2^r) - \frac{1}{c_2} (\delta p_2^i - \delta p_2^r); \\ & \delta p_1^t = \left(1 + 2 \frac{U}{c_1} \right) (\delta p_2^i + \delta p_2^r) - 2 \frac{U c_2}{c_1^2} (\delta p_2^i - \delta p_2^r). \end{aligned} \quad (8)$$

From this we find that the acoustic conductance at the flame front is

$$\begin{aligned} \zeta = & \frac{\rho_2 c_2}{\rho_1 c_1} - (\rho_1 - \rho_2) c_2 A + (\gamma - 1) \left(1 - \frac{c_1^2}{c_2^2} \right) \frac{U c_2}{c_1^2} + \\ & + 2 (\rho_1 - \rho_2) A [c_1 - (\rho_1 - \rho_2) A c_2^2] \frac{U c_2}{c_1^2}. \end{aligned} \quad (9)$$

The reflection coefficient $k = \delta p_2^r / \delta p_2^i$ is related to ζ by the equation $k = (1 - \zeta) / (1 + \zeta)$. From the system of equations (2) we can also determine the refractive index $\delta p_1^t / \delta p_2^i$ which comes out to be

$$I = \frac{2}{1 + \zeta_0} \left[1 + 2(\rho_1 - \rho_2) A U \frac{c_2^2}{c_1^2} - \frac{B}{1 + \zeta_0} \frac{U}{c_1} \right],$$

where

$$\zeta_0 = \rho_2 c_2 / \rho_1 c_1 - (\rho_1 - \rho_2) c_2 A; \\ B = \{(\gamma - 1)(1 - c_1^2/c_2^2) + 2(\rho_1 + \rho_2) A [c_1 - (\rho_1 - \rho_2) A c_2^2]\} c_2^2/c_1^2.$$

Equation (9) shows that the acoustic conductance at the flame front consists (in the first approximation at least) of a sum of terms representing various physical factors. The first term is the acoustic conductance of a contact gap with a density rise equivalent to that of the flame. The second term, which contains the physical constant A , represents the effects of the flame reaction on weak perturbations. Since A is generally positive the second term is negative and thus decreases the acoustic conductance of the flame. Thus even in zero order approximation it becomes apparent that the changes in the flame propagation velocity induced by a weak wave constitute an important effect. With increasing A the amplitudes of the reflected and transmitted waves increase. The third term, which is an infinitesimal of the first order, represents the entropy wave which separates the combustion products formed before and after the interaction. The fourth term is a first order approximation to the change in the flame propagation velocity.

When a compression wave encounters a flame front moving in the opposite direction the resulting perturbation in the burning mixture consists of an incident and a reflected compression wave, while through the combustion products a transmitted compression wave and an entropy wave are propagated; the variation in the flame propagation velocity can be related to the pressure perturbation by the equation $\delta U = A(\delta \rho_1 + \delta \rho_1')$. In this case the acoustic conductance and the refractive index are given by the equations:

$$\zeta' = \frac{\rho_1 c_1'}{\rho_2 c_2} - (\rho_1 - \rho_2) c_2 A \frac{c_2}{c_1} + (\gamma - 1) \left(1 - \frac{c_1^2}{c_2^2} \right) \frac{U c_2}{c_2^2} \frac{c_2}{c_1} - 2(\rho_1 - \rho_2) A U \left(\frac{c_2}{c_1} \right)^3; \quad (11)$$

$$I' = \frac{1}{1 + \zeta_0'} \left[1 - 2(\rho_1 - \rho_2) A U \frac{c_2^2}{c_1^2} - \frac{B'}{1 + \zeta_0'} \frac{U}{c_1} \right],$$

where

$$\zeta_0' = \rho_1 c_1 / \rho_2 c_2 - (\rho_1 - \rho_2) c_2 A c_2 / c_1; \quad B' = [(\gamma - 1)(1 - c_1^2/c_2^2) - 2(\rho_1 - \rho_2) c_2 A] c_2^2 / c_1^2. \quad (12)$$

Equation (11) shows that when $A=0$ the zero order approximation again yields an acoustic conductance for the flame equal to that of an equivalent contact gap. Unlike Equation (9), where the reflected and the transmitted waves had the same sign as the incident, Equation (11) shows that at moderately small A the reflected wave has a sign opposite to that of the incident while the transmitted wave retains the same sign as the incident. At the same time the amplitude of the reflected wave decreases with increasing A . Otherwise the individual components of Equation (11) have the same physical significance as do the corresponding terms of Equation (9). Of some interest is also the limiting space $\rho_1 \gg \rho_2$, which represents a solid burning on the surface. Equation (9) shows that in this case the acoustic conductance of the flame front is always negative and equal to

$$\zeta_k = -(\rho_1 - \rho_2) c_2 A. \quad (13)$$

Consequently the reflected wave is reinforced.

It should be noted that the applicability of Equations (9)-(13) is limited to moderately large values of A . Otherwise under the impact of a weak wave the flame might generate waves of ultimate intensity, which would fall beyond the framework of a linear treatment.

The constant A is the coefficient of flame propagation velocity under conditions of adiabatic pressure variations in the burning mixture. It can be determined either from the Zel'dovich-Frank-Kamenetskii formula for

the velocity of flame propagation [8] or experimentally. The experiments are usually designed to determine the flame propagation velocity as a function of the initial temperature at fixed pressure or as a function of pressure at a fixed temperature. The resulting pressure or temperature dependent coefficients for the velocity of flame propagation under various conditions may be either positive or negative. That is why A can be positive, negative, or zero.

As an example let us examine the combustion of an air-methane mixture. Previous experiments have shown [9] that in this case the velocity is relatively independent of pressure. We can assume, therefore, that A can be determined from the simple function $U = U(T_c)$. In a mixture containing 10% methane and with $P = 1$ atm at $T_0 = 20^\circ$ we have $T_c = 2100^\circ$ and $\Delta U / \Delta T = 0.2$ cm/sec-deg, while the individual terms of Equation (9) are:

$$\frac{\rho_2 c_2}{\rho_1 c_1} = 0,35; (\rho_1 - \rho_2) c_2 A = 0,002; (\gamma - 1) \left(1 - \frac{c_1^2}{c_2^2}\right) \frac{U c_2}{c_1^2} = 0,0009;$$

$$2 (\rho_1 - \rho_2) c_2 A \left[\frac{c_1}{c_2} - (\rho_1 - \rho_2) c_2 A \right] \frac{c_2}{c_1} \frac{U}{c_1} = 3,5 \cdot 10^{-6}.$$

Thus we see that when we take into account variations induced in the flame propagation velocity by the interaction, the acoustic conductance of the flame front is reduced by 0.5%. We have also estimated that in some cases the reduction may amount to several percent. The effect may become very important if the compression wave should recross the flame front many times as a result of reflections.

LITERATURE CITED

1. S. M. Kogarko, Zhur. Tekh. Fiz. 30, 1, 110 (1960).
2. G. D. Salamandra and I. K. Sevost'yanova, Zhur. Tekh. Fiz. 29, 11, 1360 (1959).
3. G. M. Bam-Zelikovich, Theoretical Hydromechanics [in Russian], Coll. No. 4 (1949); Coll. No. 9 (1952).
4. Poa T'ieh-Ch'u, Coll. Problems in Combustion and Detonation Waves, 4th Intl. Symp. [in Russian] (Moscow, 1958), p. 411.
5. N. Manson, Proc. VII Int. Congr. Appl. Mech., 2, 187 (1948).
6. S. M. Kogarko and V. I. Skobelkin, Doklady Akad. Nauk SSSR, 120, No. 6, 1280 (1958).
7. S. M. Kogarko, V. I. Skobelkin, and A. N. Kozakov, Doklady Akad. Nauk SSSR, 122, No. 6, 1046 (1958).
8. Ya. B. Zel'dovich and D. A. Frank-Kamenetskii, Zhur. Fiz. Khim. 12, 1, 100 (1938).
9. L. N. Khitrin, The Physics of Combustion and Detonation [in Russian], 1957.
10. K. I. Shchelkin, Izvest. Akad. Nauk SSSR, Energetika i Avtomatika, No. 5, 86 (1959).

All abbreviations of periodicals in the above bibliography are letter-by-letter transliterations of the abbreviations as given in the original Russian journal. Some or all of this periodical literature may well be available in English translation. A complete list of the cover-to-cover English translations appears at the back of this issue.

SPREADING OF MERCURY OVER A FREE ZINC SURFACE,
AS CONNECTED WITH THE STUDY OF STRENGTH
REDUCTION BY ADSORPTION

B. D. Summ, Yu. V. Goryunov, N. V. Pertsov and E. D. Shchukin
M. V. Lomonosov Moscow State University
(Presented by Academician P. A. Rebinder, December 9, 1960)
Translated from *Doklady Akad. Nauk SSSR*, Vol. 137, No. 6
pp. 1413-1415, April, 1961
Original article submitted December 4, 1960

A rapid penetration of atoms from the melt into the precorrosion zone by means of two-dimensional migration along the defects of the crystal structure and the walls of nucleated microcavities is an essential condition for reducing the strength of metals under the action of molten adsorption-active metallic coatings [1,2]. In one of our last communications we have described the developing of macroscopic corrosion cracks in zinc sheets under the action of locally applied small mercury droplets [3]. These experiments allowed us to clarify directly, for the first time, the role of mercury migration in the development of cracks and connect the kinetics of their growth with two peculiar competitive processes: the spreading of mercury along the walls of the crack to the precorrosion zone (surface migration) and the absorption of mercury through the crack walls along their entire length (three-dimensional diffusion).

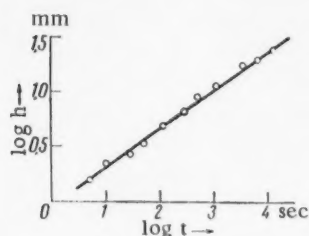


Fig. 1. The rise of a mercury stain plotted versus time.

In the present investigation we have studied the spreading of mercury over a free zinc surface (in the absence of mechanical stresses)*. The experiments were carried out at room temperature on technical zinc sheets (98.7% Zn) with a thickness of 1.85 mm. In order to remove the oxide layer the samples were treated with 12% nitric acid, then rinsed with water and immersed in a tank with a 10% solution of ammonia, in which it was kept throughout the experiment.

The first series of experiments was carried out on vertically kept sheets with a width of 2.0-2.5 cm and a length up to 30 cm. The lower end of the sheet was brought in contact with mercury which wetted the entire lower edge of the zinc. A sufficiently great amount of mercury was taken so that it practically did not diminish during the experiment ("linear source with infinite capacity"). Right after contact between zinc and mercury has been achieved, an easily visible bright mat stain with a clearly outlined front begins to spread upwards along the surface of the sheet. At the first moment (a small fraction of a second) the stain front moves at a quite high velocity (about a centimeter per second); later on the rate of spreading rapidly slows down. The position of the stain front was read visually through the tank wall (a glass wall) by means of a scale which had been ruled previously on the sample. A series of such experiments gave a good quantitative reproducibility in the results. It was found that the height h over which the stain rises is a power function of the time t (Fig. 1).

The second series of experiments was carried out on horizontally kept square sheets. A small mercury droplet (from a few tenths of a milligram to several times ten milligrams) was placed on the center of the sheet ("point source", or, strictly speaking, since it has a small finite radius, "source with finite capacity"). In this case the

* G. I. Varicheva took part in the investigation.

spreading of mercury over the zinc surface is divided in three consecutive and clearly distinguishable stages. The flattening of the droplet is the first and very shortest (fraction of a second) stage. The droplet turns into a "small pool" with a shining mirror-like surface; the size depends, of course, upon the amount of mercury. For amounts of 10 mg the radius of the circle occupied by mercury is 3-4 mm at the end of the flattening stage.

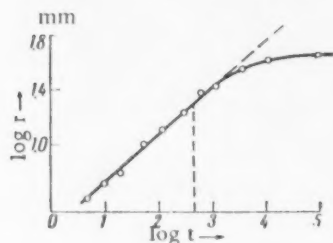


Fig. 2. The radius of the mercury stain plotted versus time. Amount of mercury $m = 10$ mg. The vertical dashed line corresponds to the moment in which the liquid mercury phase in the center of the stain disappears.

a droplet of 10 mg is shown in Fig. 2 (the observations were started a few seconds after the onset of the second stage). In Fig. 3 the final stain radius R (two hours after the droplet has been applied) is plotted on a logarithmic scale versus the weight of mercury.

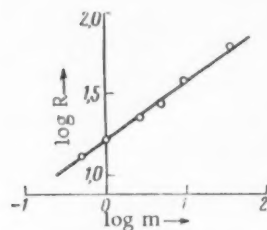


Fig. 3. The relation between the final stain radius and the weight of mercury.

Promptly after the droplet has flattened, the second, main, stage, which is comparable with the above-described spreading of mercury along a vertical sheet, starts. Namely, from the rim of the mirror-like "poollet" a bright mat stain with an accurately circular shape begins to spread; in the first moment the front moves at a rate attaining ~ 1 cm/sec; then the rate falls regularly. During several minutes, dependent upon the weight of the mercury droplet, liquid mercury is visible while it is retained in the central part of the circle; it dries up and its shining luster disappears; the third stage sets in. The stain grows very slowly; meanwhile the characteristic linear relation between the logarithm of the stain radius and the logarithm of time, which is found in the second stage, is no longer met. After some hours the stain growth stops completely (it should be noted that when a layer with a strongly developed structure is present on the sheet surface, the spreading rate of the stain along the grains differs somewhat from that across and, because of this, the stain gets an ellipsoidal shape). The growth of the stain radius with time for

A series of experiments was also carried out to simulate on a horizontal sheet "a point source with infinite capacity": for this purpose, as the mercury in the central part of the circle dried up, (before stage II ended) new mercury was added successively in small portions. Finally, some experiments were done to observe vertical spreading of mercury from "a point source with infinite capacity": for this we used samples in the form of segments with an angle of 60° cut from sheet. The segment was kept with its top down and the top was brought in contact with a sufficiently great amount of mercury. The experiments indicated that the course of the process (stage I excluded) is practically the same, when the sheet is kept horizontally or vertically.

In all cases where "a source with infinite capacity" was used (and also in stage II for a source with infinite capacity) the spreading of the mercury front could be described as a power function of time: $r \sim t^n$; dependent upon the experimental conditions, values of about 0.3 to 0.4 are found for the exponent n .

The results of these experiments closely resemble the data on the spreading of cracks in zinc sheets at the local application of mercury [3]; in the latter case the same stages are found, namely flattening of the droplet, the spreading of mercury by surface migration from the source, which visibly retains liquid mercury and, finally, a slow redistribution of the mercury which is still present in the very fine surface layers, when the source has already disappeared. It is evident that, in the above-described experiments on the spreading of mercury over a zinc surface in the absence of mechanical stresses, the kinetics are also determined by the competition between surface diffusion of mercury and its penetration (diffusion) into the bulk of zinc. In this connection the following fact is interesting; if, soon after stage II has ended, a new amount of mercury is put in the center of the stain, then the addition appears to be "additive": the stain takes the same final size as it should have got, if the total amount had been applied at once. But, if a second droplet is applied after 2-3 hours, when stage III has already come to a complete stop, there is no longer additivity: if the second amount is equal to the first one, the stain size practically does not change; if the second amount is greater, then the final stain radius approximately corresponds to the greater one of the droplets.

Mechanical tests also confirm the essential role of volume diffusion (absorption) of mercury in the kinetics of the spreading over a zinc surface. We have shown previously [2] that a mercury film with a thickness of $\sim 1\mu$ causes embrittlement of zinc. In the said paper it has been established that if the sheet is bended soon after an experiment, then the entire surface occupied by the mercury stain is covered by a network of fine cracks. However, if the sample is not bended soon after an experiment, but this is done several hours later on, then cracking of the surface is not found; this means that nearly all mercury which originally is located on the surface succeeds in diffusing into the bulk of the zinc.

It should be expected that the strength reduction of the zinc within the reach of the spreading stain will be more clearly manifested when thin samples are tested. A corresponding series of experiments was carried out on zinc wire of high purity (99.99 % Zn) with a diameter of 0.6 mm and a length of 10-15 cm. The samples were placed vertically in the tank and during a fixed time kept in contact with mercury. Then they were withdrawn from the tank and exposed to a very mechanical test: at a constant rate they were wound on a rod with a diameter of 3 cm. At this radius of curvature the wire which we used bended easily and cracking was not found, when no mercury was present. The sample was wound on the bar starting from the upper wire end untouched by mercury. At a certain distance from its lower end (as a rule, just at that point which the visible mercury front had succeeded in reaching) the sample broke. The experiments gave the following results:

Contact time of sample with mercury	1	5	20	60	min
Length of region turned brittle	7	15	25	41	mm

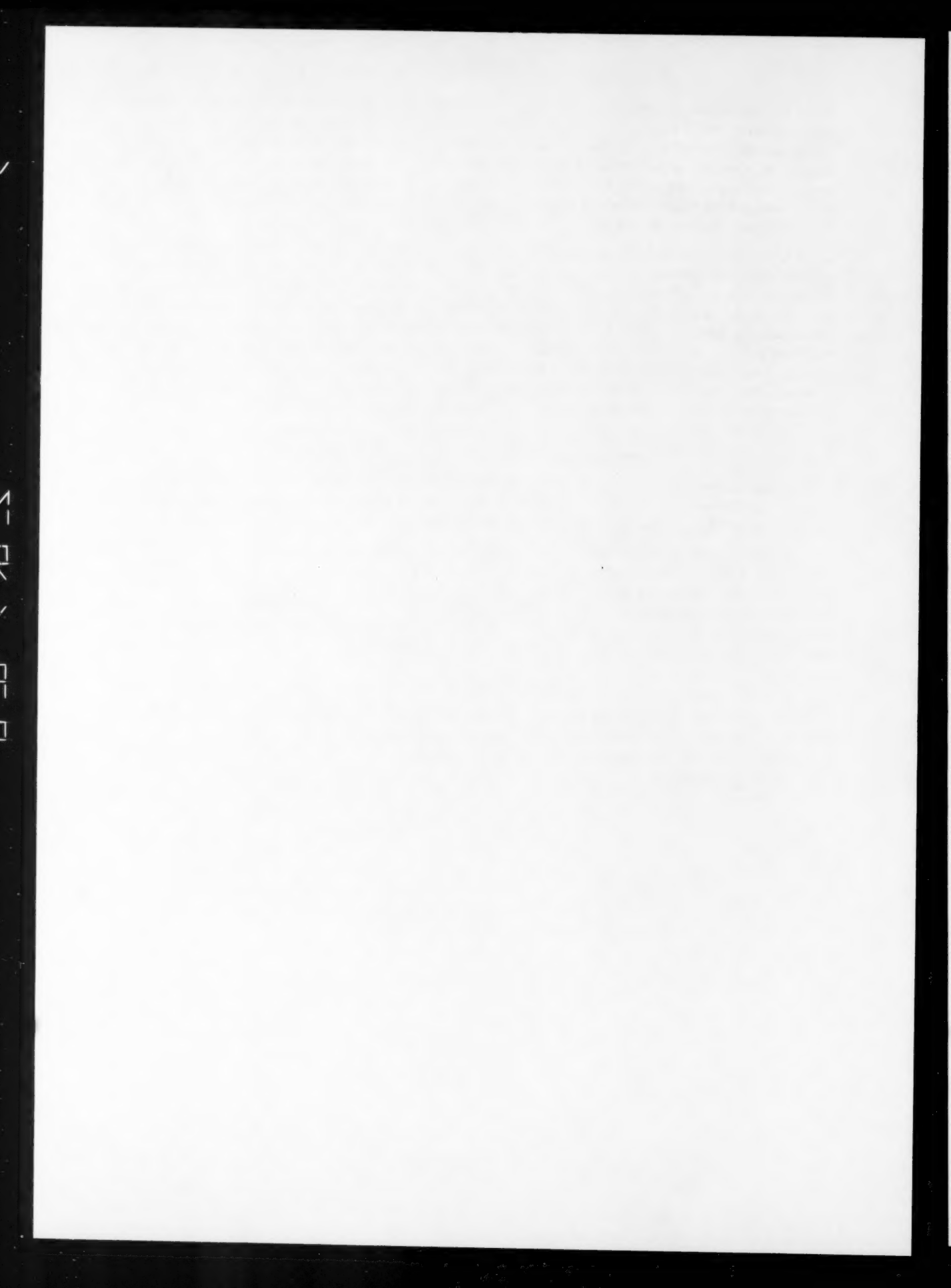
These data on the whole give the same relation between the height of the mercury rise and time as was found above (compare Fig. 1). Small numerical discrepancies are connected, obviously, with the difference in purity of the samples, the quality of their surfaces and the grain size.

It should be remarked that spreading of mercury over the zinc surface could only be observed, if the experiments were done in a medium which prevented the formation of an oxide film. The optimum conditions for stain growth were obtained by using a 10-20 % solution of ammonia. When the concentration of ammonia was lowered to 2.5-5 %, the spreading was slowed down somewhat. When a 5 % solution of hydrochloric acid or sodium hydroxide was used as medium preventing the oxidation of zinc, the results were practically the same as have been found in a 10 % solution of ammonia.

LITERATURE CITED

1. P. A. Rebinder, V. I. Likhtman and L. A. Kochanova, *Doklady Akad. Nauk SSSR*, **111**, 1284 (1956).
2. E. D. Shchukin, N. V. Pertsov and Yu. V. Goryunov, *Kristallografiya*, **4**, 887 (1959).
3. B. D. Summ, Yu. V. Goryunov, N. V. Pertsov, E. D. Shchukin and P. A. Rebinder, *Doklady Akad. Nauk SSSR*, **136**, No. 6 (1961).

All abbreviations of periodicals in the above bibliography are letter-by-letter transliterations of the abbreviations as given in the original Russian journal. Some or all of this periodical literature may well be available in English translation. A complete list of the cover-to-cover English translations appears at the back of this issue.



THE MANIFESTATION OF AUTONOMY BY ELECTRON GROUPINGS IN THE LUMINESCENCE SPECTRA OF COMPLICATED MOLECULES

D. N. Shigorin, N. A. Shcheglova and N. S. Dokunikhin

L. Ya. Karpov Physicochemical Institute

(Presented by Academician A. N. Terenin, November 9, 1960)

Translated from Doklady Akad. Nauk SSSR, Vol. 137, No. 6

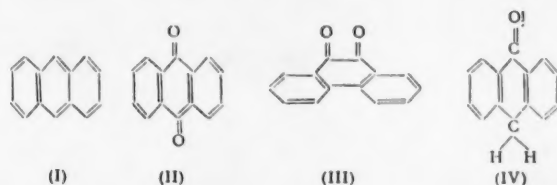
pp. 1416-1419, April, 1961

Original article submitted November 2, 1960

By a quantum-mechanical discussion of the electron levels in simple molecules with multiple bonds it was shown that excitation is connected with the participation of π - and p-electrons of chromophoric groups ($>C=C<$, $C=O$, etc.) and that substituents (auxochromes) influence the position of these levels. So, in molecules containing $C=C$ -bonds (ethylene, etc.) the $\pi \rightarrow \pi^*$ ($N \rightarrow V$) transition: $\sigma^2 \pi^2 \rightarrow \sigma^2 \pi \pi^*$ is the most probable one. In compounds containing chromophores with heteroatoms ($C=O$; $C=S$; NO_2 , $-N=N-$; $-N=O$, etc.) the $n \rightarrow \pi^*$ ($N \rightarrow Q$) transition in which one p-electron from a nonbonding orbital of the heteroatom is transferred to the antibonding π -orbital of the multiple bond: $\sigma^2 \pi_x^2 Y_L^2 \rightarrow \sigma^2 \pi_x^2 Y_L \pi_x^*$ is the most probable transition giving rise to absorption at long wavelengths.

Therefore, those groups of atoms which are directly connected with the other parts of the molecule by exchange interaction and are mainly responsible for the electronic excitation of the entire molecule are called chromophores.

Does the autonomy of the electron groupings chromophores manifest itself in emission (luminescence spectra) as well as in absorption? In order to solve the problem raised we have investigated the luminescence spectra of a whole series of complicated molecules:



(anthraquinone, thioindigo and its derivatives, etc.) in diluted solutions in n-paraffinic hydrocarbons ($C = 10^{-4} - 10^{-5}$ mole/liter) at $T = 77^\circ K$. The experimental results are shown in Fig. 1.

An analysis of the quasiline spectra which we have obtained for the luminescence of anthraquinone (II), α - and β -monohalide derivatives of anthraquinone; α -methyl, α -phenyl, α -methoxyanthraquinone, phenanthraquinone (III), anthranone (IV), etc. [2-4] shows that the intensive spectral bands, just as the suitably taken weaker ones, lie at mutual distances which on the average are equal to 1664 cm^{-1} (for III and IV 1686 cm^{-1}) and correspond to the valency vibration of the chromophoric $C=O$ group in the electronic ground state. Consequently, in the electronic-vibration spectra of compounds with the said group, the vibrational structure is characterized

by the valency vibrations of the chromophoric C=O group, which is mainly responsible for the electronic excitation of the system ($n \rightarrow \pi^*$ -transition) not only in the absorption spectra but also in the luminescence spectra. The frequencies of the totally symmetric vibrations of the condensed aromatic system analogous to anthracene are not characteristic for the quasiline spectra of anthraquinone and its derivatives. On the contrary, in the line spectrum of anthracene (I) luminescence, according to data of É. V. Shpol'skiĭ and co-workers [1], the vibrational fine-structure is characterized by the frequencies of the totally symmetric vibrations of the condensed aromatic

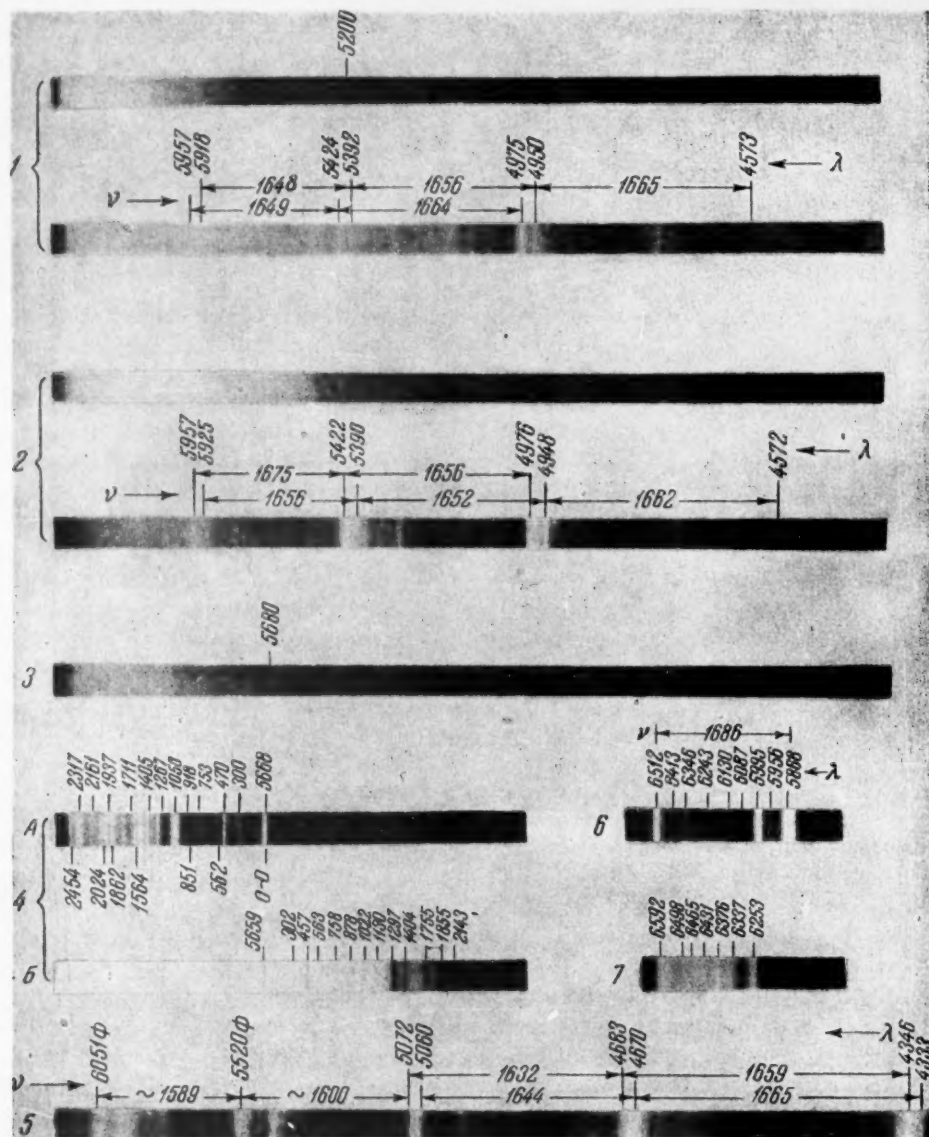
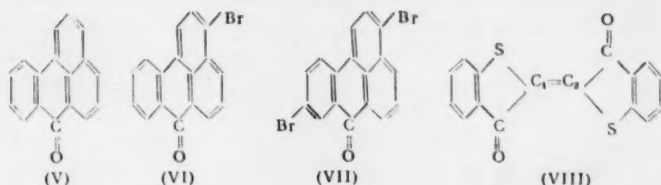


Fig. 1. Luminescence spectra of anthraquinone derivatives in heptane at 77° K. a) $\lambda_{\text{Hg}} = 313 \text{ m}\mu$, b) $\lambda_{\text{Hg}} = 365 \text{ m}\mu$: 1) α -chloranthraquinone; 2) 1,8-hydroxyanthraquinone; 3) 1,5-dihydroxyanthraquinone; 4) 1,4,5,8-tetrahydroxyanthraquinone (a- emission, b- absorption); 5) anthraone (in hexane), the short-wave part of the spectrum for $\lambda_{\text{main}} = 4043 \text{ \AA}$ is not shown in photograph; 6) phenanthraquinone; 7) monobromomesobenzanthrone.

system, which is responsible for the electronic excitation ($\pi \rightarrow \pi^*$ -transition). Further, the vibrational structure of the quasiline spectra in the luminescence of the molecules which we have studied: mesobenzanthrone (V), its bromoderivatives (VI, VII), thioindigo (VIII) and its derivatives [5] are not characterized by the frequencies of the C=O valency vibrations, although the said compounds have C=O groups in common.



The spectra of mesobenzanthrone and its derivatives (V-VII) are characterized by the vibration frequencies of the condensed aromatic system. So, in these compounds the C=O group is not responsible for the electronic excitation, and therefore, it is not a chromophore for these molecules. The electronic excitation in these molecules is brought about by the π -electron system of the aromatic rings ($\pi \rightarrow \pi^*$ -transition). In the quasiline spectra given by thioindigo in absorption and luminescence the vibrational fine-structure, clearly, is characterized by the frequencies of the $>C_1=C_2<$ valency vibrations (1540 cm^{-1}) and not by the C=O frequencies, as was the case for anthraquinone and its derivatives. Consequently, in thioindigo the $C_1=C_2$ group is the chromophore which determines the electronic excitation ($\pi \rightarrow \pi^*$ -transition) and, therefore, the frequency of its valency vibration appears so characteristically in the quasiline spectra of absorption and emission. The facts given indicate that in the absorption and luminescence spectra of complicated molecules a certain autonomy of the electron groupings (chromophores), which are mainly responsible for the electronic excitation, is manifested and the frequencies of the valency vibration of the chromophoric groups are the chief characteristic in the vibrational structure of the electronic-vibrational (quasiline) spectra.

In complicated molecules containing several chromophoric groups, just that group which provides the smallest energy difference between the ground state and the first excited level ($h\nu_{\min} = E_{1,e} - E_{0,e}$) takes part directly in the excitation discussed. Above it has been remarked that the quasiline spectra of complicated molecules in which autonomy of the chromophoric groups is manifested can be observed only at low temperatures in diluted solutions in paraffinic hydrocarbons. Under normal conditions the electronic spectra of complicated molecules are characterized by very diffuse bands. The reason lies in the fact that in complicated molecules the interaction between electron motion and nuclear vibrations is very high. As a result of this interaction, electronic energy is converted into vibration energy of the nuclei; if, initially, the vibrational energy is localized in one or a few degrees of freedom, then, at a later instant, it is redistributed throughout the entire molecule and this is the reason why the vibrational structure of the spectrum is diffuse [6]. However, the probability of an energy redistribution over the vibrational degrees of freedom does not depend only upon the total vibrational energy content of the system, the properties of the medium, temperature, but the interactions between the separate degrees of freedom, as is determined by particularities of the chemical molecular structure (conjugation, coplanarity, etc.), are also important features. At low temperatures (where the total vibrational energy content and the interaction between the various degrees of freedom are decreased), when there is no interaction with the solvent and between the luminescent molecules themselves, and the interaction between the chromophoric group (C=O) and the rest of the molecule (II-IV) is also relatively weak, the excitation energy, which, initially, is mainly localized on the electronic and vibrational levels of the chromophore (C=O), will be redistributed much more slowly over the other vibrational degrees of freedom. This also means that the fraction of electronic energy which at excitation is converted into vibrational energy will be mainly distributed over the vibrational levels of the chromophoric group which is responsible for the excitation. Because of this, the vibrational fine-structure will be characterized, to a considerable extent, by the frequencies of the normal vibrations of the chromophoric group and this is in agreement with the facts given here.

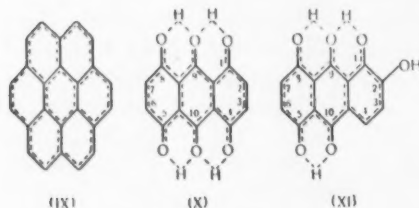
Our investigations have shown that in the luminescence spectra (in diluted solutions in paraffins at low temperatures) of those molecules which contain two different groups the excitation of electronic transitions (states) corresponding to these groups is possible. Dependent upon the excitation conditions (λ , T, medium), one may obtain any of two, or both electron states simultaneously, and observe two spectra (luminescence). So, α -chloranthra-

quinone contains two different carbonyl (chromophoric) groups: in excitation with $\lambda = 365 \text{ m}\mu$ one observes a continuous spectrum ($\lambda_{\text{main}} = 5200 \text{ \AA}$), which obviously is connected with an electronic $n \rightarrow \pi^*$ -transition in the $\text{C}=\text{O}$ group near to the chlorine atom, and in excitation with $\lambda = 313 \text{ m}\mu$ the continuous spectra remains, but a new spectrum with a vibrational fine-structure at $\lambda_{\text{main}} = 4573 \text{ \AA}$ corresponding to an electronic $n \rightarrow \pi^*$ -transition in the free $\text{C}=\text{O}$ group makes its appearance (Fig. 1).

In the 1,8-dihydroxyanthraquinone molecule there are also two sharply different carbonyl groups. Upon exciting with $\lambda = 365 \text{ m}\mu$ a continuous spectrum ($\lambda_{\text{main}} = 5516 \text{ \AA}$) is obtained and upon exciting with $\lambda = 313 \text{ m}\mu$, besides this, a new spectrum appears with a vibrational fine-structure ($\lambda_{\text{main}} = 4572 \text{ \AA}$) corresponding to an electronic ($n \rightarrow \pi^*$) transition in the free $\text{C}=\text{O}$ group. The carbonyl group which participates in the formation of an hydrogen bond requires less energy for its excitation than does the free group. The character of the luminescence spectra of 1,5-dihydroxyanthraquinone and 1-hydroxyanthraquinone does not depend upon the frequency of the exciting light. The influence of the auxochromes (Hal , OH , NH_2 , etc.) upon the molecular spectra manifests itself in shifting and broadening the bands, in changing the intensity sequence (in agreement with the Franck-Condon principle and sometimes in changing completely the vibrational structure of the spectrum [3,4]).

In the α -hydroxy derivatives of anthraquinone the OH group forms a hydrogen bond with the chromophoric $\text{C}=\text{O}$ group, mainly by π -electron interaction. If acceptor-donor interaction played a predominant role in the formation of the hydrogen bond, then the excitation of the molecule (accompanied by a $n \rightarrow \pi^*$ -transition) would result in breaking the hydrogen bond and by this the luminescent properties of the compound would be lost. This is confirmed by the fact that in the α -amino derivatives of anthraquinone the luminescence is much less than in the α -hydroxy-derivatives. It has been established [7] that the orthoaminoazo compounds give no luminescence at all, whereas the orthohydroxyazo compounds fluoresce brightly. When an internal hydrogen bond is formed under participation of the amino group, the condition of coplanarity is insufficiently met and, therefore, in the excited state the hydrogen bond may be weakened or even broken, because the acceptor-donor interaction has been upset (as a result of the $n \rightarrow \pi^*$ -transition) and the participation of the NH group in the π -electron interaction is little effective.

A new fact, which confirms that in the excited state of the α -hydroxy derivatives of anthraquinone the hydrogen bond is preserved and consolidated and this bond has even a strong influence upon the nature of the excited state, is given by luminescence spectrum of 1,4,5,8-tetrahydroxyanthraquinone in which each $\text{C}=\text{O}$ group takes part in the formation of two hydrogen bonds. This gives four additional quasi-aromatic rings having π -electron interaction with the three additional original rings, so that there results a system of seven rings which may be called a peculiar quasicoronene (X).



A vibration analysis of the quasiline absorption and emission spectra of this compound has shown that the electronic excitation is accomplished at the expense of a $\pi \rightarrow \pi^*$ -transition. In the spectra there are frequencies which are similar to those of coronene, but there are also found bands at 1267 , 1404 and 1564 cm^{-1} , which are characteristic for the vibrations of anthracene [8,9]. The vibrational structure of the quinalizarin (XI) spectrum is also characterized by the frequencies of the aromatic system. In the 1,4,5,8-tetrahydroxyanthraquinone (X) and quinalizarin (XI) molecules a new chromophoric system comprising

rings with hydrogen bonds arises at excitation. Because of this, the vibrational structure of the quasiline spectra is not characterized by the frequencies of the $\text{C}=\text{O}$ valency vibrations.

An analysis of the luminescence spectra of β -substituted anthraquinones (Br , I , $\text{R}-\text{O}-\text{C}=\text{O}$) allows us to draw the conclusion that (under comparable excitation conditions) the intensity of the chromophore ($\text{C}=\text{O}$) combination band and that of the band corresponding to the $0''-0'$ -transitions change antipatically.

The facts discussed confirm the idea [10] that in complicated molecules local many-center electronic orbitals may exist in which a certain assemblage of π -electrons participates and moves in the field of the directly mutually connected nuclei, but upon which the more remote surrounding exerts only a certain perturbation. The manifestation of autonomy of chromophoric groupings in the absorption and emission spectra of complicated molecules, dependent upon the composition and the excitation conditions, is the object of further investigations.

The authors express their gratitude to Academician A. N. Terenin for his valuable suggestions in the discussion of the present paper.

LITERATURE CITED

1. É. V. Shpol'skii, *Uspekhi Fiz. Nauk*, **68**, 51 (1959); **71**, 215 (1960).
2. D. N. Shigorin, N. A. Shcheglova, R. N. Nurmukhametov and N. S. Dokunikhin, *Doklady Akad. Nauk SSSR*, **120**, 1242 (1958); *Izvest. Akad. Nauk SSSR, Ser. Fiz.* **23**, 37 (1959).
3. D. N. Shigorin, N. A. Shcheglova, N. S. Dokunikhin and V. A. Puchkov, *Doklady Akad. Nauk SSSR*, **132**, 1372 (1960).
4. D. N. Shigorin, N. A. Shcheglova and N. S. Dokunikhin, *Izvest. Akad. Nauk, Ser. Fiz.* **24**, 778 (1960); *Doklady Akad. Nauk SSSR*, **133**, 420 (1960).
5. R. N. Nurmukhametov, D. N. Shigorin and N. S. Dokunikhin, *Izvest. Akad. Nauk SSSR, Ser. Fiz.* **24**, 728 (1960).
6. B. I. Stepanov, *Luminescence of Complicated Molecules* [in Russian] (Minsk, 1960).
7. R. N. Nurmukhametov, D. N. Shigorin, Yu. I. Kozlov and V. A. Puchkov, *Abstracts of the Proceedings of the XIII Conference on Spectroscopy* [in Russian] (Moscow, Branch Physical-Mathematical Sciences, Acad. Sci. USSR Press, 1960).
8. É. V. Shpol'skii and L. A. Klimova, *Izvest. Akad. Nauk SSSR, Ser. Fiz.* **23**, 23 (1959).
9. E. Y. Bowen, B. Brocklehurst, *J. Chem. Soc.*, 1954, 3875.
10. D. N. Shigorin, *Zhur. Fiz. Khim.* **25**, 737 (1951); **30**, 2753 (1956); **32**, 1739 (1958).
11. T. N. Bolotnikova, *Izvest. Akad. Nauk SSSR, Ser. Fiz.* **23**, 29 (1959).

All abbreviations of periodicals in the above bibliography are letter-by-letter transliterations of the abbreviations as given in the original Russian journal. Some or all of this periodical literature may well be available in English translation. A complete list of the cover-to-cover English translations appears at the back of this issue.



REACTION KINETICS FOR THE REDUCTION
OF DIPHENYL - m - TOLYLCARBINOL WITH ISOPROPYL
ALCOHOL BY TRANSFER OF NEGATIVELY CHARGED HYDROGEN
IN THE SYSTEM $H_2SO_4 - H_2O$

S. G. Éntelis, R. P. Tiger, G. V. Épple, and N. M. Chirkov

The Institute of Chemical Physics of the Academy of Sciences of the USSR

(Presented by Academician V. N. Kondrat'ev, November 4, 1960)

Translated from Doklady Akad. Nauk SSSR, 137, No. 6

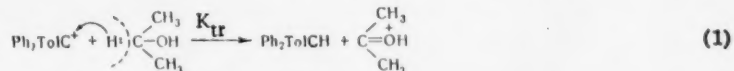
pp. 1420-1423, April, 1961

Original article submitted October 31, 1960

In recent years it has been shown that a number of organic oxidation-reduction reactions include the stage of transfer of negatively charged hydrogen. There have been several investigations of the mechanism and kinetics of these reactions [1-4]. A particular study has been made of the reduction of triphenylcarbinol (TPC) by aliphatic alcohols in an aqueous H_2SO_4 medium. In order to find out how the reactivity of a triarylcarbinol altered with structure, we chose diphenyl-m-tolylcarbinol (DPTC) as our triarylcarbinol and investigated the kinetics of its reduction by isopropyl alcohol.

The reaction was carried out in an H_2SO_4 medium, with acid concentrations from 44 to 64%, and at temperatures from 40 to 60°. The DPTC concentration in the reaction mixture was about 10^{-4} M, and the isopropanol concentration was varied from 0.1 to 1.5 M. The course of conversion was followed by measuring the change in optical density with time at $410\text{ m}\mu$; this wave length corresponds to the absorption maximum of the ionized form of DPTC. The experimental method has been described previously [6].

By analogy with triphenylcarbinol [1,4], we assumed that the limiting stage would be the acceptance of a hydride ion from isopropanol by the Ph_2TolC^+ carbonium ion, formed by ionization of DPTC:



It is not difficult to show [4] that the expression for the observed effective velocity constant has the form:

$$k_{ef} = k_{tr} \left(\frac{K_{Ar_3COH} c_0}{1 + K_{Ar_3COH} c_0} \right) \left(\frac{1}{1 + K_{ROH} h_0} \right) [ROH], \quad (2)$$

where k_{ef} is the observed first order velocity constant; k_{tr} is the velocity constant for the elementary act of hydride transfer; K_{Ar_3COH} and K_{ROH} are the equilibrium constants for the protonization of carbinol and alcohol ($K_{Ar_3COH} = [Ar_3C^+]/[Ar_3COH] c_0$; $K_{ROH} = [ROH_2^+]/[ROH] h_0$); c_0 and h_0 are the negative antilogarithms respectively of the Deno and Hammett acidity function [5].

The experiments were carried out with excess isopropanol, so that the concentration of the latter hardly altered during an experiment, and the observed kinetics were pseudo first order. The values of the effective velocity constants were found from the slopes of the kinetic curves plotted on semilogarithmic paper.

We made a detailed study of the variation of k_{ef} with H_2SO_4 concentration at various alcohol concentrations. Table 1 shows the results obtained over the above-stated temperature range.

It is clear from Table 1 that the observed bimolecular constants $k_0 = k_{ef}/C_{alc}$ varied with changing isopropanol concentration. For example, at low H_2SO_4 concentrations and low temperatures, the value of k_0 diminished with increasing alcohol concentration, owing to the effect of the alcohol on the acidity of the medium [5]. This phenomenon affected the interpretation, so the observed values of k_{ef} were interpolated to $C_{alc} = 0.1$ mole/liter at which concentration the effect of the alcohol on the acidity of the medium could be neglected [6].

TABLE 1

40 °C				50 °C				54 °C				60 °C			
H_2SO_4 , %	C_{alc} , mole/liter	$k_{ef} \cdot 10^2$, min ⁻¹	$k_0 \cdot 10^2$, liter/mole·min	H_2SO_4 , %	C_{alc} , mole/liter	$k_{ef} \cdot 10^2$, min ⁻¹	$k_0 \cdot 10^2$, liter/mole·min	H_2SO_4 , %	C_{alc} , mole/liter	$k_{ef} \cdot 10^2$, min ⁻¹	$k_0 \cdot 10^2$, liter/mole·min	H_2SO_4 , %	C_{alc} , mole/liter	$k_{ef} \cdot 10^2$, min ⁻¹	$k_0 \cdot 10^2$, liter/mole·min
	0,431	2,85	6,62	46,40	0,132	2,99	22,6	49,88	0,243	7,60	31,3	45,80	0,198	7,54	38,2
	0,635	3,22	5,17		0,198	2,76	13,9		0,315	11,05	35,1		0,199	8,16	41,0
	0,887	4,26	4,81		0,349	6,90	19,7		0,410	16,3	39,8		0,289	12,42	43,1
	1,234	5,30	4,30		0,651	10,60	16,2		0,765	21,4	28,0		0,517	14,49	28,1
					1,00	6,54	6,54		0,777	24,2	31,1		0,596	21,0	38,6
	0,162	1,38	8,52	46,80	0,095	2,53	26,7	46,31	0,135	3,88	28,8	46,80	0,158	7,86	50,0
	0,363	3,20	8,92		0,320	5,75	18,0		0,366	5,68	15,5		0,198	10,10	51,5
	0,634	5,18	8,18		0,422	6,45	15,3		0,453	11,2	24,8		0,298	12,65	42,5
	1,014	6,67	6,56		0,590	8,96	15,2		0,613	14,25	23,3		0,431	19,55	45,1
	1,397	7,60	5,44		0,965	14,3	14,8		0,620	18,2	29,3		0,575	20,70	36,0
49,34	0,198	2,30	11,00	49,30	0,096	2,12	22,1	47,11	0,103	6,20	60,1	49,35	0,138	7,36	53,3
	0,209	2,13	10,20		0,278	6,45	23,2		0,202	6,67	33,0		0,224	10,80	48,3
	0,595	6,10	10,25		0,396	10,30	26,0		0,410	11,7	28,6		0,281	13,40	47,7
	0,944	8,66	9,20		0,715	11,90	16,7		0,510	14,7	28,3		0,298	11,70	39,3
	1,144	9,02	7,91		0,776	16,55	21,4		0,617	15,2	24,7		0,410	17,70	43,2
	1,340	11,40			8,52								0,413	21,90	53,0
													0,581	26,50	45,0
49,82	0,155	1,46	9,43	49,90	0,168	3,22	19,1	53,40	0,201	4,60	22,9	50,05	0,218	11,05	50,7
	0,325	3,53	10,80		0,226	5,40	23,7		0,374	9,90	26,5		0,271	13,30	49,0
	0,429	4,37	10,40		0,379	9,95	26,3		0,633	17,5	27,6		0,300	15,20	50,6
	0,919	7,13	7,77		0,628	14,60	23,3						0,391	21,80	55,17
					0,980	19,35	19,8						0,665	31,80	47,9
													0,671	36,60	54,5
53,30	0,083	0,73	8,74	55,90	0,201	6,45	32,1	56,12	0,144	2,39	16,6	50,80	0,185	8,05	43,5
	0,184	1,49	8,10		0,252	3,95	15,7		0,322	5,44	16,9		0,286	9,43	33,0
	0,202	1,62	8,03		0,405	11,30	27,9		0,405	6,75	16,7		0,415	20,7	49,3
	0,317	4,37	13,80		0,754	10,60	14,1		0,514	9,85	19,1		0,436	23,9	52,7
	0,321	4,18	13,00		1,00	16,50	16,5		0,620	12,05	19,4		0,593	30,8	52,0
	0,774	7,31	9,45												
	1,010	9,20	9,15												
	1,110	11,12	10,10												
	1,303	11,70	8,97												
	1,580	16,1	10,10												
55,96	0,183	1,02	5,56									56,10	0,134	3,68	27,4
	0,830	5,63	6,77										0,269	7,82	29,1
	0,422	2,78	6,60										0,276	8,17	29,6
	0,653	4,16	6,37										0,466	13,60	29,1
	0,821	4,90	5,97										0,780	24,80	31,8
	1,460	11,50	7,83												

Figure 1 shows the variation of k_{ef} with acid concentration at $C_{alc} = 0.1$ mole/liter. It is clear that, as with Ph_3COH reduction [4], the curves for different temperatures all showed a maximum, whose position (at 49.5% H_2SO_4) was practically independent of temperature. The reason for the similarities of the curves relating k_{ef} and H_2SO_4 concentration is that the effective velocity constant is a complex function of the true velocity constant, the protonization constant of isopropanol, the ionization constant of DPTC, and the acidity of the medium. With increasing H_2SO_4 concentration, there is an increase in the term $K_{Ar_3COH}C_0/(1 + K_{Ar_3COH}C_0) = b$, characterizing DPTC ionization, and a decrease in the term $1/(1 + K_{ROH}h_0)$, characterizing the part played by the unprotonized form of the alcohol. Thus k_{ef} , which contains both terms according to equation (2), must be a function with a maximum at a given H_2SO_4 concentration.

Table 2 shows the temperature variation of k_{ef} and the corresponding activation energies E_{ef} , for different H_2SO_4 concentrations, at $C_{alc} = 0.1$ mole/liter. E_{ef} decreased with increasing acid concentration, as would be expected from the theory of the reaction mechanism [4].

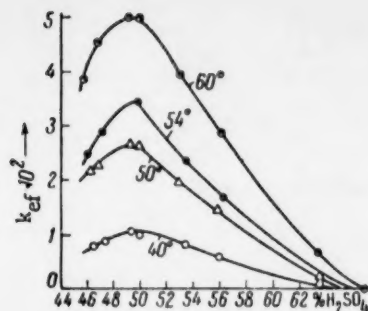


Fig. 1. Variation of k_{ef} with H_2SO_4 concentration at different temperatures. Calc = 0.1 mole/liter.

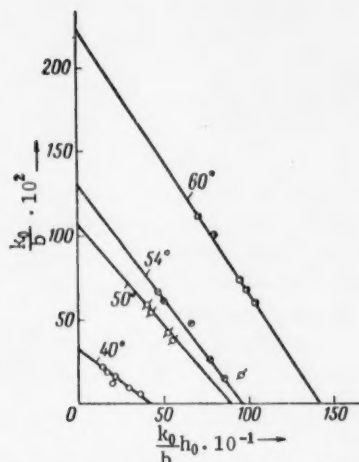


Fig. 2. Graphical determination of the values of k_{tr} and pK_{ROH} .

TABLE 2

H_2SO_4 , %	$k_{ef} \cdot 10^2$, min ⁻¹				E_{ef} , kcal/mole
	40 °C	50 °C	54 °C	60 °C	
46,0	0,75	2,15	2,40	4,00	17,7
48,0	1,00	2,55	3,25	4,90	17,6
49,0	1,10	2,70	3,45	5,05	16,1
50,0	1,07	2,65	3,40	5,00	15,9
52,0	0,93	2,20	2,75	4,32	15,6
54,0	0,80	1,80	2,15	3,55	16,0
56,0	0,65	1,47	1,75	2,90	15,5

trostatic interaction, either ion-dipole or dipole-dipole, may considerably increase the collision probability between reacting particles. Secondly, interaction of reacting molecules with solvent may lead to a decrease in the rotational degrees of freedom, which are responsible for the low values of the pre-exponential terms in reactions between polyatomic molecules*. The expression for the true velocity constant has the form:

$$k_{tr} = 9,6 \cdot 10^{11} e^{-20300/RT}. \quad (4)$$

* This explanation was suggested by Professor N. D. Sokolov in a contribution to the Conference on Heterolytic Reactions at Kiev in May 1960.

It is clear from equation (2) that in order to calculate velocity constants for the act of hydride transfer, k_{tr} , it is necessary to know the values of K_{Ar_3COH} and K_{ROH} . We therefore used the method of [5] to measure the DPTC basicity constant $K_B^{Ar_3COH} = 1/K_{Ar_3COH}$ at the various temperatures.

In our case, the isopropanol protonization constants were determined simultaneously with the true hydride transfer velocity constants. By using equation (2), and replacing k_{ef} by $k_0[ROH]$, it is not difficult to derive the expression:

$$\frac{k_0}{b} = k_{tr} - \frac{k_0}{b} h_0 K_{ROH}. \quad (3)$$

The graph relating k_0/b and $k_0 h_0/b$ is a straight line, whose intercept on the k_0/b axis is equal to k_{tr} . The slope of the line gives the value of K_{ROH} . Figure 2 shows the relations between k_0/b and $k_0 h_0/b$ at 40, 50, 54, and 60° for Calc = 0.1 mole/liter. Table 4 shows the results obtained for the hydride transfer velocity constants and the isopropanol basicity constants ($K_B^{ROH} = 1/K_{ROH}$).

It is interesting to compare the basicity constants of DPTC and TPC [4] with the velocity constants for the process of hydride transfer. The introduction of a methyl group into one of the benzene rings of TPC has little effect on the properties of the carbinol, but it is clear that the increase in basicity, i. e. the increase in stability of the corresponding cation, reduces its capacity to combine with the hydride ion. For example, for TPC at 60°, $pK_B = -6.17$ and $k_{tr} = 5.39 \times 10^{-2}$ liter/mole · sec [4], while for DPTC, $pK_B = -6.05$ and $k_{tr} = 3.72 \times 10^{-2}$ liter/mole · sec, i. e. the increase in pK_B of 0.12 units produces a decrease in the logarithm of the velocity constant such that $\Delta \log k_{tr} = -0.16$.

From the data in Table 4 we can calculate the true activation energy $E_{tr} = 20300 \pm 600$ cal/mole and the preexponential term $A = 9,6 \times 10^{11}$ liter/mole · sec.

It should be noted that, as in the case of TPC, the value of the preexponential term is close to that calculated, $Z_0 = 1.1 \times 10^{11}$ liter/mole · sec, from the formula for an ideal solution, assuming that $r_{ROH} = 3.1$ Å and $r_{Ar_3C^+} \sim r_{Ar_3COH} = 4.5$ Å.

The appearance of "normal" preexponential terms in reactions between polyatomic polar molecules in the liquid phase is not in accordance with the theory of absolute velocities, and, though it has been known for some time [7], has not received a satisfactory explanation. There are two possible factors tending to increase the preexponential term in such cases. Firstly, the existence of an elec-

TABLE 3

Temp., °C	35	40	50	54	60
$pK_B^{Ar,COH}$	-6,16	-6,14	-6,095	-6,075	-6,05

$\Delta H = (2100 \pm 100) \text{ cal/mole}; \Delta S = -21,5 \pm 0,1 \text{ cal/mole} \cdot \text{degree}$

TABLE 4

Temp., °C	40	50	54	60
$k_{tr} \cdot 10^3, \frac{\text{liter}}{\text{mole} \cdot \text{sec}}$	5,32	18,7	21,5	37,2
pK_B^{ROH}	-3,14	-2,95	-2,87	-2,80

TABLE 5

$H_2SO_4, \%$	55,90	53,20	49,80	49,34	47,40	46,40
$K_0 \cdot 10^3, \frac{\text{liter}}{\text{mole} \cdot \text{sec}}$	$\left\{ \begin{array}{l} \text{calc.} \\ \text{exp.} \end{array} \right.$					
	0,995	1,49	1,79	1,78	1,55	1,31
	1,05	1,50	1,67	1,83	1,50	1,33

From the temperature variation of the basicity constant we calculated the heat of protonization of the alcohol $\Delta H = 8100 \pm 1000 \text{ cal/mole}$ and the entropy $\Delta S = +11,4 \pm 0,1 \text{ cal/mole} \cdot \text{degree}$. This value of ΔH is in satisfactory agreement with that derived from our previous data [4]. Substituting the values of k_{tr} , $K_{Ar,COH}$, and K_{ROH} in equation (2), we obtained the following equation for calculating the observed bimolecular constants:

$$k_0 = 9,6 \cdot 10^{11} e^{-20300/RT} \left[\frac{2,08 \cdot 10^{-3} e^{-2100/RT} c_0}{1 + 2,08 \cdot 10^{-3} e^{-2100/RT} c_0} \right] \left[\frac{1}{1 + 3,09 \cdot 10^2 e^{-8100/RT} h_0} \right]. \quad (5)$$

Values of k_0 for 40°, calculated from equation (5), are compared with the experimental values in Table 5. It is clear that the two sets of values agree very well. This confirms our basic assumption that the limiting stage of the reaction was the interaction between the ionic form of diphenyltolylcarbinol and the isopropanol molecule.

LITERATURE CITED

1. P. D. Bartlett, J. D. McCullum, J. Am. Chem. Soc. **78**, 1441 (1956).
2. R. Stewart, Canad. J. Chem. **35**, 766 (1957).
3. R. Stewart, J. Am. Chem. Soc. **79**, 3057 (1957).
4. S. G. Entelis, G. V. Épple, and N. M. Chirkov, Doklady Akad. Nauk SSSR **136**, No. 3 (1961).
5. N. C. Deno, J. J. Jaryzelski, A. Schriesheim, J. Am. Chem. Soc. **77**, 3044 (1955).
6. S. G. Entelis, G. V. Épple, and N. M. Chirkov, Doklady Akad. Nauk SSSR **130**, 826 (1960).
7. Moelwyn-Highes, Kinetics and Reactions in Solutions [Russian Translation] (1937).

* This explanation was suggested by Professor N. D. Sokolov in a contribution to the Conference on Heterolytic Reactions at Kiev in May, 1960.

ERRATA

Vol. 135, Nos. 1-6,
November-December, 1960

On p. 1149 of the article by V. I. Gusynin and V. L. Tal'roze, the table should read as follows:

Quencher	Luminescing solution	\bar{z} , liter/ mole	\bar{y} , liter/mole	\bar{x} , liter/mole
Methanol CH_3OH	Terphenyl in dioxane	115 ± 12	$0,66 \pm 0,09$	$-0,09 \pm 0,04$
Ethanol $\text{C}_2\text{H}_5\text{OH}$		115 ± 12	$0,93 \pm 0,15$	$-0,06 \pm 0,04$
Propanol $\text{C}_3\text{H}_7\text{OH}$		115 ± 12	$1,18 \pm 0,16$	—
Hexanol $\text{C}_6\text{H}_{13}\text{OH}$		115 ± 12	$1,82 \pm 0,55$	—
Nonanol $\text{C}_9\text{H}_{19}\text{OH}$		115 ± 12	$2,88 \pm 0,42$	—
Water		115 ± 12	$0,23 \pm 0,03$	—
Carbon tetrachloride	Terphenyl in dioxane	62	28	18
The same	Terphenyl in xylene	415	217	10

*For comparison, we give values characterizing quenching by water and carbon tetrachloride of the luminescence of a solution of terphenyl in dioxane (our own measurements) and xylene (results taken from [3]).

SIGNIFICANCE OF ABBREVIATIONS MOST FREQUENTLY
ENCOUNTERED IN SOVIET PERIODICALS

FIAN	Phys. Inst. Acad. Sci. USSR.
GDI	Water Power Inst.
GITI	State Sci.-Tech. Press
GITTL	State Tech. and Theor. Lit. Press
GONTI	State United Sci.-Tech. Press
Gosenergoizdat	State Power Press
Goskhimizdat	State Chem. Press
GOST	All-Union State Standard
GTTI	State Tech. and Theor. Lit. Press
IL	Foreign Lit. Press
ISN (Izd. Sov. Nauk)	Soviet Science Press
Izd. AN SSSR	Acad. Sci. USSR Press
Izd. MGU	Moscow State Univ. Press
LEIIZhT	Leningrad Power Inst. of Railroad Engineering
LET	Leningrad Elec. Engr. School
LETI	Leningrad Electrotechnical Inst.
LEIIZhT	Leningrad Electrical Engineering Research Inst. of Railroad Engr.
Mashgiz	State Sci.-Tech. Press for Machine Construction Lit.
MEP	Ministry of Electrical Industry
MES	Ministry of Electrical Power Plants
MESEF	Ministry of Electrical Power Plants and the Electrical Industry
MGU	Moscow State Univ.
MKhTI	Moscow Inst. Chem. Tech.
MOPI	Moscow Regional Pedagogical Inst.
MSP	Ministry of Industrial Construction
NII ZVUKSZAPIOI	Scientific Research Inst. of Sound Recording
NIKFI	Sci. Inst. of Modern Motion Picture Photography
ONTI	United Sci.-Tech. Press
OTI	Division of Technical Information
OTN	Div. Tech. Sci.
Stroiizdat	Construction Press
TOE	Association of Power Engineers
TsKTI	Central Research Inst. for Boilers and Turbines
TsNIEI	Central Scientific Research Elec. Engr. Lab.
TsNIEI-MES	Central Scientific Research Elec. Engr. Lab.- Ministry of Electric Power Plants
TsVTI	Central Office of Economic Information
UF	Ural Branch
VIESKh	All-Union Inst. of Rural Elec. Power Stations
VNIIM	All-Union Scientific Research Inst. of Metrology
VNIIZhDT	All-Union Scientific Research Inst. of Railroad Engineering
VTI	All-Union Thermotech. Inst.
VZEI	All-Union Power Correspondence Inst.

Note: Abbreviations not on this list and not explained in the translation have been transliterated, no further information about their significance being available to us. — Publisher.

Soviet Journals Available in Cover-to-Cover Translation

ABBREVIATION	RUSSIAN TITLE	TITLE OF TRANSLATION	PUBLISHER	TRANSLATION BEGAN
				Vol. Issue Year
AÉ	Atomnaya énergiya	Soviet Journal of Atomic Energy	Consultants Bureau	1 1 1956
Akust. zh.	Akusticheskii zhurnal	Soviet Physics - Acoustics	American Institute of Physics	1 1 1955
Astr.(onl). zh(urn).	Antibiotiki	Antibiotics	Consultants Bureau	4 1 1959
Avto(mat). svarka	Astronomicheskii zhurnal	Soviet Astronomy-AJ	American Institute of Physics	34 1 1957
	Avtomaticheskaya svarka	Automatic Welding	British Welding Research Association (London)	
	Avtomatika i Telemekhanika	Automation and Remote Control	Instrument Society of America	1 1959
	Biofizika	Biophysics	National Institutes of Health*	27 1 1956
	Biokhimiya	Biochemistry	National Institutes of Health*	1 1 1957
	Byulleten' éksperimental'noi biologii i meditsiny	Bulletin of Experimental Biology and Medicine	Consultants Bureau	21 1 1956
DAN (SSSR)			Consultants Bureau	41 1 1959
Dokl(ad)y AN SSSR				
		The translation of this journal is published in sections, as follows:		
		Doklady Biochemistry Section	American Institute of Biological Sciences	106 1 1956
		(Includes: Anatomy, biophysics, cytology, ecology, embryology, endocrinology, evolutionary morphology, genetics, histology, hydrobiology, microbiology, morphology, parasitology, physiology, zoology sections)	American Institute of Biological Sciences	112 1 1957
		Doklady Botanical Sciences Sections (Includes: Botany, phytopathology, plant anatomy, plant ecology, plant embryology, plant physiology, plant morphology sections)		
		Proceedings of the Academy of Sciences of the USSR, Section: Chemical Technology	Consultants Bureau	106 1 1956
		Proceedings of the Academy of Sciences of the USSR, Section: Chemistry	Consultants Bureau	106 1 1956
		Proceedings of the Academy of Sciences of the USSR, Section: Physical Chemistry	Consultants Bureau	112 1 1957
		Doklady Earth Sciences Sections (Includes: Geochemistry, geology, geophysics, hydrogeology, mineralogy, paleontology, petrography, permafrost sections)		
		Proceedings of the Academy of Sciences of the USSR, Section: Geochemistry	American Geological Institute	124 1 1959
		Proceedings of the Academy of Sciences of the USSR, Section: Geology	Consultants Bureau	106- 1 1957- 123 6 1958
		Proceedings of the Academy of Sciences of the USSR, Sections: Geology	Consultants Bureau	106- 1 1957- 123 6 1958
		Soviet Physics-Doklady (Includes: Aerodynamics, astronomy, crystallography, cybernetics and control theory, electrical engineering, energetics, fluid mechanics, heat engineering, hydraulics, mathematical physics, mechanics, physics, technical physics, theory of elasticity sections)	The American Mathematics Society	131 1 1961
		Proceedings of the Academy of Sciences of the USSR, Applied Physics Sections (does not include mathematical physics or physics sections)		
		Wood Processing Industry	American Institute of Physics	106 1 1956
		Telecommunications		
		Entomological Review	Consultants Bureau	106- 1 1956- 117 1957
		Pharmacology and Toxicology	Timber Development Association (London)	9 1959
		Physics of Metals and Metallurgy	Massachusetts Institute of Technology*	1 1957
		Sechenov Physiological Journal USSR	American Institute of Biological Sciences	38 1 1959
		Plant Physiology	Consultants Bureau	20 1 1957
		Geochemistry	Acta Metallurgica*	5 1 1957
		Soviet Physics-Solid State	National Institutes of Health*	1 1957
		Measurement Techniques	The Geochemical Society	4 1 1957
		Bulletin of the Academy of Sciences of the USSR: Division of Chemical Sciences	American Institute of Physics	1 1958
			Instrument Society of America	1 1959
			Consultants Bureau	1 1952
Derevoobrabat. prom-st'.				
		promyshlennost'		
		Élektrosvyaz		
		Entomologicheskoe obozrenie		
		Farmakologiya i toksikologiya		
		Fizika metallov i metallovedenie		
		Fiziologicheskii zhurnal im. I. M. Sechenova		
		Fiziologiya rastenii		
		Geokhimiya		
		Fizika tverdogo tela		
		Izmeritel'naya tekhnika		
		Izvestiya Akademii Nauk SSSR: Otdelenie khimicheskikh nauk		

continued

Izv. AN SSSR, (Metall), i top.	Izv. AN SSSR Ser. fiz(ich).	Izv. AN SSSR Ser. geofiz.	Izv. AN SSSR Ser. geol.	Kauch. i rez.	(see Met. i top.) Izvestiya Akademii Nauk SSSR: Seriya fizicheskaya Izvestiya Akademii Nauk SSSR: Seriya geofizicheskaya Izvestiya Akademii Nauk SSSR: Seriya geologicheskaya Kauchuk i rezina Kinetika i kataliz Koks i khimiya	Bulletin of the Academy of Sciences of the USSR: Physical Series Bulletin (Izvestiya) of the Academy of Sciences USSR: Geophysics Series Izvestiya of the Academy of Sciences of the USSR: Geologic Series Soviet Rubber Technology Kinetics and Catalysis Coke and Chemistry USSR	1	1954	Columbia Technical Translations
Kolloidn. zh(urn).					Kolloidnyi zhurnal Kristallografiya Metallovedenie i termicheskaya obrabotka metallov Metallurg Metallurgiya i topiiva Mikrobiologiya Optika i spektroskopiya Pochvovedenie Prirostozenie	Colloid Journal Soviet Physics - Crystallography Metal Science and Heat Treatment of Metals Metallurgist Russian Metallurgy and Fuels Microbiology Optics and Spectroscopy Soviet Soil Science Instrument Construction	18	1959	American Geological Institute Research Association of British Rubber Manufacturers
Metalov. i term. obrabot. metal.					Kinetika i kataliz Koks i khimiya	Kinetics and Catalysis Coke and Chemistry USSR	1	1959	American Geophysical Union
Met. i top. Mikrobiol. OS					Kinetika i kataliz Koks i khimiya	Kinetics and Catalysis Coke and Chemistry USSR	1	1959	American Geological Institute Research Association of British Rubber Manufacturers
Pribory i tekhn. éksperimenta éks(perimenta)	Prikl. matem. i mekh.				Kinetika i kataliz Koks i khimiya	Kinetics and Catalysis Coke and Chemistry USSR	1	1959	American Geological Institute Research Association of British Rubber Manufacturers
PTÉ					Kinetika i kataliz Koks i khimiya	Kinetics and Catalysis Coke and Chemistry USSR	1	1959	American Geological Institute Research Association of British Rubber Manufacturers
Radiotekh. Radiotekh. i élektronika					Kinetika i kataliz Koks i khimiya	Kinetics and Catalysis Coke and Chemistry USSR	1	1959	American Geological Institute Research Association of British Rubber Manufacturers
Stek. i keram. Svaroch. proiz-vo	Teor. veroyat. i prim.				Kinetika i kataliz Koks i khimiya	Kinetics and Catalysis Coke and Chemistry USSR	1	1959	American Geological Institute Research Association of British Rubber Manufacturers
Tsvet. Metall'y					Kinetika i kataliz Koks i khimiya	Kinetics and Catalysis Coke and Chemistry USSR	1	1959	American Geological Institute Research Association of British Rubber Manufacturers
UFN					Kinetika i kataliz Koks i khimiya	Kinetics and Catalysis Coke and Chemistry USSR	1	1959	American Geological Institute Research Association of British Rubber Manufacturers
UKh					Kinetika i kataliz Koks i khimiya	Kinetics and Catalysis Coke and Chemistry USSR	1	1959	American Geological Institute Research Association of British Rubber Manufacturers
UMN					Kinetika i kataliz Koks i khimiya	Kinetics and Catalysis Coke and Chemistry USSR	1	1959	American Geological Institute Research Association of British Rubber Manufacturers
Usp. fiz. nauk					Kinetika i kataliz Koks i khimiya	Kinetics and Catalysis Coke and Chemistry USSR	1	1959	American Geological Institute Research Association of British Rubber Manufacturers
Usp. khim(ii)					Kinetika i kataliz Koks i khimiya	Kinetics and Catalysis Coke and Chemistry USSR	1	1959	American Geological Institute Research Association of British Rubber Manufacturers
Usp. matem. nauk					Kinetika i kataliz Koks i khimiya	Kinetics and Catalysis Coke and Chemistry USSR	1	1959	American Geological Institute Research Association of British Rubber Manufacturers
Usp. sovr. biol.					Kinetika i kataliz Koks i khimiya	Kinetics and Catalysis Coke and Chemistry USSR	1	1959	American Geological Institute Research Association of British Rubber Manufacturers
Vest. mashinostroeniya					Kinetika i kataliz Koks i khimiya	Kinetics and Catalysis Coke and Chemistry USSR	1	1959	American Geological Institute Research Association of British Rubber Manufacturers
Vop. gem. i per. krov					Kinetika i kataliz Koks i khimiya	Kinetics and Catalysis Coke and Chemistry USSR	1	1959	American Geological Institute Research Association of British Rubber Manufacturers
Vop. onk.					Kinetika i kataliz Koks i khimiya	Kinetics and Catalysis Coke and Chemistry USSR	1	1959	American Geological Institute Research Association of British Rubber Manufacturers
Vop. virusol.					Kinetika i kataliz Koks i khimiya	Kinetics and Catalysis Coke and Chemistry USSR	1	1959	American Geological Institute Research Association of British Rubber Manufacturers
Zavodsk. lab.(oratoriya)					Kinetika i kataliz Koks i khimiya	Kinetics and Catalysis Coke and Chemistry USSR	1	1959	American Geological Institute Research Association of British Rubber Manufacturers
ZhAKh Zh. anal(it). khimii					Kinetika i kataliz Koks i khimiya	Kinetics and Catalysis Coke and Chemistry USSR	1	1959	American Geological Institute Research Association of British Rubber Manufacturers
ZhETF					Kinetika i kataliz Koks i khimiya	Kinetics and Catalysis Coke and Chemistry USSR	1	1959	American Geological Institute Research Association of British Rubber Manufacturers
Zh. éksperim. i teor. fiz.					Kinetika i kataliz Koks i khimiya	Kinetics and Catalysis Coke and Chemistry USSR	1	1959	American Geological Institute Research Association of British Rubber Manufacturers
ZhFKh Zh. fiz. khimii					Kinetika i kataliz Koks i khimiya	Kinetics and Catalysis Coke and Chemistry USSR	1	1959	American Geological Institute Research Association of British Rubber Manufacturers
ZhMEI Zh(urn). mikrobiol. épidemiologii i immunobiologii					Kinetika i kataliz Koks i khimiya	Kinetics and Catalysis Coke and Chemistry USSR	1	1959	American Geological Institute Research Association of British Rubber Manufacturers
ZhNKh					Kinetika i kataliz Koks i khimiya	Kinetics and Catalysis Coke and Chemistry USSR	1	1959	American Geological Institute Research Association of British Rubber Manufacturers
Zh(urn). neorgan(ich). khim(ii)					Kinetika i kataliz Koks i khimiya	Kinetics and Catalysis Coke and Chemistry USSR	1	1959	American Geological Institute Research Association of British Rubber Manufacturers
Zh(urn). obshch(ei) khimii					Kinetika i kataliz Koks i khimiya	Kinetics and Catalysis Coke and Chemistry USSR	1	1959	American Geological Institute Research Association of British Rubber Manufacturers
ZhPKh					Kinetika i kataliz Koks i khimiya	Kinetics and Catalysis Coke and Chemistry USSR	1	1959	American Geological Institute Research Association of British Rubber Manufacturers
Zh(urn). prikl. khimii					Kinetika i kataliz Koks i khimiya	Kinetics and Catalysis Coke and Chemistry USSR	1	1959	American Geological Institute Research Association of British Rubber Manufacturers
ZhSKh					Kinetika i kataliz Koks i khimiya	Kinetics and Catalysis Coke and Chemistry USSR	1	1959	American Geological Institute Research Association of British Rubber Manufacturers
Zh(urn). strukt. khimii					Kinetika i kataliz Koks i khimiya	Kinetics and Catalysis Coke and Chemistry USSR	1	1959	American Geological Institute Research Association of British Rubber Manufacturers
ZhTF					Kinetika i kataliz Koks i khimiya	Kinetics and Catalysis Coke and Chemistry USSR	1	1959	American Geological Institute Research Association of British Rubber Manufacturers
Zh(urn). tekhn. fiz.					Kinetika i kataliz Koks i khimiya	Kinetics and Catalysis Coke and Chemistry USSR	1	1959	American Geological Institute Research Association of British Rubber Manufacturers
Zh(urn). vyssh. nervn. deyat. (im. P. Pavlova)					Kinetika i kataliz Koks i khimiya	Kinetics and Catalysis Coke and Chemistry USSR	1	1959	American Geological Institute Research Association of British Rubber Manufacturers

*Sponsoring organization. Translation through 1960 issues is a publication of Pergamon Press.

